K.M. Wijnberg

Morphologic behaviour of a barred coast over a period of decades

Nederlandse Geografische Studies / Netherlands Geographical Studies

ISSN 0169-4839

Morphologic behaviour of a barred coast over a period of decades

Nederlandse Geografische Studies / Netherlands Geographical Studies

ISSN 0169-4839

Nederlandse Geografische Studies 195

Morphologic behaviour of a barred coast over a period of decades

K.M. Wijnberg

Utrecht/Amsterdam, 1995

Koninklijk Nederlands Aardrijkskundig Genootschap/
Faculteit Ruimtelijke Wetenschappen Universiteit Utrecht

CIP-GEGEVENS KONINKLIJKE BIBLIOTHEEK, DEN HAAG

Wijnberg. K.M.

Morphologic behaviour of a barred coast over a period of decades / K.M. Wijnberg. - Utrecht : Koninklijk Nederlands Aardrijkskundig Genootschap ; Utrecht : Faculteit Ruimtelijke Wetenschappen Universiteit Utrecht. - Ill., fig., tab. - (Nederlandse geografische studies, ISSN 0169-4839 ; 195)
Ook verschenen als proefschrift Universiteit Utrecht, 1995. - Met lit. opg. - Met samenvatting in het Nederlands.
ISBN 90-6809-211-1
Trefw.: geomorfologie ; kusten ; Nederland / fysische geografie.

ISBN 90-6809-211-1 (NGS)
ISBN 90-6266-125-4 (Thesis)

Gedrukt door Drukkerij Elinkwijk b.v. Utrecht.

Here earth and water seem to strive again,
Not chaos-like together crush'd and bruis'd,
But, as the world, harmoniously confus'd:
Where order in variety we see,
And where, tho' all things differ, all agree.

A. Pope, Windsor-Forest (1704)

Acknowledgements

This thesis is the result of about five years of research at the Institute for Marine and Atmospheric research Utrecht (IMAU) in the coastal section of the Department of Physical Geography. During this period I benefited from the support of, and inspiring and open discussions with many people. I'm grateful to all these people, of whom I want to mention here some in particular.

First of all, I am grateful to my supervisor Prof. Dr. Joost Terwindt for the open discussions we had on the challenging topic of Large Scale Coastal Behaviour, and for giving me a lot of freedom to pursue my ideas. I am also greatly indebted to Prof. Dr. Ir. Leo van Rijn (Utrecht University/Delft Hydraulics) for the stimulating and pleasant collaboration in developing the WAVIS model (Chapter 6), and for reading and commenting on the draft version of this thesis. Special appreciation is extended to Prof. Dr. Rob Holman (Oregon State University), for his valuable suggestions on the draft version of the thesis. I especially profited from his suggestions concerning the expression of morphologic change in terms of sediment transport patterns (Chapter 5 and 6). Furthermore, I'm very grateful for his help in creating the opportunity for me to continue my career in science. Dr. Huib de Swart (IMAU) is gratefully acknowledged for his thorough review of the manuscript as well as for the interesting discussions we had throughout the years.

I am especially thankful to Dr. Aart Kroon (IMAU), for the many inspiring discussions, for the encouragements, and for the numerous and valuable suggestions on the manuscript. Besides, I enjoyed his company during many workaholic dinners at 'de Uithof'.

The work on large-scale coastal behaviour presented in this thesis could never have been accomplished without the unique data sets on nearshore bathymetry gathered over the years by the *Rijkswaterstaat*. Furthermore, their data on the wave climate have been very valuable for this study as well. I wish to thank Trudy Nijland and Lia Walburg (Rijkswaterstaat, RIKZ) for providing me with the profile data. Bram Roskam (Rijkswaterstaat, RIKZ) has been very co-operative in providing the wave climate data and discussing them with me. I am also indebted to Ir. Dick Rakhorst (Rijkswaterstaat, Directie Noord-Holland), who searched the Rijkswaterstaat archives for old bathymetric maps of the Holland coast (Chapter 4).

I gratefully acknowledge the *Rijks Geologische Dienst* for allowing me to use their core archive. Special appreciation is expressed to Dr. Dirk Beets for his assistance in selecting the cores, as well as for discussing them with me. Lilian van de Zande of the Drawing Department of our Faculty is kindly thanked for doing the tedious job of drawing these cores for Appendix 2.

I wish to thank all colleagues and former colleagues who took me into the field and out onto the sea to keep me in touch with the elements of nature. The 'sandy colleagues' - Piet Hoekstra, Klaas Houwman, Aart Kroon, Jan van de Meene, Gerben Ruessink, Ad Stolk, and Felix Wolf - are greatly acknowledged for

providing me with field data and discussion when I made up another 'large-scale' theory that needed confrontation with the real world. Special appreciation is extended to Felix 'Mac' Wolf with whom I shared an office for several years. Next to the many inspiring and open discussions we had on coastal behaviour on any scale, I enjoyed the pleasant working atmosphere which certainly helped me getting through the final stage of writing this thesis. The fact that he generously let me take over his 'Mac', helped me a lot to finish this thesis. In addition to all the 'sandy colleagues', I wish to thank Alfred, Bart, Celia, Erik-Jan, Hans, Heleen, Henk ('bedankt voor de reservering...'), Jaap, Nathalie, Wilfried, and Willem, for creating such an enjoyable and inspiring atmosphere to work in.

Finally, I wish to thank my parents for their genuine interest in my work, and for stimulating me throughout the years to really go for the things that interest me. And last but not least, I am deeply obliged to Ivo for his everlasting support, for taking me skiing when I thought I had no time to do so, and for his understanding that 'megaribbels' were such an important part of my life during the final stage of the completion of this thesis.

CONTENTS

List of Figures 13
List of Tables 17
List of Appendices 17

1 Decadal behaviour of large coastal stretches: an introduction

1.1 Introduction 19
1.2 Scale concept 22
1.2.1 Time scales and spatial scales in coastal behaviour 22
1.2.2 Process scales in coastal behaviour 23
1.3 Dealing with decadal behaviour of the Holland coast 26
1.3.1 Introduction 26
1.3.2 Approaches to the study of large-scale coastal behaviour 27
1.3.3 Studying decadal developments of the Holland coast from field data 29
1.4 Objectives and outline of the thesis 32

2 The study area: the Holland coast

2.1 Introduction 35
2.2 Setting of the study area 35
2.2.1 Introduction 35
2.2.2 Morphology 35
2.2.3 Wind, waves, tides, and river outflow 40
2.2.4 Sediment 56
2.2.5 Paleogeography 60
2.2.6 Antropogenic influences 63
2.3 Previous studies on the decadal behaviour of the Holland coast 66
2.3.1 Introduction 66
2.3.2 Shoreline studies 67
2.3.3 Sediment budget studies 69
2.3.4 Morphologic studies 72
2.4 Discussion and conclusions 74

3 Method to extract decadal morphologic behaviour from high-resolution, long-term bathymetric surveys

3.1 Introduction 77
3.2 The morphologic data base JARKUS 77
3.3 Concept of analysis of decadal morphologic behaviour 78
3.4 Quantification of cross-shore profile behaviour 79
3.4.1 Quantification of horizontal profile shift 79
3.4.2 On the quantification of profile shape change 80
3.4.3 Empirical eigenfunction analysis applied to nearshore profiles 81
3.4.4 Empirical eigenfunction analysis and moving window approach 84
3.4.5 Some additional remarks on the quantification of profile behaviour 86
3.5 Representation of alongshore coherence in cross-shore profile behaviour 87

4 Decadal morphologic behaviour along the Holland coast

4.1 On the morphological interpretation of empirical eigenfunctions 91
4.1.1 The empirical eigenfunctions 91
4.1.2 The weightings on the empirical eigenfunctions 94
4.1.3 On the interpretation of the 'alongshore coherence' plots 98
4.2 Alongshore coherence in decadal profile developments 101
4.2.1 The cross-shore position of the sub-aqueous profile 101
4.2.2 The mean profile 104
4.2.3 Secondary morphologic features 106
4.2.4 Relation between profile shape change and cross-shore profile shift 109
4.2.5 Relation between profile steepness and the second and third eigenfunction 114
4.3 Regional differences in decadal morphologic behaviour 114
4.3.1 Identification of 'LSCB-regions' 114
4.3.2 Explanation of the locations of boundaries between 'LSCB-regions' 117
4.4 Discussion 122
4.5 Conclusions 128

5 Multi-year behaviour of multiple bar systems along the Holland coast

5.1 Introduction 131
5.2 Morphologic behaviour of multiple bar systems 132
5.3 Bar system behaviour and implied patterns of nearshore sediment transport 148
5.3.1 Introduction 148
5.3.2 Sediment transport patterns based on gross sediment budget considerations 149
5.3.3 Sediment transport patterns based on profile considerations 153
5.3.4 Conclusions 158
5.4 Hypothesis on the dynamics of cyclic bar system behaviour 160
5.5 Discussion 164
5.6 Conclusions 165

6 The systematic, offshore degeneration of the outer bar

6.1 Introduction 167
6.2 Definition of wave climate parameters on the outer bar 167
6.3 Model for estimating wave climate parameters on the outer bar 169
6.3.1 Introduction 169
6.3.2 Wave model description 170
6.3.3 Near-bed orbital velocity asymmetries 174
6.4 Wave climate parameters on the outer bar 181
6.4.1 Wave model input 181
6.4.2 Wave climate properties on the outer bar in relation to the development stage of the outer bar 188
6.5 The effect of offshore wave station, shoreline orientation, and profile shape on wave climate parameters on the outer bar 194
6.5.1 Introduction 194
6.5.2 Sensitivity of wave climate parameters on the outer bar to offshore wave station, shoreline orientation, and profile shape 195
6.5.3 The relation between shoreline orientation and the occurrence of bar degenerating conditions 201
6.6 On the transport capacity during bar-degenerating conditions 203
6.6.1 Introduction 203
6.6.2 Transport gradients across the outer bar 203

6.7 The duration of the bar system cycle: the Noord-Holland bar system versus the Zuid-Holland bar system 207
6.8 Discussion and conclusions 210

7 General discussion and conclusions

7.1 Decadal and sub-decadal morphologic behaviour of large coastal stretches 211
7.2 Recommendations for further research 215

Summary 217
Samenvatting 219
References 223
Appendices 231
Curriculum Vitae 245

FIGURES

1.1	Location of the study area	20
1.2	Primary scale relationship	23
1.3	Coastal morphodynamic system	24
1.4	Schematic overview of applied scale concepts	25
1.5	Concept for analysing decadal behaviour	30
1.6	Schematic overview of the analysis of decadal behaviour of the Holland coast	32
2.1	Geomorphologic setting of the study area	36
2.2	Morphologic terminology in the coastal zone	37
2.3	Some morphometric characteristics of the Holland coast shoreface	38
2.4	Shoreface morphology between km 0 and km 30	39
2.5	Inshore profile steepness along the Holland coast	39
2.6	Shoreline orientation along the Holland coast	40
2.7	Shoreface morphology along the Holland coast	41
2.8	Water levels in relation to varying wave conditions, wave station MPN	43
2.9	Wave climate at wave station YM6	44
2.10	Average monthly mean wave height at wave station YM6	46
2.11	Directional distribution of low-frequency wave energy, various wave stations	46
2.12	Position of measurement stations for waves, currents, and water levels	47
2.13	Average monthly mean wave height and average yearly mean wave height, various wave stations	47
2.14	Average yearly mean wave height per directional sector, various wave station	48
2.15	Wave climate at wave station ELD	49
2.16	Wave climate at wave station MPN	50
2.17	Wave climate at wave station EUR	51
2.18	Frequency distribution of H_{E10}, various wave stations	53
2.19	Tidal range along the Holland coast	54
2.20	Tidal curves along the Holland coast	55
2.21	Positions tide stations	56
2.22	Horizontal and vertical tide along the Holland coast	57
2.23	Median grain size at the high tide and low tide waterline along the Holland coast	58
2.24	Temporal variation in the cross-shore distribution of median grain size	59
2.25	Nearshore distribution of median grain size along the Holland coast	59
2.26	Location of some paleogeographic features along the Holland coast	61
2.27	Location of engineering structures and beach nourishments along the Holland coast	65
2.28	Qualitative overview of sediment budgets along the Holland coast	70
2.29	Present-day position and 1896 position of the 7 m and 10 m depth contours	73
3.1	High tide water levels along the Holland coast	80
3.2	Analysed length of nearshore profiles	85
3.3	Number of profiles per window	85
3.4	Example of first, second, and third empirical eigenfunction	87
3.5	Examples of extrapolated first eigenfunctions	88
3.6	Examples of extrapolated (re-arranged) second eigenfunctions	88
3.7	Example of depth deviation plotted in Sheet 1, Figure b	89

4.1 First empirical eigenfunctions along the Holland coast 91
4.2 Second and third empirical eigenfunctions along the Holland coast 92
4.3 Examples of the interpretation of weightings on the first three eigenfunctions 93
4.4 Residual variance explained by the second and third eigenfunctions 94
4.5 Results eigenfunction analysis of profiles in window km 41-42, with observed and reconstructed profiles 95
4.6 Results eigenfunction analysis of profiles in window km 69-70, with observed and reconstructed profiles 96
4.7 Results eigenfunction analysis of profiles in window km 12-13, with observed and reconstructed profiles 97
4.8 Examples reconstruction of incomplete profiles by three eigenfunctions 97
4.9 Maximum anomalies of the position of the +1m contour relative to its time-averaged position 98
4.10 Mean depth at 750 m seaward distance of the +1m contour 99
4.11 Results eigenfunction analysis of profiles in window km 31-32 100
4.12 Illustration cyclic bar system behaviour by eigenfunctions and observed profiles 100
4.13 Spatial and temporal coherence in fluctuations of shoreline position, km 30-52 102
4.14 Direction and statistical significance of linear correlations of shoreline position versus time 103
4.15 Examples illustrating the presence of some remainders of bar topography in the first eigenfunction 105
4.16 Direction and statistical significance of linear correlations of profile steepness versus time 106
4.17 First eigenfunctions in windows km 3-4 to km 7-8 107
4.18 Onshore movement of bar as derived from eigenfunctions 107
4.19 Definition sketch of 'discontinuities in alongshore coherence', 'return period of bar topography', and 'folds in isolines of equal weighting' 109
4.20 Geometric relations between changes in the shoreline position and the shape of the complete nearshore profile 110
4.21 Relation between sign of the weightings on the second and third eigenfunction and bar positions relative to the shoreline near km 84 111
4.22 Relation between sign of the weightings on the second and third eigenfunction and bar positions relative to the shoreline near km 31 112
4.23 Direction and statistical significance of linear correlations of weightings on respectively the first, second, and third eigenfunction versus the shoreline position 113
4.24 Direction and statistical significance of linear correlations between weightings on the first, second, and third eigenfunction 115
4.25 Cross-shore profiles prior to and after the construction of the IJmuiden harbour moles, north of IJmuiden 119
4.26 Cross-shore profiles prior to and after the construction of the IJmuiden harbour moles, south of IJmuiden 120
4.27 Cross-shore profiles near km 52, situation 1910 versus today 121
4.28 Cross-shore profiles near km 58, situation 1910 versus today 121
4.29 Changes in the alongshore trends in shoreline orientation and the position of boundaries of LSCB-regions 122
4.30 Differences in bar system morphology north and south of IJmuiden 125
4.31 Variation in inshore profile steepness within and among Region 3 and Region 4 126
4.32 Mean profile and 'secondary' morphology for window km 40-41 and window km 99-100 127

5.1 Morphodynamic systems concept underlying the analysis of multi-year bar system behaviour 132
5.2 Comparison eigenfunctions based on TAW-profiles and based on JARKUS-profiles, window km 84-85 133
5.3 Comparison eigenfunctions based on TAW-profiles and based on JARKUS-profiles, window km 40-41 134
5.4 Average, seasonal standard deviation of the cross-shore depth measurements at km 84.25 135
5.5 Nearshore profiles in 'winter storm period', km 84.25 136
5.6 Nearshore profiles in 'summer season', km 84.25 137
5.7 Twenty profile surveys near km 41, December 1970 to August 1973 138
5.8 Nearshore bathymetry between km 58 and km 69 in 1984 139
5.9 Nearshore bathymetry between km 65 and km 76 in 1983 139
5.10 Nearshore bathymetry between km 65 and km 76 in 1984 140
5.11 Bar behaviour between km 32.50 and km 42.75 141
5.12 Bathymetry in 1976 and 1973, km 32 - km 49 142
5.13 Development of rhythmic topography between km 35 and km 47, 1966-1968 143
5.14 Development of rhythmic topography between km 32 and km 39, 1983-1985 144
5.15 Nearshore bathymetry between km 80.5 and km 90.5 in 1982 145
5.16 Nearshore bathymetry between km 65 and km 76 in 1982 145
5.17 Scales of alongshore 'rhythmicity' observed in the outermost well-developed bar 146
5.18 Outer bar degeneration sequence near km 40 147
5.19 Average correlation between the elevation of the outer bar crest and the cross-shore position of the bar located landward of it 148
5.20 Definition sketch bar volume 149
5.21 Potential transport components that may be involved in the degeneration of the outer bar 150
5.22 Sediment budget situation near Katwijk 151
5.23 Change in sediment volume enclosed in the zone between 800 m and 1400 m seaward from the RSP reference line near Katwijk over the period 1970-1980 152
5.24 Derivation of net cross-shore transport near km 84.25, period 1979-1981 154
5.25 Volume change in the inner and outer nearshore zone over the period 1979-1981 near Katwijk 155
5.26 Bathymetry in the vicinity of km 84.25 in 1979 and 1981 156
5.27 Net longshore transport in the inner nearshore zone near Katwijk over the period 1979-1981 157
5.28 Volume change in the nearshore zone over the period 1965-1967 near Egmond 158
5.29 Nearshore bathymetry between km 31 and km 42 in 1965 and 1967 159

6.1 Breaking coefficient γ 172
6.2 Bed profile, wave height, mean water level and fraction of breaking waves; Egmond case 175
6.3 Bed profile, wave height, and fraction of breaking waves; flume test 176
6.4 Tripod position for measuring near-bed velocity at Terschelling field site 177
6.5 Calculated and measured near-bed orbital velocity characteristics; Terschelling site 178

6.6 Near-bed, orbital velocity asymmetry as a function of near-bed, peak onshore orbital velocity; observations near Terschelling versus model computations 179
6.7 Near-bed, orbital velocity asymmetry as a function of near-bed, peak onshore orbital velocity at about 3.5 m water depth; observations versus model computations 179
6.8 Tripod position for measuring near-bed velocity at Egmond field site 180
6.9 Empirical relationships between wave height and wave period at wave stations MPN and YM6 183
6.10 Empirical relationship between T_{m02} and $T_{1/3}$ 183
6.11 Distinction between swell conditions and conditions with predominantly wind waves 184
6.12 Relation between wave height and water level for varying angles of wave propagation, wave station MPN 186
6.13 Nearshore profiles used in computations near Katwijk and Egmond 187
6.14 Examples of composite input profiles 188
6.15 Nearshore wave climate parameters as a function of development stage of the outer bar 189
6.16 Sensitivity of the ratio R to the definition of the boundaries between morphologically inactive conditions, bar-maintaining conditions and bar-degenerating conditions 190
6.17 Cumulative percentage of occurrence of wave conditions with increasingly higher fractions of breaking waves on the outer bar 191
6.18 Smoothed values of the nearshore wave climate parameters as a function of development stage of the outer bar 193
6.19 Sensitivity of the parameter %ACT 196
6.20 Sensitivity of the parameter %DGEN 198
6.21 Sensitivity of the parameter %MAIN 199
6.22 Sensitivity of the parameter R 200
6.23 Distribution of %DGEN over the angles of incidence 202
6.24 Degeneration of the outer bar and related net cross-shore transports near Katwijk: 1981-1983 204
6.25 Near-bed, peak onshore orbital velocity and asymmetry on the outer bar during bar-degenerating conditions 209

In appendix:

A.1 Estimates of the accuracy of the position of the 7 m and 10 m depth contour 240

TABLES

2.1	Some properties of the data sources on which the presented wave climate is based	45
2.2	Engineering works along the Holland coast	64
2.3	Beach nourishments along the Holland coast up to 1990	66
6.1	Some hydrodynamic properties of the conditions at the Terschelling site that were used for model verification	178
6.2	Offshore wave input for model calculations presented in Figure 6.17	181
6.3	Discrete representation of an offshore wave field: an example	185
6.4	Values of TRANSPOR input parameters	205
6.5	Example of transport computations for bar-degenerating conditions	206
6.6	Mean annual volume transport across the outer bar near Katwijk	206

In appendices:

A.1	Estimated effect of refraction on wave height near MPN	231
A.2	Core identification numbers in Geological Survey data base	238
A.3	Input wave climate applied in Katwijk case study	241
A.4	Input wave climate applied in Egmond case study and profile shape sensitivity analysis	241
A.5	Input wave climate applied in shoreline orientation sensitivity analysis and wave station sensitivity analysis	242
A.6	Input water levels for varying wave conditions applied in Katwijk case study	243
A.7	Input water levels for varying wave conditions applied in shoreline orientation sensitivity analysis and wave station sensitivity analysis	243
A.8	Input water levels for varying wave conditions applied in Egmond case study and profile shape sensitivity analysis	244

APPENDICES

1	Model estimates of wave refraction effects near wave station MPN	231
2	Stratigraphy along the Holland coast	232
3	Accuracy of the 1896 position and the present-day position of the 7 m and 10 m depth contour	239
4	Input wave climates	241
5	Input water levels	243

Sheet 1 Alongshore coherence in the temporal behaviour of the shoreline and the profile shape (gatefold)

1 DECADAL BEHAVIOUR OF LARGE COASTAL STRETCHES: AN INTRODUCTION

1.1 Introduction

In low-lying, densely populated countries like the Netherlands the understanding of large-scale and long-term changes of the coast is of vital importance. Proper coastal management requires insight in the influence of large engineering works on long-term coastal development, probably involving large coastal stretches. Moreover, insight in the natural long-term developments of coastal areas is required to prepare for unwanted future developments. This preparation may range from building protection works for threatened areas, to intervening in the coastal system to slow down unwanted natural developments or to displace the unwanted developments to areas where they are no threat to society.

Recently, indications of an increasing rate of sea level rise gave an impulse to the research on the natural, long-term behaviour of large coastal stretches. The possible acceleration of sea level rise (e.g. Warrick and Oerlemans, 1990) induced a need to predict the morphologic response of coastal areas to this phenomenon, especially the response to be expected in the near future. Such predictions require knowledge of the natural behaviour of large coastal areas (including the nearshore bathymetry), with lengths in the order of tens of kilometres, over a time span of decades (tens of years). This type of process-response knowledge was lacking and is still in its infancy today (e.g. Zitman et al., 1990; Terwindt and Battjes, 1990; De Vriend, 1991; De Vriend et al., 1993; Fenster and Dolan, 1993; Cowell and Thom, 1994).

In the Netherlands, the establishment that knowledge of coastal behaviour on large length and time scales was lacking resulted in considerable efforts on this subject. These efforts included both modelling and analysis of long-term field data (e.g. De Vriend and Roelvink, 1989; Stive, 1989; Louisse et al., 1990; De Ruig and Louisse, 1991). This study is part of the effort recently put in the analysis of long-term field data, especially bathymetric data. The analysis is confined to the behaviour of a long coastal stretch without inlets: the Holland coast (Figure 1.1; also see Section 2.2).

Field data based studies on decadal behaviour of large, inlet-free coastal areas are generally restricted to shoreline developments. Field studies on decadal coastal behaviour that include the developments of the sub aqueous morphology are scarce, because of a lack of suitable data sets. Large bathymetric data sets generally have either a large spatial dimension or a large temporal dimension, but usually not both (Terwindt and Wijnberg, 1991). By the author's knowledge, the only suitable data bases are the Dutch bathymetric data base 'JARKUS' -analysed in this study- and the Egyptian bathymetric data base for the Nile Delta coast (e.g. Fanos et al., 1991). The bathymetric data base of a part

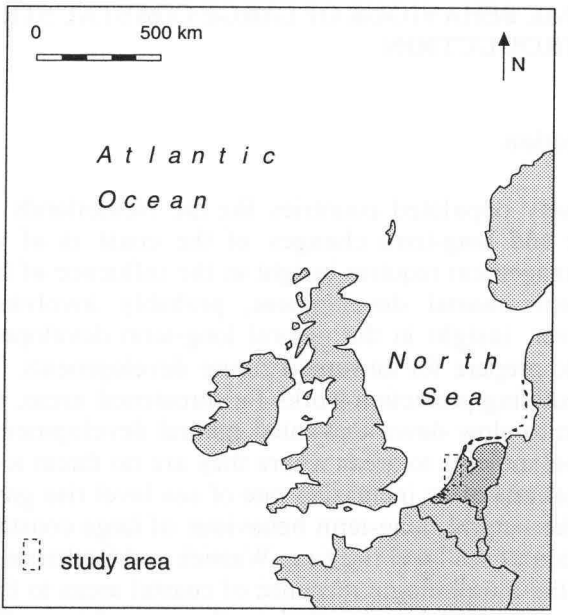

Figure 1.1: Location of the study area: the Holland coast

of the northern Danish coast may be suitable too, regarding the temporal extent of 17 year and the spatial extent of 80 km alongshore and up to 3 km cross-shore (Christiansen and Bowman, 1990). The temporal and cross-shore resolution of this data set, respectively 2 year and 150 m, is rather coarse in comparison to the other two data sets. It is still unknown, however, what the proper resolution is for the study of decadal behaviour of large coastal areas.

Some of the recent analyses of the two latter bathymetric data bases (Nile Delta data base: Fanos et al., 1991; Inman et al., 1992; Khafagy et al., 1992; Danish data base: Christiansen and Bowman, 1990) resulted in descriptions of multi-year morphologic behaviour. Quantitative relations between morphologic behaviour and controlling factors were not presented.

Model studies on decadal coastal developments of large, inlet-free coastal areas generally involve Bruun-type modelling (e.g. Bruun, 1988; Scientific Committee on Ocean Research Working Group 89, 1991). This type of modelling combines some morphometric 'rules' (read 'assumptions') with the conservation of mass to determine the response of the coastal profile to changes in sea level in terms of a new equilibrium profile. These models usually lack the alongshore dimension and do not include sediment transport processes. Consequently, these types of models add little to the understanding of the time-dependent development of the coastal system.

The one-line and n-line beach plan-shape models (e.g. Bakker, 1968; Dijkman et al., 1990) are also based on the existence of some equilibrium shape of the nearshore profile, but these models include the longshore dimension. Further, some schematised transport expression is formulated based on substantial a priori assumptions about the relevant hydrodynamic forces that drive the large-scale coastal behaviour. Other relevant physical processes will be tied-up in site-specific calibration factors. Therefore, the n-line type models may essentially be considered as sophisticated methods of extrapolation but they add little to the true understanding of decadal developments of large, inlet-free coastal areas.

Models that take into account the processes that physically transport the sediment by including short-term process knowledge will suffer from the limited accuracy of sediment transport formulations (Roelvink and Stive, 1990). In addition, our present-day lack of knowledge on appropriate input reduction or model reduction (De Vriend et al., 1993; De Swart, 1995) is a major obstacle in formulating a useful model for the decadal development of coastal morphology of large areas.

The study presented in this thesis aims at increasing the basic knowledge on decadal behaviour of large coastal stretches, focusing on sub-aqueous morphologic developments. This 'basic knowledge' covers a wide range of topics, for example the nature of the morphologic behaviour of large coastal stretches over a time span of decades and the relevant boundary conditions for the coastal behaviour on these scales. Another topic is the often presumed relationship between spatial scales and time scales in coastal behaviour. To obtain this type of knowledge, the decadal behaviour of the Holland coast will be analysed. The analysis is considered a case study of decadal behaviour of large coastal stretches; it does not aim at making predictions of coastal developments, although the obtained knowledge eventually will be of use in formulating models that might me able to make such predictions.

The scale concept is an essential concept for this study, because it determines the approach to the analysis of the decadal behaviour of the Holland coast. The general approach to the study of the behaviour of this coast (see Section 1.3 and 1.4) is based on a presumed relationship between time scales and spatial scales in coastal behaviour and a presumed relation between process scales and scales of coastal behaviour. The presumed relationship between time scales and spatial scales in coastal behaviour is also an underlying concept in formulating a method of analysis for the bathymetric data set (see Chapter 3). In addition, the scale concept is useful for positioning the studied coastal behaviour in a wider framework of coastal developments.

1.2 Scale concept

1.2.1 Time scales and spatial scales in coastal behaviour

In the definition of scales of coastal behaviour it is often assumed -implicitly or explicitly- that time scales and spatial scales are related. Recently, behaviour of coastal stretches of tens of kilometres length on time scales of decades has been called large-scale coastal behaviour (Terwindt and Battjes, 1990; List, 1993). The coupling of these specific time scale and length scale did not emerge from thorough analyses of coastal behaviour but is merely the result of the present-day interest in coastal behaviour on those two specific scales. The actual relation between length scales and time scales is still a matter of discussion (e.g. De Vriend, 1991).

The relationship between time scales and spatial scales is often assumed to be monotonic increasing, i.e. time scale increases with spatial scale. This assumption expresses the basic intuition that for a noticeable change of a large stretch of coast more sediment has to be redistributed than for a noticeable change of a small stretch of coast. For example, the amounts of sediment involved in a few degrees change of the shoreline orientation will be quite different along a coastal stretch of 100 km length and along a coastal stretch of only 1 km length. Further, a noticeable change of a large stretch of coast generally involves a larger part of the cross-shore profile. This implies that morphological changes at larger depths are involved. As a consequence, large-scale developments require transport of sediment at larger depths than small-scale developments. Generally, the hydrodynamic conditions that induce sediment transport at deeper water occur less frequently than the hydrodynamic conditions that induce sediment transport at shallower water. Therefore, bathymetric changes at larger depths tend to occur at a slower rate than at smaller depths. The assumed relation between time scale and spatial scale is therefore not only based on the amounts of sediment involved in the coastal change but also on the depths involved.

In coastal systems spatial scales are usually anisotropic: the alongshore length scale is larger than the related cross-shore length scale. In this study, the spatial scale will be defined by the alongshore length scale. The associated cross-shore scale is indirectly defined by the time scale that is linked with the alongshore length scale. The closure depth associated with that time scale and the bed slope in the nearshore zone determine the cross-shore length scale.

In this study, it is assumed that the coupling between time scales and spatial scales in coastal behaviour exists. Consequently, the notion of 'the' scale of coastal behaviour refers to some coupled set of time scale and spatial scale. The magnitude of the time scale associated with a coastal development at a specific spatial scale is not necessarily invariant but may be site-specific (Terwindt and Kroon, 1993).

1.2.2 Process scales in coastal behaviour

The coastal behaviour at all scale levels is ultimately the result of net transport of sediment particles due to waves and currents. It is assumed, though, that the net transports at the various scale levels are the result of different characteristics of the hydrodynamic processes. For example, at a small scale level, beach development depends on the hour to hour variation in water level and offshore wave height. At an intermediate scale level, the alternation of calm periods and stormy periods may be more relevant for the coastal behaviour than the hour-to-hour variation of hydrodynamic conditions. At a large scale level, possibly overall characteristics of the wave climate are more appropriate to explain the coastal behaviour. The latter would imply that the individual realisations of storm and calm weather sequences are no longer important at this scale level, provided the realisations originate from a constant probability distribution of wave height, wave period and wave direction. In other words, it is assumed that at each scale level in the coastal system a different filter is applied to the incoming energy.

The foregoing assumption is closely related to the assumption of 'primary-scale relationship' proposed by De Vriend (1991). The primary-scale relationship states that a process of a certain scale will be in dynamic interaction with coastal behaviour of a similar scale; that same process will be an extrinsic condition for coastal behaviour on a smaller scale and will be just noise for coastal behaviour on a larger scale (Figure 1.2). The concept of primary-scale relationship implies that at a certain scale level of coastal behaviour, the smaller scale process-response relationships are considered to produce noise, and the larger scale

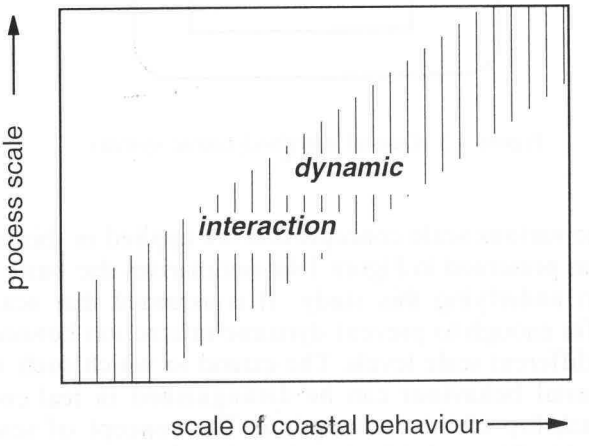

Figure 1.2: Primary scale relationship (after: De Vriend, 1991)

process-response relationships are considered to produce extrinsic boundary conditions. Further, the assumption of primary-scale relationship implies that for each scale level a specific morphodynamic system can be identified. In a coastal morphodynamic system the motion of water induces a net sediment transport which at its turn induces a morphologic change. The water motion is induced by energy input in the system through waves and currents and is influenced by the bottom topography (Figure 1.3). Following the primary-scale relationship, different aspects of the water motion, the mechanism of sediment transport, and the morphology will be relevant to the morphodynamic systems at the different scale levels.

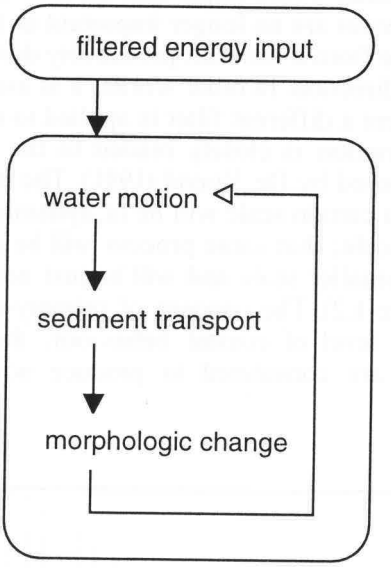

Figure 1.3: Coastal morphodynamic system

In Figure 1.4 the various scale concepts that are applied in this study are integrated. The diagram presented in Figure 1.4a summarises the basic perception of the coastal system underlying this study. It is assumed that scales of coastal behaviour will differ enough to prevent dynamic interaction between morphodynamic systems of different scale levels. The extend to which such well separated scale levels in coastal behaviour can be distinguished in real coastal systems determines the tenability of this assumption. The concept of scales in coastal behaviour presented in Figure 1.4 further describes that the time scale and spatial scale of morphologic developments are forced by the scales of variation in the forcing energy input as well as by the scales of variation in the boundary conditions imposed by the larger scale morphodynamic system (Figure 1.4b and 1.4c).

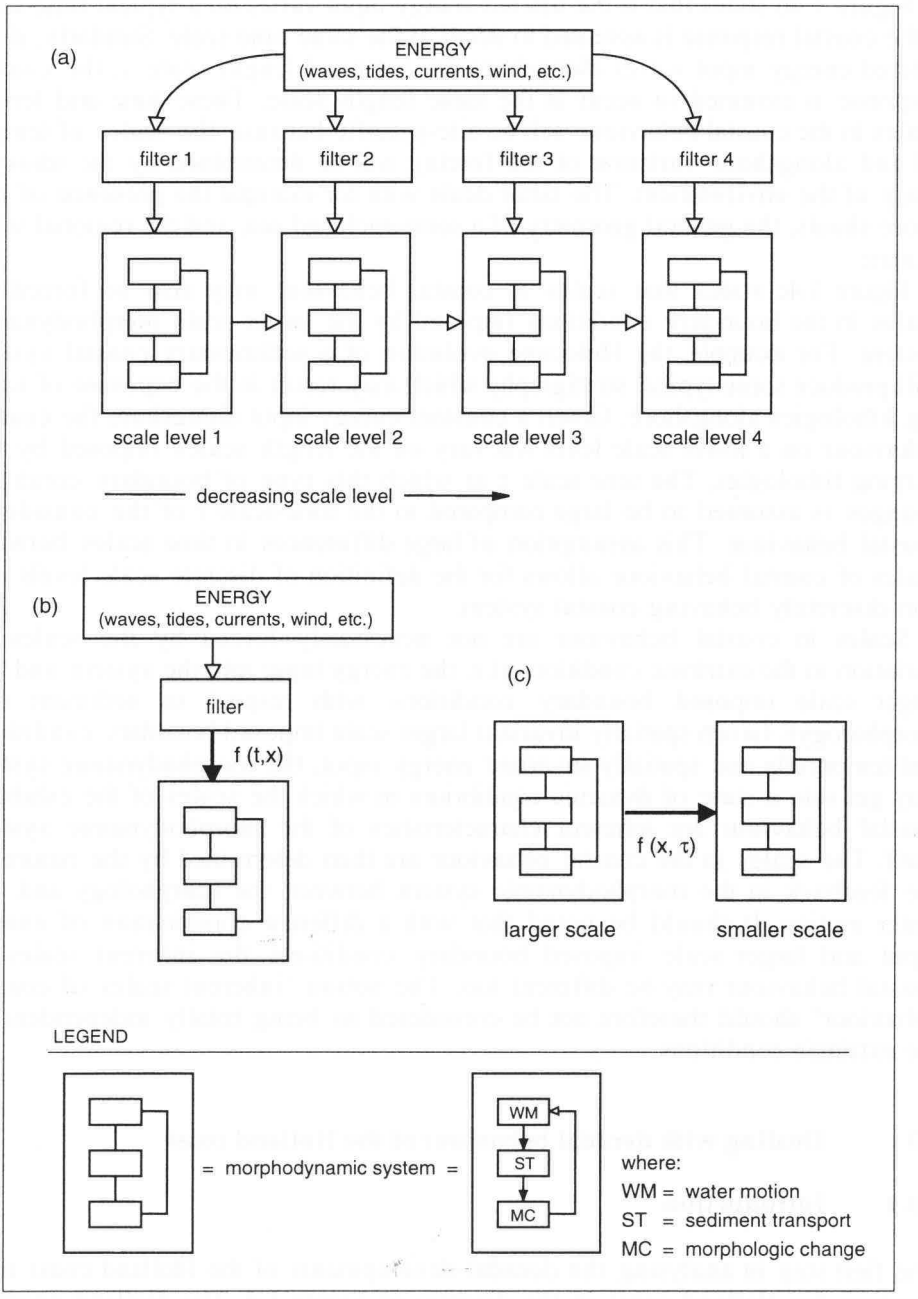

Figure 1.4: Schematic overview of applied scale concepts. (a) Scale relationships in the coastal system; (b) energy input into the coastal morphodynamic system; (c) larger scale imposed boundary conditions

Figure 1.4b states that if the filtered energy input varies on a typical time-scale t, the coastal response is assumed to occur at the same time scale. Similarly, if the filtered energy input varies alongshore on a typical length scale x, the coastal response is assumed to occur at the same length scale. These time and length scales in the coastal behaviour will be site-specific because the scales of temporal and alongshore variation of the forcing will be determined by the idiosyncrasy of the environment. The latter deals with for example the presence of offshore shoals, the general geometry of a semi-enclosed sea, and the regional wind climate.

Figure 1.4c states that scales in coastal behaviour may also be forced by scales in the boundary conditions imposed by the larger scale morphodynamic system. For example, the Holocene evolution of a sedimentary coastal system will produce some typical stratigraphy which may result in the exposure of varying lithologies alongshore. Given a constant energy input alongshore the coastal behaviour on a lower scale level will vary on the length scales imposed by the varying lithologies. The time scale τ at which this type of boundary condition changes is assumed to be large compared to the time-scale t of the considered coastal behaviour. This assumption of large differences in time scales between scales of coastal behaviour allows for the definition of discrete scale levels in a non-discretely behaving coastal system.

Scales in coastal behaviour are not necessarily forced by the scales of variation in the extrinsic conditions (i.e. the energy input into the system and the larger scale imposed boundary conditions with respect to sediment and morphology). Given spatially invariant larger scale imposed boundary conditions and temporally and spatially invariant energy input, the morphodynamic system may get into a state of dynamic equilibrium in which the scales of the exhibited coastal behaviour are inherent characteristics of the morphodynamic system itself. The scales in the coastal behaviour are then determined by the nature of the feedback in the morphodynamic system between the morphology and the water motion. It should be noted that with a different combination of energy input and larger scale imposed boundary conditions the inherent scales of coastal behaviour may be different too. The notion 'inherent scales of coastal behaviour' should therefore not be considered as being totally independent of the extrinsic conditions.

1.3 Dealing with decadal behaviour of the Holland coast

1.3.1 Introduction

The first step in analysing the decadal developments of the Holland coast is to position the Holland coast in the diagram of Figure 1.4. The Holland coast is assumed to be a morphologic entity with its own morphodynamic system, because it has a typical character that differs from the neighbouring coastal stretches. The Holland coast is a wave-dominated, inlet-free coast. Neighbouring

coastal stretches, of a comparable scale level, are a coastal stretch consisting of a chain of barrier islands and a coastal stretch consisting of a set of peninsulas separated by estuaries and tidal basins (Figure 1.1 and Figure 2.1). The Holland coast is arbitrarily defined as the large-scale level. The length scale related to this large-scale level is tens of kilometres. The time scale of shoreline developments observed along the Holland coast over a 120 year period is in the order of decades (see Van Straaten, 1961). Therefore, the site-specific time scale of the behaviour of this large-scale morphologic entity is expected to be in the order of decades.

Next, the larger scale morphodynamic system that will impose boundary conditions to the Holland coast morphodynamic system has to be defined. The higher scale level, or the mega-scale level, is considered to include a set of the above mentioned large-scale morphologic entities, e.g. the North Sea coast from Belgium to Denmark. A typical length scale is hundreds of kilometres for this specific example of a mega-scale morphologic entity. The developments of this morphologic entity include, for example, the development from a barrier island type of coast to a continuous, inlet-free type of coast or vice versa. These types of developments are typical for developments that occurred in this area during the Holocene (Beets et al., 1992). Therefore, the time scale related to the mega-scale level is many hundreds of years to thousands of years.

So, to understand decadal developments of the Holland coast knowledge is required of the boundary conditions imposed by the Holocene developments, the large-scale filter for the energy input boundary condition, and the large-scale morphodynamic system itself.

1.3.2 Approaches to the study of large-scale coastal behaviour

The boundary conditions for large-scale coastal behaviour resulting from the Holocene evolution are the morphology, the stratigraphy and some possibly present background erosion or accretion rate. The morphologic boundary condition consists of, for example, the presence and location of headlands and the related general shape of the shoreface. The morphologic boundary condition is also referred to as the pre-existing morphology. The background erosion or accretion rate deals with the presence of sediment sinks or sources that operate on the scale of Holocene evolution. For example, a tidal basin associated with a barrier island type of coast may be silting up due to a net import of sediment. One of the sources for the sediment supply can be an adjoining stretch of coast, such as a continuous, inlet-free stretch of coast. The resulting retreat of the inlet-free stretch of coast is a result of the mega-scale behaviour and can not be explained by the 'local' large-scale morphodynamic system of the inlet-free stretch of coast. Quantitative studies on Holocene developments (e.g. Pool, 1992; Cowell et al., 1993) will give insight in the order of magnitude of background erosion or accretion rates for large-scale coastal behaviour.

Identifying the large-scale morphodynamic system deals with identifying relevant expressions for its components: the 'large-scale water motion', the 'large-scale sediment transport' and the 'large-scale morphology'. The definition of the relevant 'large-scale water motion' deals with defining the appropriate 'large-scale filter' for the energy input into the large-scale morphodynamic system. At present, it is still a matter of discussion how the components of the large-scale morphodynamic system should be derived. Some researchers follow the approach of up scaling small-scale, physical and semi-empirical knowledge on water motion and sediment transport (e.g. Roelvink and Stive, 1990; Chesher, 1993; Latteux, 1993). Alternatively, the morphodynamic system can be studied at the scale of interest by analysing long-term observations of the coastal system.

The up scaling of small-scale knowledge involves the averaging over time and space of hydrodynamic processes and sediment transport processes for which mathematical equations have been formulated on the small scale ('process filtering'). Another possibility is the reduction of input data for the small-scale process models ('input filtering').

A drawback of using the up scaling approach is that only processes are considered that are important on the small-scale. Process terms that are not important on the small scale, hence not included in the mathematical formulations, may happen to be important on the 'large' scale. Further, the small-scale formulations that can be averaged, still have difficulties with describing the small-scale morphologic developments. So, even correctly averaged formulations for water motion and sediment transport will not necessarily describe the large-scale morphologic developments well. Further, the small-scale formulations have to be averaged successively over the small-scale and the meso-scale level. The errors from the small scale formulations will be amplified every time the non-linear mathematical system is integrated to a larger scale (Terwindt and Battjes, 1990). In this approach, 'large-scale morphology' is implicitly defined by the morphologic changes that the averaged expressions for water motion and sediment transport produce.

The study of the coast on the scale of interest involves the analysis of long term data sets of bathymetry, hydrodynamics and sediments, covering a large area with sufficient resolution. Which resolution is actually sufficient, can only be determined afterwards, regarding the present level of knowledge. The analysis of a long-term and large area covering bathymetric data set will reveal what is an appropriate characterisation of 'large-scale morphology'. In addition, the amount of 'noise' induced by meso-scale behaviour can be determined.

Qualitative insight in the large-scale morphodynamics derived from the analysis of the field data may be translated into parametric relations, relating the large-scale morphologic behaviour to 'large-scale water motion' parameters and to relevant aspects of the substrate. To end up with a predictive model, an expression for the 'large-scale sediment transport' component of the large-scale morphodynamic system is required. Possibly, new expressions can be derived by combining the empirical knowledge condensed in parametric relations and the theoretical knowledge on the structure of large-scale transport expressions. The

latter being derived from the up scaling of transport formulations. This subject will not be discussed any further here, because the formulation of a predictive model is outside the scope of this study. A comprehensive review on the subject is presented by De Vriend et al. (1993).

The main drawback of studying the coast on the scale of interest is that the properties and limitations of the few long-term data sets that are available today, will also limit the types of coastal characteristics that can be studied. This applies to the bathymetric data sets as well as to the data sets on hydrodynamic properties and sediment properties. Further, the simple approach of comparing alongshore changes in morphologic behaviour to alongshore changes in boundary conditions suffers from the uncertainty about what properties of the boundary conditions should be characterised and how to include combined effects of for example waves and tides.

Both the up-scaling approach and the approach of studying the coastal behaviour on the scale of interest have their merits and their drawbacks. What holds for both approaches is the long way ahead to a full understanding of coastal behaviour on the large-scale level.

1.3.3 Studying decadal developments of the Holland coast from field data

In this study on decadal developments of large coastal stretches the approach of studying the coast at the scale of interest is chosen. This approach will make a start with revealing the type of morphologic behaviour that actually occurs on these scales, for the character of that behaviour is largely unknown.

Insight in the operation of the large-scale morphodynamic system requires the identification of the relevant boundary conditions imposed by the Holocene evolution, the definition of the large-scale filter for the energy input, and a proper description of the components of the morphodynamic system itself. In a first approach the morphodynamic system is simplified by putting the water motion component and the sediment transport component into one black box process component (Figure 1.5). This simplified system will be analysed from long-term field data. First, a proper definition of the energy input and the boundary conditions has to be found. Next, time series of filtered energy input and morphologic changes can be used to develop some parametric relationship or empirical transfer function to describe the black box process.

Given the general lack of knowledge on large-scale coastal behaviour, the first problem to tackle is a very basic one, viz. finding proper characterisations of the energy input and the boundary conditions. To find such characterisations it is hypothesised that along the Holland coast stretches of coast exist that exhibit different decadal morphologic developments. For convenience, these stretches

will be called 'LSCB-regions'. It is assumed that the alongshore variation in decadal coastal developments is controlled by :
(a) alongshore varying large-scale filtered energy input
(e.g. wave climate characteristics, tidal characteristics), or
(b) alongshore varying sediment-related constraints
(e.g. grain size of the substrate), or
(c) alongshore varying morphology-related constraints
(e.g. shoreline orientation, shoreface morphology), or
(d) combinations of a, b, and c.

In this approach it is assumed that the spatial scales in the decadal behaviour of the Holland coast are forced by spatial variation in the extrinsic conditions. This line of approach is chosen because potentially relevant extrinsic conditions vary along the Holland coast (see Chapter 2). However, the possibility of a much more complicated situation in which inherent scales of coastal behaviour play a role should be kept in mind.

Human interventions along the Holland coast, ranging from local beach nourishments to the construction of engineering works (see Section 2.2.6), may affect the behaviour of the Holland coast as well. It is unknown whether these interventions just add local noise to the large-scale morphodynamic system, or whether they act as boundary conditions that induce large-scale alongshore differences in decadal behaviour. Human interventions are classsified under the categories (b) and (c).

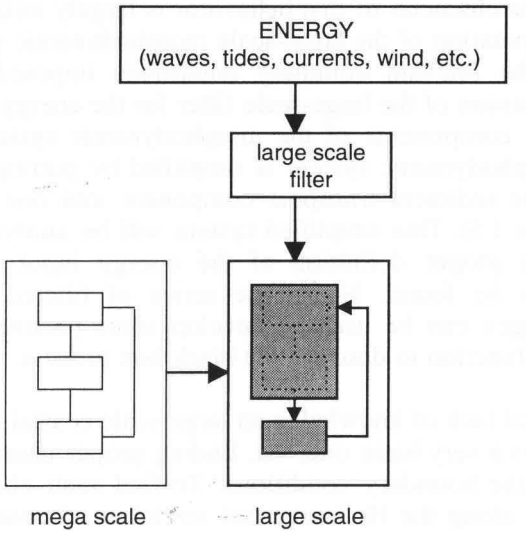

Figure 1.5: Concept for analysing decadal behaviour of the Holland coast

Identifying the cause of alongshore variations in decadal developments will indicate which aspects of the extrinsic conditions are important for the functioning of the large-scale morphodynamic system. It is assumed that the relevant variables co-vary with the alongshore changes in large-scale coastal behaviour. Furthermore, it is assumed that a gradual alongshore change in the external 'input conditions' of the morphodynamic system (energy, sediment, pre-existing morphology) results in a gradual change in morphologic response. For example, if tidal range is the controlling variable, a gradual alongshore change in tidal range is expected to result in a gradual alongshore change in coastal behaviour going with gradual transitions between LSCB-regions. The relation between 'input conditions' and morphologic response is probably not linear. It is assumed, however, that the non-linearity does not cause abrupt changes in the morphologic response, although this is theoretically possible. The gradual changes in the shoreline position along the Holland coast over the last century (Van Straaten, 1961) indicate that this is probably a tenable assumption for the Holland coast.

The first step in this approach is to analyse large-scale morphologic developments from a long-term data set of coastal profiles along a large stretch of coast. The analysis will reveal what type of developments occur on a decadal time scale. Further, it will show whether LSCB-regions exist, and whether the boundaries are sharp or gradual. The temporal extent of the available bathymetric data set is 'only' 28 years. As a consequence, it is not a priori known whether the large-scale coastal behaviour will emerge from the field data (Figure 1.6). If not, this implies that over a time span of three decades the 'noise' produced by the meso-scale behaviour is dominating trends related to the large-scale behaviour. The understanding of decadal coastal behaviour then involves the understanding of the fluctuations generated by the meso-scale coastal behaviour. The scale levels mentioned in Figure 1.5 should then be changed, viz. 'mega-scale' should be replaced by 'large-scale' and 'large-scale' should be replaced by 'meso-scale'.

For the analysis of the energy input into the morphodynamic system long-term wave data are available as well as data on the wind climate and some tidal characteristics (Figure 1.6). For the boundary conditions imposed by the mega-scale, data are available on the stratigraphy and on the morphologic setting (the presence of shoreface connected ridges, the general orientation of the shoreline, etc.). Additionally, a limited data set exists of grain sizes of nearshore surface sediment.

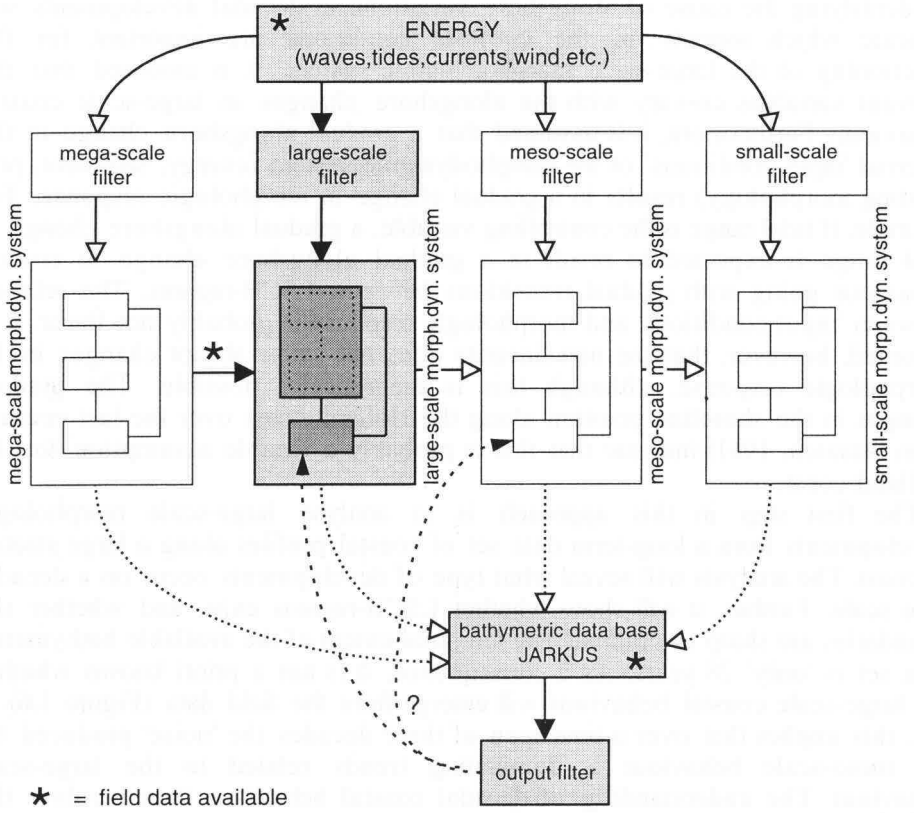

Figure 1.6: Schematic overview of the analysis of decadal behaviour of the Holland coast

1.4 Objectives and outline of the thesis

The general aim of the study is to increase the knowledge on decadal behaviour of large coastal stretches. This will be accomplished by making a case study of the decadal behaviour of the Holland coast, based on large data bases of field data. The decadal behaviour of the Holland coast has been identified for the time-being as coastal behaviour at the large-scale level. The establishment that the length scale of tens of kilometres is (probably) inherently coupled to the time scale of decades along the Holland coast, implies that the alongshore changes in decadal developments will be interrelated over distances of tens of kilometres. Consequently, the decadal coastal developments can only be understood when the full length of the Holland coast is considered.

In line with the presented point of view on the subject of large-scale coastal behaviour, the following objectives are formulated:

(1) Determine the nature of decadal behaviour along the Holland coast and determine the spatial scales involved. This includes verifying the assumption that 'LSCB-regions' exist and, if the existence is confirmed, determining the location and nature of the boundaries between those regions.
(2) Identify the extrinsic conditions that are relevant for the observed coastal behaviour, e.g. grain size, tidal range, mean annual wave-height, shoreline orientation.
(3) Explain the observed coastal behaviour in terms of phenomenological relationships and possibly involved mechanisms.

The first objective requires the elaboration of a method that effectively quantifies large-scale morphological changes from a large bathymetric data set (Chapter 3), such to explore the existence of 'LSCB-regions' and the location and nature of the boundaries between these regions (Chapter 4) (Wijnberg and Terwindt, 1995). The identification of relevant factors for the observed large-scale coastal behaviour will be approached in a 'statistical' manner, i.e. by correlating the location of LSCB-boundaries to the alongshore distribution of potentially controlling factors such as grain size, tidal range, etc. (Chapter 2 and Chapter 4). The explanation of the observed coastal behaviour in terms of phenomenological relationships and possibly involved mechanisms focuses on the multi-year behaviour of the multiple bar systems along the Holland coast (Chapter 5 and Chapter 6).

2 THE STUDY AREA: THE HOLLAND COAST

2.1 Introduction

This chapter on the study area serves as a general introduction into the study area, but it also serves as an outline of the boundary conditions of the large-scale morphodynamic system of the Holland coast. This outline includes the alongshore variability of mega-scale imposed boundary conditions concerning sediment and morphology. In addition, the outline includes the alongshore variability of processes that, in a filtered form, may put energy into the large-scale morphodynamic system of the Holland coast (Figure 1.5). The alongshore variations described in Section 2.2 will be used in Chapter 4 to explain the location of the LSCB-regions identified in that chapter. Further, the summary in Section 2.3 of the current knowledge on decadal morphologic changes along the Holland coast, outlines the alongshore variability in decadal coastal behaviour and the possibility to recognise LSCB-regions.

2.2 Setting of the study area

2.2.1 Introduction

The Holland coast is a sandy, inlet-free, wave-dominated coast. Several names are in use to indicate the Holland coast, such as 'Central Dutch Coast', 'Central Netherlands Coast' (e.g. Short, 1992) or (in Dutch) 'Schone Kust' and 'Gesloten Kust'. The length of this coastal stretch is about 120 km and the orientation of the slightly curved coastline is essentially NNE-SSW. The Holland coast faces the southern part of the semi-enclosed North Sea basin. To the north the North Sea basin is wide open to the Atlantic Ocean (Figure 1.1). To the south the basin is connected to the Atlantic Ocean by a narrow strait.

Along the full length of the Holland coast, a series of beach poles is present with an alongshore spacing of usually 250 m. This series of beach poles serves as a reference line for the monitoring of coastal developments. The beach poles are numbered according to their distance to Den Helder, following the coastline (Figure 2.1). For example, the distance from beach pole 38.25 to Den Helder along the coastline is 38.25 km. The series of beach poles is called -in Dutch- the 'Rijks Strand Palen lijn', and will be abbreviated as RSP reference line.

2.2.2 Morphology

The description of the morphology deals with the shoreface and the nearby parts of the inner shelf as well as the inshore and the beach (Figure 2.2). The inshore extends seaward from the fore shore to just beyond the surf zone (Shore Protection

Manual, 1984). The bathymetry in the inshore area is described relatively briefly, considering the abundance of available bathymetric data, because it is analysed in more detail in Chapter 3 and 4.

On the inner shelf a series of low-relief, shoreface connected ridges is present in front of the central part of the Holland coast (Figure 2.1). The sand ridges are located at a depth of about 18 m, and have a height of about 2 m and a cross-bank width of about 5 km. The ridges slowly migrate in the direction of the flood current (northward) at a rate of about 1 m/yr (Van de Meene, 1994). Considering the large spatial scales involved in the study of decadal developments of the Holland Coast, the decadal change in the bathymetric boundary conditions due to the ridge migration is negligibly small.

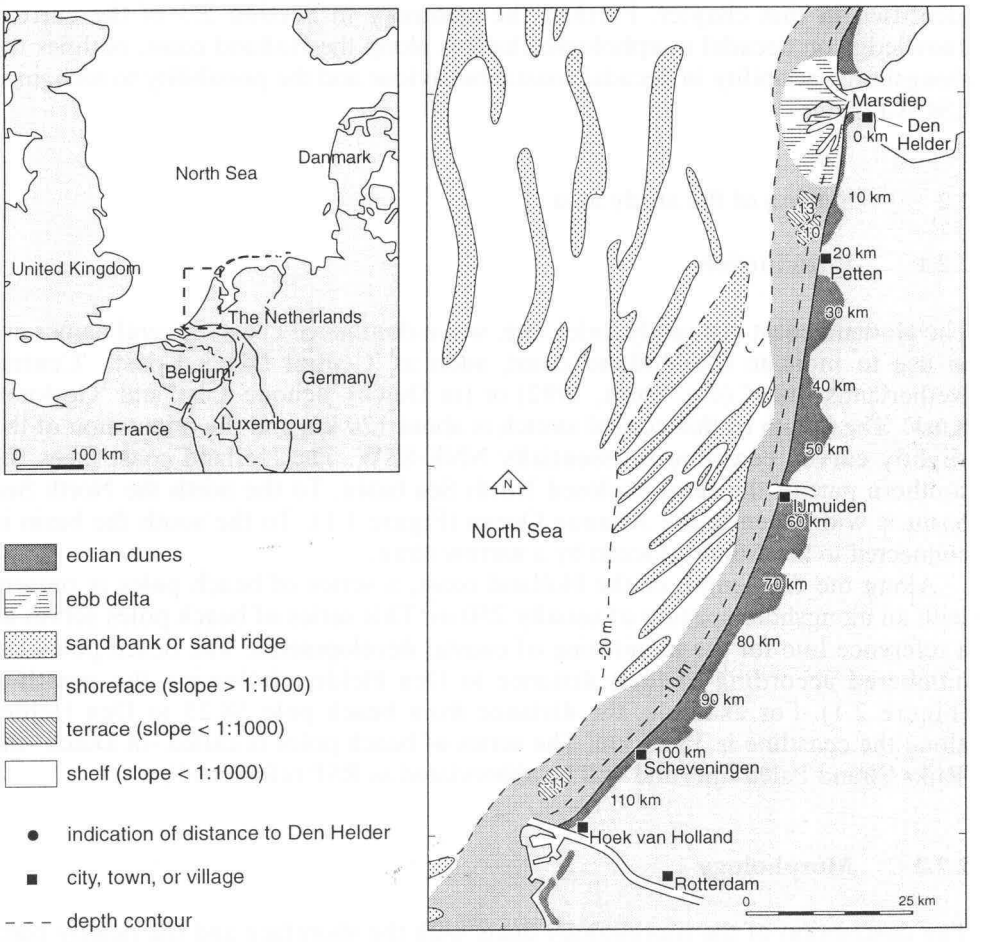

Figure 2.1: Geomorphologic setting of the study area

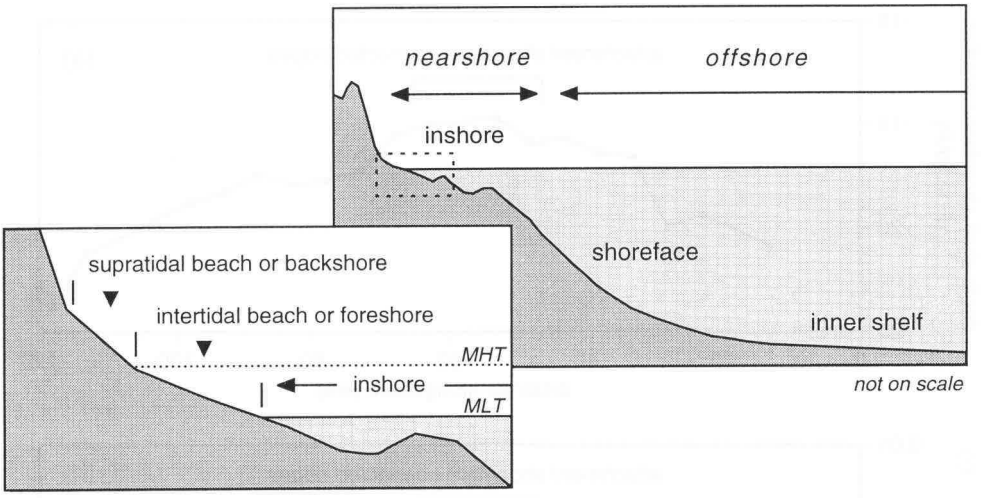

Figure 2.2: Morphologic terminology in the coastal zone

The depth at which the transition from shoreface to shelf floor occurs also varies alongshore. According to Stolk (1989), this transition generally occurs between 15 and 20 m water depth (Figure 2.3a). The average slope of the shoreface in front of the Holland coast varies roughly between 1:150 and 1:450 (Figure 2.3b). The flattening of the shoreface in the central part near IJmuiden coincides with the location where the sand ridges of the inner shelf connect to the shoreface.

Terrace-like interruptions of the concave shaped shoreface exist near km 15 and km 115 (Van Alphen and Damoiseaux, 1988). Near km 15, two natural terraces exist at respectively 10 m and 13 m water depth. The shallowest terrace of the two is called the 'Pettemer Polder'. The origin of these terraces is unknown (Beets, pers. comm.). On the southern 'terrace' a ridge feature is present which has a shore normal orientation (Figure 2.4). Near km 115, an artificial terrace exists at about 11 m water depth. This terrace, called 'Loswal Noord', is the result of repeated dumping of spoil from dredging operations.

The Holland coast is bordered to the north by a tidal inlet called the Marsdiep. The ebb-delta of this tidal inlet determines the offshore bathymetry from km 0 up to about km 10. A flood-tidal channel on this delta -the 'Nieuw Schulpen Gat'- is located very close to the shore. Consequently, the behaviour of this channel has a considerable influence on the behaviour of this coastal stretch (see Chapter 4).

Mean slopes in the surf zone generally vary between 0.0065 (≈1:150) and 0.017 (≈1:60) (Figure 2.5). The mean slopes refer to the mean profile slope across the first 750 m seaward of the +1m contour. Estimates of the mean slope from the shoreline down to 8 m water depth (Short, 1991) exhibit a similar alongshore pattern.

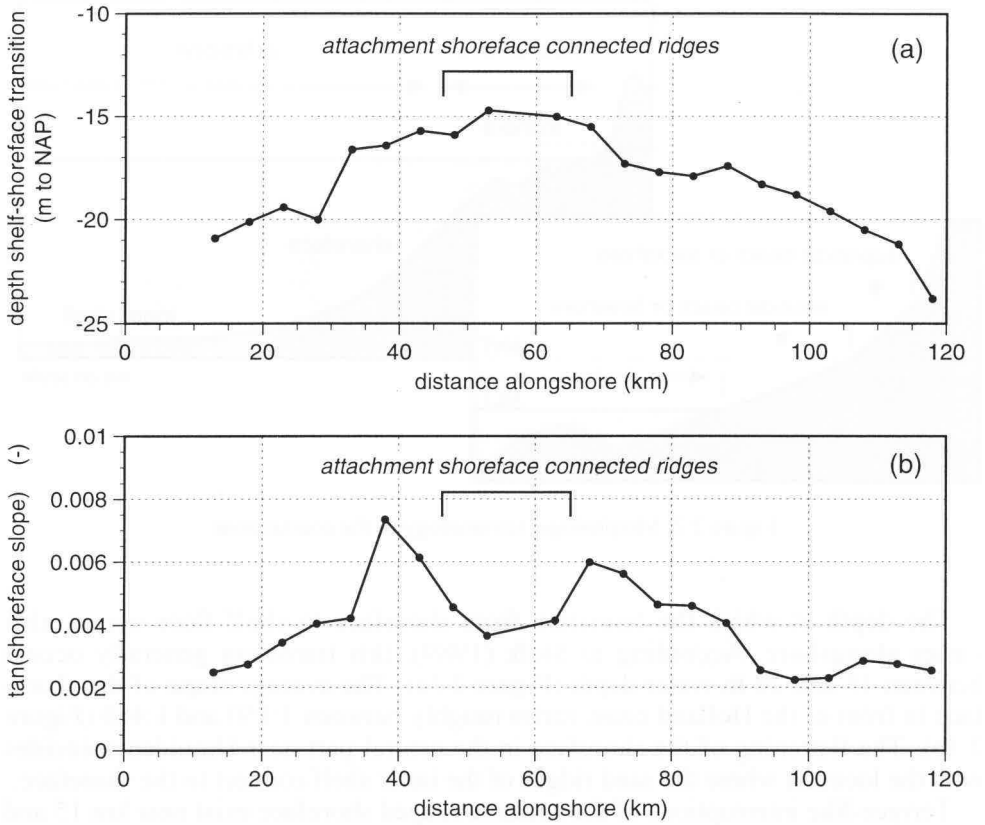

Figure 2.3: Some morphometric characteristics of the Holland coast shoreface, based on data from Stolk (1989). (a) Depth of shelf-shoreface transition; (b) shoreface slope

Breaker bars are present along the major part of Holland coast. The number of breaker bars varies between 1 and 4. Generally, the cross-shore spacing of the bars north of IJmuiden harbour is larger than south of it. North of IJmuiden the spacing is about 300 to 400 m, whereas south of IJmuiden it is about 200 to 240 m (Short, 1991). In addition, south of IJmuiden, between km 60 and km 96, the outer bar is generally one continuous body of sand, whereas north of IJmuiden, between km 27 and km 48, this is usually not the case (Knoester, 1990). According to De Vroeg (1987), the breaker bars are oriented obliquely to the shoreline at a small angle.

The widths of the intertidal beach and supratidal beach are relatively constant alongshore. The intertidal beach, represented by the horizontal distance between the -1m contour and the +1m contour, is about 75 m wide (Knoester, 1990). The supratidal beach, represented by the horizontal distance between the +1m contour and the +3m contour, is about 40 m wide (Knoester, 1990).

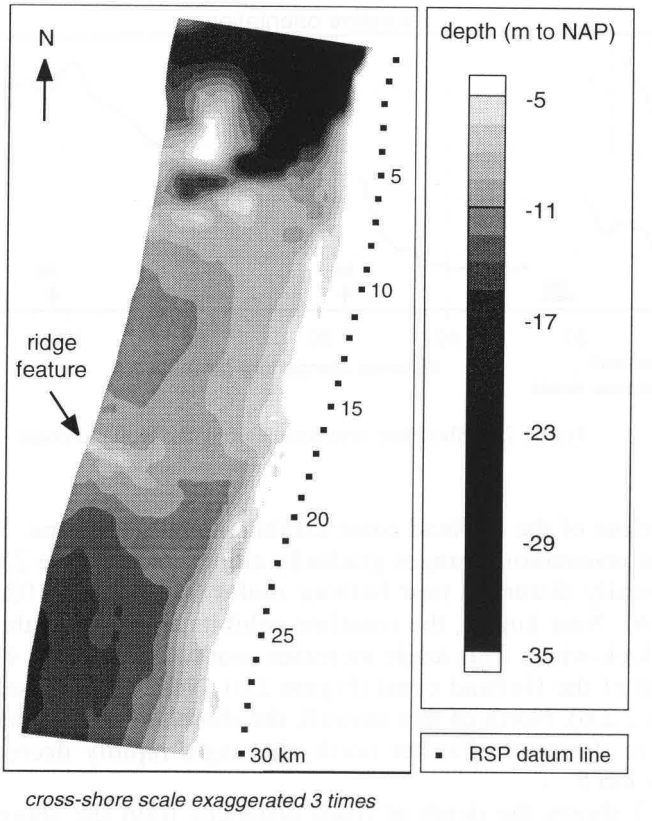

Figure 2.4: Shoreface morphology between km 0 and km 30 (based on extended survey 1985)

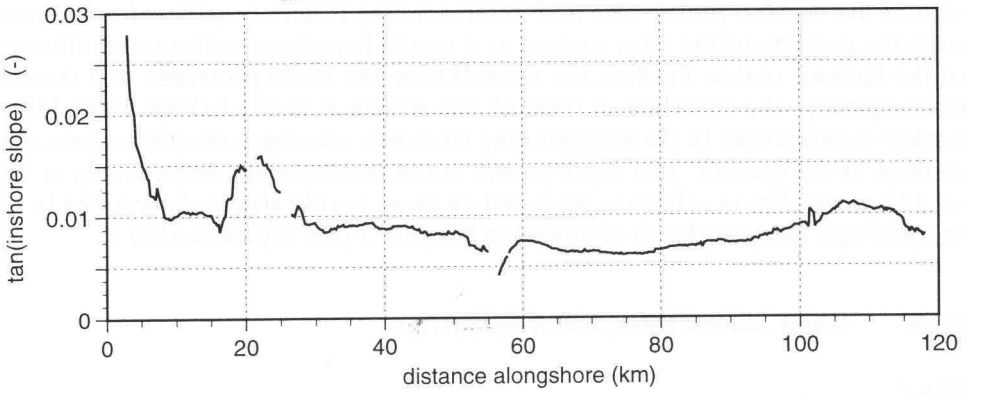

Figure 2.5: Inshore profile steepness along the Holland coast; derived from first eigenfunctions (see Chapter 3)

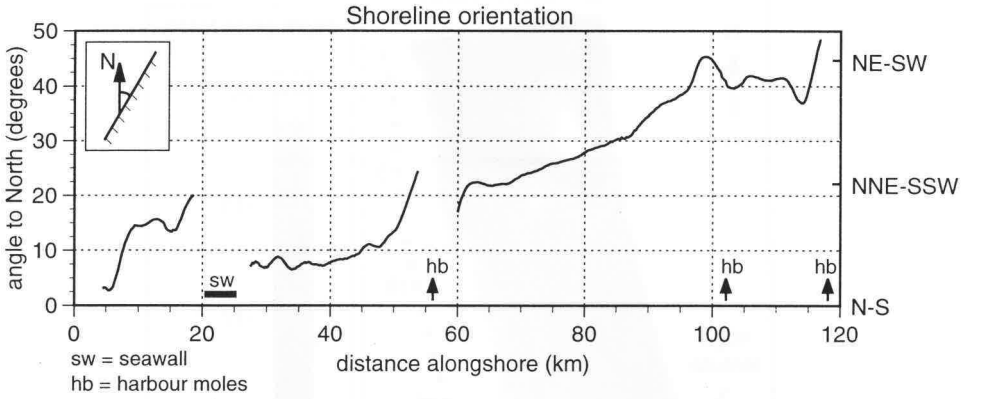

Figure 2.6: Shoreline orientation along the Holland coast

The shoreline of the Holland coast exhibits a concave shape. South of km 25, the shoreline orientation changes gradually alongshore (Figure 2.6). This gradual change is locally disturbed near harbour moles (km 56, km 102, km 118.5; see Section 2.2.6). Near km 25, the coastline exhibits an angle of about 8 degrees to the north (clock-wise). This angle increases southward to about 42 degrees at the southern end of the Holland coast (Figure 2.6). Near km 25 a seawall is present (see Section 2.2.6). North of this seawall, the shoreline exhibits an angle of about 15 degrees to the north. Farther north, the angle rapidly decreases to about 3 degrees near km 5.

Figure 2.7 shows the depth at fixed distances from the shoreline, giving an impression of the shoreface morphology. In the plot, the shoreline is defined as the +1m contour, except near the 2.5 km long harbour moles of IJmuiden (km 56). At this location 'the shoreline' is represented by the RSP reference line, because the +1m contour migrated seaward up to several hundreds of metres due to the extension of the harbour moles. The RSP reference line is here considered to approximate the position of the +1m contour as it would have been without the influence of the harbour moles. Further, the seawall near km 20-25 protrudes into the sea. Consequently, the shoreline in front of this stretch is located about 75 to 150 m further seaward than in the neighbouring stretches, causing a steeper inshore zone in front of the seawall. The depth values in the inshore zone -respectively at 255 m, 495 m and 750 m offshore- are based on mean profile shapes determined in the morphologic analysis that is described in Chapter 3 (viz. eigenfunction 1).

2.2.3 Wind, waves, tides, and river outflow

Wind

The wind climate of the southern North Sea is largely determined by W-E tracking, mid-latitude low pressure systems (Barry and Chorley, 1982). Seasonal

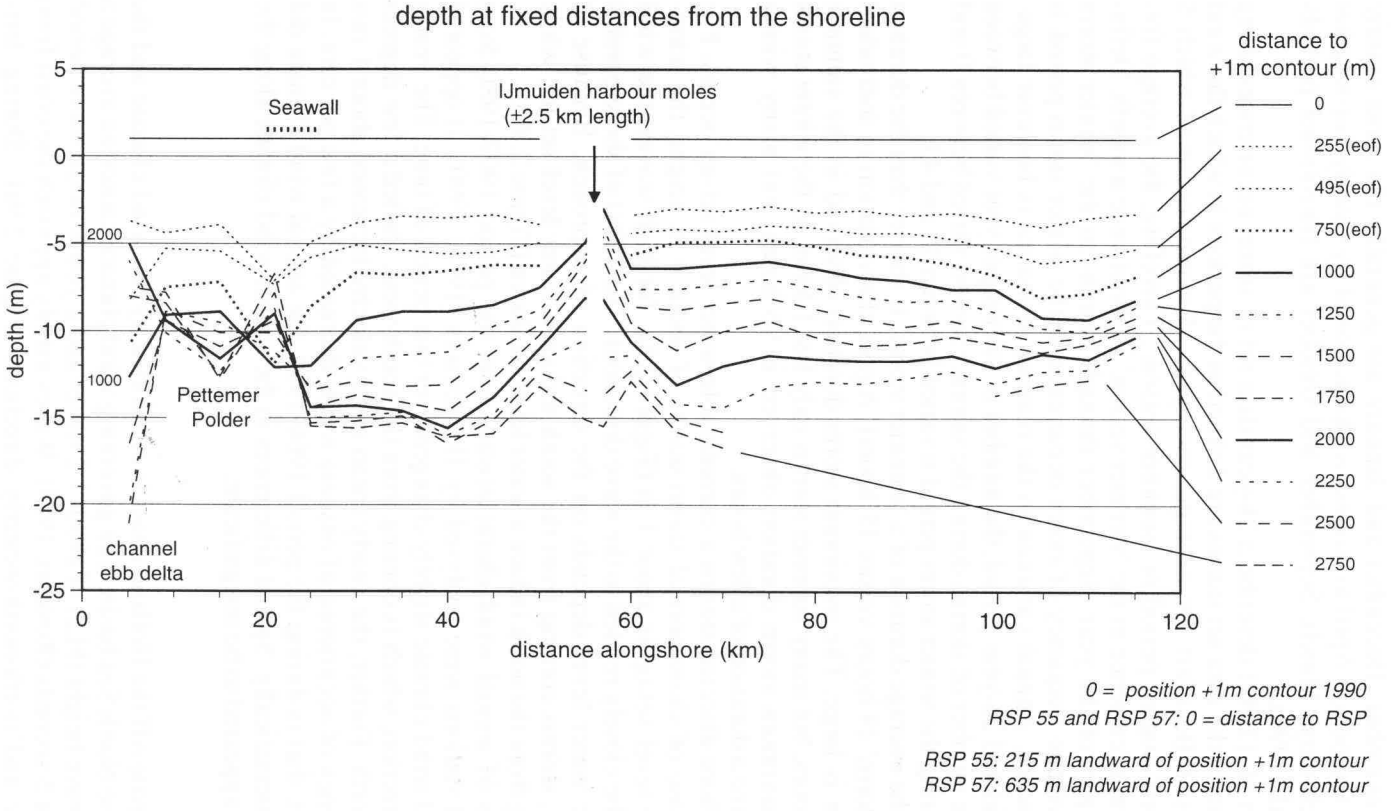

Figure 2.7: Shoreface morphology along the Holland coast (based on extended profile surveys of 1990)

variations in the atmospheric circulation patterns cause seasonal variation in the storminess. November, December and January are generally the most stormy months, while the period April to August is characterised by mainly fair-weather conditions. February, March, September and October are transitional periods (Augustijn et al., 1990).

Augustijn et al. (1990) describe a 26-year data set of storm occurrences along the Dutch coast. In the data set storms are defined as the periods in which the wind force is at least 8 Beaufort. On average, each year 35 storms occur of which 5 during the April-August period or 'summer season'. Therefore, the average frequency of storm occurrence in the 'summer season' is about once a month. Defining the other part of the year -September through March- as the 'winter storm period', the average frequency of storm occurrence in the winter storm period is about once a week. Annual variation in the number of storms is however large. Over the considered 26-year period, the number of storms per year varied between 13 and 48. The number of storms during the summer season varied between 0 and 10 whereas during the winter storm period it varied between 10 and 43.

Generally, the average duration of a 'summer storm' is shorter than the duration of a 'winter storm' (9 hours versus 15 hours). Again, the variation in individual storm duration is large. The maximum storm duration observed in the summer season is 50 hours, but many summer storms only last 1 hour. In the winter storm period, the maximum storm duration observed is 96 hours, but many winter storms only have a duration of a few hours.

During onshore directed storms a considerable water level set-up occurs. For example, in case of shore-normal storm waves of about 4 m height, the wind-induced water level set-up is about 1 m (Figure 2.8a; for high waves, the wind direction will be closely related to the wave direction). The effect of shore-parallel storms on the water level depends on the direction of approach. Because of Coriolis force, storms coming from the south induce a water level set-up, while storms coming from the north induce a water level set-down (Figure 2.8b).

Time series of annual wind characteristics over the period 1907-1980 from offshore wind stations were analysed by Hoozemans (1989; 1990). It appeared that the annual wind climate slightly changed over this period of time. The yearly mean wind direction, which is coming from the south-west, shifted a few degrees towards the north. Further, the yearly mean wind velocity increased about 1 m/s and the frequency of occurrence of onshore winds decreased by a few per cent. In the recent past, that is during the period 1960-1980, the annual wind climate did not change systematically. Spatial differences in the annual wind climate along the Holland coast appeared to be insignificant.

Waves

The wave climate off the Holland coast is controlled by the wind climate and the geometry of the North Sea basin. The governing wind climate causes on average a yearly mean wave height (H_{m0}) of about 1.2 meter and a yearly mean wave period (T_{m01}) of about 5 seconds (Roskam, 1988). Waves mainly approach the coast from south-westerly and north-north-westerly directions (Figure 2.9a). During fair-

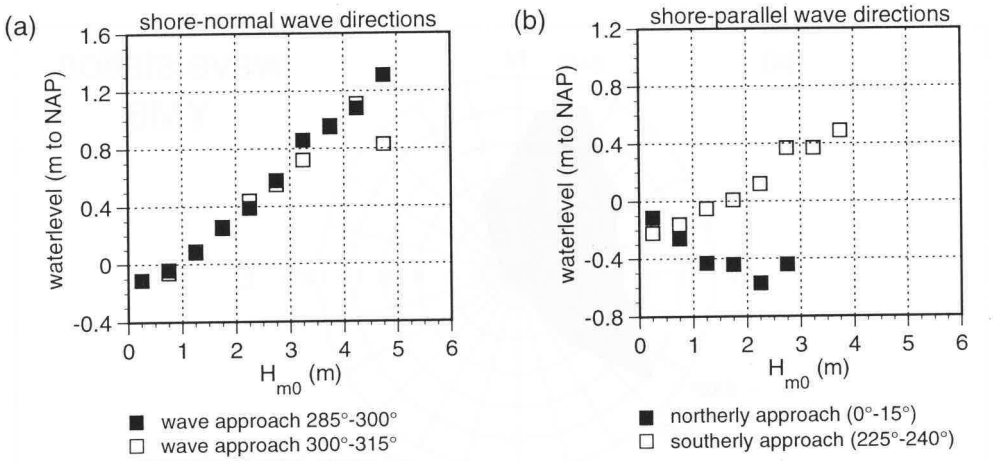

Figure 2.8: Water levels in correlation with varying wave conditions at wave station MPN. (unpublished data *Rijkswaterstaat*.) (a) shore-normal waves (and wind); (b) shore-parallel waves (and wind).

weather (H_{m0}<1m) waves approach the coast most often from the north-westerly directions (Figure 2.9b). During 'normal' storm conditions (1.5m < H_{m0}<3.5m) waves often approach from south-westerly directions (Figure 2.9c). During 'extreme' storm conditions (H_{m0}>4.5m) the dominant directions of wave approach are west and north-west (Figure 2.9d). The specific wave climate classes are derived by grouping wave height classes with similar directional distributions.

The seasonal variation in the storminess of the wind climate is clearly reflected in the wave climate. In the stormy winter months (November through January), the monthly mean wave height is about 1.7 m, while in the summer season (April through August) the monthly mean wave height is about 1 m (see Figure 2.10).

The presence of swell is hard to detect in the wave records. According to Roskam (1988) the energy in the low-frequency part of the wave spectrum (0.03 Hz - 0.10 Hz) may be used as an indicator of swell. Analyses of this part of the spectrum indicate that about 20 % of time swell is distinctly present (Rijkswaterstaat, 1994).

The geometry of the North Sea basin is such that swell - generated on the Atlantic Ocean and the northern North Sea - will always approach the Holland coast from northerly directions (Figure 1.1 and Figure 2.11).

Alongshore differences in the wave climate of the Holland coast are small. At four stations wave parameters have been recorded over more than a decade. These stations are Eierland (ELD), IJmuiden06 (YM6), platform Meetpost Noordwijk (MPN) and Euro-platform (EUR) (Figure 2.12a).

Wave directions are recorded at the four stations since 1985 respectively 1989 (Table 2.1). At those times, non-directional waverider buoys and wave poles were

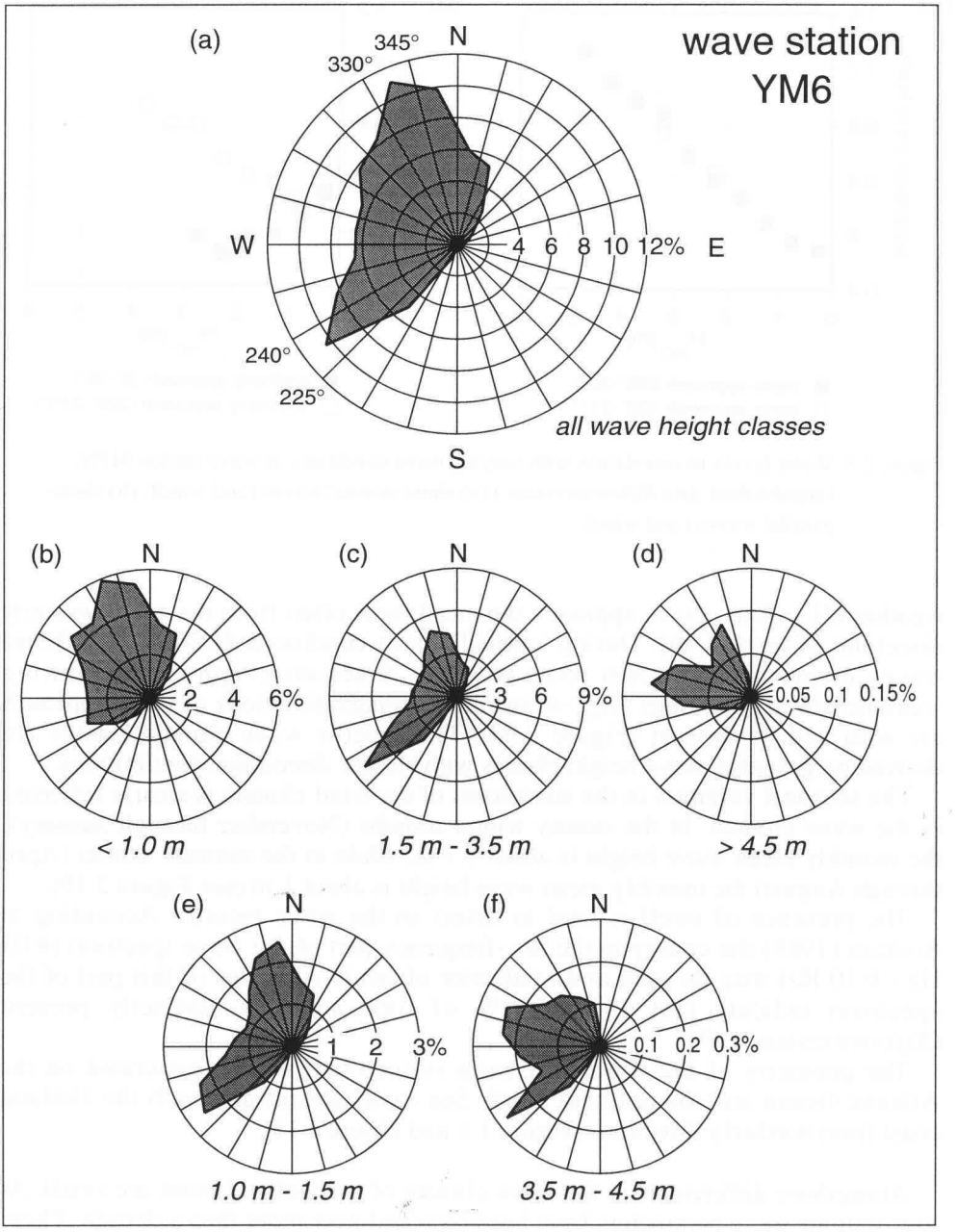

Figure 2.9: Wave climate at wave station YM6 (unpublished data *Rijkswaterstaat*)

replaced by wavec buoys (see Table 2.1). Wave directions in the period prior to the installation of the wavec buoys were predicted from wind directions by applying empirical relations between wave directions and wind directions (Roskam, 1994). These relations were separately defined for each wave station, based on all available measurements of the wave direction and wind direction between 1985 and 1991. Different relations were defined for different wind velocities and wind directions (Roskam, 1994).
The mean monthly wave heights (H_{m0}), as well as the mean annual wave heights per directional sector are very much alike for wave stations ELD, YM6, and EUR (Figures 2.13 and 2.14). The data of wave station MPN are clearly deviating, both for onshore and offshore directed waves. The frequency distributions of wave directions (Figures 2.15a, 2.9a, 2.17a) reveal a southward decrease in westerly wave directions going with a slight increase in south-westerly and north-north-westerly wave directions. MPN is again a clearly deviating station (Figure 2.16a).

Table 2.1: Some properties of the data sources on which the presented wave climate is based

	Eierland (ELD)	IJmuiden06 (YM6)	Meetpost Noordwijk (MPN)	Euro-Platform (EUR)
measurement device	waverider/ wavec	waverider/ wavec	wave pole*/ wavec	wave pole*/ wavec
water depth	26 m	21 m	18 m	31 m
record length wave climate	Sept. 1979 - Dec. 1991	Jan. 1979 - Dec. 1991	Jan. 1979 - Dec. 1991	Nov. 1982 - Dec. 1991
record length wave direction	1989 - Dec. 1991	1989 - Dec. 1991	1985 - Dec. 1991	1985 - Dec. 1991
% estimated wave direction	68%	74%	73%	52%
wind station	De Kooy/ Den Helder (land station)	IJmuiden semaphore (land station)	MPN (offshore station)	EUR (offshore station)
water level station	Den Helder harbour	IJmuiden harbour	MPN (offshore station)	EUR (offshore station)

*) measurement device recording water level fluctuations by a vertical array of sensors

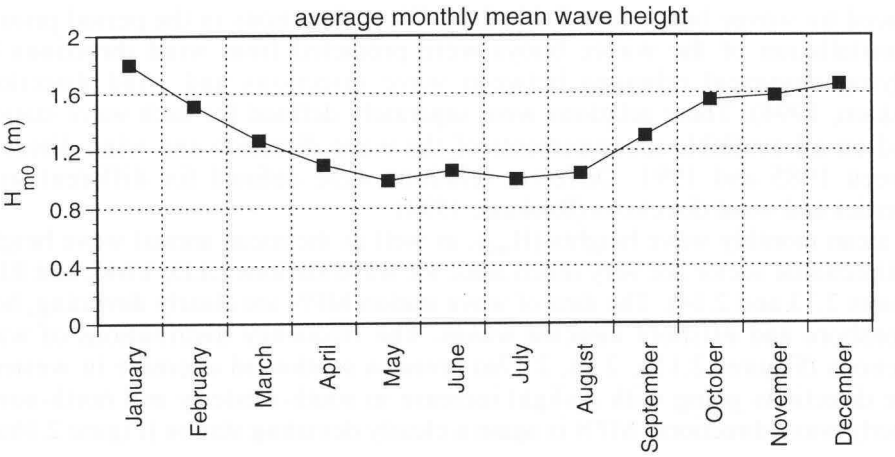

Figure 2.10: Average monthly mean wave height at wave station YM6 (unpublished data *Rijkswaterstaat*).

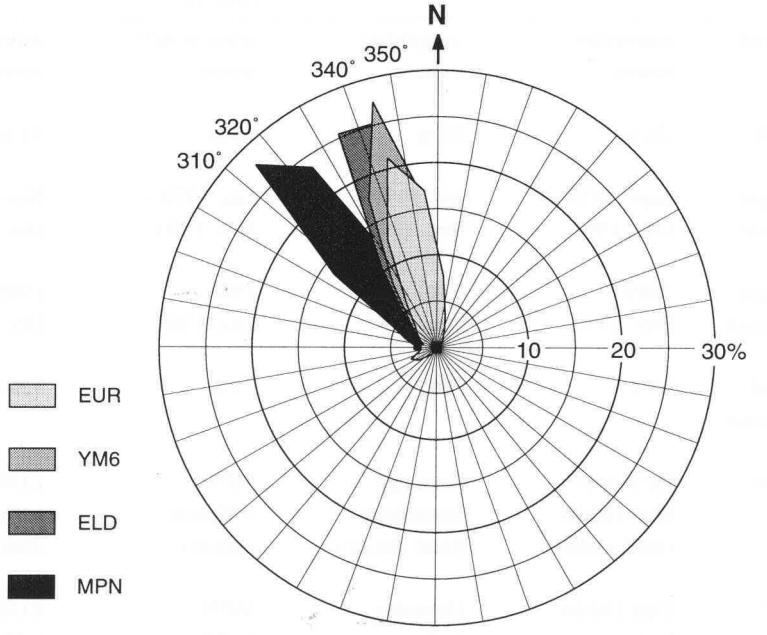

Figure 2.11: Directional distribution of low-frequency wave energy (0.03 Hz-0.10 Hz) at wave station ELD, YM6, MPN, and EUR (unpublished data *Rijkswaterstaat*).

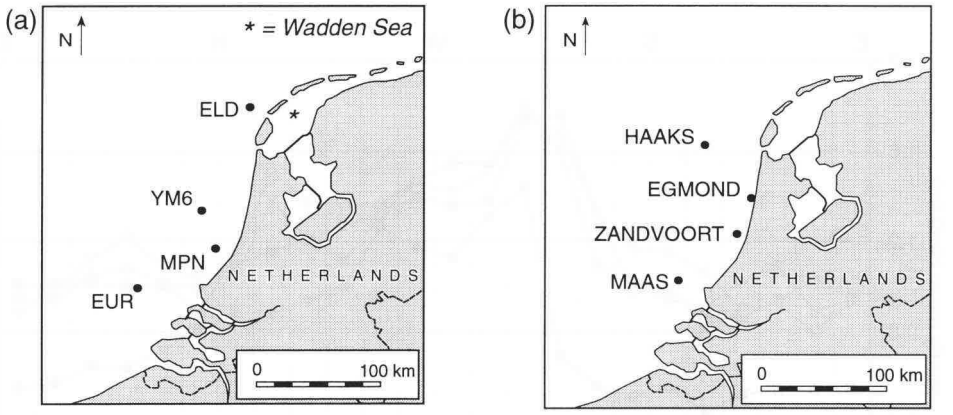

Figure 2.12: Position of measurement stations. (a) Wave measurements; (b) combined measurements of currents and water levels.

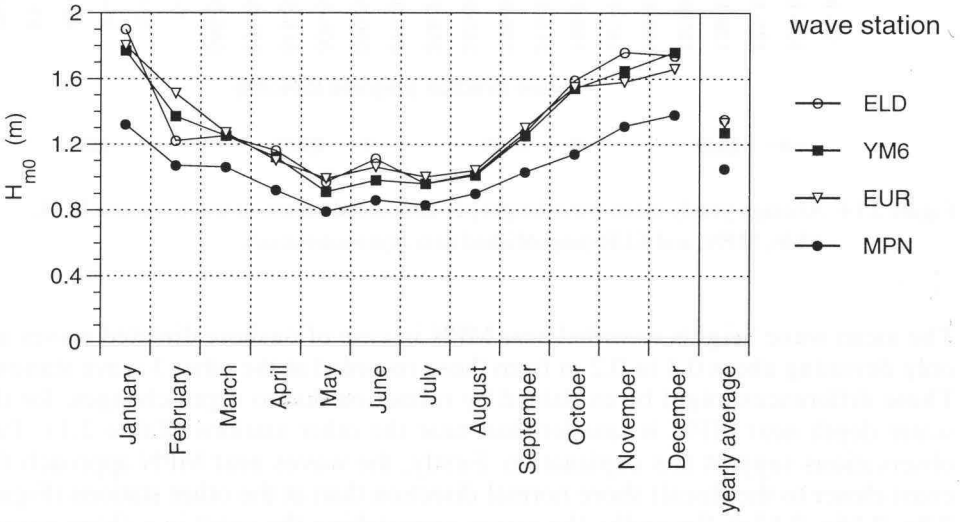

Figure 2.13: Average montly mean wave height and average yearly mean wave height at wave stations ELD, YM6, MPN, and EUR (unpublished data *Rijkswaterstaat*)

The smaller wave heights near MPN in case of offshore directed wave propagation can be explained by the shorter fetch experienced by waves passing MPN, due to the proximity of the land. It is remarkable though that this effect is negligible for station ELD. A possible explanation, which is just hypothetical, is that offshore wind velocities are larger near ELD because the Wadden Sea has a smaller roughness than the land surface near MPN.

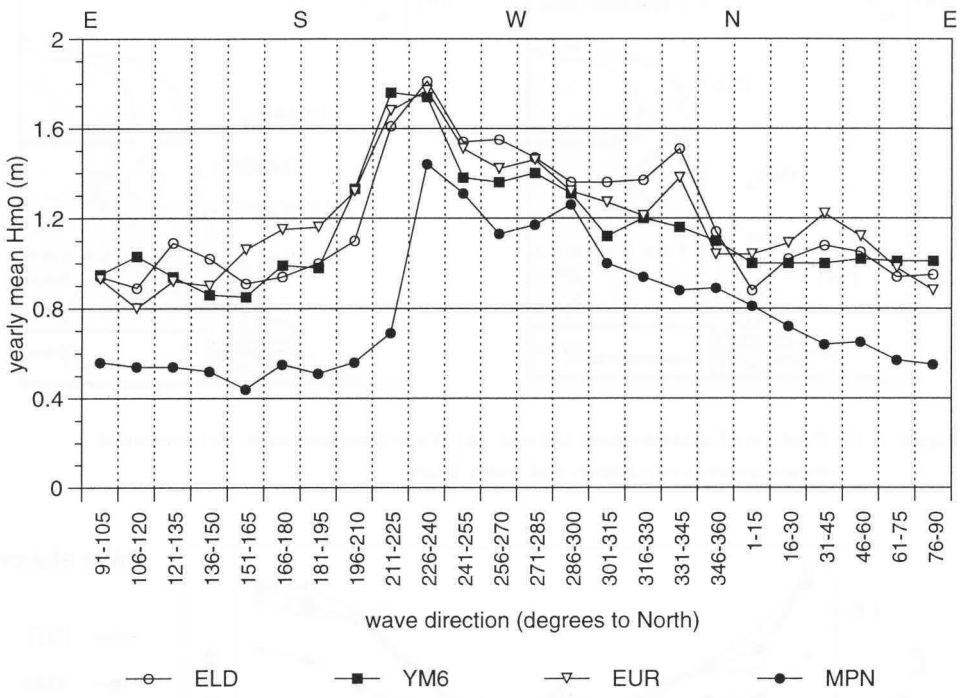

Figure 2.14: Average yearly mean wave height per directional sector, at wave stations ELD, YM6, MPN, and EUR (unpublished data *Rijkswaterstaat*).

The mean wave heights recorded near MPN in case of onshore directed waves are only deviating about 0.1 to 0.2 m from those recorded at the other 3 wave stations. These differences might be explained by refraction due to depth changes, for the water depth near MPN is smaller than near the other stations (Table 2.1). Two observations support this explanation. Firstly, the waves near MPN approach the coast closer to the (local) shore normal direction than at the other stations (Figure 2.9a, 2.16a, 2.17a). Secondly, the waves approaching the coast in a shore normal direction, which is about 300° near MPN, hardly deviate in height from those measured at the other stations (Figure 2.14). The wave heights of obliquely incident waves in the sectors 240°-255° and 0°-15° recorded at MPN are also similar to the wave heights recorded at the other stations in those particular sectors. This similarity may be explained by the fact that these sectors of MPN include the refracted high waves from the sectors 225°-240° respectively 15°-30° at deeper water. Model calculations of wave height decrease near MPN due to refraction compare well to the observed decrease in wave heights (Appendix 1).

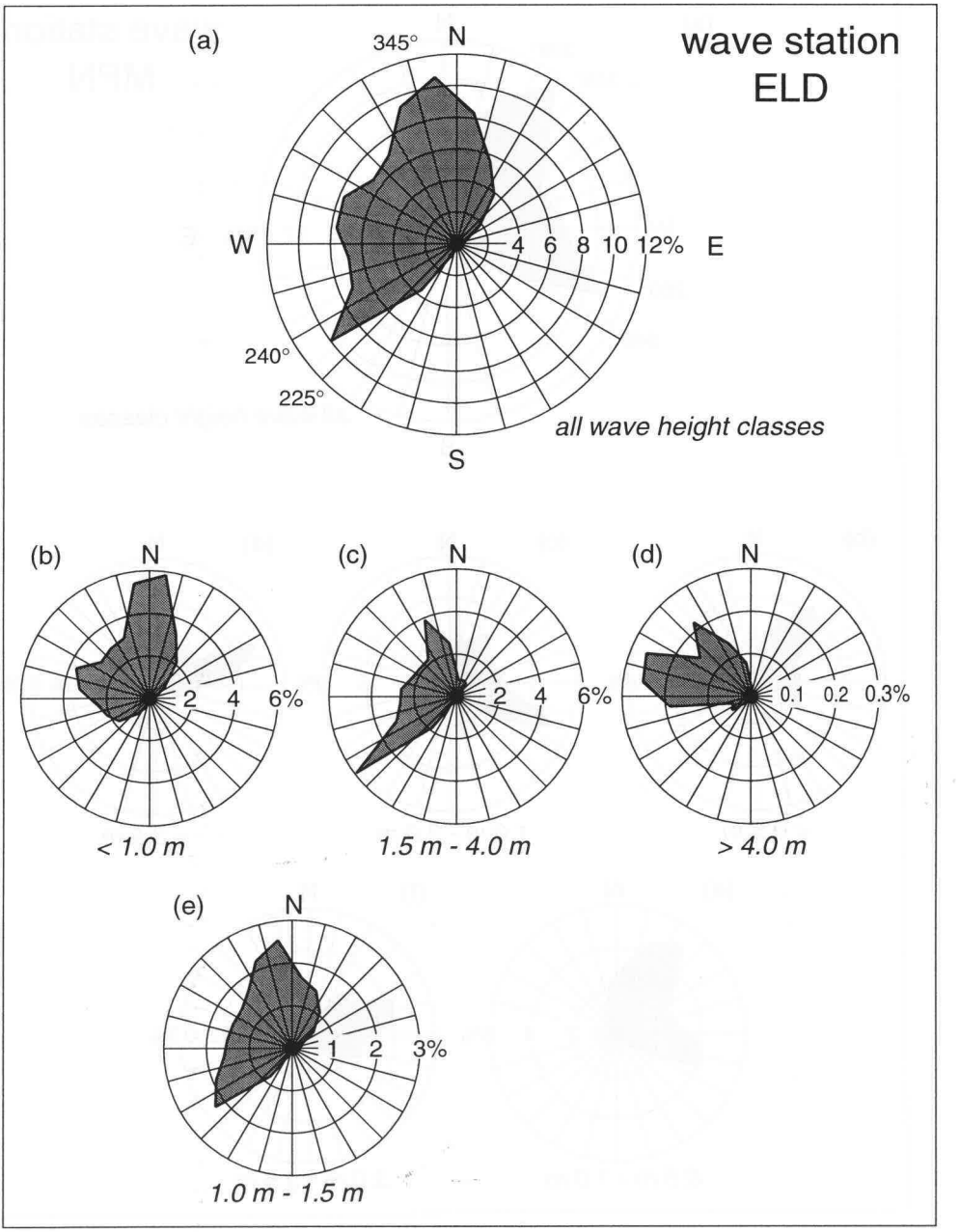

Figure 2.15: Wave climate at station ELD (unpublished data *Rijkswaterstaat*).

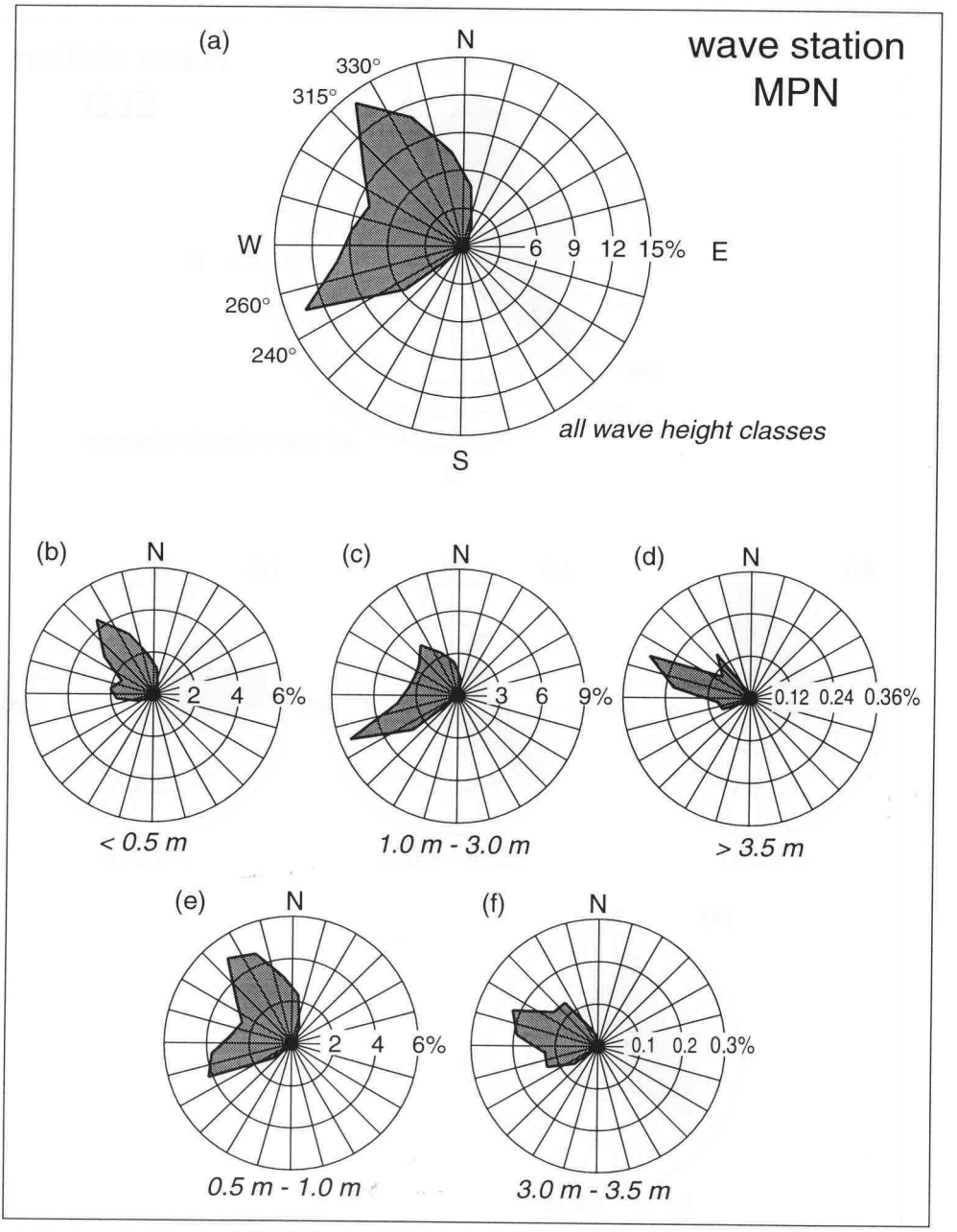

Figure 2.16: Wave climate at station MPN (unpublished data *Rijkswaterstaat*).

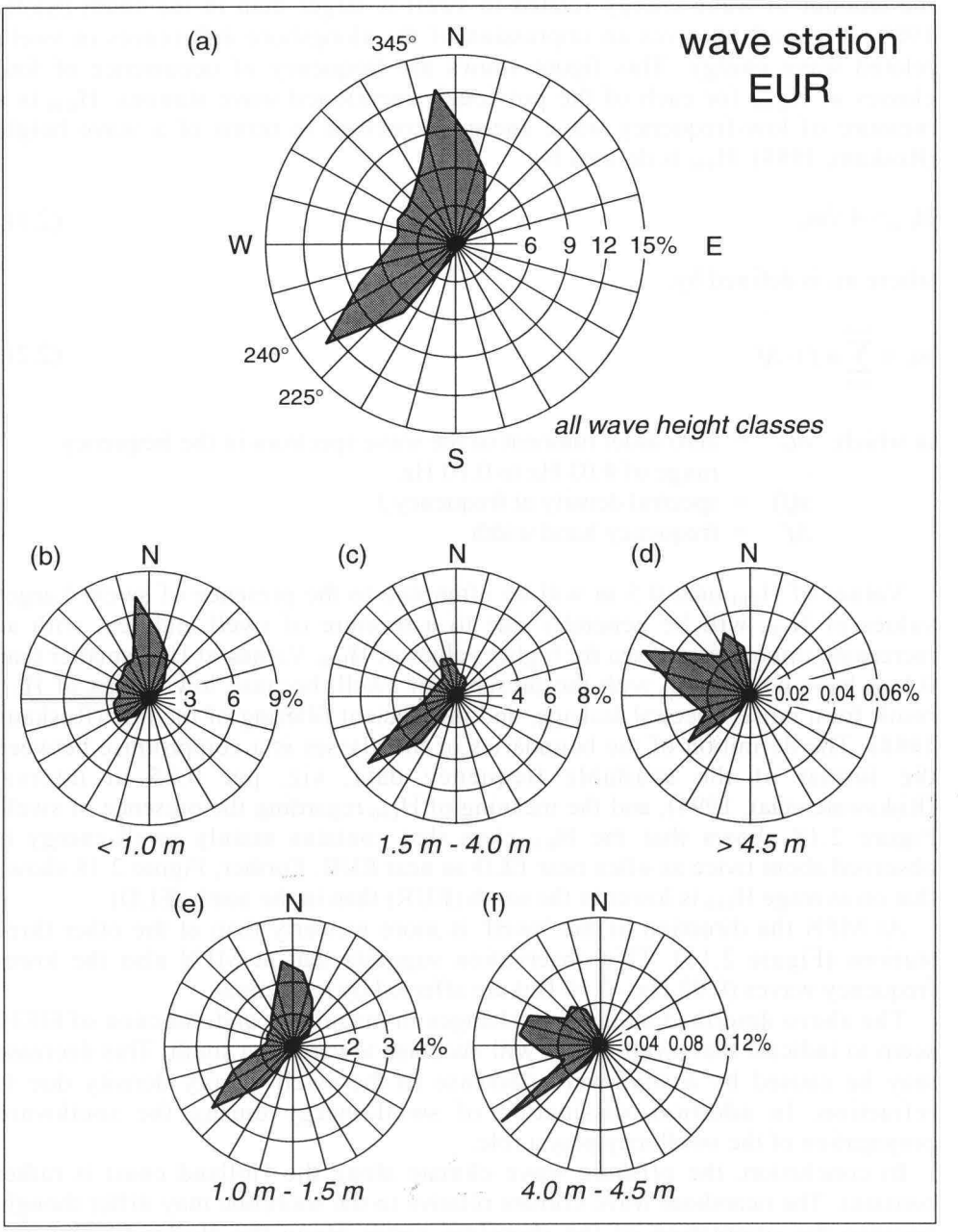

Figure 2.17: Wave climate at station EUR (unpublished data *Rijkswaterstaat*).

The knowledge on alongshore differences in swell is rather limited. In the north the amount of wave energy related to swell is larger than in the south (Stolk, 1989). Figure 2.18 gives an impression of the alongshore differences in swell-related wave energy. This figure shows the frequency of occurrence of four classes of H_{E10}, for each of the previously mentioned wave stations. H_{E10} is a measure of low-frequency wave energy expressed in terms of a wave height (Roskam, 1988). H_{E10} is defined by:

$$H_{E10} = 4\sqrt{m_0} \tag{2.1}$$

where m_0 is defined by:

$$m_0 = \sum_{0.03}^{0.10} s(f) \cdot \Delta f \tag{2.2}$$

in which: m_0 = zero order moment of the wave spectrum in the frequency range of 0.03 Hz to 0.10 Hz.
$s(f)$ = spectral density at frequency f
Δf = frequency band width

Values of H_{E10} near 0.5 m will be often due to the presence of swell. Larger values of H_{E10} will be generally due to a mixture of swell and sea, with an increasing importance of sea for higher values of H_{E10}. Values of H_{E10} smaller than 0.1 m have no relation with the presence of swell, because low values of H_{E10} result from noise, spectral leakage, and insufficient filtering of the tide (Roskam, 1988). The definition of the boundaries of the classes is a compromise between the format of the available frequency data, viz. per 0.25 m interval (Rijkswaterstaat, 1994), and the meaning of H_{E10} regarding the presence of swell. Figure 2.18 shows that the H_{E10}-class that contains mainly swell-energy is observed about twice as often near ELD as near EUR. Further, Figure 2.18 shows that on average H_{E10} is lower in the south (EUR) than in the north (ELD).

At MPN the direction of the 'swell' is more westerly than at the other three stations (Figure 2.11). This observation suggests that at MPN also the lower frequency waves (0.03 Hz - 0.10 Hz) are affected by refraction.

The above described alongshore changes in magnitude and direction of HE10 seem to indicate that swell height will decrease towards the south. This decrease may be caused by a southward decrease in the swell energy density due to refraction. In addition, dissipation of swell-energy during the southward propagation of the swell may play a role.

In conclusion, the offshore wave climate along the Holland coast is rather constant. The nearshore wave climate relative to the shoreline may differ though, because the orientation of the shoreline varies along the Holland coast and because alongshore differences in the morphology of the shoreface exist.

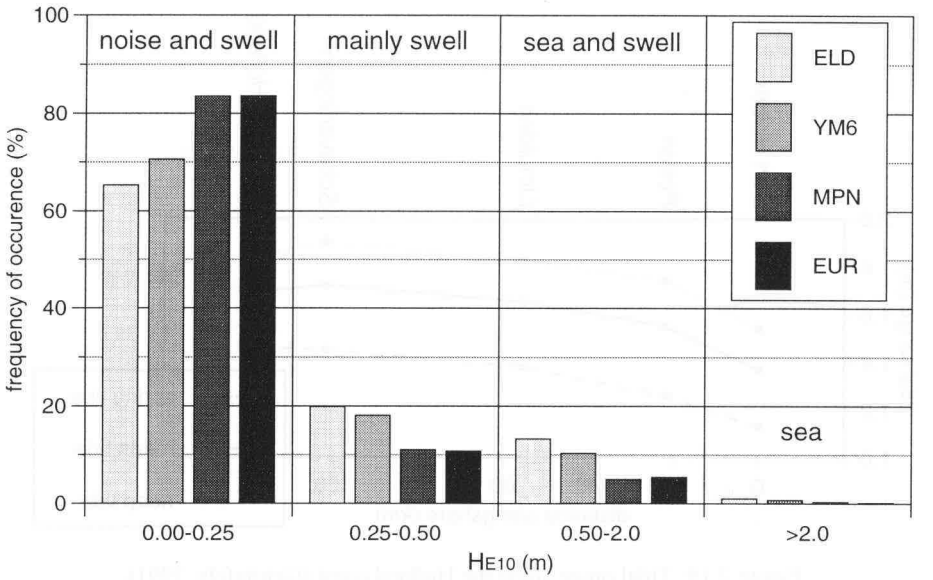

Figure 2.18: Frequency distribution of H_{E10} (see text) at wave stations ELD, YM6, MPN, and ELD (unpublished data *Rijkswaterstaat*)

Tides

The Holland coast is a micro-tidal coast. The mean tidal range is about 1.6 m and peak tidal current velocities generally do not exceed 1 m/s. Some alongshore variation exists in the tidal ranges. Near Hoek van Holland and Scheveningen the mean tidal range is about 1.7 m. This decreases to about 1.6 m near IJmuiden, 1.45 m near Petten and 1.4 m near Den Helder (Getijtafels, 1991). The tide station of Den Helder is located in the tidal inlet and is consequently not necessarily representative for tidal levels along the nearby part of the coast that faces the open sea. Figure 2.19 illustrates the alongshore change in mean tidal range as well as in spring and neap tidal range (Getijtafels, 1991).

The tidal curves along the Holland coast are asymmetric. The character of the asymmetry varies alongshore. This is illustrated in Figure 2.20, which shows the shapes of tidal curves at the 5 coastal tide stations during a mean tide situation. Additionally, the tidal curves of some nearby offshore stations are shown. The locations of the tide stations are shown in Figure 2.21.

The phase difference between the horizontal tide (the tidal current) and the vertical tide (the water level elevation) is not constant alongshore (Figure 2.22 and Figure 2.12b). At the southern boundary of the Holland coast the horizontal tide and vertical tide are almost in phase. At the northern boundary, however, the horizontal tide and vertical tide are about 50 degrees out of phase. This means that the water level signal lags the velocity signal on average by about 1¼ hour.

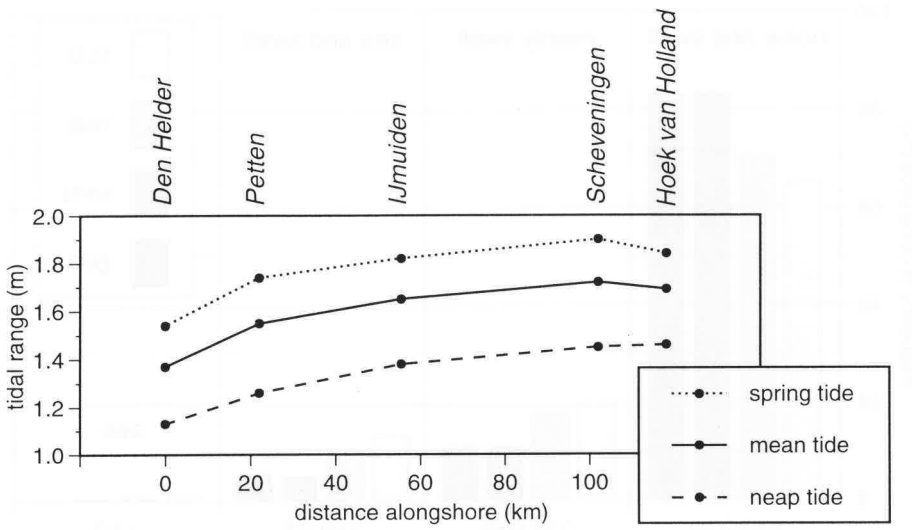

Figure 2.19: Tidal range along the Holland coast (Getijtafels, 1991)

These conclusions are based on the differences in phase of the M_2-components of the vertical tide and the horizontal tide at stations Maas and Haaks (Figure 2.22a and 2.22d) (Van den Berg, 1987). The M_2-components are derived from the tidal signal (currents or water levels) by harmonic analysis and they characterise the semi-diurnal variation in surface elevation and current velocity due to the tide.

Surveys of surface elevation and current velocities near Zandvoort (Van de Meene, 1994) and Egmond (Houwman and Hoekstra, 1994) reveal an approximate phase difference of about 30 degrees between the horizontal and vertical tide (Figures 2.22b and 2.22c, and Figure 2.12b). Therefore, the phase shift between vertical tide and horizontal tide seems to change rather gradually along the Holland coast.

River outflow

At the southern boundary of the study area, the River Rijn (Rhine) flows out into the North Sea. The average discharge of the River Rijn is about 2200 m^3/s (Visser, 1993). A part of this discharge enters the North Sea at Hoek van Holland, flowing through Rotterdam Harbour. The other part flows out into the North Sea through the estuaries located south of the Holland coast. The discharge through Rotterdam Harbour is kept constant at 1500 m^3/s as long as possible by manipulating sluices (Visser, 1993).

The outflow of the River Rijn causes a density driven circulation in front of the Holland coast. This circulation causes an onshore directed near-bottom current of a few centimetres per second (Visser et al., 1991). The alongshore extent of this cross-shore circulation depends on the discharge of the River Rijn and the wind

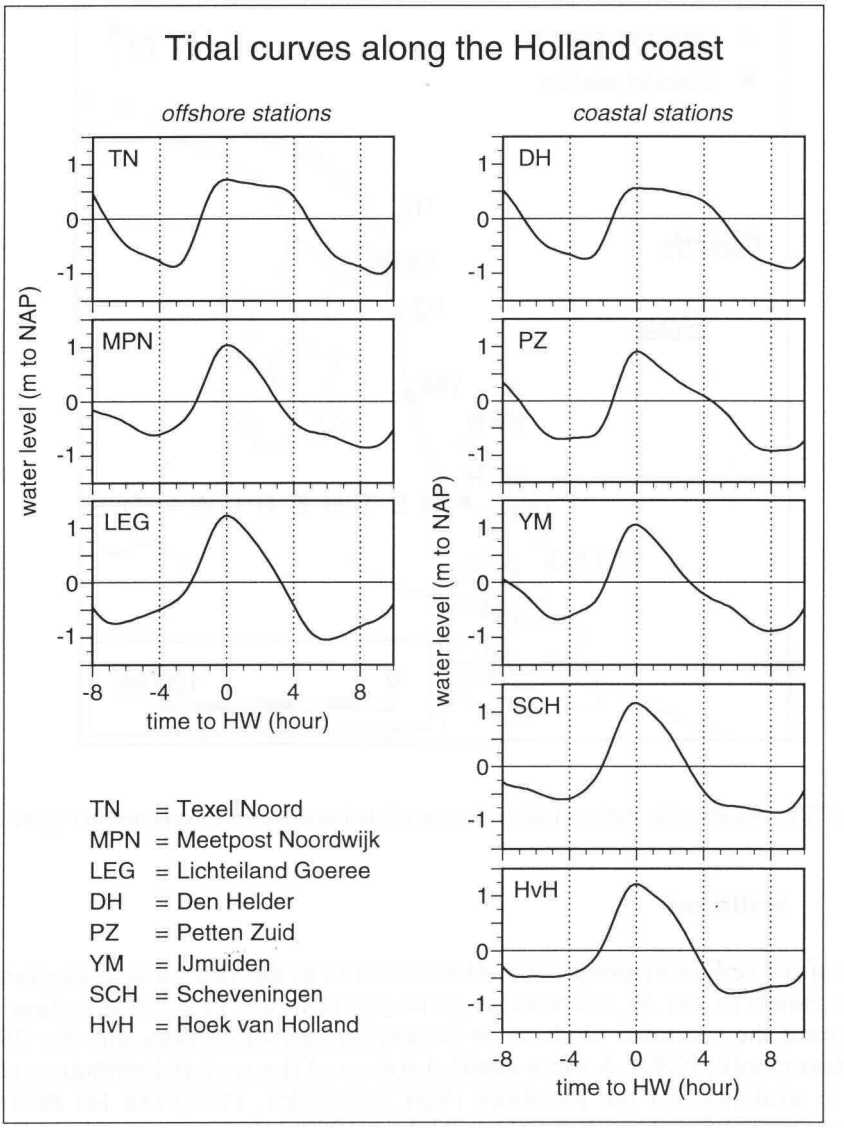

Figure 2.20: Tidal curves along the Holland coast (*Rijkswaterstaat*)

conditions, but may reach as far north as km 20 (Van Alphen et al., 1988). Under average conditions the alongshore extent of the cross-shore circulation reaches as far north as about km 85 (Van Alphen et al., 1988).

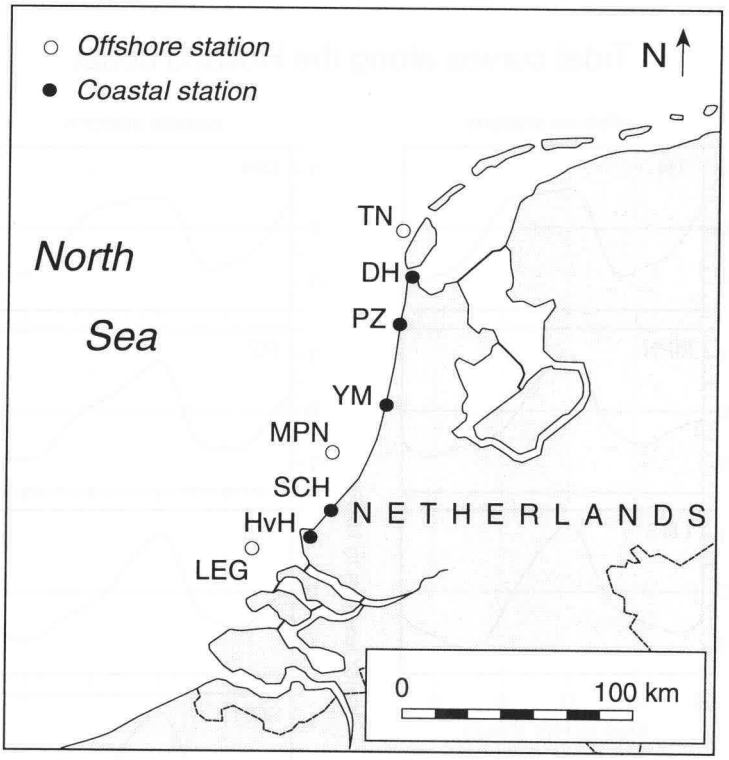

Figure 2.21: Position tide stations (abbreviations of station names are explained in Figure 2.20)

2.2.4 Sediment

Most of the sediment along the Holland coast is in the fine sand to medium sand range. South of km 30, the median grain size is in the 125-250 μm class, while northward the sediment tends to be somewhat coarser, getting into the 250-500 μm class (Stolk, 1989). A more detailed survey of the spatial distribution of grain sizes is available for the foreshore (Van Bemmelen, 1988) and for the inshore between km 37.5 and km 109.5 (Van Alphen, 1987).

At mean high water level the median grain size varies alongshore between 195 μm and 380 μm, with an average of 262 μm. At mean low water level the median grain size varies alongshore between 185 μm and 420 μm, with an average of 286 μm (Van Bemmelen, 1988; Short, 1991). Most of the alongshore grain size variation occurs over distances of 10 km or less (Figure 2.23). Distinct large-scale trends across both sediment populations can not be observed. Possibly present subtle trends will be small in comparison to the variation occurring within 10 km.

The inshore sediments were sampled in two campaigns. South of km 76.5 the sediments were sampled in October 1986, while the sediments north of this

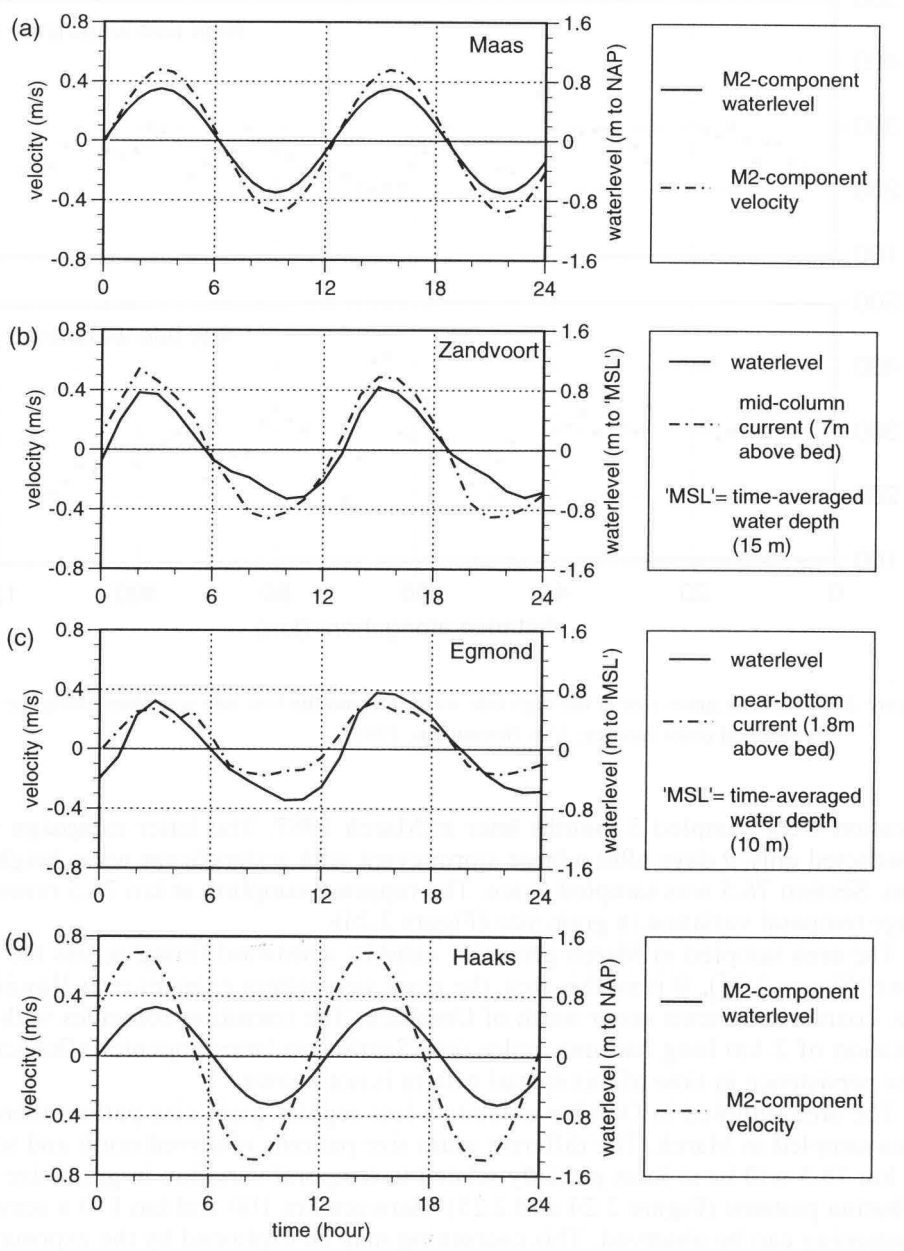

Figure 2.22: Horizontal and vertical tide along the Holland coast. (a) Maas (after: van den Berg, 1987); (b) Zandvoort (courtesy Van de Meene); (c) Egmond (after: Houwman and Hoekstra, 1994); (d) Haaks (after: Van den Berg, 1987).

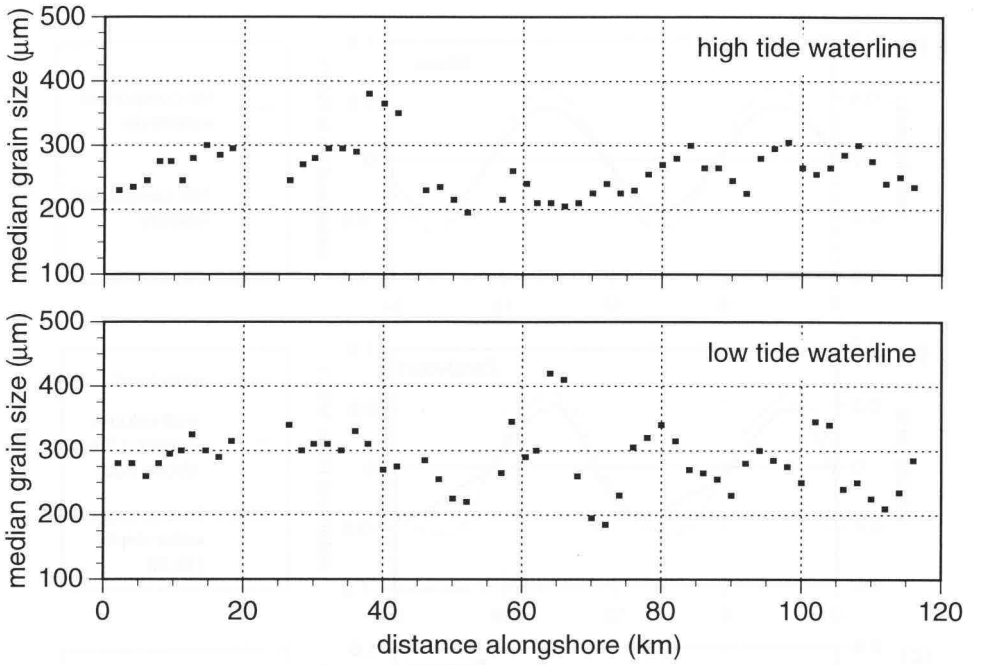

Figure 2.23: Median grain size at the high tide waterline and the low tide waterline along the Holland coast (source: Van Bemmelen, 1988).

location were sampled 5 months later in March 1987. The latter campaign was conducted only 9 days after a large storm event with a significant wave height of 5 m. Section 76.5 was sampled twice. The repeated sampling at km 76.5 reveals a large temporal variation in grain size (Figure 2.24).

The area sampled in March generally exhibits a seaward fining across the surf zone (Figure 2.25). Within this area, the grain size pattern changes near IJmuiden, viz. coarser sediments occur north of IJmuiden. The transition coincides with the location of 2 km long harbour moles (see Section on 'antropogenic influences'). The persistence in time of this spatial pattern is not known.

The area sampled in October exhibits a less regular grain size pattern than the area sampled in March. The different grain size patterns observed north and south of km 76.5 will be at least partially related to temporal variation in grain size distribution patterns (Figure 2.24 and 2.25). Between km 100 and km 110 a seaward coarsening can be observed. This coarsening may be explained by the exposure of older deposits, although extensive beach nourishment southward of this area during the late summer of 1986 may also have influenced the grain size composition (Van Alphen, 1987).

In conclusion, the surface sediments in the nearshore zone along the Holland coast do not seem to exhibit a distinct alongshore trend in grain size. 'Small-scale'

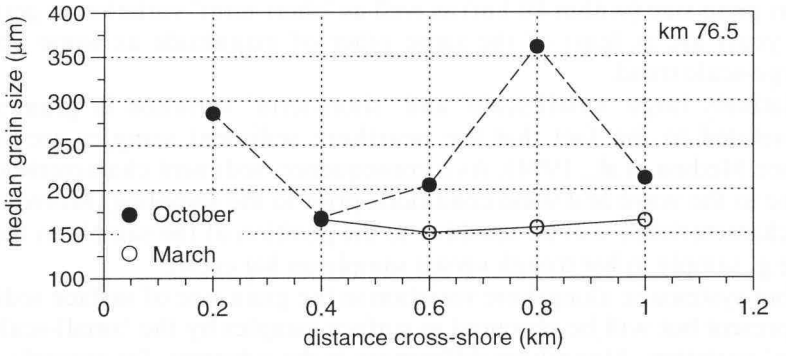

Figure 2.24: Temporal variation of median grain size in the cross-shore direction (source: Van Alphen, 1987)

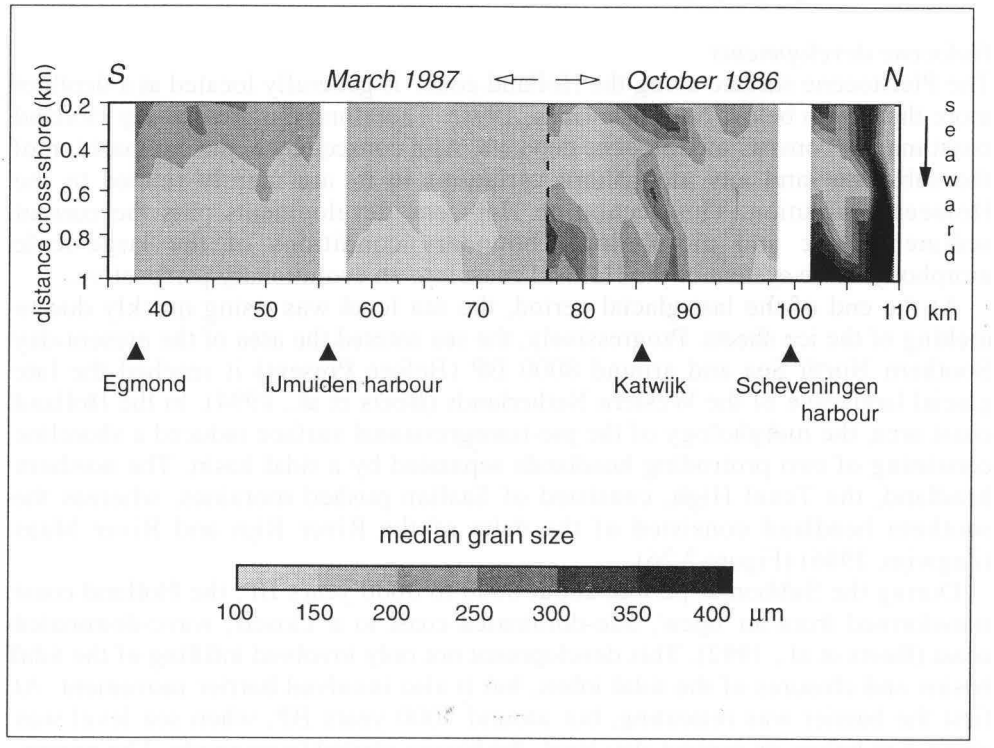

Figure 2.25: Spatial variation of median grain size in the nearshore zone of the Holland coast (after: Van Alphen, 1987)

variation in grain size (within 10 km) as well as 'short-term' variation in grain size (within a year) are at least of the same other of magnitude as some possibly present large-scale trend.

The relatively large 'small-scale' and 'short-term' variation in grain size is probably related to the fact that the nearshore sediment samples are surface samples (see Medina et al., 1994). As a consequence, sediment characteristics will be sensitive to the wave and wind conditions prior to the sampling. Moreover, the sediment characteristics will be sensitive to the position of the sample in the morphology (e.g. sample in bar trough versus sample on bar crest).

Subtle but systematic alongshore variation in the grain size of surface sediments might be present but will be obscured in surface samples by the 'small-scale' and 'short-term' variation. Alongshore differences in the substrate, for example, might induce a systematic alongshore variation in grain size. The likelihood of this situation along the Holland coast will be discussed in the following section on the paleogeographic setting of the study area.

2.2.5 Paleogeography

Holocene developments

The Pleistocene surface along the Holland coast is generally located at a depth of more than 15 m below NAP (De Gans, 1991). Therefore, the present-day Holland coast mainly consists of Holocene deposits. As a consequence, the composition of the substrate -and any alongshore variations in it- are mainly related to the Holocene evolution. This section on Holocene developments puts the current sedimentologic and morphologic boundary conditions of the large-scale morphodynamic system of the Holland coast into an evolutionary perspective.

At the end of the last glacial period, the sea level was rising quickly due to melting of the ice sheets. Progressively, the sea entered the area of the present-day Southern North Sea and around 8000 BP (Before Present) it reached the late glacial landscape of the Western Netherlands (Beets et al., 1994). In the Holland coast area, the morphology of the pre-transgressional surface induced a shoreline consisting of two protruding headlands separated by a tidal basin. The northern headland, the Texel High, consisted of Saalian pushed moraines, whereas the southern headland consisted of the delta of the River Rijn and River Maas (Zagwijn, 1986) (Figure 2.26).

During the Subboreal period, about 6000 to 3000 years BP, the Holland coast transformed from an 'open', tide-dominated coast to a 'closed', wave-dominated coast (Beets et al., 1992). This development not only involved infilling of the tidal basins and closures of the tidal inlets, but it also involved barrier movement. At first the barrier was retreating, but around 5000 years BP, when sea level was about 5 m below its present-day level, the barrier started to prograde. The progradation of the barrier resulted in an alternation of ridges and beach plains. On the ridges relatively low dunes were formed with a maximum height of 10 m: the Older Dunes. Dunes were lacking on the moist beach plains in between the ridges.

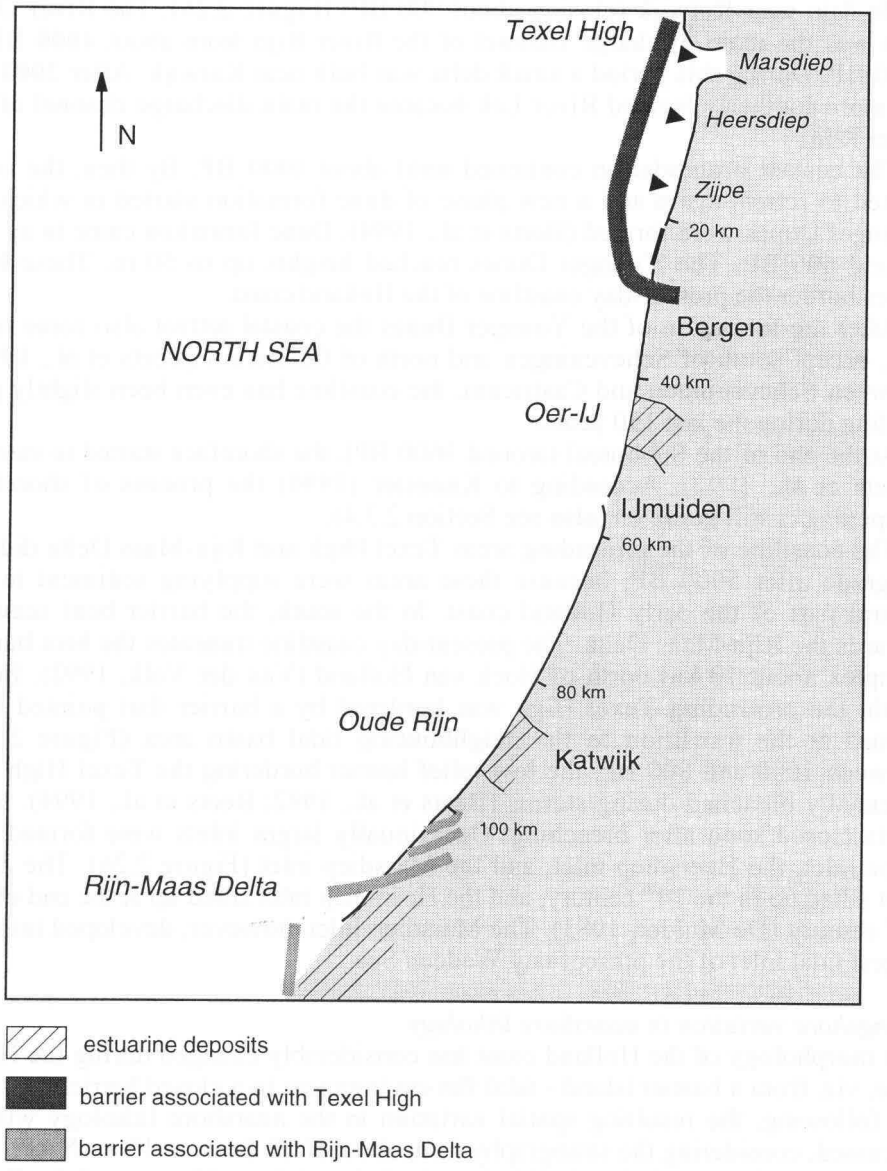

Later on, the beach plains were filled in with peat. In Roman times, the dunes were stabilised by vegetation (Van der Valk, 1992).

Around 3300 BP, all tidal channels were silted up and the tidal inlets were closed (Beets et al., 1994). Only two inlets connected to branches of the River

Rijn were still open: the Oer-IJ near Castricum (closing about 2000 BP) and the Oude Rijn near Katwijk (closing about 900 BP) (Figure 2.26). The River Oude Rijn was the main discharge channel of the River Rijn from about 4000 BP to 2000 BP. During this period a small delta was built near Katwijk. After 2000 BP the more southerly located River Lek became the main discharge channel of the River Rijn.

The coastal progradation continued until about 1000 BP. By then, the coast started to retreat again and a new phase of dune formation started in which the Younger Dunes were formed (Beets et al., 1994). Dune formation came to an end around 600 BP. The Younger Dunes reached heights up to 50 m. These high dunes border the present-day coastline of the Holland coast.

After the formation of the Younger Dunes the coastal retreat also came to an end, except south of Scheveningen and north of Castricum (Beets et al., 1994). Between Scheveningen and Castricum, the coastline has even been slightly prograding during the last 150 years.

At the end of the Subboreal (around 3600 BP), the shoreface started to steepen (Beets et al., 1992). According to Knoester (1990) the process of shoreface steepening is still going on (also see Section 2.3.4).

The coastline of the protruding areas Texel High and Rijn-Maas Delta did not prograde after 5000 BP, because these areas were supplying sediment to the central part of the early Holland coast. In the south, the barrier bent seaward towards the Rijn-Maas Delta. The present-day coastline truncates the bent barrier complex about 10 km north of Hoek van Holland (Van der Valk, 1992). In the north, the protruding Texel High was bordered by a barrier that pointed land inward at the transition to the neighbouring tidal basin area (Figure 2.26). Between 1000 and 800 BP, the low-relief barrier bordering the Texel High was repeatedly breached during storms (Beets et al., 1992; Beets et al., 1994). Most inlets closed soon after breaching. Occasionally larger inlets were formed: the Zijpe inlet, the Heersdiep inlet, and the Marsdiep inlet (Figure 2.26). The Zijpe inlet silted up in the 14th century, and the Heersdiep inlet silted up at the end of the 15th century (De Mulder, 1983). The Marsdiep inlet, however, developed into the largest tidal inlet of the present-day Wadden Sea.

Alongshore variation in nearshore lithology

The morphology of the Holland coast has considerably changed during the Holocene, viz. from a barrier island - tidal flat environment to a closed barrier coast. In the following, the resulting spatial variation in the nearshore lithology will be discussed, considering the stratigraphy from about NAP down to 10 m -NAP.

The alongshore variation in lithology is deduced from 82 cores of the Dutch Geological Survey (Appendix 2). The cores were sampled along the coast between km 1 and km 118. All cores were sampled on the beach or in the dunes, with a maximum distance to the beach of 1 km. Most of the cores were sampled within 0.5 km distance of the beach. Various devices were used for the coring, which resulted in varying accuracy of grain size estimates. In addition, the objectives for coring varied (e.g. scientific background, engineering background) and the

accuracy of the core description by various observers seemed to be variable. The presence of this 'observational noise' should be kept in mind when judging the alongshore variation in lithology.

Starting in the north, the first marked change in lithology occurs near km 29 (Appendix 2). Deposits north of km 29 are characterised by the presence of clay and peat layers. South of km 29, peat layers are absent and clay layers -if present- are generally thinner and located at larger depths. This change in lithology occurs at the location of the land inward bending barrier near Bergen (Figure 2.26). In the area protected by the barrier connected to the Texel High, clayey and peaty deposits could be formed. This type of deposits will now be exposed on the shoreface, because of the ongoing erosion of the Texel High area since Subboreal times. South of the hooked barrier sandy deposits are dominating, because this area formerly consisted of tidal inlets that were later closed by sandy sediments supplied by the nearshore area.

The former Oer-IJ inlet intersects with the present-day coastline between about km 42 and km 48 (Westerhof et al., 1987) (Figure 2.26). The deposits filling this inlet between NAP and 10 m -NAP do not show a distinct lithology that clearly differs from the neighbouring deposits.

The Oude Rijn deposits near Katwijk are located between about km 84 and km 93 (Beets, pers. comm.) (Figure 2.26). Except for core 59, these deposits do not reveal a lithology that is clearly different from the neighbouring cores. Core 59 contains more clay than the neighbouring cores, which may be related to the more land inward location of this core (viz. about 800 m land inward).

Van Alphen (1987) ascribes the coarseness of the surface sediment at 1000 m offshore between km 100 and 110 to the exposure of older deposits (see Section 2.2.4). Near km 105, very coarse sand (class 420-200 μm) is present at about 11 m and 14 m depth. At 1000 m offshore the sea bed is located at about 10 m -NAP. Therefore, the upper layer is probably the source of coarse sediment referred to by Van Alphen (1987).

South of about km 111 the number and thickness of clayey layers increase. This area is the alluvial plain of the Rijn-Maas Delta, which started to erode in the Subboreal period. From 3000 BP onward this area was repeatedly invaded by the sea and tidal basins were formed behind the prograding barrier complex. These areas were lateron filled by tidal flat deposits (Beets et al., 1994).

In conclusion, considering the observational noise, only two boundaries in substrate lithology can be identified, viz. near km 29 and near km 111. Subtle alongshore differences in the mean grain size, for example near former inlets, can not be determined from this data source.

2.2.6 Antropogenic influences

Human intervention in the development of the Holland coast nearly dates back to the middle ages. As early as the 16th century a seawall was built near Petten (Figure 2.27). This seawall was the earliest predecessor of the present-day

'Hondsbossche and Pettemer Seawall'. The seawall had to be relocated to a more landward position several times because of ongoing erosion north and south of the seawall. The last relocation was in 1823 (Table 2.2) (Stolk, 1989). Erosion still goes on, and nowadays the seawall is again a structure that protrudes into the sea. Another seawall was constructed near Scheveningen in 1895 (Table 2.2 and Figure 2.27). In the next years it was extended to a total length of 2.5 km (Eversdijk, 1989).

Groins were built along the eroding southern and northern parts of the coast from the late 18th century up to the early 20th century (Table 2.2 and Figure 2.27). Only the groins built in front of the seawall near Petten were connected to a hard structure. (Verhagen and Van Rossum, 1989). In the second half of the 19th century, harbour moles were constructed near Hoek van Holland (km 119), Scheveningen (km 102) and IJmuiden (km 55.5) (Table 2.2 and Figure 2.27). These harbour moles were extended seaward in the late sixties and early seventies of the present century (Verhagen, 1989a). Near Katwijk (km 86), a discharging sluice was constructed in 1807, near the mouth of the River Oude Rijn (Van Ommering, 1988). The discharging capacity of this sluice was increased in 1984.

Table 2.2: Engineering works along the Holland coast

	Activity	Period	Spatial scale
Seawalls			
Hondsbossche and Pettemer Seawall (km 20 - km 26)	construction most recent relocation	about 1550 1823	? 6 km (alongshore)
Scheveningen (km 102)	construction extension	1895/1896 1896, 1902, and 1907	140 m (alongshore) total length: 2.5 km (alongshore)
Groins			
km 2 - km 31	construction	1838-1935	
km 98 - km 118	construction	1776-1896	
Harbour moles			
IJmuiden (km 55/56)	construction extension	1865 - 1879 1962 - 1967	1.5 km (cross-shore) southern mole +1.5 km northern mole +1 km
Scheveningen (km 102)	construction extension	1900-1908 1968-1970	groin length + 0.5 km
Hoek van Holland (km 118)	construction extension	1864-1874 1968-1972	2 km (cross-shore) northern mole: + 3 km
Discharging sluice			
Katwijk (km 86)	construction increase discharge capacity	1807 1984	

Finally, in the last few decades beach nourishments have been applied on several locations (Table 2.3 and Figure 2.27).The data on nourishments along the Holland coast in Table 2.3 are derived from Stolk (1989) for the period up to 1988, and from Van Rijn (1995) over the period 1989-1990.

Human influence in the dune landscape started to increase in the middle of the 19th century. Nowadays, only 7 km of the fore-dune along the Holland coast is in a natural condition, viz. km 3-4, km 8-11, km 18-19, and km 53-55 (Arens, 1994). The remaining stretch of fore dunes is subjected to varying degrees of human interference. The dune management varies from adjusting slopes or even complete remodelling the fore dune to planting marram grass and building sand fences.

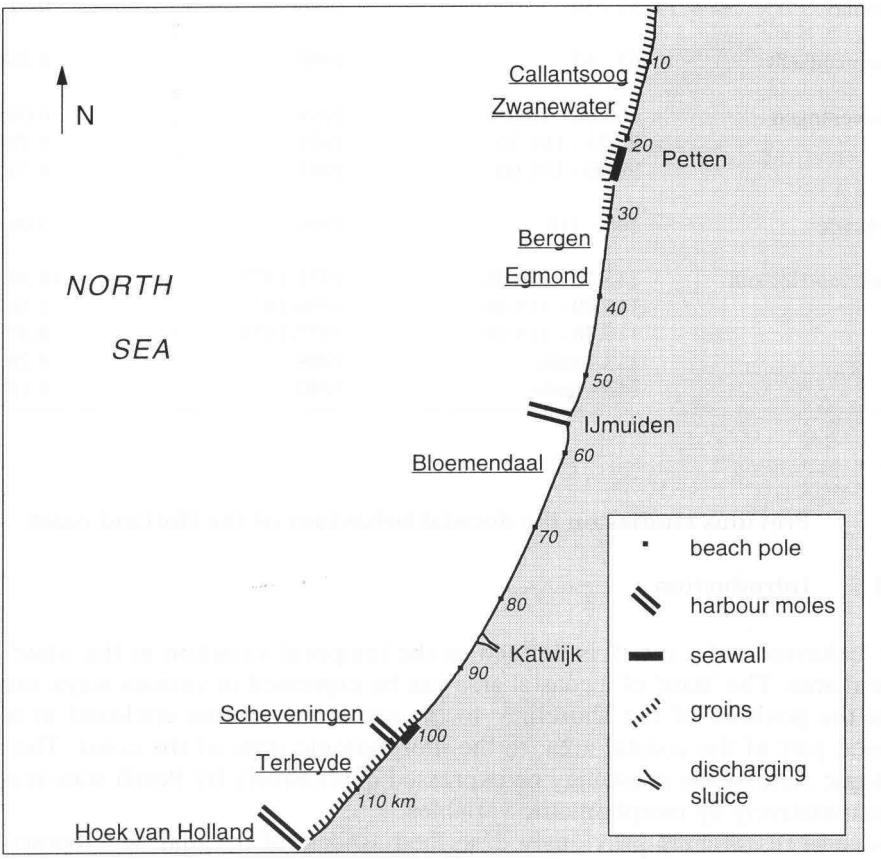

Figure 2.27: Location of man-made structures and beach nourishments along the Holland coast; underlined place names indicate nourishment sites.

Table 2.3: Beach nourishments along the Holland coast up to 1990

	RSP-location	Period	Nourishment volume (10^6 m^3)
Callantsoog	11.50 - 13.60	1976-1977	0.35
	11.50 - 13.60	1979-1980	0.47
	10.00 - 14.00	1986	1.30
Zwanewater	13.00 - 19.00	1987	1.85
Bergen	32 - 34	1990	0.45
Egmond	37 - 39	1990	0.32
Bloemendaal	62 - 63	1990	0.26
Scheveningen	100.00 - 101.50	1969	0.045
	99.75 - 101.50	1975	0.79
	99.00 - 101.00	1985	0.33
Terheyde	108 - 116	1986	3.00
Hoek van Holland	115.70 - 119.00	1971-1972	18.94
	115.70 - 119.00	1976-1977	1.50
	115.70 - 119.00	1977-1978	0.87
	118 - mole	1988	0.20
	118 - mole	1990	0.18

2.3 Previous studies on the decadal behaviour of the Holland coast

2.3.1 Introduction

The 'behaviour of a coast' is defined as the temporal variation in the 'state' of a coastal area. The 'state' of a coastal area can be expressed in various ways, ranging from the position of the shoreline, to the sediment volume enclosed in a predefined part of the coastal area, to the morphologic state of the coast. The morphologic state of the coast may be expressed qualitatively by beach state models, or quantitatively by morphometric variables.

Several researchers previously described aspects of decadal developments of the Holland coast. The earliest descriptions considered the coastal behaviour in terms of shoreline position (e.g. Wentholt, 1912; Van Straaten, 1961; Edelman, 1961). Later, when data from two decades of coastal profile monitoring became available, several sediment budget studies were conducted (Kohsiek, 1988; De Ruig, 1989; Van Vessem and Stolk, 1990; De Ruig and Louisse, 1991). Recently, new budget calculations were made based on 3 decades of profile data

(Bouwmeester et al., in prep.; Groenendijk, in prep.; Van Rijn, 1995). Also based on the JARKUS data base, Knoester (1990) described the decadal coastal behaviour of the Holland coast in terms of morphologic changes.

In the following, the aspects of previous studies on decadal developments of the Holland coast that are relevant for the present study will be described. Relevant aspects are: the nature of decadal developments, the alongshore variation in the developments and the locations where transitions take place, and the mechanisms that are suggested to explain the observed behaviour.

2.3.2 Shoreline studies

The studies on decadal behaviour of the Holland coast shoreline are based on a data set of annual recordings of the position of 'the' shoreline every kilometre alongshore. The shoreline is represented by three contours viz. the high tide waterline, the low tide waterline and the dune foot. The annual monitoring of the three contours started in 1843 along the northern part of the Holland coast (km 0-km 70). Since 1857 the full stretch is monitored (Wentholt, 1912).

All studies on decadal shoreline behaviour showed that north of Egmond and south of Scheveningen the coastline is retreating. In between, the shoreline is slightly prograding (e.g. Wentholt, 1912; Van Straaten, 1961; Edelman, 1961; De Valk and Zitman, 1987; Kohsiek, 1988). The observation of this pattern is independent of the varying length of the time series used by the various researchers. For example, Wentholt only used 40 year of shoreline data, whereas De Valk and Zitman used time series of 128 year. The 'Egmond' boundary was located by the various researchers between km 36 (De Valk and Zitman, 1987) and km 43 (Van Straaten, 1961). The 'Scheveningen' boundary was located between km 94 (Van Straaten, 1961; De Valk and Zitman, 1987) and km 104 (Edelman, 1961).

The average rates of shoreline movement over the last 140 years were quantified by Van Vessem (in: Stolk, 1989). South of Scheveningen an average retreat occurred of about 0.35 m/yr, excluding the area just north of the harbour moles of Hoek van Holland that prograded due to human interference (see Section 2.2.6). From Scheveningen to Egmond an average progradation of 0.25 m/yr occurred, with a much larger progradation near the Harbour moles of IJmuiden. North of Egmond the average shoreline retreat was found to be about 0.9 m/yr.

The physical explanation for this large-scale erosion-progradation pattern is often ascribed to gradients in the longshore transport (Stive, 1989). The concave shape of the Holland coast induces gradients in the wave-driven longshore transport. Further, the Marsdiep tidal inlet at the northern boundary of the Holland coast is believed to produce a gradient in the longshore sediment transport in the northern part of the Holland coast. This gradient should result from the sand importing nature of the Wadden Sea and from the sheltering effect of the ebb-tidal delta for waves coming from the north and north-west. According to Stive and Eysink (1989), the effect of the sand import by the Wadden Sea reaches at least as

far south as Egmond. They conclude this from the calibration procedure of their large-scale coastal model, which required a considerable adaptation of the modelled longshore transport along the above mentioned stretch.

Further, differential rates of tectonic sinking have been put forward to explain the alongshore differences in shoreline migration (Wiersma, 1991). Beets (1994) elucidates the role of the lithology in the sensitivity of the northern and southern ends of the Holland coast to long-term erosion. Beets states that on the long-term, the presence of clay layers in these areas increases the rate of erosion. On the short-term clay layers are erosion resistant, but once eroded they cause an irreversible loss of sediment volume from the local coastal system, because the fine material is easily transported out of the source area. Sand, on the contrary, is more likely to be redeposited within the local coastal system after an erosion event, causing redistribution of sediment rather than an immediate loss of sediment volume.

Superimposed on the above mentioned general trend, temporal fluctuations in shoreline position were observed along large parts of the Holland coast (Van Straaten, 1961; De Valk and Zitman, 1987). From the beginning of the observations till about 1866 the shoreline exhibited a general advance. Then, a period of retreat occurred which slowed down in the period 1878-1886. The retreat was followed by a distinct advance that gradually decreased to very small values around 1910. This development is most clearly observed in the position of the low tide line and is almost absent in the position of the dune foot.

Van Straaten (1961) revealed a correlation between the superimposed shoreline retreat during the period 1866-1886 and a relatively frequent occurrence of south-westerly and westerly winds, accompanied by an increase in precipitation and lower mean annual temperatures. In addition, Van Straaten showed that the shoreline retreat ended earlier in the north (1876-1880) than in the south (1880-1888). The transition occurred near km 70. A physical explanation for these observations was not found, among other things because of a lack of bathymetric data.

Verhagen (1989b) suggests that, superimposed on the above mentioned shoreline behaviour, other systematic shoreline behaviour is present, viz. 'sand waves'. 'Sand waves' are defined by Verhagen as '... longshore wave-like movements of the shoreline, measured in a horizontal plane'. To arrive at the 'sand wave' phenomenon he subtracted linear trends from the shoreline position time series (low tide line) to remove the long-term trends of erosion and accretion respectively. The superimposed long-term shoreline fluctuations described by Van Straaten (1961) were removed under the assumption that everywhere along the coast, the magnitude of the fluctuation was equal to the average change in position along the coast. For each year Verhagen calculated the average change in shoreline position from the detrended time series. The resulting time series of alongshore-averaged shoreline position change was then subtracted from all detrended time series. In the resulting manipulated data set, Verhagen recognised longshore wave-like movements in the shoreline position. However, this mode of shoreline

behaviour is hard to recognise in the contour plot that Verhagen presented to illustrate the existence of this phenomenon along the entire Holland coast. Further, no explanation is available for this phenomenon along the Holand coast.

2.3.3 Sediment budget studies

Sediment budget studies for the Holland coast are based on coastal profile data contained in the JARKUS data base. These profiles usually start in the dune area and end about 800 m seaward of the RSP reference line. Since 1963 the profiles are annually surveyed at fixed locations that are about 250 m apart. More information on the JARKUS data base is given in Section 3.2. Further, every 5 year coastal profiles are surveyed up to about 2500 m from the RSP reference line: the so-called 'extended profile surveys'. The alongshore spacing of these extended profile surveys is 1 km. The 5-yearly surveying of profiles started in 1965.

Several researchers made a study on 'the' sediment budget of the Holland Coast based on the coastal profile data sets (e.g. Kohsiek, 1988; De Ruig, 1989; Van Vessem and Stolk, 1990). They all describe the budget in terms of a linear increase or decrease of sediment volume in a pre-defined control volume. The major difference between the various budget studies is the choice of alongshore and cross-shore boundaries to define the control volumes for which the linear trends are determined. For example, Kohsiek (1988) used fixed distances to the RSP reference line to define the cross-shore boundaries of the control volume, whereas Van Vessem and Stolk (1990) used depth contours. The alongshore width of control volumes varied between 1 km (De Ruig, 1989) and several tens of kilometres (Van Vessem and Stolk, 1990). Recently, Bouwmeester et al. (in prep.), Groenendijk (in prep.) and Van Rijn (1995) made new sediment budget calculations for the Holland coast, using longer time series of profile data. The definition of the control volumes again varied among the studies, with none of the definitions being equal to those used in previous studies.

In the time series of sediment volume, the year-to-year fluctuations are generally an order of magnitude larger than the year-to-year change due to the linear trend (Van Vessem and Stolk, 1990; Bouwmeester et al., in prep.). Therefore, the statistical significance of the linear trends needs some considerations. Bouwmeester et al. (in prep.) illustrated that linear trends determined per profile line over a 30 year period do not often differ statistically significant from zero along the Holland coast. This implies that it is well possible that the calculated trends are not present in the real world, but that they are just a chance result of sampling random fluctuations and additional measurement errors. Generally, increasing the alongshore width of the control volume, by including more profile lines, tends to reduce the year-to-year variation of volumes by averaging out the effect of the small-scale spatial fluctuations. Although this approach was applied in several studies, no one evaluated the effect on the statistical significance of the linear trends.

In the following, the general trends resulting from the various budget studies of the Holland coast are summarised (Figure 2.28). Rates of erosion or accretion, if mentioned, only indicate the order of magnitude of the volume changes. Exact rates of change have little meaning here because of the varying definition of the control volumes in the various studies and because of the questionable reliability of the linear trends due to the large scatter in the data. For the same reasons, the location of alongshore boundaries, if mentioned, is only indicative.

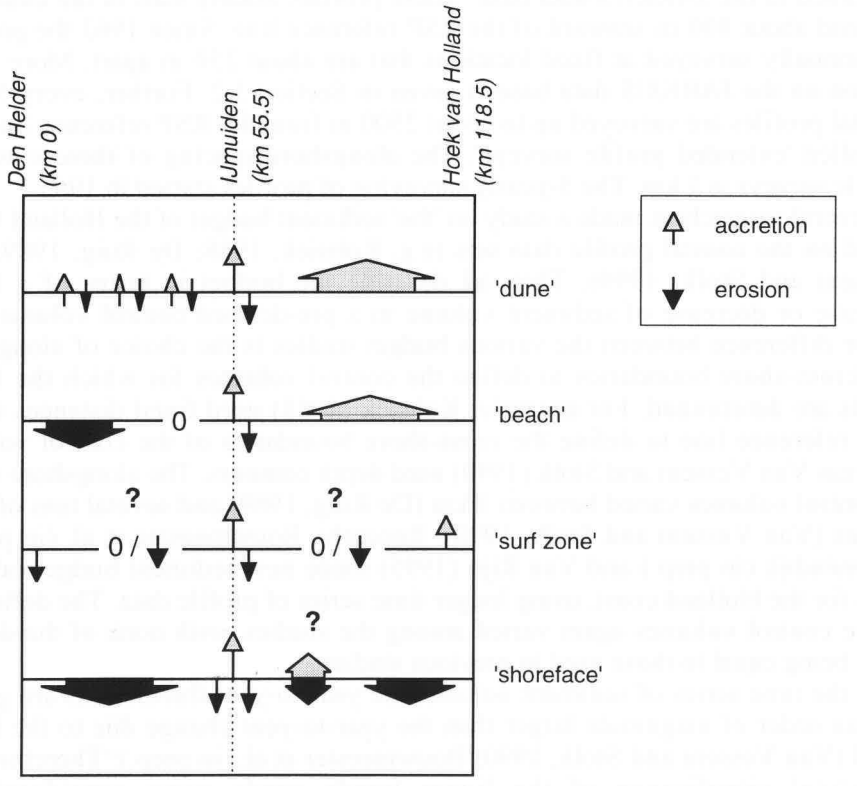

Figure 2.28: Qualitative overview of sediment budgets along the Holland coast; based on De Ruig (1989), Bouwmeester et al. (in prep.), and Van Rijn (1995).

The dune area is generally gaining sediment. Apparently, the sediment is effectively entrapped by the marram grass on the fore-dune and by other dune management activities (De Ruig, 1989). Between km 64 and km 93 the average rate of accretion is order 5 to 10 cubic meters per year per meter coast alongshore ($m^3/m/yr$). Alongshore fluctuations in the rate of sediment gain are small in this area. North of IJmuiden (km 55) the dunes both gain and lose sediment, with

losses and gains alternating over short distances (Bouwmeester et al., in prep.). No physical explanation is given for this variable pattern.

Some distance away from the harbour moles of IJmuiden dune erosion occurs, especially south of the moles near km 60-62.5. This dune erosion is related to the offshore and nearshore erosion that is occurring due to the extension of the harbour moles. This extension influenced the tidal currents and the wave-driven currents in the vicinity of the moles (De Ruig and Louisse, 1991).

The beach zone seems to be losing some sediment north of Egmond (about km 37) at a rate of a few $m^3/m/yr$. The year-to-year fluctuations are generally an order of magnitude larger than the trend in this area (Bouwmeester et al., in prep.). Between km 64 and km 114 the beach seems to be gaining some sediment (order 1 $m^3/m/yr$). According to Bouwmeester et al. (in prep.) the accretion trend is statistically significant.

Due to the extension of the IJmuiden harbour moles, considerable accretion occurred on the beaches close to the harbour moles (km 51-km 60). Neighbouring beach sections have lost sediment, especially between km 60 and km 63. Close to the harbour moles of Hoek van Holland, between km 114 and km 118, the beach gained sediment.

The inshore is gaining sediment near the harbour moles of IJmuiden (about km 52 to km 59). Neighbouring inshore sections are losing sediment, especially near km 60-67. Near the harbour moles of Hoek van Holland the inshore is gaining sediment, approximately between km 100 and km 118. The gain is only statistically significant between km 113 and km 118 (Bouwmeester et al., in prep.). Further, the inshore near the 'Nieuw Schulpen Gat' is losing sediment (between about km 0 and km 8), due to the landward migration of a flood-tidal channel on the Marsdiep ebb-tidal delta.

Along the remaining part of the Holland coast, the volume of sediment contained in the inshore has both been described as decreasing (De Ruig, 1989) and as being stable (Bouwmeester et al., in prep.). Probable causes for these different results are the different definitions of the control volumes for the budget calculations, the different length of the analysed time series, and the large scatter of the yearly sediment volumes. According to De Ruig (1989), sediment losses occur at a rate of a few $m^3/m/yr$. The differences between the actual measurements and the trend (i.e. the residuals) are large. The standard deviation of those residuals is on average one hundred m^3/m (Bouwmeester et al., in prep.).

The sediment budgets calculated for the shoreface are based on only a few extended profile surveys. De Ruig (1989) had only 4 values available to fit linear trends. Van Rijn (1995) added data from the 1990 survey, as well as data from the 1965 survey that was only carried out south of km 97 and north of km 72. De Ruig (1989) omitted the 1965 survey from his analysis because the volumes determined from the 1965 survey were quite deviating and consequently would be dominating trends along the stretches where profiles were surveyed in 1965.

Both authors showed that the shoreface zone is losing sediment over large stretches, but that the area near the harbour moles of IJmuiden (km 50-60) is gaining sediment. De Ruig (1989) calculated additional gain of sediment on the

shoreface between km 70 and km 80, and a stable amount of sediment between km 80 and km 90. According to Van Rijn (1995) these areas are losing sediment. Van Rijn (1995) attributes the sediment losses on the shoreface to gradients in the longshore transport.

In the aforementioned studies, the definition of the seaward boundary of the control volume for the shoreface sediment budget is largely enforced by the fixed length of the extended profiles, rather than determined by physical reasoning. This fact, in combination with the small number of observations available yet, implies that sediment budgets of the shoreface should be considered as rather tentative estimates.

Several modelling studies have been conducted to explain the observed sediment budget (e.g. Roelvink and Stive, 1990; Dijkman et al., 1990). These studies suffer from the general problems mentioned in Chapter 1 regarding up scaling of small-scale process knowledge to larger scales. Therefore, these models are not capable of explaining the observed sediment budget conclusively. Calibration of the models with the observed budgets remains a critical requirement to let the models match reality.

2.3.4 Morphologic studies

A description of decadal behaviour of the Holland coast in terms of morphologic changes was presented by Knoester (1990). Knoester summarised temporal and alongshore changes of the nearshore morphology by a large set of morphometric variables. Knoester mainly based his description on the JARKUS data base.

The analyses presented by Knoester (1990) revealed that the width of the supratidal beach, represented by the horizontal distance between the +1m contour and the +3m contour, is generally stable, except near large engineering works. Close to the harbour moles of Hoek van Holland and the harbour moles of IJmuiden the supratidal beach is widening, and some distance away from the moles it is narrowing. The supratidal beach is also narrowing just south and north of the seawall near Petten.

The intertidal beach, represented by the area between the -1m contour and the +1m contour, shows a tendency to widen locally over stretches of about 5 km length. In between, no statistical significant change in beach width occurs. The widening occurs at a rate of about 1 m/yr. This pattern is not explained.

The decadal behaviour of the subtidal part of the nearshore profile and the alongshore variation in it, if any, has not been described satisfactorily yet. Knoester tried to characterise this behaviour by the behaviour of two depth contours. However, given the limitations of available data sets along the Holland coast, the description of the decadal behaviour of the subtidal nearshore profile by changes in depth contour positions has several drawbacks. The seaward extent of the JARKUS data set not always includes the seaward limit of the breaker bar zone. In addition, the value of the deepest surveyed depth contour varies among

the profiles in the JARKUS data set, because of the fixed cross-shore survey length and the alongshore varying profile steepness. Therefore, the deepest depth contour present in most JARKUS profiles will be well within the zone of breaker bars along large parts of the coast. As a consequence, the behaviour of such a depth contour will be largely influenced by the position and behaviour of breaker bars. So, the behaviour of the deeper parts of the profiles in the JARKUS data set can not be adequately described by one common depth contour. The latter was illustrated by Knoester (1990) who used the -5 m contour for this purpose.

The 5-yearly, extended profile surveys extend well beyond the zone of breaker bars, but the present-day number of surveys is too small for a reliable description of morphologic behaviour during the past 2 decades (see Section 2.3.3). Therefore, Knoester (1990) tried to compare the present-day positions of the -7 m contour and the -10 m contour to the positions of these contours in 1896. Knoester concludes that the position of the -7 m contour shifted landward about 50 m, excluding the prograding and stable areas close to the harbour moles of IJmuiden and Hoek van Holland. The position of the -10 m contour shifted landward by about 100 m to 150 m along most parts of the Holland coast, again excluding the prograding areas near the harbour moles of IJmuiden and Hoek van Holland. Further, north of km 20 the behaviour of the -10 m contour becomes more complicated, because of the southward migration of this contour near the Pettemer Polder (Knoester, 1990) (Figure 2.29).

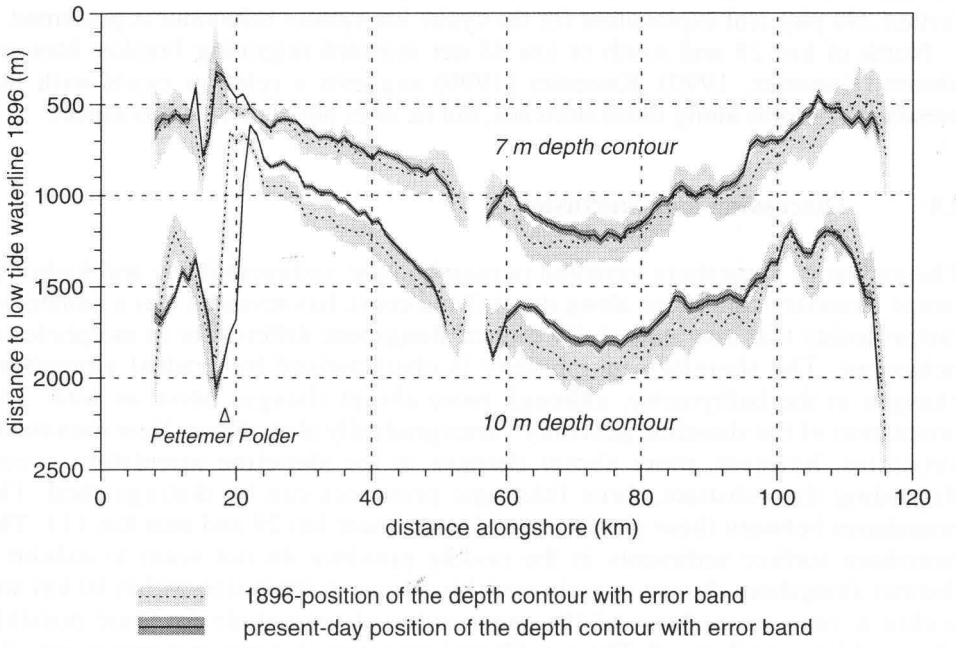

Figure 2.29: Present-day position and 1896 position of the 7 m and 10 m depth contours.

The change in the positions of the -7 m contour and -10 m contour seems considerable, but the accuracy of the surveys should be considered for a more balanced appraisal of the figures presented by Knoester (see Appendix 3). The change in position of the -7 m contour is generally within the range of the estimated accuracy of the depth contour position (Figure 2.29). Therefore, little can be concluded about the behaviour of the -7 m contour.

The change in the position of the -10 m contour is generally just at the edge of the accuracy range. Locally the landward shift of the -10 m contour exceeds the accuracy range, viz. between about km 20 and km 40, and between about km 60 and km 70. Along most other stretches the position of the -10 m contour may have remained unchanged since 1896, though landward shifting remains a possible option.

From km 30 to km 90 -a multiple barred stretch of coast- breaker bars exhibit multi-year cyclic behaviour. This cyclic behaviour consists of a net seaward migration of all bars with the outer bar fading away and with a new bar developing near the shoreline (Edelman, 1974; De Vroeg, 1987; Knoester, 1990; Houwing, 1991). The time span required to complete one cycle varies alongshore. Between km 30 and km 50 the estimates of the required time span vary between 15 and 27 years, whereas between km 60 and km 90 the time span estimates vary between 3 and 5 years (De Vroeg, 1987; Knoester, 1990). Both De Vroeg and Knoester mention that the bar behaviour between km 60 and km 90 is more coherent than between km 30 and km 50, but they do not elaborate this aspect any further. No physical explanation for the cyclic bar system behaviour is presented.

North of km 28 and south of km 98 net seaward migrating breaker bars are absent (Knoester, 1990). Knoester (1990) suggests a relation exists with the presence of groins along those stretches, but he does not elaborate this aspect.

2.4 Discussion and conclusions

The outline of alongshore variation in morphologic, sedimentologic and hydrodynamic boundary conditions along the Holland coast, has revealed that a number of factors exists that may potentially induce alongshore differences in morphologic behaviour. The shoreface morphology is characterised by gradual alongshore changes in the bathymetry, although more abrupt changes occur as well. The orientation of the shoreline generally varies gradually alongshore. Near man-made structures, however, more abrupt changes in the shoreline orientation occur. Regarding the substrate, three lithologic provinces can be distinguished. The boundaries between these provinces are located near km 29 and near km 111. The nearshore surface sediments in the middle province do not seem to exhibit a distinct alongshore change in grain size. Variations in grain size within 10 km and within a year are at least of the same order of magnitude as some possibly obscured large-scale trend. The non-filtered processes that may put energy into the large-scale morphodynamic system seem to vary only gradually along the Holland

coast (tides, 'swell', density-driven circulation). Some processes may even be quite constant along this stretch (wind and wind waves).

Human intervention in the coastal system, in terms of constructing engineering works, dates back more than a century. This implies that the large-scale morphodynamic system has had considerable time to adapt to these interventions. Some of the man-made structures, however, have been substantially enlarged about 2 decades ago. It is not clear to what extent the large-scale morphodynamic system has adjusted itself to that situation.

The previous studies on decadal developments of the Holland coast have shown that alongshore differences indeed exist: in shoreline behaviour, in sediment budgets, and in morphologic developments. The alongshore differences in coastal behaviour described in various studies can not easily be used to define LSCB-regions. The degree of detail in which alongshore variation is described varies among the studies. Furthermore, the total number of variables used in the various studies is too large to get an overview of coherence in alongshore differences. In addition, notwithstanding the large number of variables used in the various studies, the developments of the morphology in the nearshore zone are still insufficiently described. For example, developments of the mean shape of the nearshore profile have not been described yet, and the alongshore coherence in the behaviour of breaker bars is still insufficiently described.

The observed decadal coastal behaviour remains largely unexplained in the various studies. At best, some correlation is found with potentially controlling factors, such as the climatic variations that have been mentioned in relation to shoreline changes. In modelling studies on sediment budgets, calibration with observed budgets is still a critical requirement to match with reality.

In conclusion, partitioning the Holland coast with respect to differences in decadal coastal behaviour is hardly possible using existing studies. To accomplish a partitioning of the coast, the coastal behaviour is preferably described by only a few variables summarising the main decadal developments. When too many variables are defined, the overview is lost and one may get confused by irrelevant details. In the following chapter (Chapter 3) a method is elaborated to summarise the decadal developments of the Holland coast with just a few variables.

3 METHOD TO EXTRACT DECADAL MORPHOLOGIC BEHAVIOUR FROM HIGH-RESOLUTION, LONG-TERM BATHYMETRIC SURVEYS

3.1 Introduction

A prerequisite for the understanding of decadal coastal behaviour is a quantitative description of large-scale morphologic developments (see Chapter 1). Previous studies revealed the nature of some decadal developments regarding the shoreline position, the sediment budget, and some morphologic characteristics. Furthermore, these studies showed that regional differences in decadal coastal behaviour exist. A coherent description of large-scale morphologic behaviour is however lacking and can not be determined from the results of previous studies (see Chapter 2).

In the following sections, a method of data analysis is elaborated to obtain a coherent and compact description of the decadal morphologic developments of the Holland coast from a data base containing nearshore profiles (JARKUS).

3.2 The morphologic data base JARKUS

The bathymetry of the Holland coast is monitored on an annual basis and contained in the JARKUS data base of the Dutch Department of Public Works (*Rijkswaterstaat*). The monitoring of this area started in 1963 in the southern part (km 99 - km 118). From 1964 on, the other part of the Holland coast (km 0 - km 99) was also included in the monitoring program.

The coastal profiles are measured from the fore-dune to approximately one kilometre seaward every 250 metre alongshore. In areas with groins the alongshore spacing of profile sections ranges between 110 metre and 310 metre, because profiles are surveyed at locations in between the groins. The alongshore position of cross-shore survey lines is marked by a permanent base line of beach poles.

The cross-shore distance between consecutive depth measurements ranges from 10 metre near the shoreline to 20 metre offshore. The sub-aerial part of the profile data (down to the low water line) was initially gathered by levelling, but since 1977 photogrammetric methods are used. The sub-aqueous part of the data (up to the low water line at least) is gathered by sounding. Usually, the sub-aerial survey and sub-aqueous survey overlap in the intertidal area. If the profiles intersect, the two profile parts are joined at the intersection point. If the profiles overlap without an intersection, some averaging procedure is applied to join the two profile parts (Kalf et al., 1993).

Profiles are usually surveyed between early April and late September. This implies that the time interval between two successive profile soundings at a

particular location may vary between 0.5 and 1.5 year. Further, it implies that the profile sampling has a seasonal bias. Little is known about seasonal changes in nearshore bathymetry along the Holland coast. Generally, spring and summer (April to September) are less stormy seasons than autumn and winter (Augustijn et al., 1990). Nevertheless, Kroon (1994) observed hardly any seasonal differences in the mean profile shape and the width and height of the sweep zone, determined over a 17-year period near km 40. Similar observations were made by Terwindt (1969) over a 4 year period near km 98-108. Further, profiles surveyed during a more than average stormy spring may have characteristics of profiles during a less than average stormy winter. Therefore, it is expected that the biased sampling does not cause a strong bias in the shapes of the profiles. Moreover, the analysis of the profiles aims at describing morphologic developments that exceed the level of seasonal changes. So, even with some seasonal bias present, long-term trends should become visible anyhow.

The sounding accuracy of the depth values is about 15 cm. The accuracy decreases to about 25 cm when ship-dependent errors are included, such as errors in the determination of the elevation of the sea surface relative to the Dutch vertical ordnance datum NAP (Glim and Visser, 1981). So, the accuracy of 15 cm applies for comparing depth differences within a single profile, and the accuracy of 25 cm applies for comparing depth differences between profiles.

The accuracy of the height measurements by photogrammetric methods is about 10 cm (Veugen, 1984). The accuracy of the levelling has not been evaluated thoroughly. Oosterwijk and Ettema (1987) mention a general value for the accuracy of height measurement by levelling of about 1 cm.

In this study, only the part below the 1m +NAP contour will be used. The 1m +NAP level approximates the high water level along the Holland coast. Therefore, most of the analysed profile data has been obtained by boat. Only the uppermost part of the profile is obtained by levelling or from aerial photographs. The data up to 1990 are analysed, starting at km 3 in the north up to km 118 in the south.

3.3 Concept of analysis of decadal morphologic behaviour

The annual 'snapshots' of the nearshore bathymetry show the cumulative result of morphologic developments on many scales. The presence or absence of a swash bar in a measured profile, for example, is determined by the wave conditions in the days to weeks prior to the survey (Kroon, 1994). Such short-term phenomena are considered to be irrelevant for the description of large-scale morphologic developments (see Section 1.2).

The objective of the analysis of the bathymetric data is to summarise only that information that is relevant to large-scale coastal behaviour, i.e. morphologic features that change on large temporal or large spatial scales. In addition, this relevant information should be compressed into only a few variables. The latter constraint is imposed to get an overview over the huge amount of information.

Previous studies (see Chapter 2) have shown that over large alongshore distances the steepness of the nearshore profile varies, as well as the bar topography. Furthermore, it has been shown that alongshore differences exist in the trends in shoreline position.

The most compact way to summarise the above mentioned type of information is in terms of sediment budgets. This type of data compression is one way and results in a loss of valuable information, such as the distribution of sediment gain or loss across the profile and the redistribution of sediment within the coastal zone. Therefore, variables directly describing morphologic features are preferred. Another reason for using morphologic variables instead of the sediment budget, is that the water motion directly interacts with the morphology. Therefore, observations of morphologic developments may give clues about possible relevant hydrodynamic forces.

The description of morphologic developments will be based on the quantification of profile characteristics. The alongshore coherence between these profile characteristics then describes the morphology. The alongshore coherence in temporal changes in profile characteristics describes the large-scale morphologic behaviour. The two main characteristics of a nearshore profile to be considered are its shape and its cross-shore position. The latter deals with the prograding or retreating nature of a coast. For example, along a prograding part of a coast the nearshore profile shifts seaward. Therefore, profile behaviour can be expressed in terms of a change in the shape of the profile and a change in the cross-shore position of the profile.

3.4 Quantification of cross-shore profile behaviour

3.4.1 Quantification of horizontal profile shift

The cross-shore shifting of the profile will be represented by the cross-shore movement of the 1m +NAP contour. The development of the shape of the profile will be analysed relative to this floating reference line. This means that only the part of the profile below 1m +NAP is analysed. From now on, the 1m +NAP contour will also be referred to as the +1m contour or as the shoreline.

The +1m contour approximates the high water level along the Holland coast (Figure 3.1) and thus approximates a process-oriented reference line. The +1m contour reasonably separates the 'sub-aerial' part of the coastal profile from the 'sub-aqueous' part. The 'sub-aqueous' part is subject to the hydrodynamic forces on a daily basis, while the 'sub-aerial' part is only subject to the hydrodynamic forces during storms.

Other contours could have been selected to separate the sub-aerial from the sub-aqueous part of the coastal profile, such as mean sea level or low water level. However, the cross-shore position of these contours is far more sensitive to the development of a swash bar than the +1 m contour. The time-series of cross-shore positions of contours below the +1m level will therefore contain more 'noise' than

the +1m contour, because swash bar development is supposed to be irrelevant for large-scale morphologic behaviour.

By analysing only the sub-aqueous part of the coastal profile to define LSCB-regions, it is implicitly assumed that the influence of the development of the sub-aqueous part on the development of the sub-aerial part is larger than vice versa.

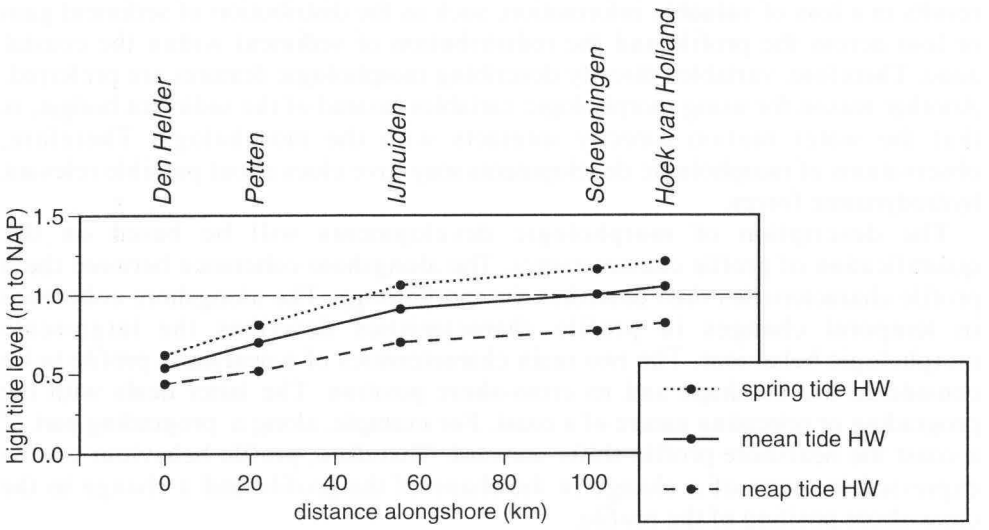

Figure 3.1: High tide water levels along the Holland coast (Getijtafels, 1991)

3.4.2 On the quantification of profile shape change

Several mathematical functions have been proposed to describe the shape of the coastal profile, but most of them do not account for a barred topography (e.g. Dean, 1977; Dean 1991; Bodge, 1992). Some authors proposed additional analyses of the bar topography by describing the deviations from the fitted (non-barred) mean profile function (e.g. De Vroeg, 1987, Helsloot, 1989). However, this type of approach tends to result in many variables which inhibits a compact and coherent description of the decadal morphologic developments. Therefore, another type of approach is chosen in which characteristic shape functions emerge from the data set itself.

Changes in the shape of nearshore profiles can be regarded as correlated changes in seabed elevation. Some of those depth variations will be irrelevant for the description of decadal morphologic behaviour, viz. the depth variations related to the small-scale and short-term coastal behaviour (see Section 1.2). These will be treated as noise. The method of analysis of the JARKUS data set should therefore remove the superfluous information on small-scale profile behaviour.

The fact that profile depths are correlated (both spatially and temporally) and that part of the changes can be regarded as noise resembles the characteristics of a regionalised variable. A regionalised variable is a variable that has properties intermediate between a truly random variable and a completely deterministic variable (Davis, 1986). The concept of a regionalised variable originates from geostatistics. Therefore, geostatistical techniques seem most appropriate to analyse the nearshore profile data set.

A wide range of geostatistical analysis techniques is available. Helsloot (1989) proposed the application of spectral analysis, considering the cross-shore profile as a stochastic time series. The presented relation between dominant frequencies and profile shape characteristics, however, was not satisfying (Terwindt and Wijnberg, 1991). The relation between dominant frequencies in the amplitude spectrum and the dimensions of the bar-trough topography was often ambiguous. In addition, the locations of bars could not be determined because the reliability of the phase spectrum was very low with generally only 1 to 3 bars present in a profile. Another geostatistical technique already applied in coastal profile analysis is principal component analysis (PCA) or -the more general form- empirical eigenfunction analysis (e.g. Winant et al., 1975). This analysis technique treats changes in the cross-shore profile as a set of correlated depth changes. The correlation structure is analysed by empirical eigenfunction analysis. Empirical eigenfunction analysis is basically the same as principal component analysis (PCA). The only difference is that PCA restricts itself to the use of a covariance or a Pearson correlation matrix while empirical eigenfunction analysis does not. Many (geo)statistical handbooks treat the subject of PCA (e.g. Davis, 1986).

Several authors applied the empirical eigenfunction technique to characterise beach profile changes (e.g. Winant et al., 1975; Vincent et al. 1976; Resio et al., 1977; Dolan et al., 1977; Aubrey, 1979; Aubrey et al., 1980; Weishar and Wood, 1983; Fisher et al, 1984; Aubrey and Ross, 1985; Lins, 1985; Zarillo and Liu, 1988). The studies of Weishar and Wood (1983) and Zarillo and Liu (1988) outline the power of empirical eigenfunction analysis to describe profile variability on respectively a large time-scale or a large length scale. None of the previous studies had to deal with bathymetric data sets with both a large temporal and a large spatial extent. Nevertheless, empirical eigenfunction analysis was selected as a promising technique to analyse the JARKUS data set.

3.4.3 Empirical eigenfunction analysis applied to nearshore profiles

The application of the empirical eigenfunction technique in the description of coastal profiles requires that every profile is described by a set of depth values at y given cross-shore locations. As a consequence, the length of the analysed profiles has to be constant. This length was set at 750 m, starting from the +1m contour, because this length was reached by most of the profiles. The cross-shore distance between depth values was chosen to be equidistant at 15 m. The depth values at the 15 m intervals were obtained by cubic spline interpolation. A data hiatus of

more than 50 m was not interpolated and short profiles were not extrapolated to reach a total length of 750 m. How these incomplete profiles are dealt with in the analysis is explained later in this section.

A set of n profiles gives n depth values at any of the m cross-shore locations. The correlation between these m samples of n depth values can be described in some correlation matrix. The m eigenvectors of this correlation matrix then describe m normal modes of cross-shore correlation in depth values. These eigenvectors are also called empirical eigenfunctions (or just 'eigenfunctions' for short), empirical orthogonal functions or principal components, depending on the type of correlation matrix that is analysed. Usually the length of these eigenvectors, or the 'amplitude' of the eigenfunction, is scaled by the square root of the corresponding eigenvalues.

Each profile is described by m depth values. Therefore, each profile can be 'plotted' in a m-dimensional data space. The set of m empirical eigenfunctions is nothing but a set of m newly defined axes. These new axes are linear combinations of the old axes. So, each of the profiles 'plotted' in the m-dimensional data space can be projected on the newly defined axes. These projections on the new axes are often called 'weightings', or 'scores' in PCA.

The measures of correlation in the correlation matrix from which the eigenvectors will be determined, can be defined in many ways. For example, the matrix can be defined as an uncorrected sum of products matrix or as a covariance matrix. In this study, an uncorrected sum of products matrix was used, which is determined by:

$$[\mathbf{U}] = (1/n) \cdot [\mathbf{D}]^{\mathrm{T}} \cdot [\mathbf{D}] \tag{3.1}$$

Where: $[\mathbf{U}] = (m \times m)$ uncorrected sum of products matrix, $[\mathbf{D}] = (n \times m)$ matrix of depth values, $[\mathbf{D}]^{\mathrm{T}}$ = transpose of $[\mathbf{D}]$, n = number of profiles in the analysis, and m = number of cross-shore depth values per profile.

The use of an uncorrected sums of products matrix has the advantage that the mean profile shape and its temporal behaviour are expressed in terms of an empirical eigenfunction with related weightings. This is not the case if a demeaned type of correlation matrix is used, such as the covariance matrix. Further, it appears that this uncorrected sums of products matrix results in a better definition of the bar topography by the second and third empirical eigenfunctions.

In mathematical notation the above described set of manipulations reads as follows. The aforementioned data matrix $[\mathbf{D}]$ consists of depth values h that are a function of the cross-shore position y and the profile observation p. The data $h(y,p)$ can be represented by a normal mode expansion of the form (Winant et al., 1975):

$$h(y,p) = \sum_{k=1}^{m} w_k(p) \cdot e_k(y) \tag{3.2}$$

where $e_k(y)$ contains the (unscaled) cross-shore eigenfunctions and $w_k(p)$ contains the profile weightings. The m eigenfunctions $e_k(y)$ are derived from the correlation matrix [**U**] (equation 3.1) by solving:

$$[\mathbf{U}] \cdot [\mathbf{E}] = \lambda_k \cdot [\mathbf{E}] \tag{3.3}$$

where [**E**] contains the m eigenvectors of matrix [**U**] and λ_k contains the corresponding m eigenvalues that are used to rank the m eigenvectors. The m eigenvectors form the m (unscaled) eigenfunctions $e_k(y)$. The weightings $w_k(p)$ on the m eigenfunctions are obtained by solving:

$$[\mathbf{W}] = [\mathbf{D}] \cdot [\mathbf{E}] \tag{3.4}$$

where [**W**] contains the weightings of the n profiles on the m eigenfunctions.

Alternatively, the matrix [**W**] can be obtained from the eigenvectors of matrix [**V**], where:

$$[\mathbf{V}] = (1/m) \cdot [\mathbf{D}] \cdot [\mathbf{D}]^{\mathrm{T}} \tag{3.5}$$

The eigenvectors of [**V**] are derived by solving:

$$[\mathbf{V}] \cdot [\mathbf{F}] = \lambda_k'' \cdot [\mathbf{F}] \tag{3.6}$$

where λ_k'' contains the m non-zero eigenvalues of [**V**], and [**F**] contains the corresponding eigenvectors. The matrix [**W**] is then derived by:

$$[\mathbf{W}] = [\mathbf{F}] \cdot \sqrt{m \cdot \lambda_k''} \tag{3.7}$$

The eigenfunctions and weightings have been calculated by the factor analysis module of the software package CSS-Statistica (StatSoft, 1991). This module rewrites the product of the first eigenfunction and the weightings on the first eigenfunction such that equation 3.2 is written as:

$$h(y,p) = \sqrt{\lambda_1} \cdot e_1(y) + \sum_{k=1}^{m} w_k'(p) \cdot e_k(y) \tag{3.8}$$

where: $w_k'(p) = w_k(p) - \sqrt{\lambda_1}$ for $k = 1$

$w_k'(p) = w_k(p)$ for $k = 2..m$

In equation 3.8, the first right hand term describes the mean profile and the second right hand term describes the deviations from the mean profile.

Incomplete profiles are not used in the computation of the eigenfunctions, that is they are not included in the calculation of the correlation matrix [**U**]. After the

eigenfunctions have been defined, the incomplete profiles are projected on the set of new axes, i.e. weightings are calculated. The data hiatus in an incomplete profile is filled with mean depth values to compute the weightings. The mean depth values are derived from the set of complete profiles.

The use of a correlation matrix that is based on non-demeaned data, has as a side effect that the weightings of the profiles on the first eigenfunction are not necessarily linearly uncorrelated to the weightings on the higher mode eigenfunctions. This is explained by the fact that the first eigenfunction has to pass through the origin of the data space. Because of this restriction, the first eigenfunction based on a non-demeaned type of correlation matrix cannot always be in the direction of maximum variance in the data. If a demeaned type of correlation matrix is used, the origin of the data space has been shifted to the arithmetical centre of the observed data and the first eigenfunction can then be defined in the direction of maximum variance in the data.

This side effect implies that morphological changes represented by profile weightings on higher mode eigenfunctions may be correlated to changes in the mean profile steepness; the latter being represented by profile weightings on the first eigenfunction. The profile weightings on eigenfunctions higher than the first mode are mutually uncorrelated (linearly).

3.4.4 Empirical eigenfunction analysis and moving window approach

The seaward extension of the bar system, the number of bars, and the bar spacing vary alongshore. Therefore, it is impossible to schematise the various bar systems with one common set of morphological meaningful empirical eigenfunctions. This implies that empirical eigenfunction techniques that simultaneously take into account the alongshore and temporal variation in the whole profile data set (e.g. Ostrowski et al., 1991), will fail to schematise the various bar systems. Therefore, the profile data has been analysed in small subsets.

Along the full length of the coast a 'window', with an alongshore width of 1 km and a temporal extent of 28 years, has been moved alongshore with a step size of 1 km. Within the window, all available profiles are summarised with three empirical eigenfunctions. Therefore, in equation 3.8 $p = p(x,t)$, where x is the alongshore location and t is the year of observation. The total analysis results in 112 sets of three empirical eigenfunctions, because near km 20-21 and km 25-26 the +1m-level is absent in the data set, and near km 55-56 a harbour is present.

The total number of profiles in a window may vary, because of missing profiles and because of differences in alongshore profile spacing (groin sections). In some windows the length of the profile that is analysed is less than 750 m. In those particular windows the portion of incomplete profiles would otherwise be too large (>25%) compared to the number of complete profiles that are used to determine the eigenfunctions. Figure 3.2 shows the analysed length per window. Figure 3.3 shows the total number of profiles per window, being composed of the number of analysed (complete) profiles and the number of incomplete profiles.

The size of the window is assumed to be small enough to avoid predetermination of boundaries of LSCB-regions. In case the decadal developments have a spatial scale of less than 1 km, this will emerge from the analysis by a lack of alongshore coherence in the profile behaviour. The empirical eigenfunction shapes based on profiles within a 1 km wide window will be more reliable than empirical eigenfunction shapes based on profiles from one location, because small-scale profile behaviour will average out better in the former. Further, the efficiency of the analysis increases by analysing profiles from more than one location together.

Usually each window includes 5 profile locations, because the alongshore spacing of profile locations is usually 250 m and profiles at both borders of the window are included. Moving the window 1 km alongshore means that the new window location has one profile location overlap with the previous window location. This overlap is a computational convenience to relate the second and third eigenfunctions in the successive windows, a relation which is not straightforward.

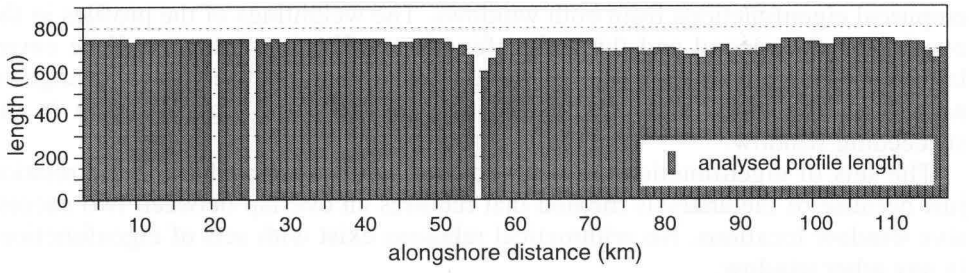

Figure 3.2: Analysed length of nearshore profiles

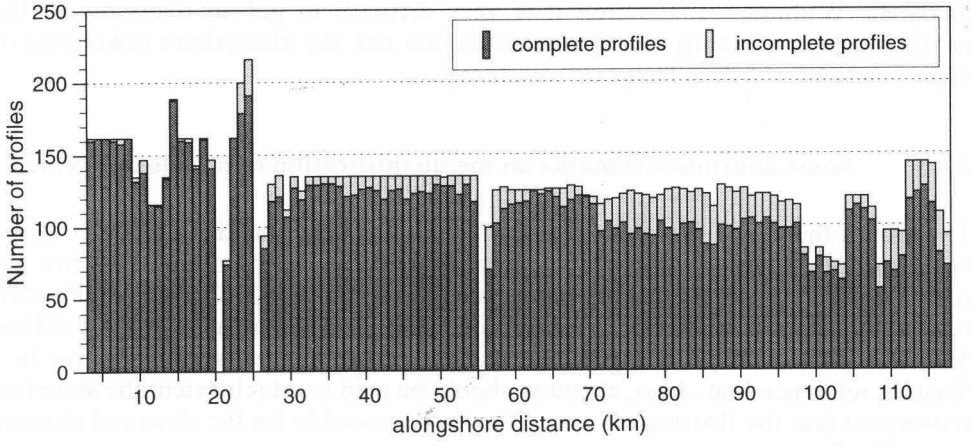

Figure 3.3: Number of profiles per window

The relation between the second and third eigenfunction in neighbouring windows is not straightforward for two reasons. Firstly, the orientation of the eigen function relative to the horizontal axis is arbitrary. This means that the second eigenfunction in window *i* may have nearly the same shape as the second eigenfunction in window (*i*-1), but mirrored around the horizontal axis. This makes alongshore comparison of empirical eigenfunction shapes unnecessarily difficult. Therefore, if necessary, eigenfunctions are mirrored around the horizontal axis.

Secondly, along a major part of the coast the second and third eigenfunction describe two modes of multiple bar topography. At many alongshore locations these two modes of bar topography occur about equally often. As a consequence, the importance of the second eigenfunction is often comparable to that of the third eigenfunction. This may result in changing names alongshore from second to third eigenfunction and vice versa for the same mode of bar topography. Again, this unnecessarily makes alongshore comparison of bar characteristics more difficult.

The profiles in the overlap between two successive windows are described by empirical eigenfunctions from both windows. The weightings of the profiles in the overlap on the second and third eigenfunctions of both windows will be correlated. The magnitude and sign of these correlations are used to re-arrange, if necessary, the order and sign of the second and third eigenfunction in the succeeding window.

The sets of eigenfunctions in neighbouring windows may have some relation just because of the analysis method that requires an overlap between two successive window locations. No arithmetical relations exist with sets of eigenfunctions in any other window.

Combination of the complex principal component analysis technique (Liang and Seymour, 1991) with the moving window approach was rejected, because it is hard to jointly visualise the results of many complex principal component analyses. Without visualisation it is very difficult to get an overview of the morphological meaning of the eigenfunctions and the alongshore coherence of eigenfunctions and their temporal weightings.

3.4.5 Some additional remarks on the quantification of profile behaviour

The aim of the above explained data manipulations is to quantify particular large-scale morphological features. It is emphasised that the manipulations are not meant to be some objective exploratory analysis of the JARKUS data set. Further, it should be kept in mind that no direct conclusions on sediment movement follow from the profile shape changes, because the profiles are analysed relative to a floating reference line. Also, attention should be paid to which extent the shoreline movement (i.e. the floating reference line) is responsible for the observed changes in profile shape.

Long-term trends in profile shape developments and cross-shore profile shift, and the correlations between the various profile characteristics will be studied by plotting the results of the above described analyses in so called 'contour plots'

(see Section 3.5) and by calculating linear correlation coefficients (R) and their statistical significance at the 1% level (p = 0.01).

3.5 Representation of alongshore coherence in cross-shore profile behaviour

The presented method of analysis results in a considerable data compression. Nevertheless, still a considerable amount of data is left. The compressed information of all 112 windows should be presented compactly to obtain an overview of this information, and thus obtain an overview of the large-scale morphologic behaviour. The compact presentation requires some additional manipulation of the data to get readable figures. In this process loss of detail is inevitable.

An empirical eigenfunction represents an average profile shape characteristic for a one kilometre stretch of coast (e.g. Figure 3.4). The alongshore variation in profile shape characteristics is represented by plotting the first three empirical eigenfunctions in 3D-diagrams (Figures 4.1 and 4.2). In some windows the analysed profile length was shorter than 750 m (Figure 3.2). Therefore, the cross-shore length of the profiles not always equals 750 m. The varying length of the mean profiles (first eigenfunctions) obscures the overview of the alongshore differences in profile steepness. Therefore, the short mean profiles have been extrapolated to reach 750 m. Extrapolation is based on the data of nearby mean profiles. Figure 3.5 shows some examples of extrapolated mean profiles. The short second and third eigenfunctions have been extrapolated too, to increase the readability of Figure 4.2. Extrapolation is based on the data of nearby eigenfunctions. Along the coastal stretch between km 71 and km 117 the extrapolation often simply consisted of adding zeros. The short eigenfunctions between km 52 and km 58

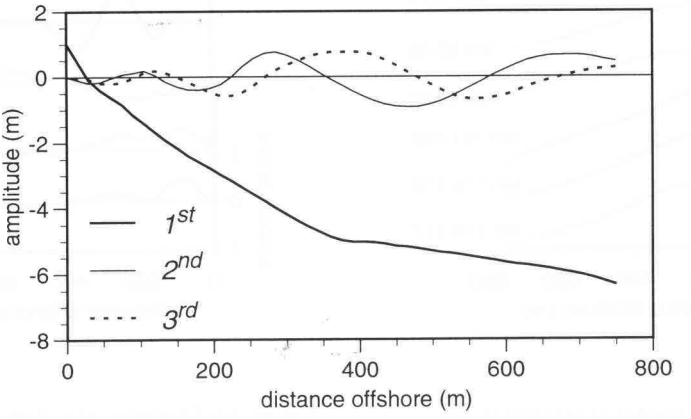

Figure 3.4: Example of first, second, and third eigenfunction

have not been extrapolated because nearby eigenfunctions were too different. Some examples of extrapolated eigenfunctions are shown in Figure 3.6.

Morphologic developments have both alongshore and cross-shore components. This spatial coherence will be accounted for by plotting the figures that quantify the profile shape and the cross-shore profile position of individual profiles into so called 'contour plots' (Sheet 1). The horizontal axes of these plots represent the alongshore location and the vertical axes represent the year of measurement. The contour lines, or isolines, connect points of equal value; the space between two successive isolines contains only points whose values are within the interval defined by the isolines. Only 2 isolines are used in the contour plots, because 3 grey-scales appeared to be the maximum possible number of grey-scales for a readable figure. The values of the isolines were chosen such that the resulting pattern was similar to the pattern emerging from plots with more isolines.

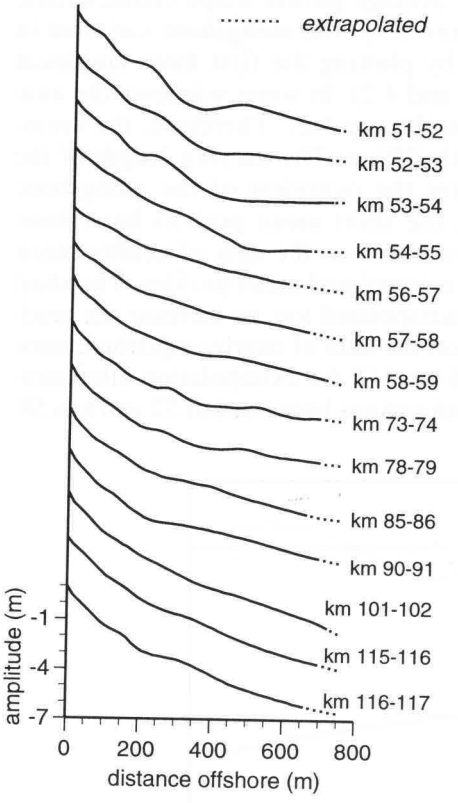

Figure 3.5: Examples of extrapolated first eigenfunctions

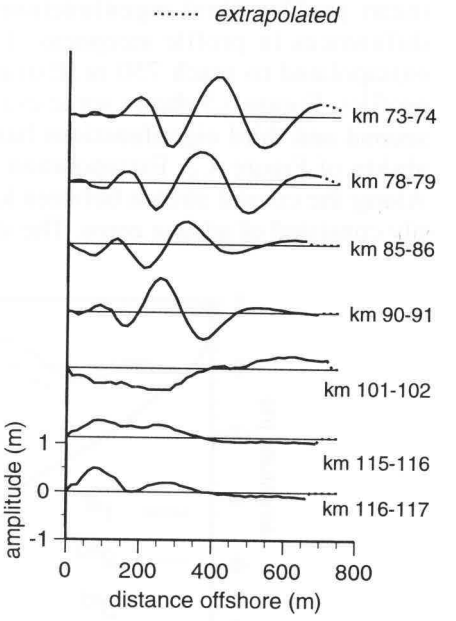

Figure 3.6: Examples of extrapolated second eigenfunctions(re-arranged)

The alongshore coherence in the cross-shore shifting of the profile (Sheet 1, Figure a) is represented by the difference between the observed cross-shore profile position ($s(x,t)$) and the local time-averaged cross-shore position ($\bar{s}(x)$), i.e.:

$$\Delta s(x,t) = s(x,t) - \bar{s}(x) \tag{3.9}$$

where:

$\Delta s(x,t)$ = anomaly in the position of the +1m contour as a function of the alongshore profile location x and the year of measurement t.

$s(x,t)$ = cross-shore position of the +1m contour relative to the base line of beach poles as a function of the alongshore profile location x and the year of measurement t.

$\bar{s}(x)$ = time-averaged position of +1m contour relative to the base line of poles as a function of the alongshore profile location x.

The alongshore coherence in the temporal variations in profile steepness is expressed in terms of deviations from the mean depth at 750 m from the shoreline (Sheet 1, Figure b). The depth deviations Δh are reconstructed from the weightings on the first empirical eigenfunctions by projecting the weighting on the first eigenfunction back into the data space by:

$$\Delta h(y,p) = w'_1(p) \cdot e_1(y) \tag{3.10}$$

where: y = 750 m, and p = profile that is reconstructed.

Therefore, the depth deviations in Figure b of Sheet 1 are *not* the differences between observed depth values and the mean depth at 750 m offshore (Figure 3.7).

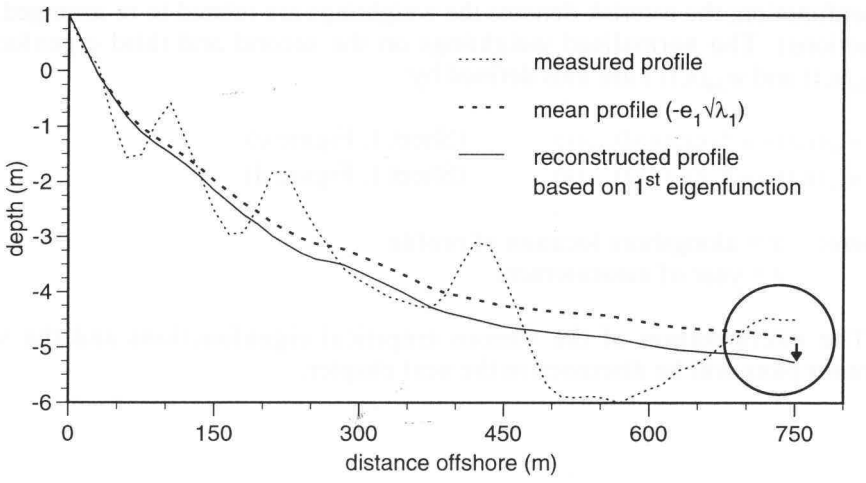

Figure 3.7: Example of anomaly of mean depth at 750 m offshore as plotted in Figure b (Sheet 1). The arrow indicates the considered depth deviation (being about -0.4 m).

In case the eigenfunction $e_1(y)$ was shorter than 750 m, the extrapolated eigenfunctions presented in Figure 4.1 were used (divided by $-\sqrt{\lambda_1}$).

The reason for using reconstructed depth values instead of weightings on the first eigenfunction is that the ship-dependent measurement errors appear in these weightings. The ship-dependent measurement error influences the profile as a whole, and therefore has a strong cross-shore correlation. The random measurement error per depth measurement, to the contrary, has no cross-shore correlation and therefore ends up in the high order empirical eigenfunctions. For example, if the vertical position of the profile relative to NAP is determined too high, then the profile will appear flatter than it actually is. Reconstructed depth deviations larger than 0.2 m are assumed to exceed this ship-dependent measurement error.

The mean profile (or first eigenfunction) is considered a first order approximation of the cross-shore profile shape. From this point of view, other profile shape characteristics may be called 'secondary' morphological features. The alongshore coherence in the temporal variations in these secondary morphological features (usually bar topography) is represented by the weightings on the second and third eigenfunction.

The range of values that the weightings on the second and third eigenfunction obtain varies alongshore. The number of grey-scales that is used to visualise the alongshore coherence in weightings is limited. As a consequence, the patterns of coherence will be obscured in areas where the range in weightings is small. This problem has been solved by normalising the weightings. The weightings on the second and third eigenfunctions are normalised by the standard deviation of the weightings per alongshore profile location x (*not* per window). The standard deviations (*SD*) of the weightings on the second and third eigenfunction are therefore only a function of x ($SD_{w2*}(x)$ and $SD_{w3*}(x)$, for respectively second and third eigenfunction; the asterisk denotes the weightings are related to re-arranged eigenfunctions). The normalised weightings on the second and third eigenfunctions ($w_{2n}(x,t)$ and $w_{3n}(x,t)$) are thus defined by:

$$w_{2n}(x,t) = w^*_2(x,t)/SD_{w2*}(x) \qquad \text{(Sheet 1, Figure c)} \qquad (3.11)$$

$$w_{3n}(x,t) = w^*_3(x,t)/SD_{w3*}(x) \qquad \text{(Sheet 1, Figure d)} \qquad (3.12)$$

where: x = alongshore location of profile
t = year of measurement

The interpretation of the various empirical eigenfunctions and the various contour plots will be discussed in the next chapter.

4 DECADAL MORPHOLOGIC BEHAVIOUR ALONG THE HOLLAND COAST

4.1 On the morphological interpretation of empirical eigenfunctions

4.1.1 The empirical eigenfunctions

Figure 4.1 shows the alongshore variation in the shape of the first eigenfunctions. The first eigenfunction describes the (local) mean profile shape ($-e_1\sqrt{\lambda_1}$). Some of the mean profiles contain a bar, for example near km 10 (Figure 4.1 and 4.3). In this case this points at the presence of a bar with a rather stable position (on the time span of 27 year). The first empirical eigenfunctions usually explain over 97 per cent of the mean square value of all the data in the window.

Figure 4.2 shows the alongshore variation in the re-arranged (scaled) second and third eigenfunctions. Figure 4.2a and 4.2b show the second and third eigenfunction when positively weighted ($e_{2*}\sqrt{\lambda_{2*}}$ (Figure 4.2a) and $e_{3*}\sqrt{\lambda_{3*}}$ (Figure 4.2b); the asterisk denotes that the eigenfunctions are re-arranged eigenfunctions). Figure 4.2c and 4.2d show the second and third eigenfunction when negatively weighted ($-e_{2*}\sqrt{\lambda_{2*}}$ and $-e_{3*}\sqrt{\lambda_{3*}}$ (Figures 4.2c and 4.2d)). The meaning of the weightings will be explained below.

The second and third eigenfunction generally represent the bar topography. When a bar is already present in the mean profile function (the first eigenfunction), the second and third eigenfunction describe modulations of the bar height and bar position, for example near km 10 (Figure 4.1, 4.2, and 4.3). When bars are absent, the second and third eigenfunction describe small modulations of the

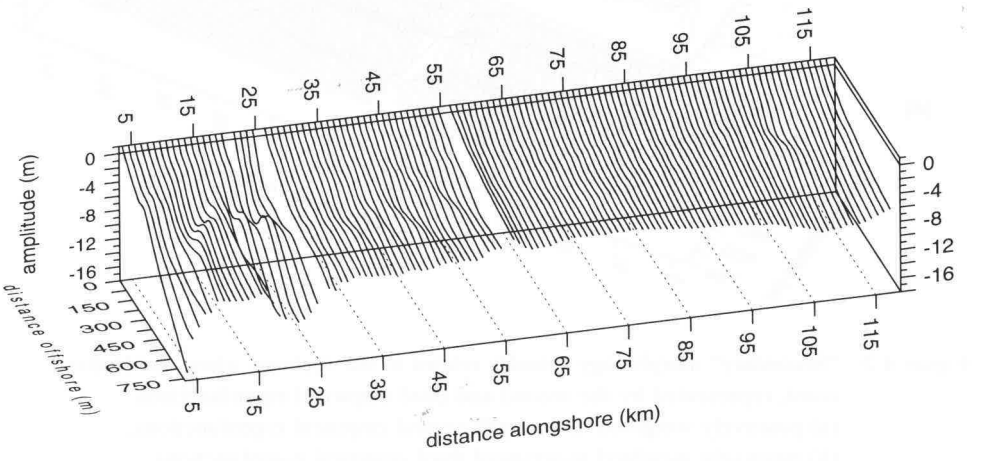

Figure 4.1: Time-averaged profile shapes along the Holland coast, represented by the first empirical eigenfunctions.

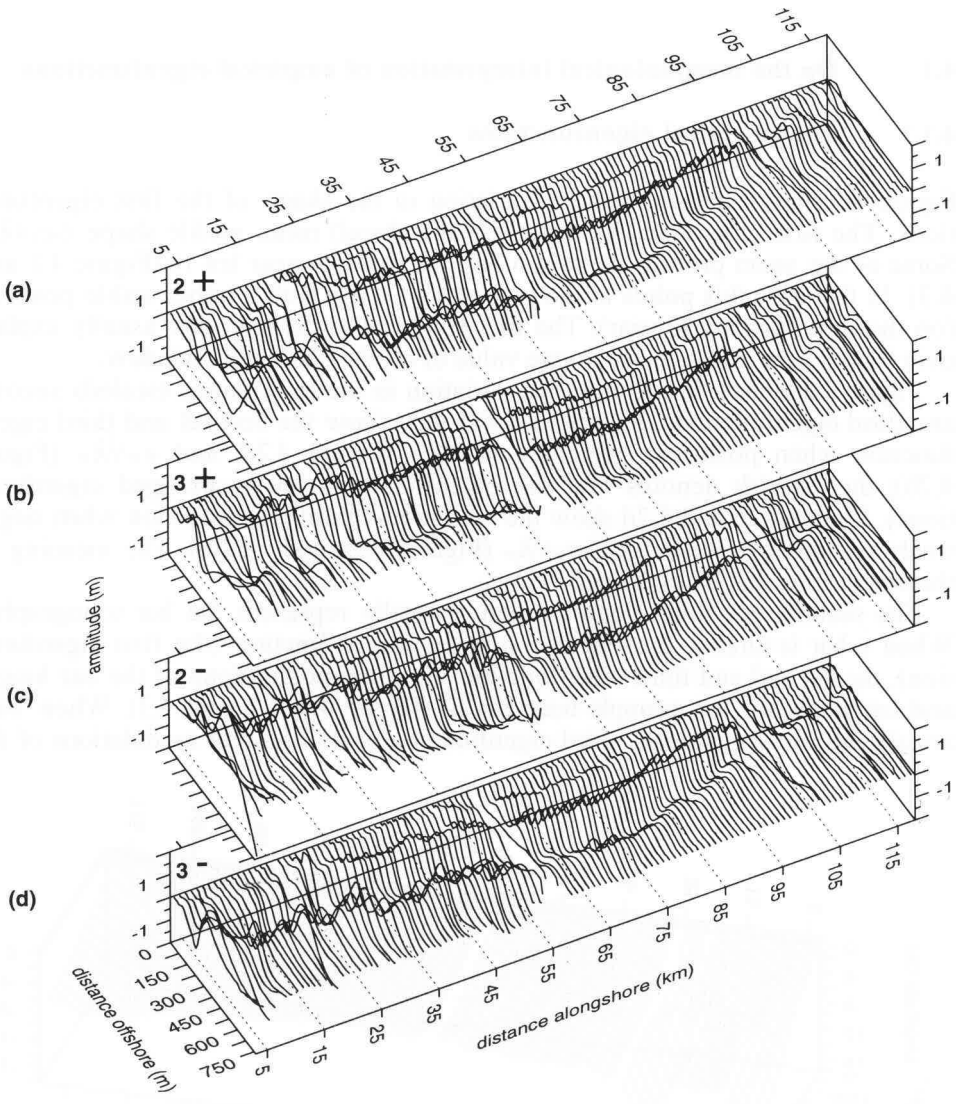

Figure 4.2: "Secondary" morphology -usually related to bar systems- along the Holland coast, represented by the second and third empirical eigenfunctions.
(a) positively weighted re-arranged second empirical eigenfunctions,
(b) positively weighted re-arranged third empirical eigenfunctions,
(c) negatively weighted re-arranged second empirical eigenfunctions,
(d) negatively weighted re-arranged third empirical eigenfunctions.

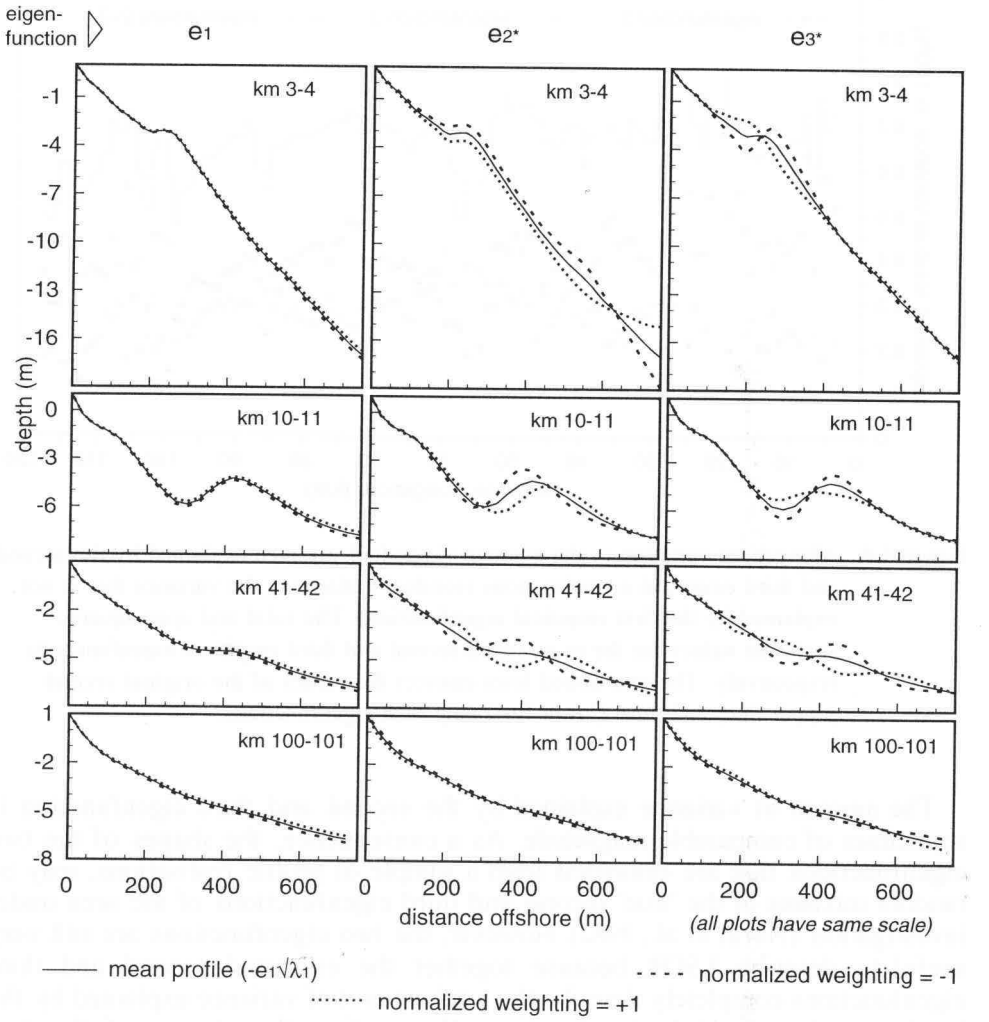

Figure 4.3: Examples of the interpretation of positive and negative weightings on the first 3 eigenfunctions. The values of the weightings are arbitrarily chosen as plus or minus the standard deviation of the normalised weightings in the window (i.e. +1 and -1).

mean profile shape, for example near km 100 (Figure 4.3). At km 3, the second eigenfunction describes the variation in concavity of the mean profile (Figure 4.3).

Generally, the second and third eigenfunction together explain about 65 to 70 per cent of the depth variance that is not explained by the first eigenfunction. The individual eigenfunctions usually explain among 25 and 45 per cent of this residual variance (Figure 4.4).

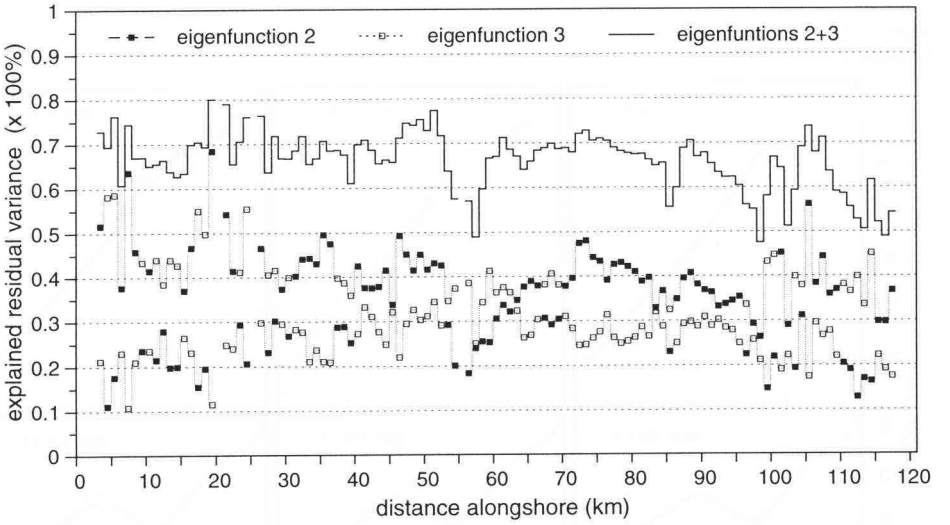

Figure 4.4: Alongshore variation in the amount of residual variance explained by the second and third empirical eigenfunctions (residual variance = the variance that is not explained by the first empirical eigenfunction). The solid and open squares represent values for the re-arranged second and third empirical eigenfunctions respectively. The two dotted lines connect the values of the original second (upper line) and third (lower line) empirical eigenfunctions.

The amount of variance explained by the second and third eigenfunction is sometimes of comparable magnitude. As a consequence, the shapes of the two eigenfunctions that are estimated from a sample of profile realisations, may be random mixtures of the 'true' second and third eigenfunctions of the area under investigation (North et al., 1982). However, the two eigenfunctions are still very useful to describe LSCB, because together the estimated second and third eigenfunctions completely describe the total amount of variance explained by the 'true' second and third eigenfunctions. In practice, the shapes of the two eigenfunctions do not appear to be fully random mixtures, because the shapes of the two modes of bar topography appear to be quite consistent over considerable alongshore distances (Figure 4.2).

4.1.2 The weightings on the empirical eigenfunctions

The weightings of an individual profile on the first three empirical eigenfunctions describe the morphology of this profile in terms of these three empirical eigenfunctions. A positive weighting on the first eigenfunction means that the observed profile is flatter than the (local) mean profile. A negative weighting means that the observed profile is steeper than the (local) mean profile (Figure 4.3).

A positive weighting on the second eigenfunction means that the topography described by the (local) second eigenfunction should be superimposed on the (local) mean profile (Figure 4.3). Usually this topography is the bar topography. A negative weighting means that the topography described by the second eigenfunction has to be mirrored around the horizontal axis before it is superimposed on the mean profile shape. The magnitude of the weighting determines the amplitude of the superimposed topography. The interpretation of the weighting of a profile on the third eigenfunction is similar to the interpretation of the weighting on the second eigenfunction.

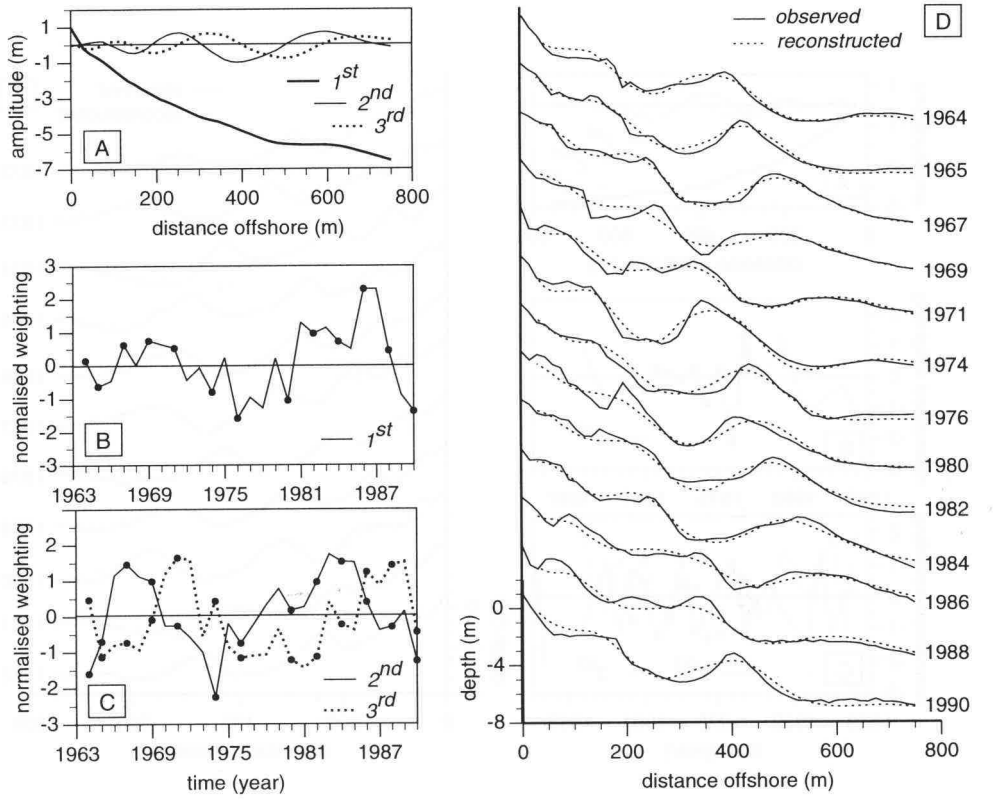

Figure 4.5: Example of the results of an eigenfunction analysis for some arbitrary window (km 41-42). (a) Shape of the first three eigenfunctions. (b) Weighting on the first eigenfunction of profiles at km 41.5. (c) Weighting on the second and third eigenfunction of profiles at km 41.5. (d) Selection of profiles observed at km 41.5 together with eigenfunction-based descriptions of these profiles. Only the first three eigenfunctions have been used to reconstruct these profiles. The black dots in Figure (b) and (c) mark the weightings that are used in the reconstruction.

Figure 4.5, 4.6, and 4.7 show examples of the results of eigenfunction analysis in three arbitrary windows (km 41-42, km 69-70, and km 12-13). These figures illustrate to what degree the three eigenfunctions approximate the observed profiles. For example, the phenomenon 'double crested bar' is not represented by using only three eigenfunctions (see Figure 4.5d, profile 1971). Figure 4.8 illustrates that incomplete profiles can be described well by three eigenfunctions.

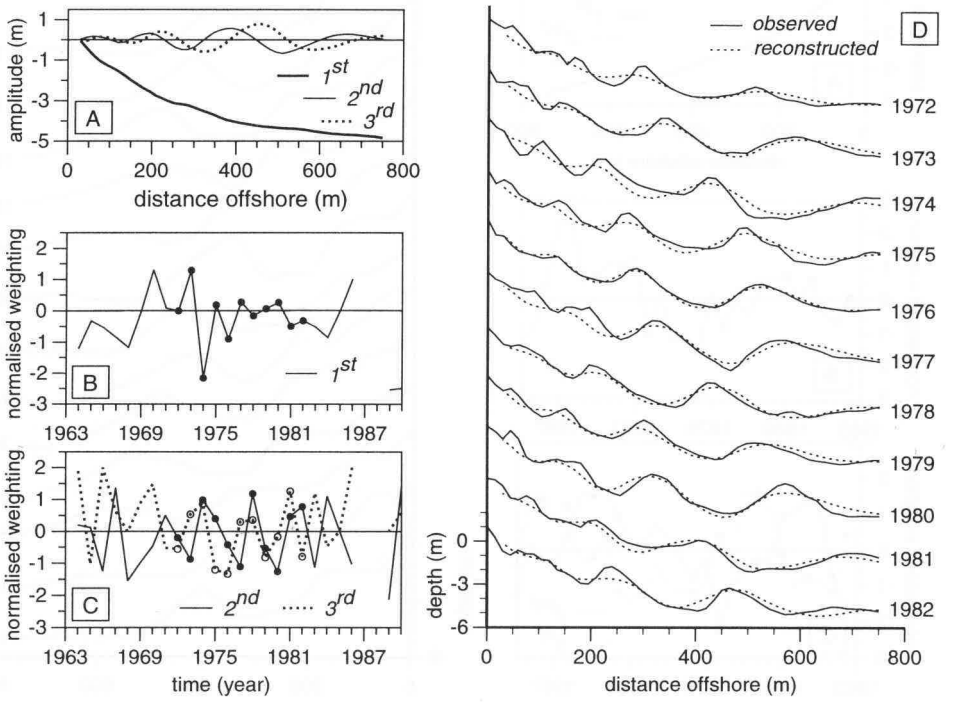

Figure 4.6: Example of the results of an eigenfunction analysis for some arbitrary window (km 69-70). (a) Shape of the first three eigenfunctions. (b) Weighting on the first eigenfunction of profiles at km 69.0 (c) Weighting on the second and third eigenfunction of profiles at km 69.0. (d) Selection of profiles observed at km 69.0 together with eigenfunction-based descriptions of these profiles. Only the first three eigenfunctions have been used to reconstruct these profiles. The dots in Figure (b) and (c) mark the weightings that are used in the reconstruction.

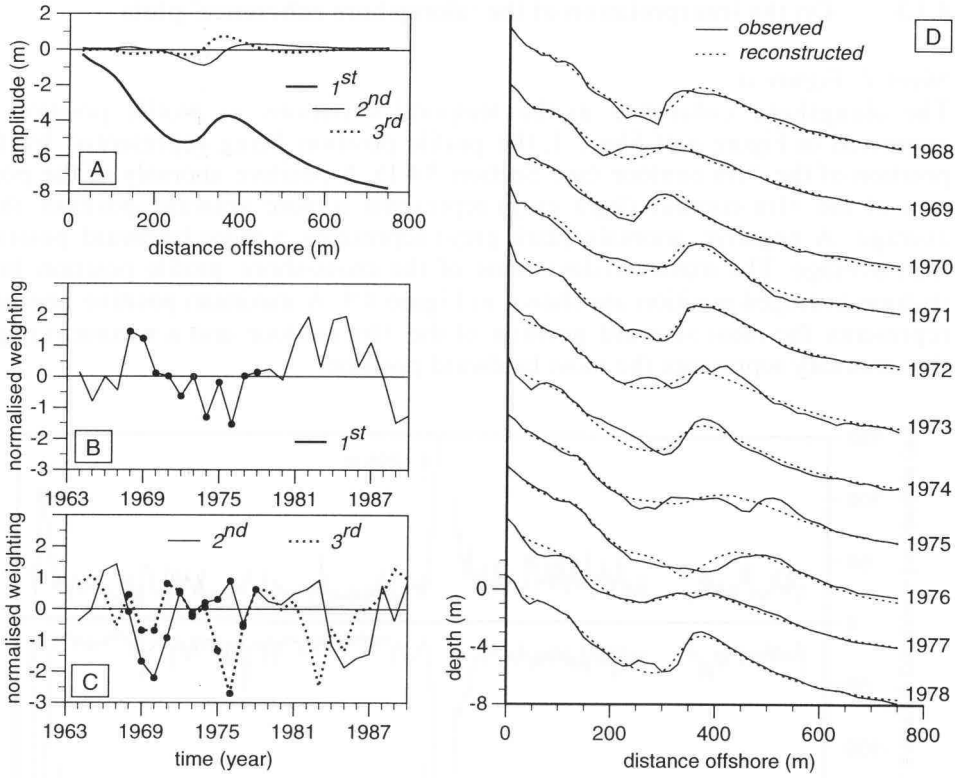

Figure 4.7: Example of the results of an eigenfunction analysis for some arbitrary window (km 12-13). (a) Shape of the first three eigenfunctions. (b) Weighting on the first eigenfunction of profiles at km 12.6 (c) Weighting on the second and third eigenfunction of profiles at km 12.6. (d) Selection of profiles observed at km 12.6 together with eigenfunction-based descriptions of these profiles. Only the first three eigenfunctions have been used to reconstruct these profiles. The dots in Figure (b) and (c) mark the weightings that are used in the reconstruction.

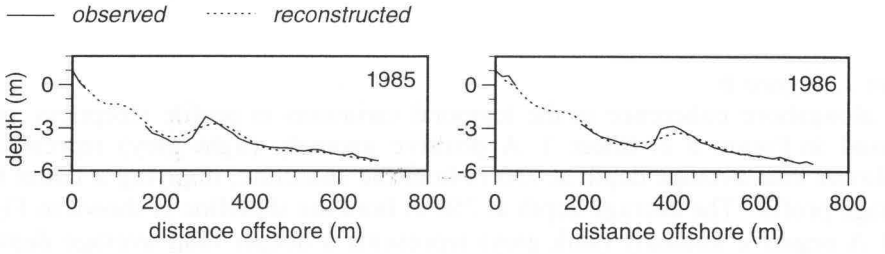

Figure 4.8: Two examples of reconstruction of incomplete profiles by three eigenfunctions

4.1.3 On the interpretation of the 'alongshore coherence' plots

Sheet 1, Figure a

The alongshore coherence in the temporal variations in profile position is expressed in Figure a of Sheet 1, the profile position being represented by the position of the +1m contour (see Section 3.4.1). A positive anomaly of the position of the +1m contour (light grey) represents a more seaward position than average. A negative anomaly (dark grey) represents a more landward position than average. The maximum deviations of the cross-shore profile position from its time-averaged position are shown in Figure 4.9. A maximum positive anomaly represents the most seaward position of the +1m contour and a maximum negative anomaly represents the most landward position.

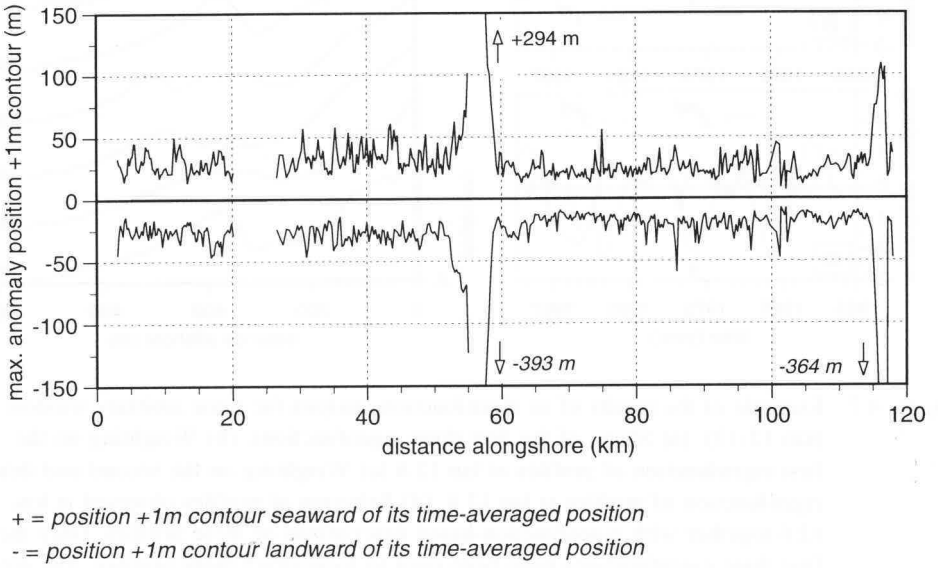

Figure 4.9: Maximum positive and negative anomalies of the position of the +1m contour relative to its time-averaged position.

Sheet 1, Figure b

The alongshore coherence in the temporal variations in profile steepness is expressed in Figure b of Sheet 1. A positive anomaly (light grey) represents a shallower than average depth at 750 m from the shoreline, implying a flatter than average profile. The average depth at 750 m from the shoreline is shown in Figure 4.10. A negative anomaly (dark grey) represents a deeper than average depth at 750 m from the shoreline, implying a steeper than average profile.

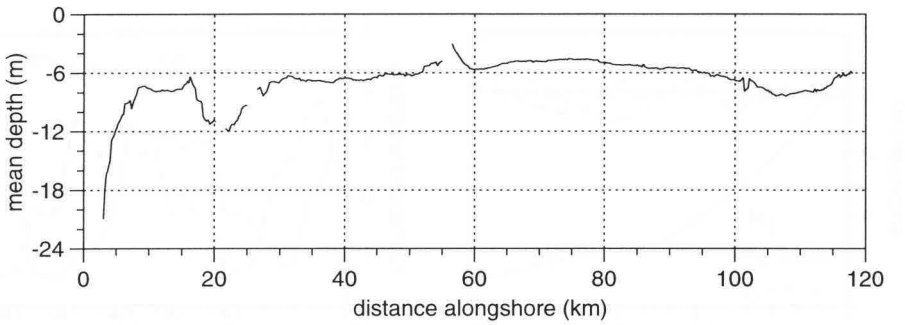

Figure 4.10: Mean depth at a distance of 750 m seaward of the +1m contour (derived from the first eigenfunctions).

Sheet 1, Figure c and Figure d

The alongshore coherence in the temporal variations in secondary morphology is expressed in Figure c and Figure d of Sheet 1. The morphological meaning of positive or negative weightings depends on the local shape of the second respectively third eigenfunction (e.g. Figure 4.3). Therefore, no common morphological interpretation exists of positive and negative weightings on the second and third eigenfunction.

An example of the interpretation of the weightings on the second and third eigenfunction is presented in Figure 4.11 and 4.12. Figure 4.11 shows the first three eigenfunctions at km section 31-32 and the weightings on the second and third eigenfunction for the profiles from the survey line at km 31.50. A positive weighting of the second (third) eigenfunction on a profile means that the bar topography in that profile compares well to that represented by the second (third) eigenfunction. A negative weighting of the second (third) eigenfunction on a profile means that the bar topography in that profile compares well to the mirror image of the topography represented by the second (third) eigenfunction. This means that bars are at trough locations and troughs at bar locations (Figure 4.12a).

The weightings of the second and third eigenfunction both exhibit the same periodicity in time but with a phase shift of 90 degrees (Figure 4.11b). Maxima in weightings of the second eigenfunction then coincide with near-zero values of the third eigenfunction and vice versa. The weightings of the second eigenfunction are leading those of the third eigenfunction. The morphological meaning of these two curves is that on the long term the bars move in a net offshore direction with the outer bar fading away at the seaward end, and with a new bar being generated near the shoreline (Figure 4.12). As a consequence, the former inner bar becomes the outer bar. This new outer bar ends up at approximately the same location as its predecessor and reduces in height at its turn, starting a new cycle.

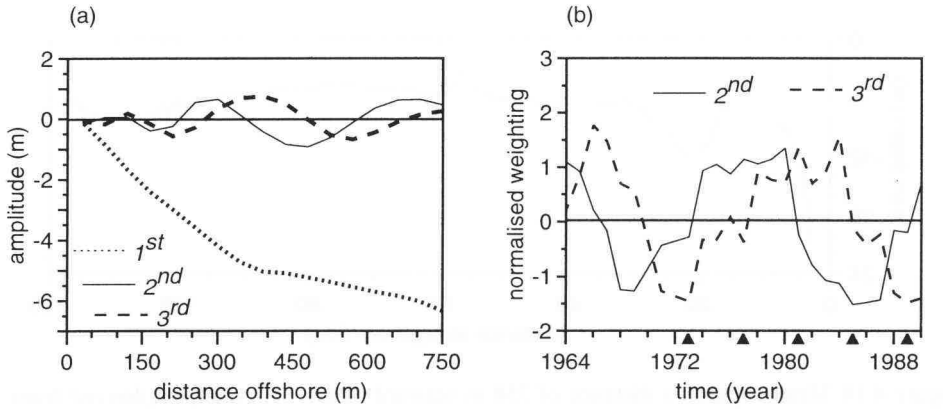

Figure 4.11: Results of the empirical eigenfunction analysis of profiles located between km 31 and km 32. (a) First three eigenfunctions; (b) Weightings on the second and third eigenfunctions of profiles located at km 31.5. (Black triangles mark the profiles that are plotted in Figure 4.12b.)

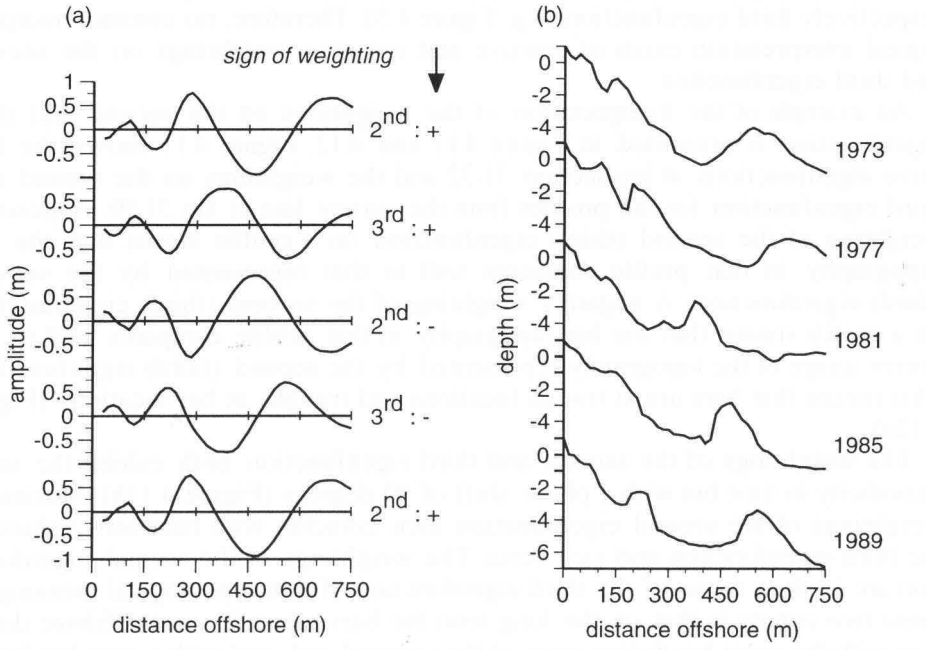

Figure 4.12: Cyclic bar system behaviour in a multiple bar system, demonstrated by (a) the second and third eigenfunction (km 31-32), (b) five selected profiles with large positive or negative weightings on either the second or the third eigenfunction (see Figure 4.11b).

The above mentioned interpretation of weightings on the second and third eigenfunction is applicable when the first eigenfunction is a (nearly) barless mean profile function and the second and third eigenfunction describe a multiple bar topography. In addition, the weightings on the second and third eigenfunction should vary periodically in time, and the periodic signals should have a phase difference of about 90 degrees. These conditions are fulfilled along large stretches of the Holland coast (approximately between km 23 and km 98). Figure 4.5 and 4.6 show two additional examples of the cyclic bar system behaviour.

For the above mentioned type of eigenfunctions the alongshore coherence in weightings on second and third eigenfunctions has the following meaning. When the shapes of the second and third eigenfunctions do not vary along a certain stretch and the weightings on the second and third eigenfunction are constant along that stretch at time *t*, then a set of straight, shore-parallel bars is present along that stretch at time *t*. When the weightings vary alongshore at time *t* -and the shapes of the eigenfunctions are still invariable alongshore- this indicates an alongshore variation in the cross-shore bar topography at time *t*. When the weightings are constant alongshore at time *t*, but the shapes of the eigenfunctions vary alongshore, this also describes an alongshore varying cross-shore bar topography. The character of the alongshore variation will depend on the local combination of eigenfunction shapes and eigenfunction weightings. The interpretation of the alongshore varying patterns shown in Figure c and d (Sheet 1) is given in Section 4.2.3 (also see Chapter 5).

4.2 Alongshore coherence in decadal profile developments

4.2.1 The cross-shore position of the sub-aqueous profile (Sheet 1: Figure a)

The cross-shore position of the sub-aqueous profile has been chosen to be represented by the cross-shore position of the +1m contour. From km 21 to 25, the Petten seawall prohibits change in the position of the +1m contour (Sheet 1: Figure a). Therefore, the seawall prohibits a change in cross-shore position of the sub-aqueous profile. The shape of the sub-aqueous profile can still change of course.

The extension of the harbour moles of IJmuiden (km 55.5) in 1962-1967 resulted in shoreline progradation directly north and south of the harbour moles (km 52-59), and shoreline retreat further south (km 59-63). Figure 4.9 reveals the magnitude of the change in shoreline position. The extension of the harbour moles of Scheveningen (km 102) in 1968-1970 also caused some shoreline progradation directly north and south of the harbour moles (km 100-104). Further north it caused some small shoreline retreat (roughly km 94-99). The extension of the harbour moles near Hoek van Holland (km 119) in 1968-1972 was combined with a large nourishment of about 19 million cubic meters of sand (km 115.7-119). These interventions caused a large progradation of the shoreline, and consequently a

seaward shift of the sub-aqueous profile (km 114-118) (Sheet 1: Figure a, and Figure 4.9).

The alongshore differences in developments of the cross-shore profile position not directly related to man-made structures are the following. From km 4 to 7 and from km 16 to 20, the shoreline shifts landward, and so does the sub-aqueous profile (given the aforementioned concept for analysing profile behaviour). The shoreline progradation between km 10 and 16 in the late eighties, seems to be related to a large nourishment in 1986 (1.3 million cubic meters between km 10 and 14). From km 7 to 10, the shoreline fluctuates around some mean position, without a clear trend.

From km 26 to 38 the shoreline shifts net landward while from km 38 to km 52 the shoreline fluctuates around some mean position, without showing a clear trend in time. From km 30 to km 52, the fluctuations in shoreline position (superimposed on any trend) seem to exhibit alongshore and temporal coherence (Sheet 1: Figure a). At every alongshore location the position of the shoreline fluctuates periodically onshore and offshore over time spans of many years. The onshore movement and offshore movement do not occur synchronously alongshore, but vary more or less periodically. The length-scale of this alongshore periodicity is about 2 km. Combination of the two observations gives the impression of a mainly southward moving pattern of periodic shoreline fluctuations (Figure 4.13).

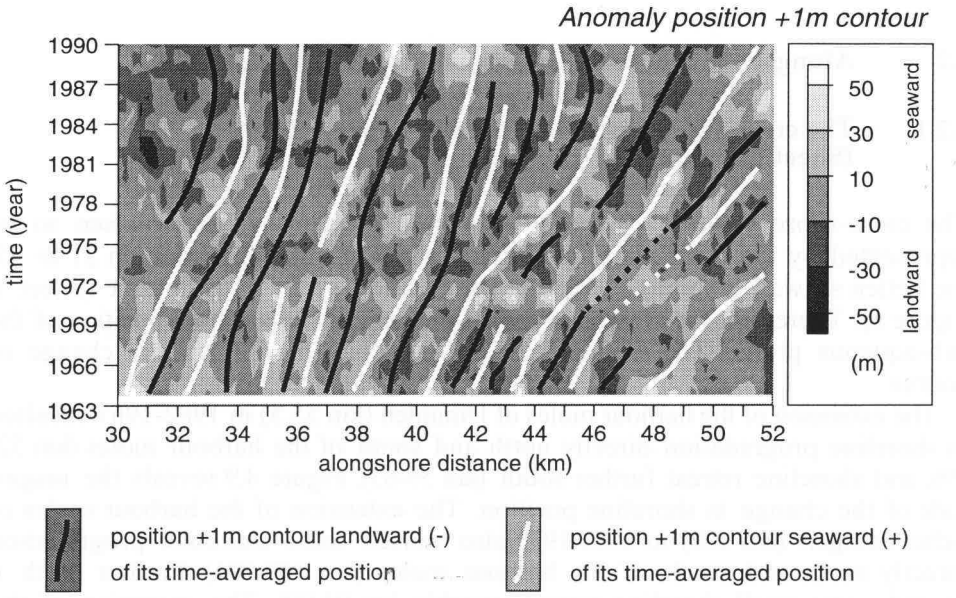

Figure 4.13: Spatial and temporal coherence in fluctuations of shoreline position, km 30-52.

From km 63 to 95 the position of the shoreline fluctuates around the time-averaged position from year to year. Some large-scale alongshore coherence in the shoreline position fluctuations is present, but longer term temporal coherence seems to be absent.

From km 104 to 114 the temporal and alongshore coherence in shoreline movement is small. Most of the fluctuations in shoreline position remain within 10 m of the time-averaged shoreline position.

Linear trends in shoreline movement (determined per window) are often not statistically significant at the 1% level (Figure 4.14). The statistically significant linear correlations generally explain less than 25 per cent of the total variance in the data (R^2). This implies that the deviations from the trend are large compared to the change in shoreline position explained by the trend. So, over a time span of nearly three decades, the fluctuations in position of the shoreline are large compared to some possibly present linear trend. In addition, the slope of these linear trends will not be representative for longer periods of time when the deviations from the trend are organised as long-term fluctuations (e.g. the pattern of shoreline retreat and progradation between km 30 and 50).

The long-term trend of shoreline retreat north of about km 40 (see Section 2.3.2) is generally present over the 3 decade period. In more detail deviations exist, such as the small stable stretch around km 10 (Sheet 1: Figure a, and Figure 4.14), and of course in front of the seawall.

The small trend of shoreline progradation that was observed over the last century in between km 40 and km 95 (see Section 2.3.2), becomes weakly visible over the 3 decade time span only south of km 63, that is south of the disturbance imposed by the IJmuiden harbour moles (Figure 4.14, and Sheet 1: Figure a).

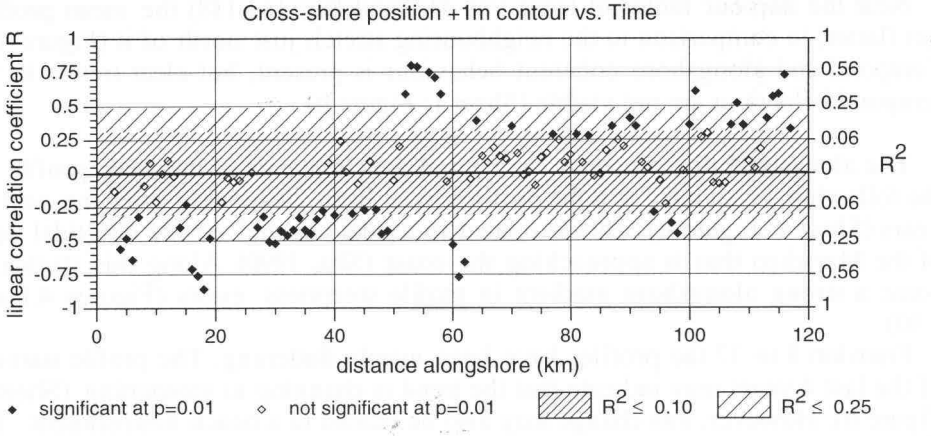

Figure 4.14: Direction and statistical significance of linear correlation of shoreline position versus time (determined per analysis window). A positive (negative) correlation means the shoreline is prograding (retreating).

North of the disturbance imposed by the IJmuiden harbour moles, i.e. north of about km 48, the position of the shoreline is more or less stable over the 3 decade period. One may even recognise a very slight tendency of shoreline retreat along this stretch between about km 40 and km 48 (Figure 4.14).

4.2.2 The mean profile (Figure 4.1, and Sheet 1: Figure b)

The impact of coastal structures on the mean profile shape is most obvious near the seawall of Petten (km 17-27) (Figures 4.1 and 4.10). The average profiles are much steeper than the surrounding profiles, because the upper part of the profile remained at a fixed location while the development of the offshore part of the profiles in front of the seawall was similar to that of the surrounding profiles. The surrounding profiles shifted landward after the seawall was constructed at its present location in 1823 (Stolk, 1989). In front of the seawall, the fluctuations of the mean profile steepness are both temporal and alongshore coherent (Sheet 1: Figure b).

Just north and south of the harbour moles of IJmuiden the profiles are flatter than the surrounding profiles (km 53-58) (Figures 4.1 and 4.10). The extension of the moles in 1962-1967 caused an additional flattening of the profiles (Sheet 1: Figure b). The flattening is mainly observed south of the moles (km 56-59). Farther south some steepening of the profiles occurred (km 59-66).

The harbour moles of Scheveningen do not seem to affect the time-averaged mean profile shape (Figure 4.1). The extension of the harbour moles in 1968-1970 has caused some flattening of the profile to the south (km 102-103) (Sheet 1: Figure b). It is not clear whether the steepening to the north (km 98.5-100.5) is also related to this human interference.

Near the harbour moles of Hoek van Holland (km 114-118) the mean profiles get flatter, in comparison to the neighbouring stretch just north of it (Figure 4.1). Temporal and alongshore coherent behaviour is present, but clear trends in the temporal behaviour are not visible (Sheet 1: Figure b).

The alongshore differences in the natural developments of the mean profile are the following. From km 3 to 8 the profiles have been steepening over the past 27 years (Sheet 1: Figure b). This is related to a tidal channel on the ebb-tidal delta of the Marsdiep that is approaching the coast (Sha, 1990). Along this stretch of coast a strong alongshore gradient in profile steepness exists (Figures 4.1 and 4.10).

From km 8 to 17 the profiles have been mainly flattening. The profile surveys of the last 4 years may indicate that the trend is changing to steepening (Sheet 1: Figure b). However, this change may also be related to a beach nourishment. The character of the mean topography on this stretch is quite correlated alongshore (Figure 4.1). From km 8 to 16 about the same profile steepness exists (Figures 4.1 and 4.10). In most profiles a bar with a relatively stable position is present. The mean profile representing km 16-17 is quite different from neighbouring profiles.

From km 27 to 53 the mean profile steepness is approximately constant (Figures 4.1 and 4.10). The mean profile tends to be more or less barless along this stretch, although several mean profile functions still contain some remainders of bar topography (Figures 4.1 and 4.15). The presence of some residual bar topography in the first eigenfunction is related to the occurrence of cyclic net offshore bar migration over about a 15 year period (see Section 4.2.3). The profile data base spans a 27 year period. Consequently, bars may have an apparently preferred position over the considered time span. Having longer time series available, the bar features will disappear from the mean profile functions (cf. mean profile functions between km 66 and km 98). Large-scale alongshore and temporal coherence in profile steepness variation exist (Sheet 1: Figure b). Longer term fluctuations in mean profile steepness seem to be present over time spans of about 10 to 20 years.

From km 66 to 98 most of the observed variation in profile steepness does not exceed the accuracy of the measurements (Sheet 1: Figure b). Generally, there is little temporal coherence between the variation in steepness. Therefore, most of the observed variation has to do with fluctuations that occur within a year.

From km 103 to 114 the variation in profile steepness exceeds the accuracy of the data more often (Sheet 1: Figure b). Some temporal coherence as well as alongshore coherence is present in the fluctuations of profile steepness, especially in the period 1969-1978. This period happens to include the period of large human intervention in the coastal system just south of this area (see Section 2.2.6).

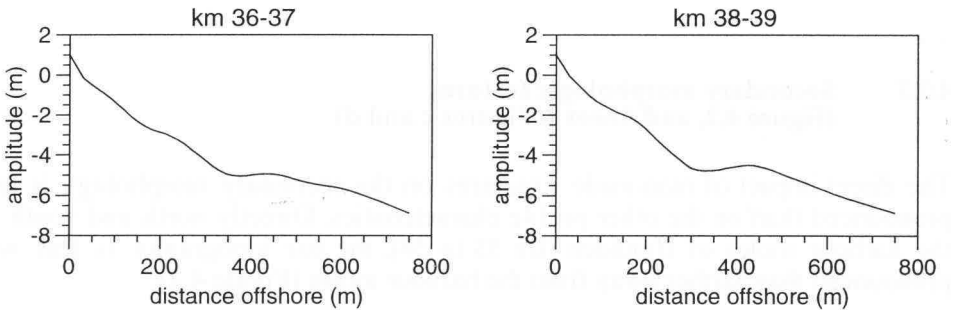

Figure 4.15: Two examples illustrating the presence of some remainders of bar topography in the first eigenfunction.

At a 1% level of significance, statistically significant linear trends are present in the temporal change in profile steepness. These significant linear trends generally explain less than 25 per cent of the total variance in the data (Figure 4.16). This implies that the deviations from the trend are usually large compared to the change explained by the trend. So, over a time span of nearly three decades, the fluctuations in profile steepness are larger than some possibly

present linear trend. Deviations from the trend that are organised as long-term fluctuations, may strongly influence the slope of linear trends (cf. Bakker and De Vroeg,1988). This situation occurs, for example, in the area between km 45 and 50.

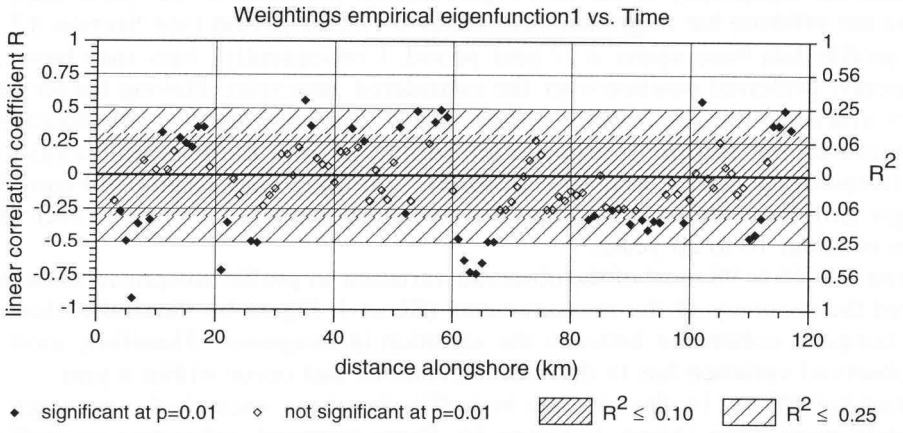

Figure 4.16: Direction and statistical significance of linear correlation of profile steepness -represented by weightings on the first empirical eigenfunctions- versus time (determined per analysis window). A positive (negative) correlation means the profile is flattening (steepening).

4.2.3 Secondary morphologic features (Figure 4.2, and Sheet 1: Figures c and d)

The direct impact of man-made structures on the secondary morphology is less pronounced than on the other profile characteristics. Directly north and south of the harbour moles of IJmuiden (km 53 to 58), the bar topography is less well pronounced than farther away from the harbour moles (Figure 4.2).

The following natural developments are observed. From km 3 to 8 a small bar at about 250 m off the shoreline is present (Figure 4.17). Through time, from km 3 to 6, this bar moves in onshore direction (Figure 4.18). Between km 6 to 8 the bar behaviour is less clearly organised. Between km 3 and 4 an important deviation from the mean profile is related to a change in concavity of the profile (Figures 4.2a, 4.2c, and 4.3). The change in concavity is related to the behaviour of a tidal channel on the ebb delta of the Marsdiep.

From km 8 to 21 a bar is present with a quite stable position over a time span of 27 years (Figure 4.1). The shapes of the second and third eigenfunction therefore relate to small modulations in height and position of the bar (Figure 4.2). These modulations do not occur in a very organised manner, in comparison to other

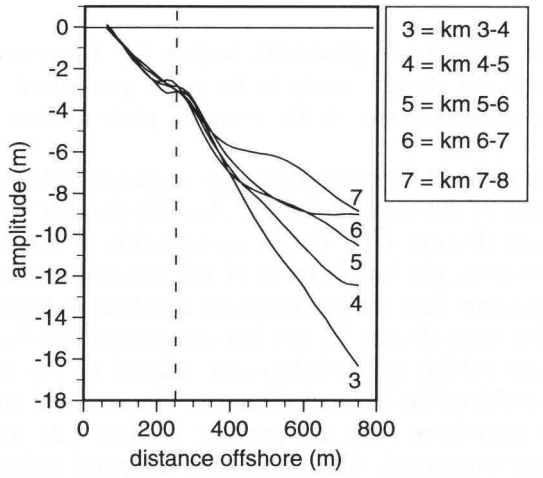

Figure 4.17:
First eigenfunctions, of windows km 3-4 to km 7-8.

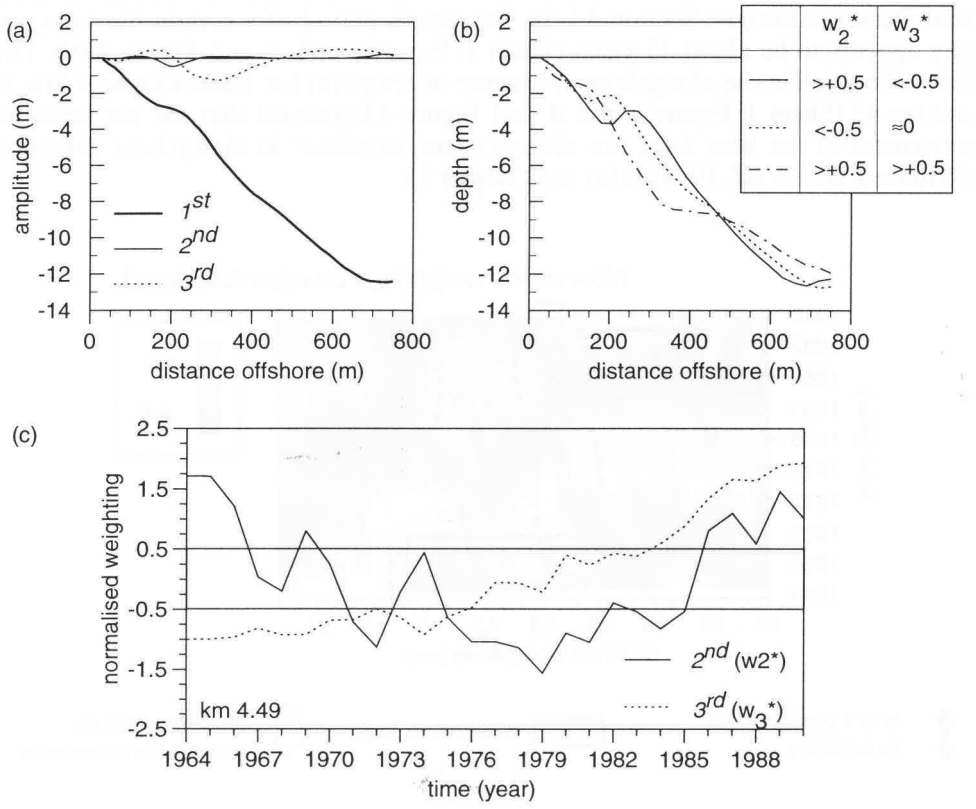

Figure 4.18: (a) First 3 eigenfunctions of window km 4-5. (b) Interpretation of weightings on eigenfunctions 2 and 3 presented in Sheet1, Figure c and d (km 4-5). (c) Example of normalised weightings on eigenfunctions 2 and 3 at km 4.49.

stretches. Between km 15 to 18 the alongshore gradients within the 1 km wide analysis window in bar position and bar height seem to be quite persistent in time. This follows from the narrow vertical bands in the contour plots (Sheet 1: Figure c and d).

From km 21 to 26, in front of the seawall, a gradual change in large-scale bar behaviour occurs. At the northern end of the seawall (km 21, km 22) one bar with a reasonably stable position is present (Figure 4.1). This is comparable to the bar behaviour north of the seawall. However, the bar in front of the seawall exhibits more coherence in its temporal behaviour than the bar north of it (Sheet 1: Figure c and d). At the southern end of the seawall (km 23, km 24) sometimes two bars are present (Figure 4.2d). These bars exhibit cyclic behaviour related to the behaviour of the multiple bar system south of the seawall (Sheet 1: Figure c and d).

From km 26 to 53 two to three nearshore bars are present (Figure 4.2). The behaviour of this bar system is very organised. The combined temporal behaviour of the second and third empirical eigenfunction shows that all bars move in a net offshore direction, with the outer bar fading away and a new bar developing near the shoreline (see Section 4.1.3). The return period of a certain bar topography appears to be about 15 years (Sheet 1: Figure c and d, and Figure 4.19). The discontinuities in the alongshore coherence in temporal bar behaviour near km 38 and km 45 (Sheet 1: Figure c and d, and Figure 4.19) reveal that the net offshore movement of the bars does not always occur 'in phase' in alongshore direction (Wijnberg and Wolf, 1994) (also see Chapter 5).

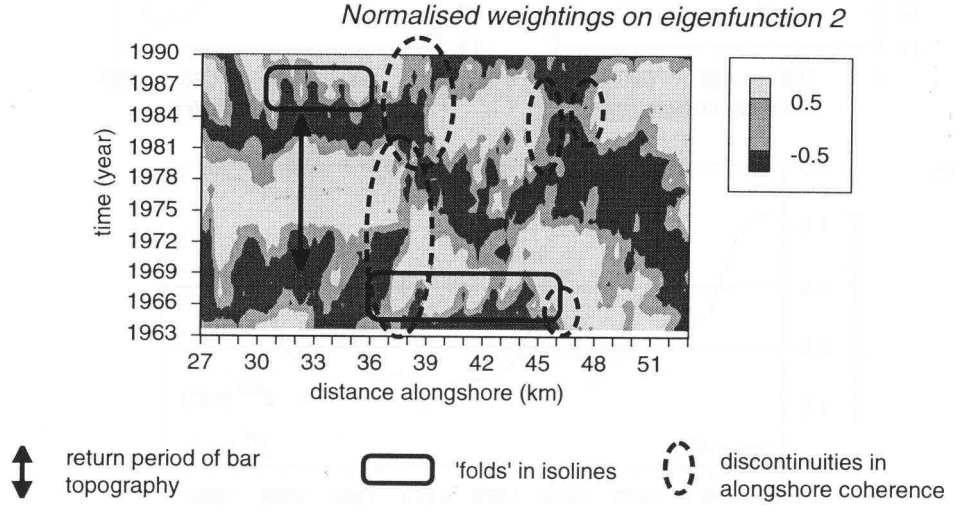

Figure 4.19: Definition sketch of 'discontinuities in alongshore coherence', 'return period of bar topography', and 'folds in isolines of equal weightings'. (Normalised weightings second eigenfunctions, km 27-53).

The 'folds' in the isolines of equal weightings, for example in Figure c of Sheet 1 between km 30 and 37 in the years 1984 to 1987 (also see Figure 4.19), indicate that a well developed rhythmic pattern is present in the bar topography over a period of several years. The alongshore scale of this rhythmic topography is about 2 km.

From km 58 to 98 another multiple bar system is present which also exhibits very organised behaviour. The number of bars in this area varies. In the central part 3 to 4 bars are present, whereas in the southern and northern part 2 to 3 bars are present (Figure 4.2). The spacing of the bars and the size of the bars in this bar system are generally smaller than in the multiple bar system between km 26 and 53. The temporal behaviour of the bars is similar to that of the bars north of IJmuiden, i.e. a net offshore movement, with the outer bar fading away, and a new bar developing near the shoreline (Figure 4.2 and Sheet 1: Figures c and d). However, the return period of a certain bar topography is much smaller, viz. about 4 year. Further, the alongshore coherence in offshore bar movement seems to be larger than in the area between km 26 and 53. Nevertheless, discontinuities in the alongshore coherence do occur, for example near km 67 in 1970 (Sheet 1: Figure c). This discontinuity is not caused by differences in the date of sounding.

The occurrence of the systematic offshore migration of the nearshore bars was already mentioned by Edelman (1974), but he did not notice the alongshore coherence in this behaviour as revealed by the eigenfunction analysis.

From km 102 to 118 generally one small bar is present (Figure 4.2). However, two low bars may be present as well, or bars may be absent. Temporal and alongshore coherence in profile behaviour exists, but it is much less well organised than it is to the north (Sheet 1: Figure c and d).

4.2.4 Relation between profile shape change and cross-shore profile shift

The shape of the sub-aqueous profile (with a fixed length) has been analysed relative to a floating reference line. When all absolute changes in the profile are restricted to the uppermost part of the sub-aqueous profile, all the above described changes in profile shape can be considered as being induced by changes in the position of the reference line. It will be examined to what extent the observed changes in profile shape are related to changes in position of the reference line (i.e. the +1m contour).

The following changes in profile shape can be (geometrically) induced by changes in position of the reference line. A shoreline retreat should result in a flattening of the profile and a more seaward position of the bars, relative to the shoreline (Figure 4.20). A prograding shoreline should result in a steepening of the profile and a relative more landward position of the bars.

If these relations exist in the profile data set, a negative correlation is to be expected between the anomaly in the shoreline position and the weighting on the first eigenfunction. When the shoreline is landward (seaward) of its time-averaged position this is described by a negative (positive) anomaly of the

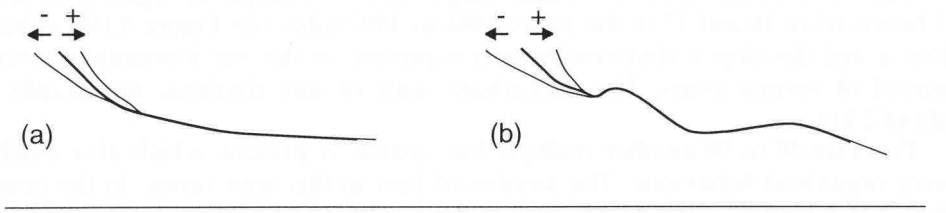

Figure 4.20: Geometric relations between changes in the shoreline position (plus the uppermost part of the profile) and the shape of the complete profile up to 750 m from the shoreline. (a) Relation shoreline position vs. profile steepness; (b) relation shoreline position vs. bar position relative to the shoreline.

shoreline position, and when the profile is flatter (steeper) than average, this is described by a positive (negative) weighting on the first eigenfunction.

The relation between the shoreline position and bar position should result in a some correlation between the anomaly in shoreline position and the weightings on the second and third eigenfunction. The sign of the correlation depends on the local shape of the eigenfunctions. For example, near km 84 a positive (negative) weighting on the second eigenfunction relates to a more landward (seaward) position of the most pronounced bars (Figures 4.21 and 4.2a,c); a positive (negative) weighting on the third eigenfunction also relates to a more landward (seaward) position of the most pronounced bars (Figures 4.21b and 4.2b,d). Another example, near km 31, shows that also the opposite relations may exist (Figures 4.22a and 4.2a,c , and Figures 4.22b and 4.2b,d). This results in negative correlations between the anomaly in shoreline position and the weightings on the second and third eigenfunction.

Linear correlations (per window) between 'weightings on the first eigenfunction' and 'shoreline position' show that the above described type of correlation between shoreline position and profile steepness only weakly exists (Figure 4.23a). Usually, less than 25 per cent of the variation in profile steepness is related to the shifting of the reference line. Locally, the direction of the correlation may be even opposite to that proposed above.

Linear correlations between 'weightings on the second eigenfunction' and 'shoreline position' and linear correlations between 'weightings on the third eigenfunction' and 'shoreline position' (Figure 4.23b and 4.23c) show that the correlation between the reference line position and the relative bar position is very weak. Generally, less than 10 per cent of the variation in bar position is correlated with a change in shoreline position. The direction of the correlation may even be opposite to that proposed above. The low correlation between shoreline position and weightings on the second and third eigenfunctions may be due to a lack of correlation between shoreline position and bar position. However, another

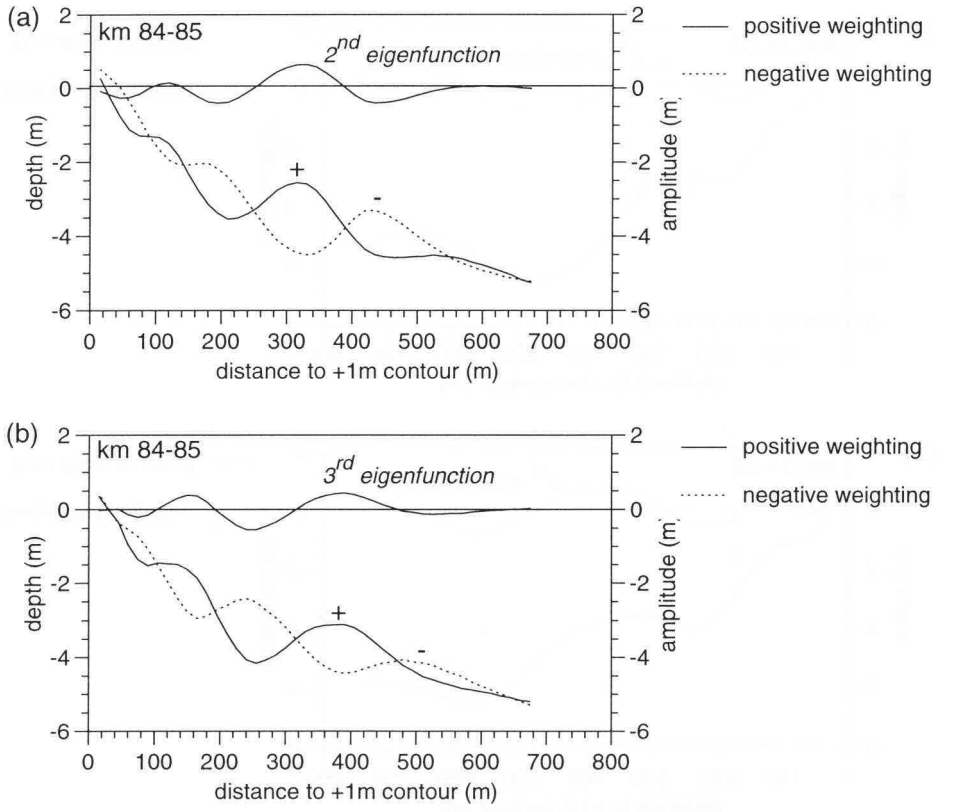

Figure 4.21: Bar position relative to the shoreline, near km 84, in relation to the sign of (a) the weighting on the second eigenfunction, (b) the weighting on the third eigenfunction.

reason for the lack of correlation may be that the description of the position of the bars by a single eigenfunction only allows for two modes of bar positions. Between these two modes the bar positions differ by about 100 to 200 m. The fluctuations in the shoreline position are generally much smaller (Figure 4.9). Therefore, the observed range of shoreline position will generally not induce a complete change of the bar position mode, i.e. a switch from a large negative weighting to a large positive weighting or vice versa.

The above findings show that the observed changes in profile shape are not simply induced by the definition of a floating reference line. Another indication that the observed profile shape behaviour is not just a function of the moving reference line follows from the comparison of Figure a of Sheet 1 to Figures b, c, and d of Sheet 1. This comparison reveals that the patterns of change in reference line position (Sheet 1: Figure a) are generally different from the patterns of change in profile shape.

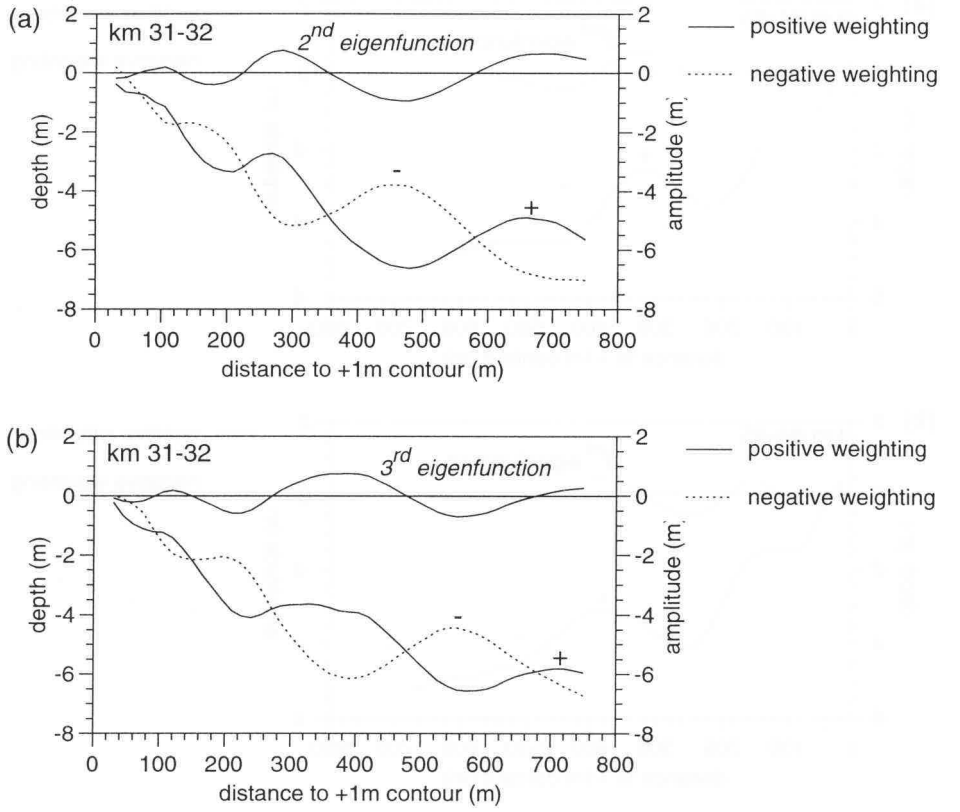

Figure 4.22: Bar position relative to the shoreline, near km 31, in relation to the sign of (a) the weighting on the second eigenfunction, (b) the weighting on the third eigenfunction.

The direction or slope of long-term *trends* in shoreline position do not seem to be related to the average shape characteristics of the nearshore profile. This is suggested by the coastal behaviour observed between km 30 and 50: the average profile shape characteristics (Figures 4.1 and 4.2) do not exhibit an alongshore gradient but the trend in shoreline movement (Sheet 1: Figure a) does, viz. from slightly retreating in the north to being stable in the south.

The *fluctuations* in shoreline position -i.e. the deviations in shoreline position from a trend, if any- do seem to be related to the temporal fluctuations in the shape of the nearshore profile. This is suggested by the southward moving pattern of shoreline retreat and progradation between km 30 and 50 (Sheet 1: Figure a), which appears to coincide with the presence of rhythmic bars that exhibit cyclic temporal behaviour (Sheet 1: Figure c and d). The alongshore scales of the two phenomena (about 2 km) coincide. The temporal scales are in the same order of magnitude. In addition, the profile steepness (Sheet 1: Figure

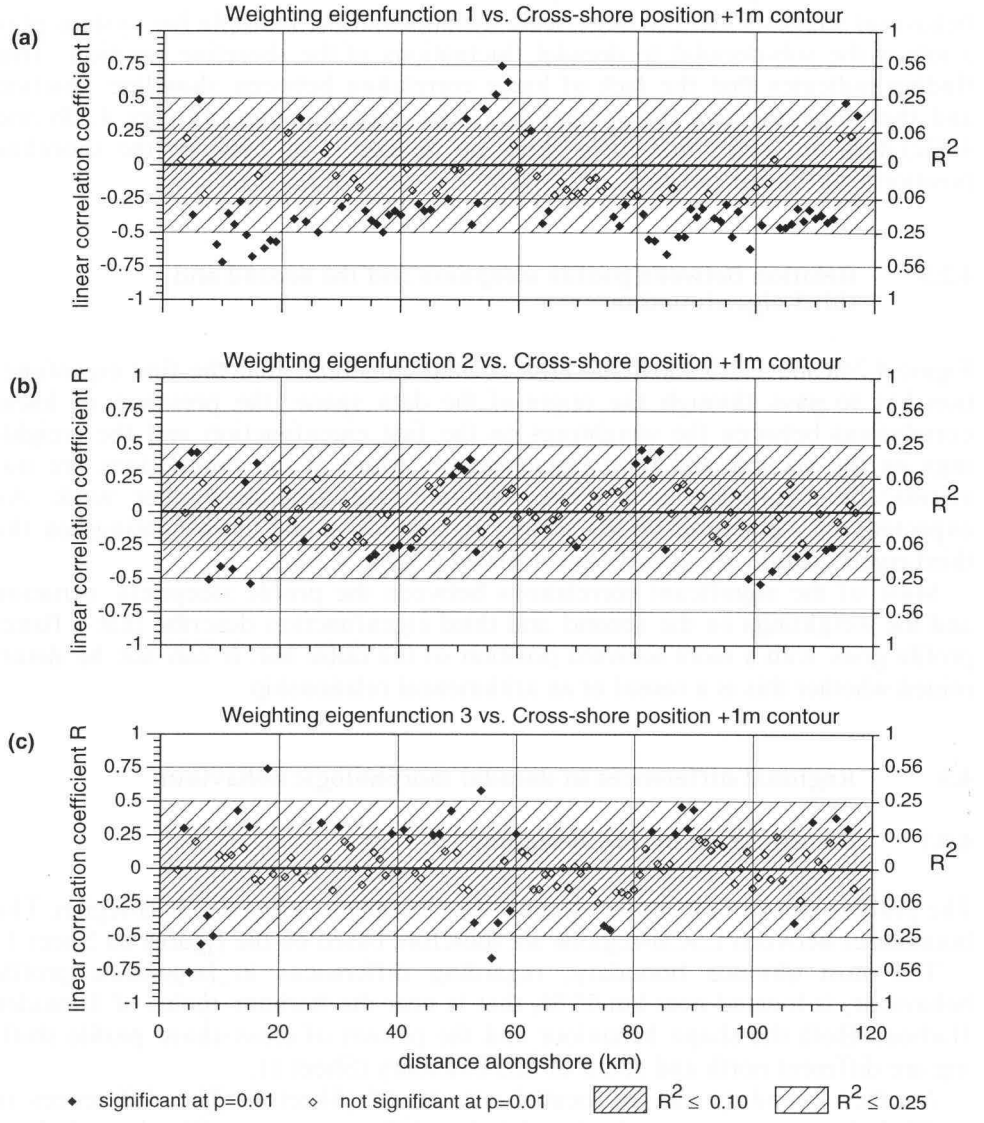

Figure 4.23: Direction and statistical significance of linear correlations (determined per analysis window) of: (a) weightings on the first empirical eigenfunctions versus the shoreline position, (b) weightings on the re-arranged second empirical eigenfunctions versus the shoreline position, (c) weightings on the re-arranged third empirical eigenfunctions versus the shoreline position.

9b) seems to exhibit some weak alongshore variation in steepening and flattening with comparable scales. Cause and effect relations were not determined, but the similarity of alongshore and temporal scales of shoreline behaviour and bar behaviour suggests that the large-scale dynamics of the multiple bar system play a role in the sub-decadal to decadal fluctuations of the shoreline position. This finding indicates that the lack of linear correlation between shoreline position and the weightings on the second and third eigenfunctions (Figure 4.23b and 4.23c) does not imply that there exists no relation at all between the shoreline position and the bar position.

4.2.5 Relation between profile steepness and the second and third eigenfunction

Figure 4.24a and 4.24b show the effect of the constraint that the first eigenfunction has to pass through the origin of the data space: the presence of linear correlations between the weightings on the first eigenfunction and the weightings on the second and third eigenfunction. Most of the correlations are not statistically significant, and those who are, are generally rather weak. As expected, the weightings on the second eigenfunction and the weightings on the third eigenfunction are linearly uncorrelated (Figure 4.24c).

Most of the significant correlations between the profile steepness variation and the weightings on the second and third eigenfunction describe that a flatter profile goes with a more seaward position of the outer bar. It can not be determined whether this is a causal or an arithmetical relationship.

4.3 Regional differences in decadal morphologic behaviour

4.3.1 Identification of 'LSCB-regions'

The profiles that exhibit similar decadal developments define a LSCB-region. The boundaries between LSCB-regions are therefore based on the figures on Sheet 1.

The most obvious boundary, regarding differences in large-scale profile behaviour, is located near km 55/56, that is near the harbour moles of IJmuiden Harbour. Both the shape behaviour and the pattern of cross-shore profile shifting are different north and south of this boundary (Sheet 1).

Another boundary can be located near km 98 (Sheet 1). The differences in profile behaviour are most clearly related to differences in profile shape behaviour, especially of the 'secondary' topography (Sheet 1: Figure c and d). The differences in the pattern of profile shifting (Sheet 1: Figure a) are largely determined by the differences in the disturbance due to human intervention, which is much larger south of this boundary (see Section 2.2.6).

A third boundary can be located near km 8 (see especially Sheet 1: Figure b, and Figure 4.2). This boundary separates an area in which the profile shape

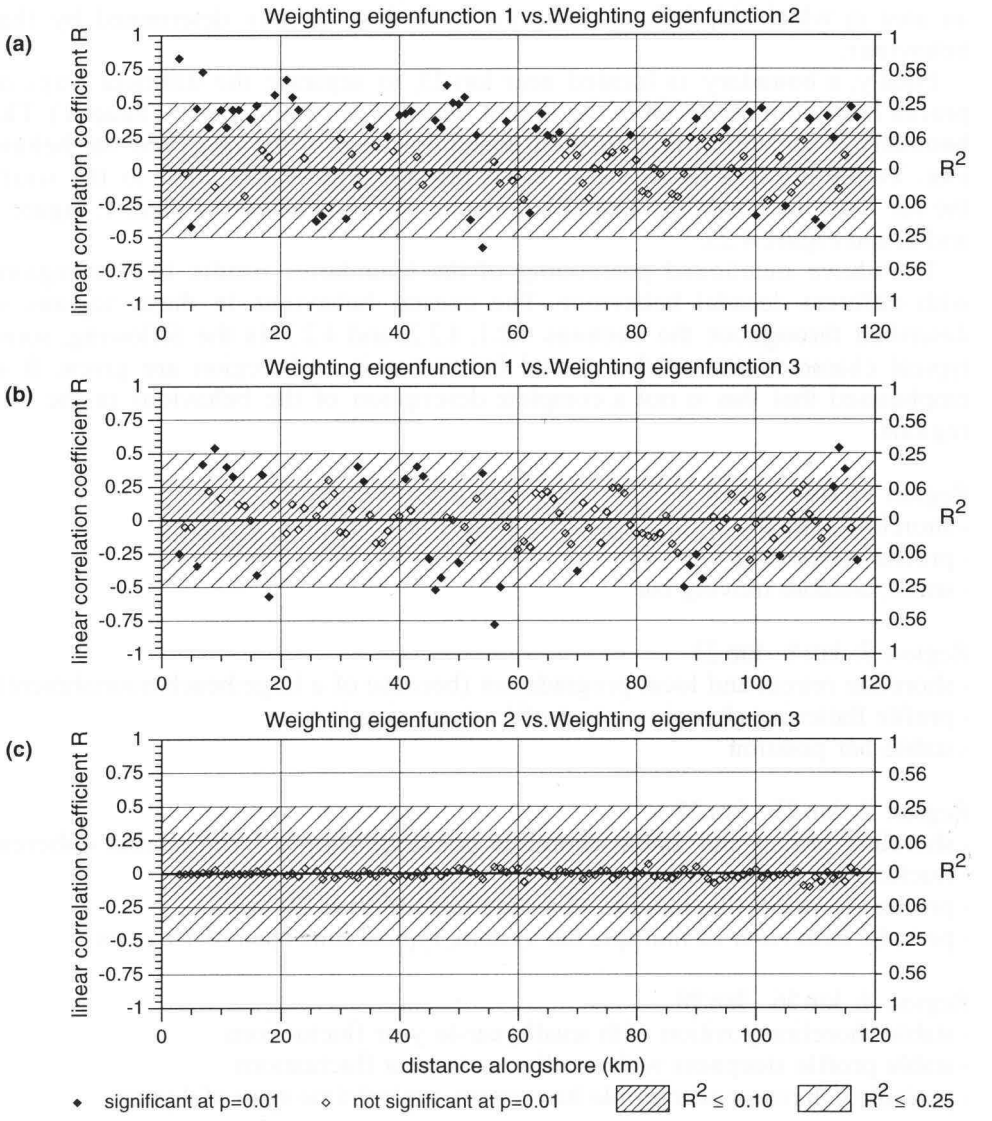

Figure 4.24: Direction and statistical significance of linear correlations (determined per analysis window) of: (a) weightings on the first empirical eigenfunctions versus weightings on the re-arranged second empirical eigenfunctions, (b) weightings on the first empirical eigenfunctions versus weightings on the re-arranged third empirical eigenfunctions, (c) weightings on the re-arrangred second empirical eigenfunctions versus weightings on the re-arranged third empirical eigenfunctions.

behaviour is largely determined by the developments of an ebb-tidal delta, from an area in which this behaviour seems to be less directly determined by that behaviour.

Finally, a boundary is located near km 23, to separate the different ways of profile behaviour observed in the region between km 8 and km 55 (Sheet 1). The boundary is located at this position mainly because of the observed bar behaviour. To the north, a rather stable bar is present (Figure 4.1), while to the south the bar behaviour exhibits spatially coherent cyclic behaviour (Sheet 1: Figure c and d, and Figure 4.2).

The above mentioned positioning of the boundaries results in five regions with different decadal behaviour. The coastal behaviour in these regions is described throughout the Sections 4.2.1, 4.2.2, and 4.2.3. In the following, some typical characteristics of the coastal behaviour in each region are given. It is emphasised that this is not a complete description of the behaviour in the five regions.

Region 1: km 3 - km 8
- shoreline retreat
- profile steepening
- small, onshore moving bar

Region 2: km 8 - km 23
- shoreline retreat and local progradation (because of a large beach nourishment)
- profile flattening changing into profile steepening in time
- stable bar position

Region 3: km 23 - km 55
- shoreline retreat and stable shoreline position; temporal and spatial coherent fluctuations in shoreline position
- profile steepness fluctuations on a time span of 10 to 20 years.
- periodic behaviour of multiple bar system, typical time span of 15 years

Region 4: km 56 - km 98
- stable shoreline position with small year-to year fluctuations
- stable profile steepness with small year-to-year fluctuations
- periodic behaviour of multiple bar system, typical time span of 4 years

Region 5: km 98 - km 118
- small shoreline fluctuations, except for man-induced shoreline progradation due to harbour mole extensions near Scheveningen and Hoek van Holland and related extensive beach nourishment km 116-119
- profile steepness fluctuations (related to human interventions ?)
- low bars sometimes present

Within the LSCB-regions, alongshore gradients in the average profile shape characteristics may exist. For example, Region 4 contains an alongshore gradient in mean profile steepness that goes with a gradient in the seaward extension of the multiple bar system and the number of bars (Figures 4.1 and 4.2). Alongshore gradients in temporal behaviour within a LSCB-region are small when compared to differences between regions.

The change in behaviour between LSCB-regions occurs over alongshore distances as short as about 2 km, except for the more gradual boundary in front of the Petten seawall. The quite sharp boundaries are especially found for the large-scale behaviour of the 'secondary' topography (Sheet 1: Figure c and d). Considering the behaviour of the profile steepness and shoreline position (Sheet 1: Figure a and b), the sharp boundaries generally apply to the differences in patterns of spatial and temporal coherence, rather than to differences in any linear temporal trends.

The analysis method has been applied to profiles of about 700 m to 750 m length. These profiles often cross the entire inshore zone. The definition of LSCB-regions would probably not have been too different if longer profiles (e.g. 1000 m length) had been available, because the profile becomes less active outside the inshore area (Kroon, 1994), i.e. little variance will be added. Besides, the depth changes on the shoreface of the Holland coast over a 3 decade time span will generally not exceed the measurement error (see Section 2.2.4). An analysis of profiles much shorter than 700 m (e.g. 250 m length) might give deviating results, because large depth changes due to migration of the outer bars are excluded from the analysis. The variance related to those large depth changes strongly determines the shape of the present second and third eigenfunctions. LSCB-regions should not be based on the behaviour of such short profiles, because much depth variation occurring on the considered time-scale is excluded in that analysis.

4.3.2 Explanation of the locations of boundaries between 'LSCB-regions'

It has been hypothesised that boundaries between LSCB-regions are caused by alongshore variation in mega-scale imposed constraints and/or by alongshore variation in large-scale energy input. Additionally, it was hypothesised that gradual changes in boundary conditions do not produce abrupt changes in behaviour (see Chapter 1). According to these hypotheses, the relatively sharp boundary between LSCB-regions should be caused by rather sharp changes in the energy input or the mega-scale imposed constraints. The parameters characterising the energy input into the coastal system change gradually alongshore (Section 2.2.3). Therefore, sediment-related constraints and morphology-related constraints, including human interventions, are more likely factors to explain the locations of boundaries between LSCB-regions.

The boundary between Region 1 and Region 2, near km 8, correlates with a change in offshore bathymetry. It appears to coincide with the southern edge of the ebb-delta that is associated with the Marsdiep Inlet. The sharp boundary in coastal behaviour occurring at this transition is explained by the fact that the coastal behaviour in Region 1 is dominated by the morphodynamics of the tidal inlet system, viz. the onshore migration of a channel on the ebb delta (Sha, 1990). Therefore, Region 1 should be considered as being part of the barrier island system rather than of the inlet-free coastal system of the Holland coast.

The boundary between Region 2 and Region 3, near km 23, is relatively gradual. The location of this boundary correlates with a change in offshore bathymetry. In front of Region 2 two terraces are present on the shoreface (Section 2.2.2), whereas such phenomena are absent in front of Region 3. Further, the transition in behaviour near km 23 occurs in front of a man-made structure, viz. a seawall. The differences in shoreface morphology may cause slight differences in the nearshore wave conditions during heavy storm events. Further, the differences in shoreface morphology impose different initial conditions for further developments. The seawall is a protruding structure (Section 2.2.6) resembling some sort of headland. The impression of the seawall functioning like a headland is reinforced by the difference in shoreline orientation north and south of this structure (Figure 2.6).

The boundary between Region 3 and Region 4, near km 55, coincides with a man-made structure, viz. a pair of harbour moles extending about 2.5 km offshore (Section 2.2.6). Further, the grain sizes of the surface sediment exhibit a change near km 55 (Section 2.2.4). The data on alongshore differences in the lithology (Appendix 2) indicate that it is unlikely that the substrate will impose such a sharp change in sediment size across km 55. Surface sediments in the nearshore zone, however, will be in dynamic interaction with the water motion and the (bar) morphology (Medina et al., 1994). Given differences in nearshore morphology, the feedback from the morphology to the water motion will cause different selective sediment transport under given energy input conditions. Therefore, the differences in surface sediment grain size north and south of km 55 are considered to be an expression of the meso-scale morphodynamic system rather than a constraint imposed on the large-scale system by the mega-scale morphodynamic system. The short term changes in the cross-shore distribution of grain size observed near km 76.5 (Figure 2.24) support this conclusion.

The harbour moles will locally affect the nearshore wave climate as well as the nearshore tidal currents, but it is hard to imagine that these moles have directly influenced the hydrodynamics over distances as large as 30 or 40 km (being the approximate lengths of Region 3 and Region 4 respectively). A more likely role of the harbour moles in causing differences in coastal behaviour is that these moles enforce an artificial boundary in a 'coastal cell'. The harbour moles inhibit interaction between the coastal stretches on either side of these moles and thus allow an independent behaviour of the two stretches. The difference in bar system

morphology between Region 3 and Region 4 is probably an example of such an independent development. The large alongshore coherence in the bar system behaviour within Region 3 as well as within Region 4, indicates that in case the harbour moles are removed the two bar systems will influence each other's behaviour.

Some indication of the influence of the harbour moles on the bar system morphology can be obtained from old bathymetric maps surveyed prior to and after the construction of the harbour moles (Staatscommissie Kraus, 1911). Cross-shore profiles derived from these maps indicate that the amplitude of the bar topography north of the harbour moles may have increased after construction of these moles (Figure 4.25). South of the present-day harbour moles, the amplitude

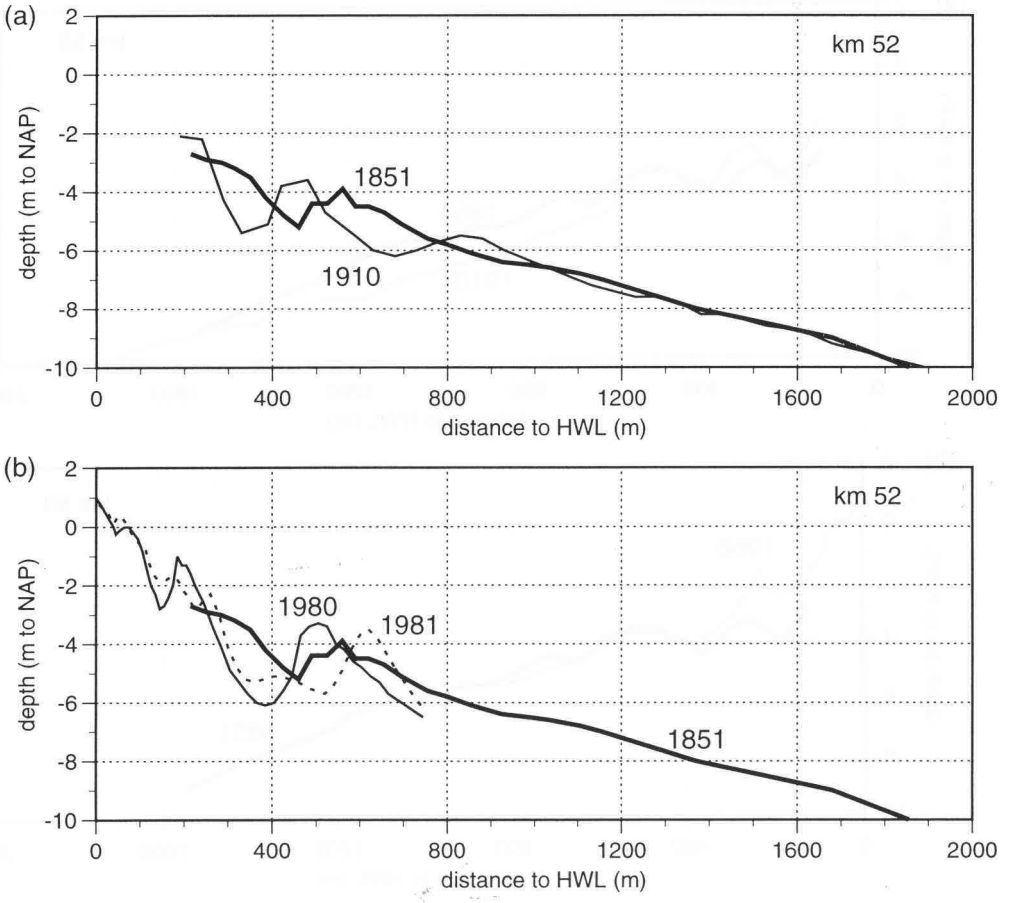

Figure 4.25: Cross-shore profiles prior to, and after the construction of the harbour moles of IJmuiden in 1865-1879. Profiles are located north of the harbour moles. (a) 1851 vs. 1910; (b) 1851 vs. today.

of the bar topography may have decreased somewhat after construction of the harbour moles (Figure 4.26). The judgement of the amount of change in the character of the bar system topography since 1851 is somewhat tentative. More obvious is the large similarity of the bar topography observed in 1910 and that observed today, especially north of the harbour moles (Figure 4.27 and 4.28). Unfortunately, the behaviour of the bars can not be determined from these surveys.

The boundary between Region 4 and Region 5, near km 98, coincides with the transition from a stretch without groins to a stretch with groins (Section 2.2.6). It is unclear whether this is a causal relationship, because a similar transition near km 31 does not induce an obvious change in decadal coastal behaviour (Sheet 1).

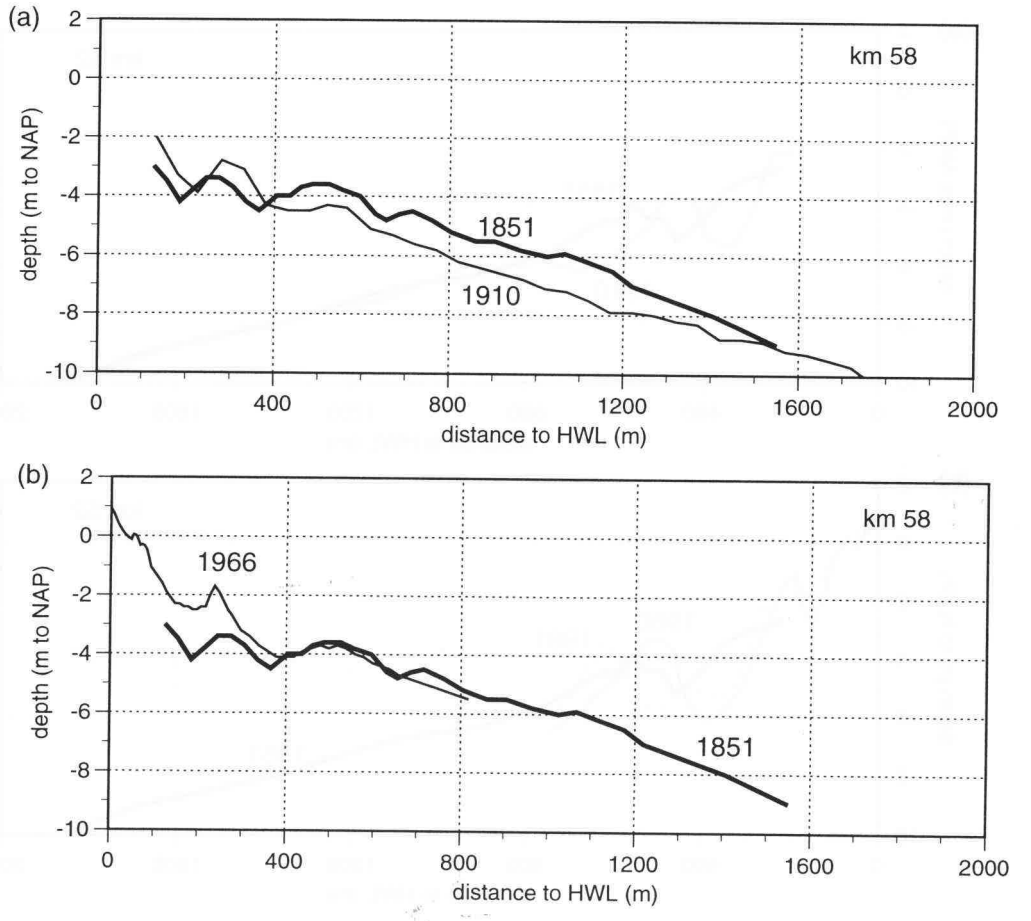

Figure 4.26: Cross-shore profiles prior to, and after the construction of the harbour moles of IJmuiden in 1865-1879. Profiles are located south of the harbour moles.
(a) 1851 vs. 1910; (b) 1851 vs. today.

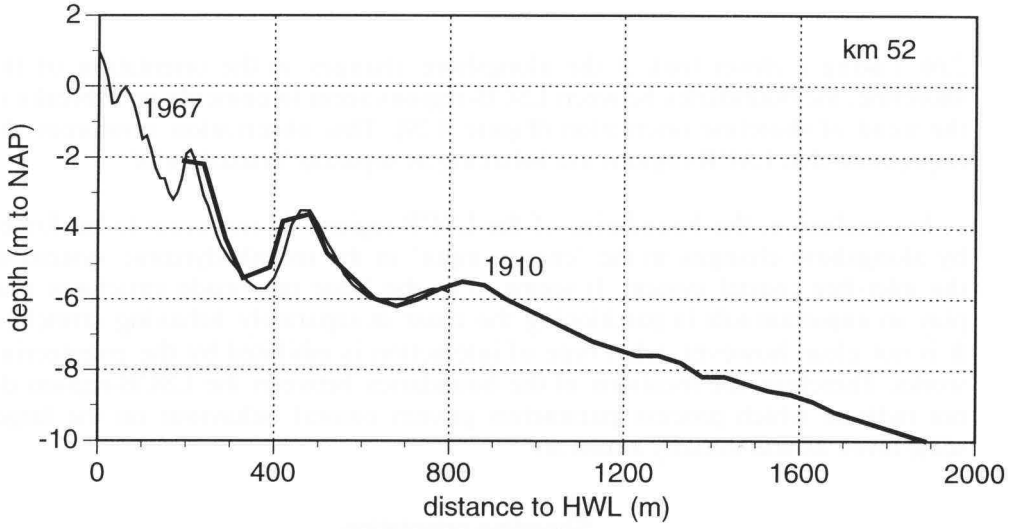

Figure 4.27: Cross-shore profiles near km 52, situation 1910 vs. today.

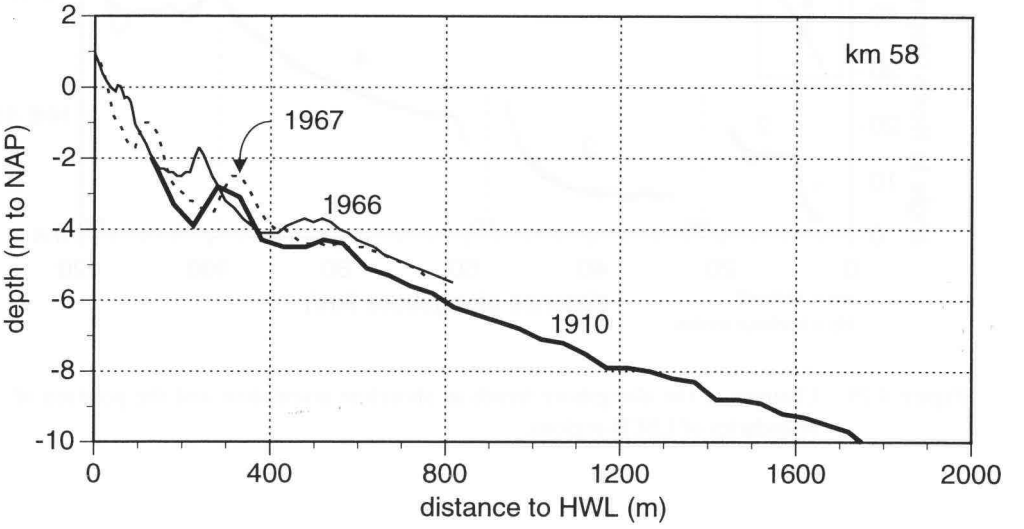

Figure 4.28: Cross-shore profiles near km 58, situation 1910 vs. today.

South of the harbour moles of Scheveningen, near km 102, the surface sediments are somewhat coarser (Figure 2.25). The consistency in time of this pattern is unknown, but the presence of coarser sediments in the substrate in this area (Appendix 2) indicates that this pattern may be permanent. The location of the change in grain size, however, does not exactly coincide with the location of the change in coastal behaviour. No explanation for this discrepancy is available. Finally, near km 98 the trend in the orientation of the shoreline changes (Figure

2.6). Taking a closer look at the alongshore changes in the orientation of the shoreline, the boundaries between LSCB-regions seem to coincide with breaks in the trend of shoreline orientation (Figure 4.29). This observation reinforces the impression that LSCB-regions are behaving as separate 'coastal cells'.

In conclusion, the boundaries of the LSCB-regions do not seem to be forced by alongshore changes in the 'energy input' in the morphodynamic system of the inlet-free coastal system. It seems to be the large man-made structures that play an important role in partitioning the coast in separately behaving stretches. It is not clear, however, what type of interaction is inhibited by the engineering works. Therefore, the locations of the boundaries between the LSCB-regions do not indicate which process parameters govern coastal behaviour on the large-scale level, as was initially aimed at.

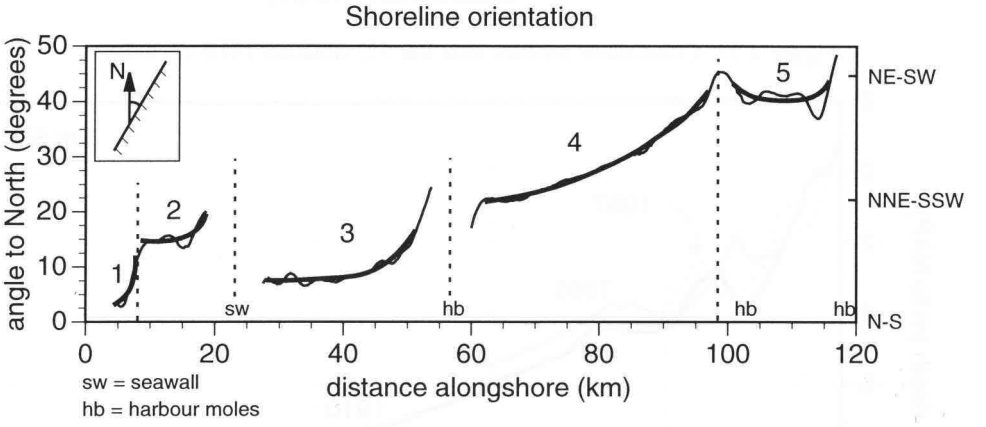

Figure 4.29: Changes in the alongshore trends in shoreline orientation and the position of boundaries of LSCB-regions.

4.4 Discussion

So far, the alongshore varying, decadal morphological developments along the Holland coast have been considered to be an expression of the large-scale morphodynamic system, because the behaviour of the complete Holland coast was expected to be associated with the decadal time scale. This assumption can now be verified from the morphologic analysis.

Establishing the time scale inherently associated with the coastal behaviour at a spatial scale of tens of kilometres is not a straightforward matter, because coherent behaviour over large alongshore distances can be produced in more than one way. Coastal behaviour that is coherent over large distances may be

produced by the large-scale morphodynamic system but may also be produced by smaller scale morphodynamic systems. When the boundary conditions and energy input for a small-scale morphodynamic system are homogeneous over large alongshore distances, this will produce coastal behaviour that is coherent over large alongshore distances in combination with a small time scale. Objective criteria are not available to distinguish true large-scale coastal behaviour from smaller scale coastal behaviour with large-scale homogeneous boundary conditions, because the current knowledge of large-scale coastal behaviour is very limited. In the following,an attempt is made to separate scales of coastal behaviour, based on the scale concepts presented in Chapter 1.

The large-scale morphologic developments of the Holland coast can be described by the alongshore coherence in the profile developments (Section 4.2). The morphologic 'state' of the Holland coast at time t consists of the shoreline position at time t and the profile shape states occurring at time t. Large-scale coastal behaviour then deals with the sequence of morphologic states of the complete Holland coast.

The morphologic state of the Holland coast appears to change only slightly over the 1963-1990 period. A small change in the configuration of the coastline occurred due to differential trend-wise shoreline behaviour (Section 4.2.1). Further, some trend-wise changes in the nearshore steepness occurred, though not in simple correlation with the large-scale shoreline behaviour (Section 4.2.2). Regarding the bar topography, the only trend-wise development over the 1963-1990 period occurred between km 3 and km 6 where a small bar moved onshore (Section 4.2.3).

The coastal stretches without visible trend-wise morphologic developments over the 1963-1990 period often exhibit slow 'fluctuations' over time spans of typically 5 to 25 year. Many fluctuations are coherent over considerable alongshore distances. Several stretches with typical coherent 'fluctuating behaviour' can be distinguished (Section 4.3.1). The coherence in behaviour within these stretches is large but the coherence in behaviour among the stretches is small.

The trend-wise change in shoreline position along the northern part of the Holland coast is at least partially caused by the background erosion induced by the mega-scale behaviour, viz. the sand import by the neighbouring tidal basin (Stive and Eysink, 1989). Superimposed on this background erosion, fluctuations may occur due to large-scale behaviour. This large-scale behaviour may be forced by the wave climate acting upon an alongshore varying, mega-scale imposed, morphologic boundary condition, viz. the pre-existing concave shape of the Holland coast (Van Straaten, 1961; Dijkman et al., 1990). From the 28-year data set it can not be determined what type of fluctuation due to large-scale behaviour is superimposed, because the exact rate of background erosion is unknown. Studies on the shoreline behaviour over the past century indicate that the rate of shoreline retreat over the last few decades has been somewhat larger than the 140-year average retreat (Van Straaten, 1961; De Valk and Zitman, 1987; Knoester, 1990)

The alongshore change in the trend in shoreline behaviour is not accompanied by a similar alongshore change in the trend in profile shape behaviour. The trend-wise steepening of the nearshore north of km 8 is related to the channel and shoal behaviour on the ebb-delta of the Marsdiep Inlet. Between km 10 and km 20 the retreating shoreline is accompanied by a flattening of the profile. The flattening is possibly representing a trend but it may be a slow fluctuation as well. Farther south, all changes in the profile shape are fluctuations rather than trends, except for the profile shape changes in the direct vicinity of large engineering works.

Coherent trends across the complete stretch of the Holland coast, such as observed in the shoreline behaviour since the mid of the 19th century (Section 2.3.2), are lacking in the JARKUS data base. This indicates that the time scale related to the behaviour of the complete Holland coast is at least many decades. Consequently, the available field data span an insufficient period of time for gaining insight into the large-scale behaviour of the Holland coast on the basis of field evidence.

The lack of coherence in behaviour among LSCB-regions seems to indicate that the alongshore varying decadal developments of the Holland coast are various expressions of meso-scale morphodynamic systems. The lack of coherence in behaviour among regions may be attributed to abruptly varying meso-scale energy input or to abruptly varying large-scale imposed boundary conditions. The abrupt change in meso-scale behaviour may also express a highly non-linear response of the meso-scale morphodynamic system to a slowly alongshore varying energy input or a slowly alongshore varying large-scale imposed boundary condition. To determine which of these possibilities is the most likely, the LSCB-region boundary near IJmuiden will be considered in more detail.

The abrupt change in meso-scale behaviour near IJmuiden is probably not due to an abrupt change in meso-scale energy input, for neither the offshore energy input nor the shoreface morphology exhibits an abrupt change near IJmuiden (see Section 2.2.2 and Section 2.2.3). The alongshore variations in shoreface morphology near IJmuiden may induce some differences in the nearshore wave climate, however, not as abrupt as the differences in coastal behaviour that are observed at either side of the harbour moles. Compared to the sharp change in coastal behaviour, the shoreface morphology exhibits a relatively gradual change (Figure 2.7).

A property that does change abruptly near IJmuiden is the general character of the bar system. The bars north of IJmuiden have larger maximum amplitudes and enclose larger volumes of sediment than those south of IJmuiden (Figure 4.30). As most of the fluctuations in the observed coastal behaviour seem to be related to the behaviour of the nearshore bars, it may be the alongshore differences in the dimensions of the bar system morphology that induce the abrupt alongshore changes in the patterns of meso-scale behaviour.

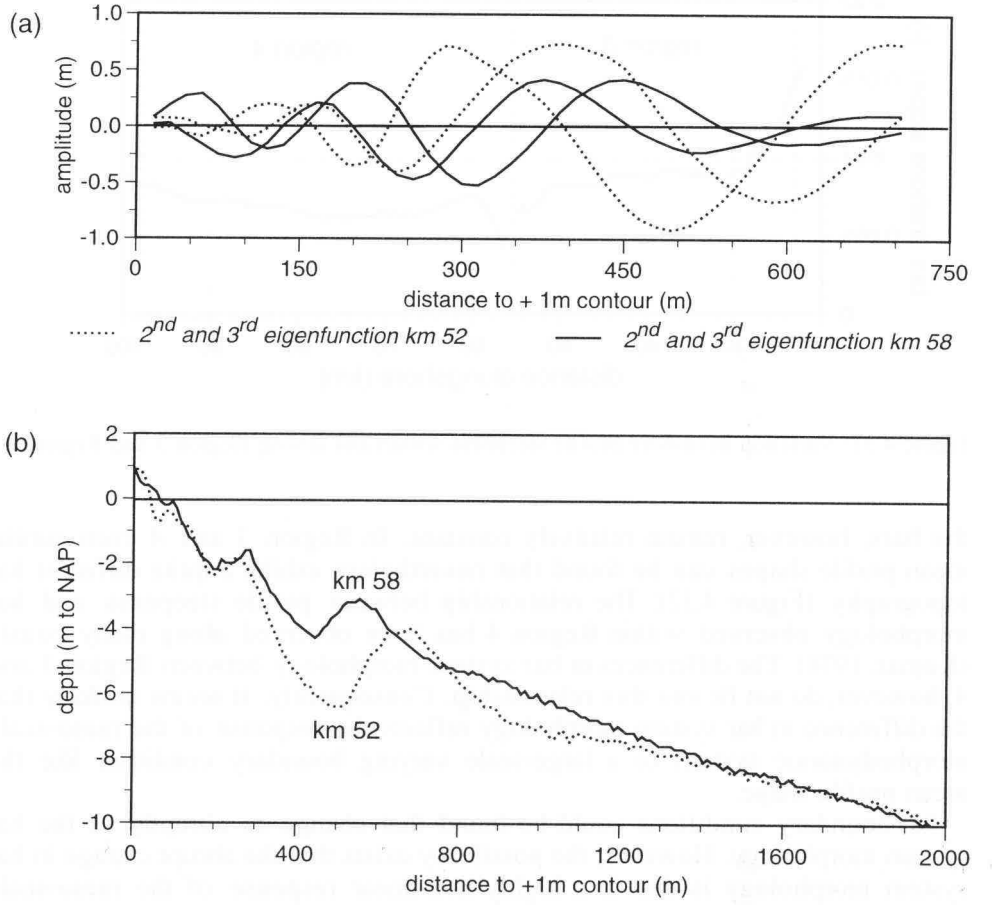

Figure 4.30: Example of differences in bar system morphology north and south of IJmuiden. (a) Second and third eigenfunction in window km 52-53 and in window km 58-59; (b) cross-shore profiles near km 52 and km 58 in 1986.

The large-scale change in the bar system morphology may be considered as a large-scale imposed boundary condition, but it may also reflect the response of the meso-scale morphodynamic system to a large-scale varying boundary condition like the mean profile shape. As will be argued in the following paragraphs, the first possibility seems to be the most likely explanation.

Along the multiple barred stretches, the mean profile is generally steeper north of IJmuiden (Region 3) than south of it (Region 4) (Figure 4.31). This correlation suggests that on steeper profiles larger bars are present. This relationship does not show up, however, within Region 4. In the latter region, an increase in the profile steepness goes with a decrease in the number of bars and a decrease in the seaward extent of the bar system (Figures 4.31 and 4.2). The dimensions of

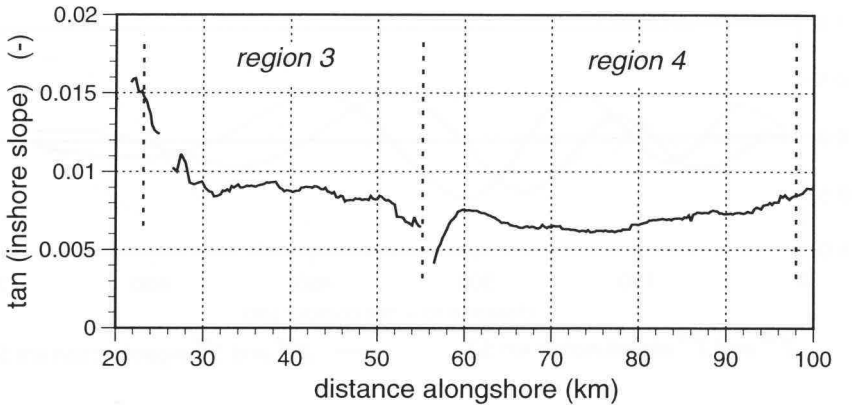

Figure 4.31: Variation in inshore profile steepness within and among Region 3 and Region 4.

the bars, however, remain relatively constant. In Region 3 and 4 even similar mean profile shapes can be found that nevertheless exhibit a quite different bar topography (Figure 4.32). The relationship between profile steepness and bar morphology observed within Region 4 has been observed along many coasts (Komar, 1976). The differences in bar system morphology between Region 3 and 4, however, do not fit into this relationship. Consequently, it seems unlikely that the difference in bar system morphology reflects the response of the meso-scale morphodynamic system to a large-scale varying boundary condition like the mean profile shape.

No boundary conditions could be found that change as abruptly as the bar system morphology. However, the possibility exists that the abrupt change in bar system morphology is due to a highly non-linear response of the meso-scale morphodynamic system to small, gradual alongshore changes in energy input or large-scale imposed boundary conditions. The existence of such a very sensitive morphodynamic system is not supported by the large consistency in time of the general differences in bar system morphology between Region 3 and 4. The lack of abrupt changes in the character of the bar system in Region 4 in response to gradual alongshore changing boundary conditions -such as shoreline orientation and profile steepness- does not indicate such a sensitivity of the morphodynamic system either. Therefore, it is concluded that the differences in bar system morphology are most probably an expression of the large-scale morphodynamic system. The differences between the bar systems north and south of the IJmuiden harbour moles may then be explained by the separate evolution of the two bar systems after construction of the harbour moles. The cyclic bar dynamics that can be observed in JARKUS are considered to be the result of the meso-scale morphodynamic system interacting with this large-scale imposed morphologic boundary condition.

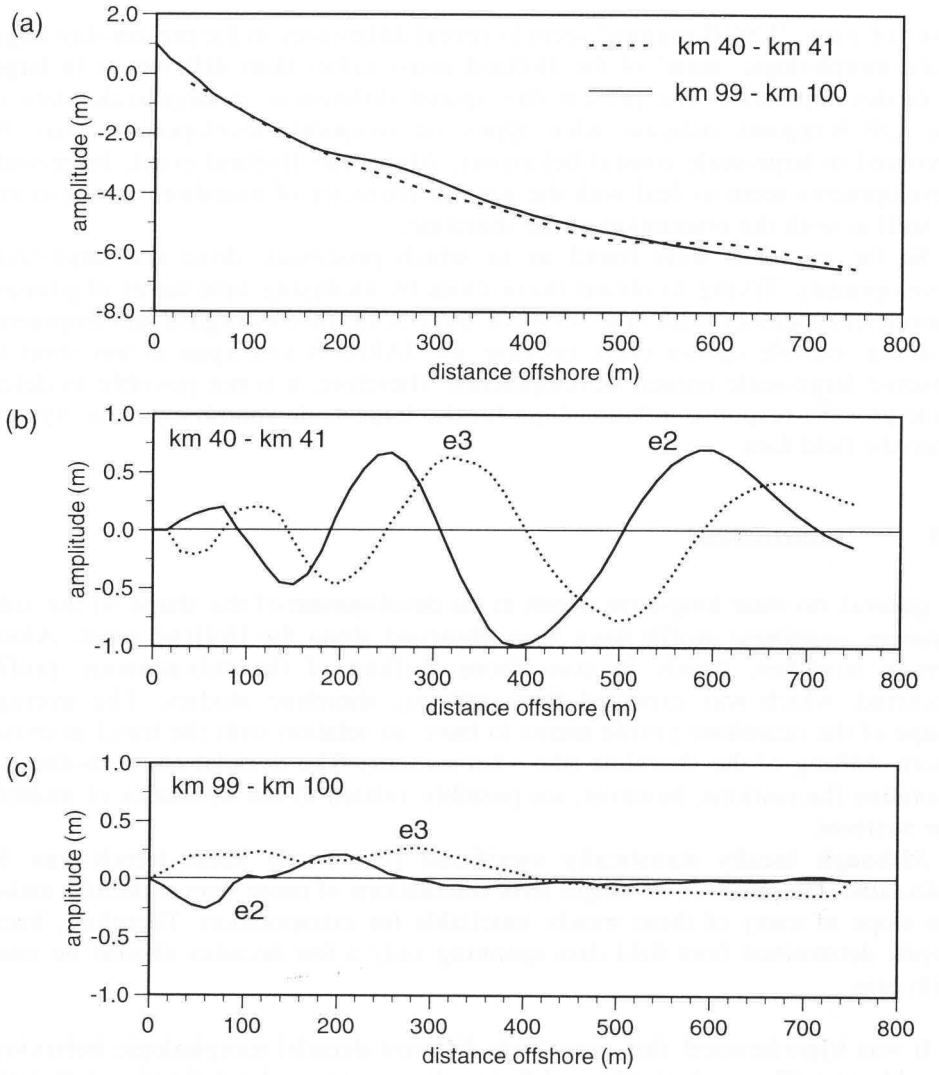

Figure 4.32: Mean profile and 'secondary' morphology for window km 40-41 and window km 99-100. (a) 'Mean profile' eigenfunction e1; (b) second and third eigenfunctions e2 and e3 for window km 40-41; (c) second and third eigenfunctions e2 and e3 for window km 99-100.

Summarising, the cyclic bar system behaviour and correlated shoreline and profile steepness behaviour are considered to be an expression of meso-scale behaviour; the scaling of the bar system (as expressed in the cross-shore eigenfunctions) is considered a large-scale imposed boundary condition. From this

point of view, 'LSCB-regions' seem to reveal differences in the present-day large-scale morphologic 'state' of the Holland coast rather than differences in large-scale developments. The present-day spatial differences in large-scale state of the LSCB-regions indicate what types of temporal developments may be involved in large-scale coastal behaviour. Along the Holland coast, large-scale developments seem to deal with the general character of nearshore bar systems, as well as with the orientation of the shoreline.

So far, no clues were found as to which processes drive the large-scale developments. Trying to obtain those clues by analysing time series of process parameters together with time series of large-scale morphological developments is not a sensible option (yet), because the JARKUS time span is too short to observe large-scale coastal developments. Therefore, it is not possible to determine process-response relationships for the large-scale morphodynamic system from the field data.

4.5 Conclusions

In general, no clear long-term trends in the development of the shape of the sub-aqueous nearshore profile have been observed along the Holland coast. Along certain stretches, trends in cross-shore shifting of the sub-aqueous profile occurred, which was expected from previous shoreline studies. The average shape of the nearshore profile seems to have no relation with the trend in cross-shore shifting of the shoreline (the +1m-contour). The decadal and sub-decadal shoreline fluctuations, however, are possibly related to the dynamics of multiple bar systems.

Although locally statistically significant (but weak) linear trends can be calculated, the presence of longer term fluctuations of more than a decade makes the slope of many of these trends unreliable for extrapolation. Therefore, linear trends determined from field data spanning only a few decades should be used with care.

It was hypothesised that areas with different decadal morphologic behaviour should exist. The analysis showed that such regions can be defined and that the boundaries between these regions are generally quite sharp.

The boundaries between 'LSCB-regions' were found to be related to man-made structures and alongshore changes in offshore bathymetry. Alongshore differences in sediment and 'energy input' seem to be of little influence on the location of the boundaries. Probably, the role of a large man-made structure in decadal coastal behaviour is that it inhibits the interaction between the coastal stretches at either side of it. This conclusion supports the presumed interrelation of decadal coastal developments over distances of tens of kilometres. An implication of this conclusion is that coastal developments that span many decades can not be properly modelled by considering only one 'representative' cross-shore profile.

The JARKUS data base spanning the 1963-1990 period basically reveals one large-scale morphologic 'state' of the Holland coast, and only offers a first glance at large-scale morphologic developments. The decadal morphologic developments along the Holland coast mainly consist of alongshore variations in meso-scale coastal behaviour due to alongshore varying large-scale imposed boundary conditions.

Since the time span of the JARKUS data base is too short to reveal large-scale morphologic developments, it is not possible to determine large-scale process-response relationships from the field data. Therefore, it is still unclear which processes drive the large-scale coastal behaviour. The current JARKUS data base is more suitable for the analysis of the meso-scale process-response relations.

5 MULTI-YEAR BEHAVIOUR OF MULTIPLE BAR SYSTEMS ALONG THE HOLLAND COAST

5.1 Introduction

Coastal developments along the Holland coast over a time span of a few decades appeared to deal mainly with meso-scale coastal behaviour. The most pronounced expression of the meso-scale morphodynamic system is the cyclic behaviour of the multiple bar systems. Therefore, this chapter will focus on the explanation of the systematic behaviour of multiple bar systems on a sub-decadal to decadal time scale.

The analysis of the systematic bar system behaviour is based on the morphodynamic systems concept presented in Chapter 1 (Figure 5.1). First the morphologic developments are characterised [1] (the bracketed number refers to the equally numbered box in Figure 5.1). Next, local sediment budgets are considered to infer possible sediment redistribution patterns going with the morphological changes [2]. The probable directions of sediment transport and the observations of the different responses of the outer bar to the mean annual wave climate in various stages of its development, are combined into an hypothesis about the relevant processes [3]. Having determined the probably relevant processes in the meso-scale morphodynamic system, the character of the meso-scale energy filter can be specified [4].

The general character of the permanently present bar system as expressed by the second and third cross-shore eigenfunctions, is considered to be a morphologic boundary condition imposed by the large-scale morphodynamic system (see Section 4.4). The nearshore bars are therefore considered to be an inherent property of the mean profile, similar to the property of a barless profile to take on, for example, some exponential or power law shape (Dean, 1977; Bodge, 1992).

Two main multiple bar systems can be distinguished along the Holland coast: the Noord-Holland multiple bar system and the Zuid-Holland multiple bar system. The Noord-Holland bar system is located in Region 3 and the Zuid-Holland bar system is located in Region 4. The two bar systems are separated by the IJmuiden harbour moles. Similarities between the Noord-Holland and Zuid-Holland bar system will be pointed out as well as the differences. Further, a hypothesis is formulated to explain the behaviour that these two bar systems have in common, viz. the multi-year, cyclic behaviour.

The analysis of the morphologic behaviour of the bar systems will be based on the second and third eigenfunctions derived from the JARKUS data base (Figure 4.2, and Sheet 1: Figure c and d). Additionally, the TAW profile data base will be used. The cross-shore profile lines monitored for the TAW data base are sampled more frequently than the profile lines in the JARKUS data base (up to 10 times per year). Unfortunately, only a few profile lines are surveyed for the TAW data base. The profile lines used in this study are located near Egmond (km 40.00,

km 40.50, and km 41.00, relative to RSP reference line) and near Katwijk (km 84.00, km 84.25 and km 84.50, relative to RSP reference line). The TAW data base will be used to evaluate the suitability of the JARKUS data base to describe the kinematics of the large-scale bar system behaviour. In addition, the TAW data base will give insight in the variability of the bar behaviour within a year.

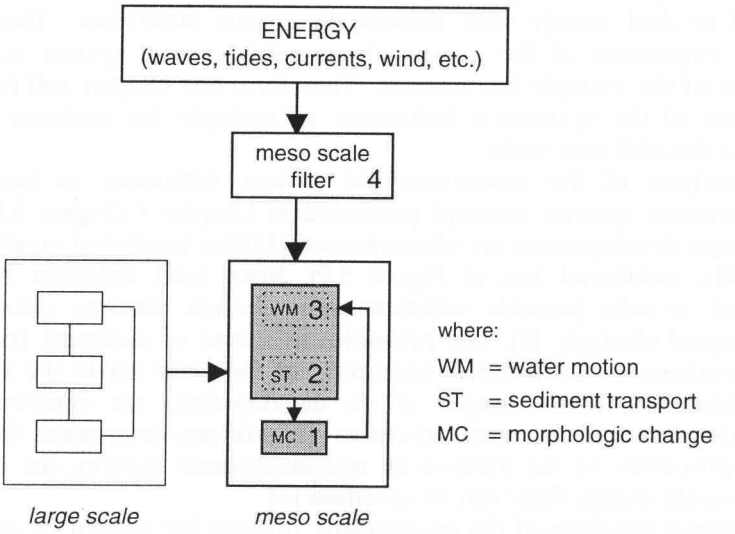

Figure 5.1: Morphodynamic systems concept underlying the analysis of multi-year bar system behaviour.

5.2 Morphologic behaviour of multiple bar systems

The description of the kinematics of multiple bar system behaviour is based on the eigenfunction analysis of the JARKUS data base presented in Chapter 4. The suitability of the JARKUS data base -which contains only annual surveys- for schematising large-scale bar system behaviour is evaluated by comparing eigenfunctions based on JARKUS to eigenfunctions based on TAW. The eigenfunctions describe all profiles available within a 1 km wide window, for the JARKUS data base and TAW data base respectively. Figure 5.2 and Figure 5.3 illustrate that the large-scale bar system behaviour as described by the annual data set is very similar to that based on more frequent profile sampling. The weightings of the TAW eigenfunctions are plotted according to their dates of survey. The weightings of the JARKUS eigenfunctions are all plotted at mid-year positions (i.e. at July 1), because this resembles the presentation of these results in the preceding chapters. As expected, the behaviour of the bar system within a year

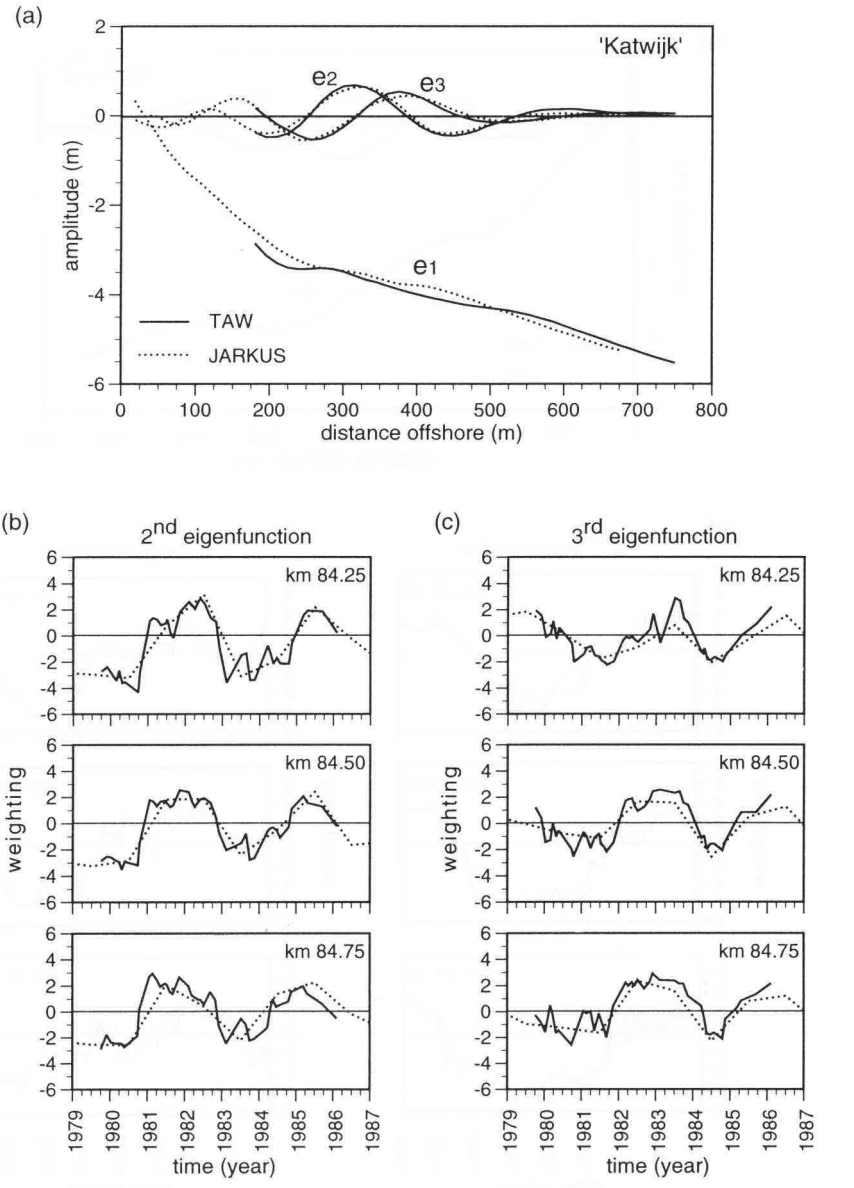

Figure 5.2: Eigenfunction analyses based on TAW profiles (km 84.00, km 84.25, and km 84.50; period 1979-1986) and on JARKUS profiles (km 84.00, km 84.25, km 84.50, km 84.75, and km 85.00; period 1964-1990) near Katwijk.
(a) First 3 eigenfunctions e1, e2, and e3; (b) Weightings on the second eigenfunction e2; (c) Weightings on the third eigenfunction e3.

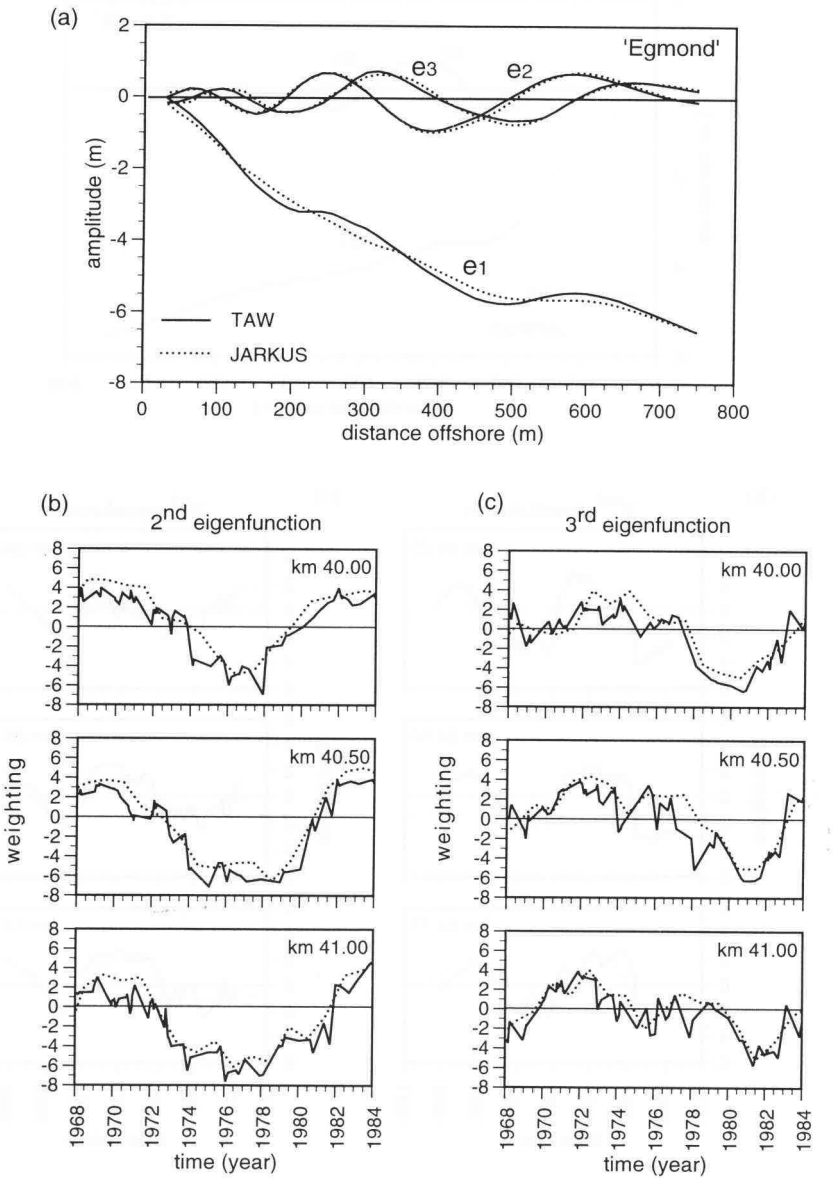

Figure 5.3 Eigenfunction analyses based on TAW profiles (km 40.00, km 40.50, and km 41.00; period 1968-1984) and on JARKUS profiles (km 40.00, km 41.25, km 40.50, km 40.75, and km 41.00; period 1964-1990) near Egmond.
(a) First 3 eigenfunctions e1, e2, and e3; (b) Weightings on the second eigenfunction e2; (c) Weightings on the third eigenfunction e3.

described by the TAW data base produces some 'noise' around the multi-year trend described by JARKUS. Major changes in the bar system are not missed by using the annual profile data base JARKUS.

The general nature of the systematic behaviour of the bar systems has been mentioned briefly in Section 4.2.3. That systematic behaviour consists of net offshore movement of all bars, with the outer bar fading away and a new bar being generated near the shoreline. The offshore migration of bars has been observed to be related to storm events (Birkemeier, 1984; Sallenger et al., 1985; Aagaard, 1990; Sunamura and Takeda, 1993; Kroon, 1994). Considering the large annual variability in the number of storms, the strength of storms, and the sequence of storm events (Section 2.2.3), the multi-year cycle of offshore bar migration observed along the Holland coast is remarkably regular in time (Sheet 1: Figure c and d). The characteristic time span of the cycle however varies with the bar system. A typical time span in the Noord-Holland bar system is about 15 years whereas in the Zuid-Holland bar system it is typically about 4 years. The cycle in the bar system development describes the return to a formerly exhibited bar topography due to the systematic and coherent behaviour of the bars. This cycle should not be confused with the 'life cycle' of each individual bar, consisting of the generation near the shoreline, the subsequent net offshore migration, and the final degeneration at its most offshore position. For example, if the cyclic behaviour of a triple bar system spans about 3 year (i.e. the return period of a certain bar topography), the life cycle of an individual bar spans about 9 year.

Profile observations from the TAW data base reveal that changes of the outer bar topography predominantly occur during the 'winter storm period', i.e. September through March (Figure 5.4 and Figure 5.5). Changes in the outer bar

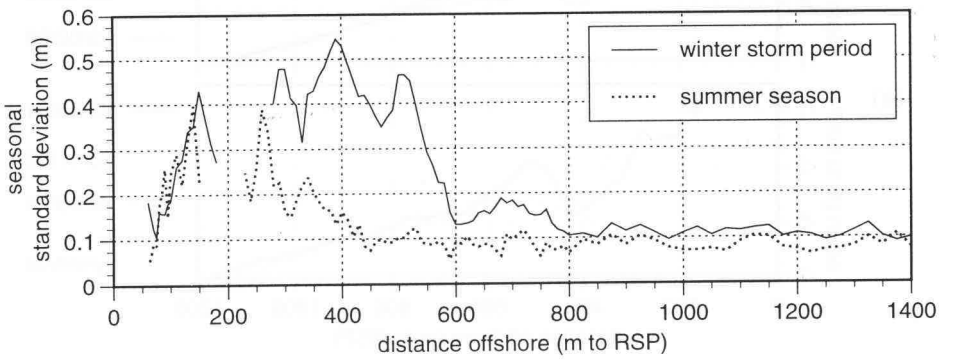

Figure 5.4 Average, seasonal standard deviation of the cross-shore depth measurements at km 84.25. The curve of the winter storm period is averaged over 5 series of 'winter' standard deviations (September-March), viz. the winters of 1979-80, 1980-81, 1981-82, 1982-83, and 1983-84. The curve of the summer season is averaged over 5 series of 'summer' standard deviations (April-August), viz. the summers of 1980, 1981, 1982, 1983, and 1984.

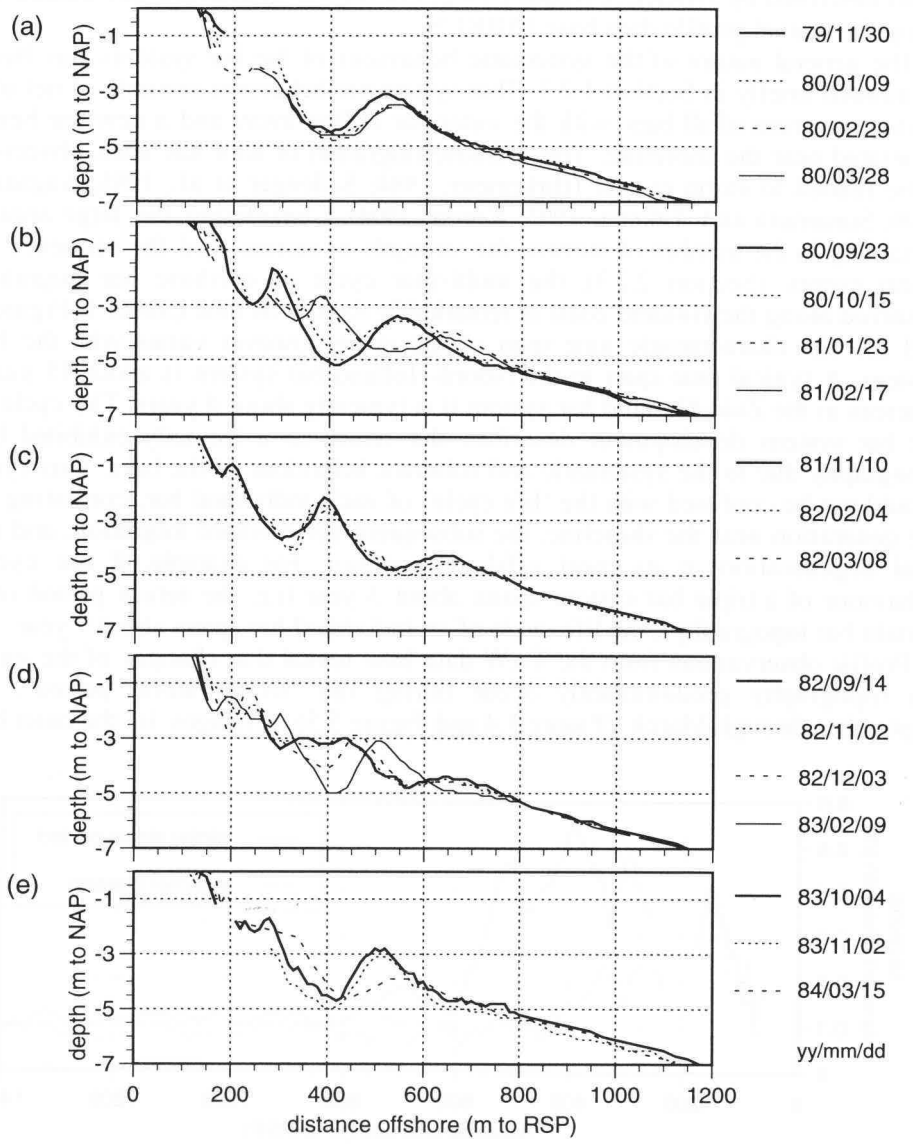

Figure 5.5: Nearshore profiles near km 84.25, 'winter storm period' (TAW data base).
(a) Winter storm period '79-'80; (b) winter storm period '80-'81;
(c) winter storm period '81-'82; (d) winter storm period '82-'83;
(e) winter storm period '83-'84;

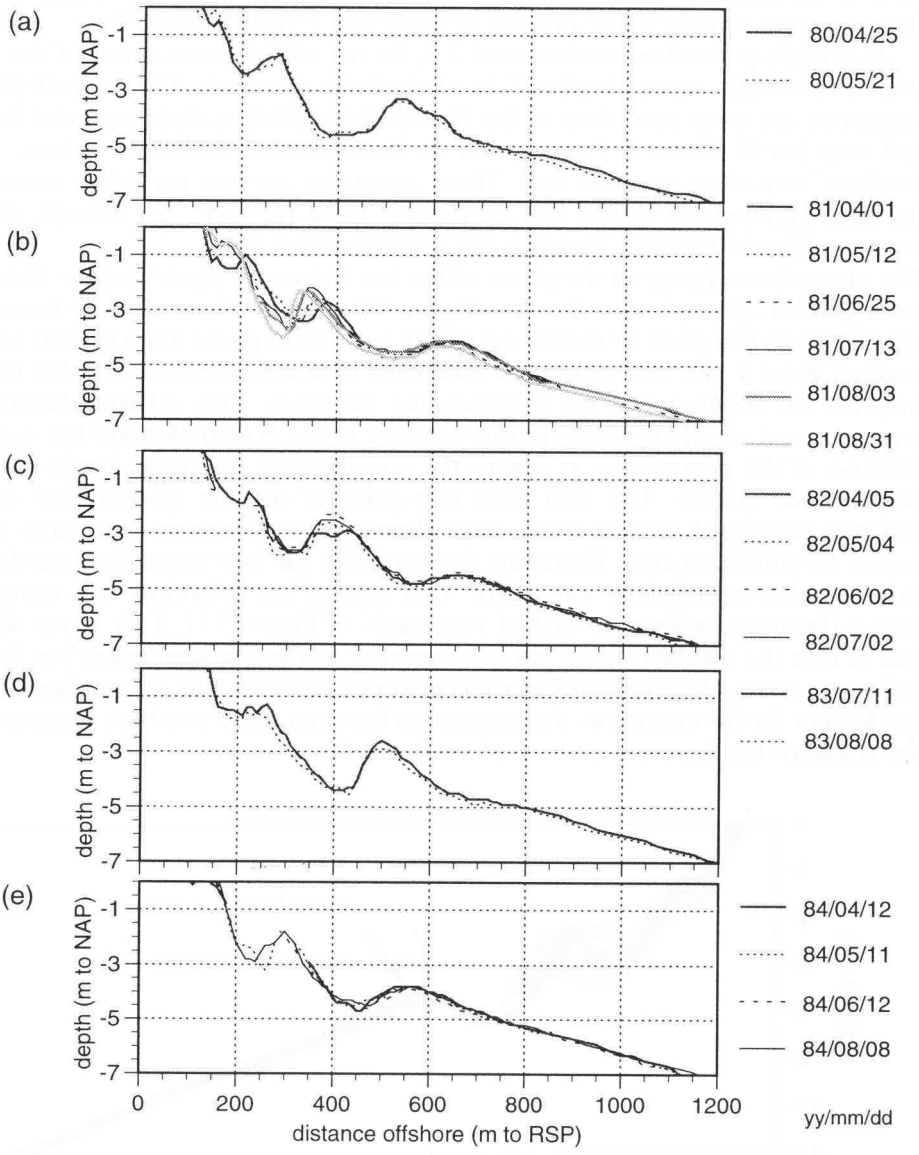

Figure 5.6: Nearshore profiles near km 84.25, 'summer season' (TAW data base).
(a) Summer season '80; (b) summer season '81; (c) summer season '82;
(d) summer season '83; (e) summer season '84;

topography during the 'summer season' can hardly be distinguished from measurement errors (Figure 5.4 and Figure 5.6). Further, profiles from the TAW data base reveal that near Egmond the outer bar can persist almost unchanged (within the measurement error) over a period of more than 2 year (Figure 5.7).

As already pointed out in Section 4.2.3, the net offshore movement of the bars does not always occur 'in phase' in alongshore direction. The 'out-of-phase' situations are most persistent in the Noord-Holland bar system, viz. near km 38 and near km 45 (Sheet 1: Figure c and d). In the Zuid-Holland bar system, 'out-of-phase' situations occur as well. These situations are less persistent in time in the Zuid-Holland bar system but they occur quite regularly, for example in the vicinity of km 65 (Sheet 1: Figure c and d; and Figure 5.8).

The alongshore change in the phase of the bar behaviour cycle may be sharp or more gradual. Examples are shown in Figure 5.9 and 5.10. Generally, the transition area between two parts of the bar system in a different phase has a typical length scale of about 2 km. The bars in the transition area exhibit behaviour that differs from the bar behaviour in the neighbouring stretches. This different behaviour emerges most clearly from the profile surveys in the Noord-Holland bar system, because of the persistence in time of the out-of-phase situations in the Noord-Holland bar system. The bars from two parts of the bar system that are in different phases of the bar cycle, make alternating attachments with each other across the transition area. Therefore, the parts of a bar in a transition area do not exhibit a clear net offshore movement. This type of bar behaviour in a transition area is illustrated within the dashed rectangles of Figure 5.11. This figure shows that at first the southern inner bar is connected to the northern outer bar. In the following years, the southern inner bar migrates seaward and the northern outer bar lowers. In the meantime, the connection between these two bars loosens and the southern bar becomes connected to the northern inner

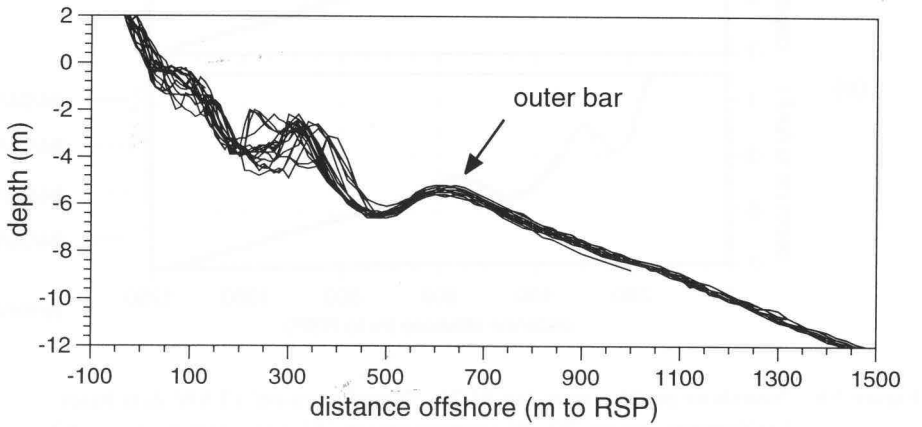

Figure 5.7: Twenty profile surveys near km 41.00, spanning the period from December 1970 to August 1973 (TAW data base).

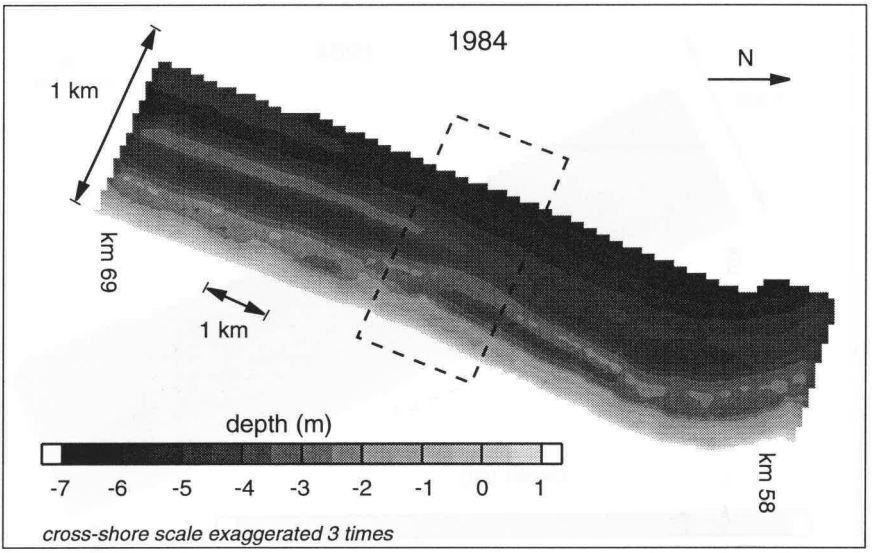

Figure 5.8: Nearshore bathymetry between km 58 and km 69 in 1984 (JARKUS data base). (Dashed box marks the transition area.)

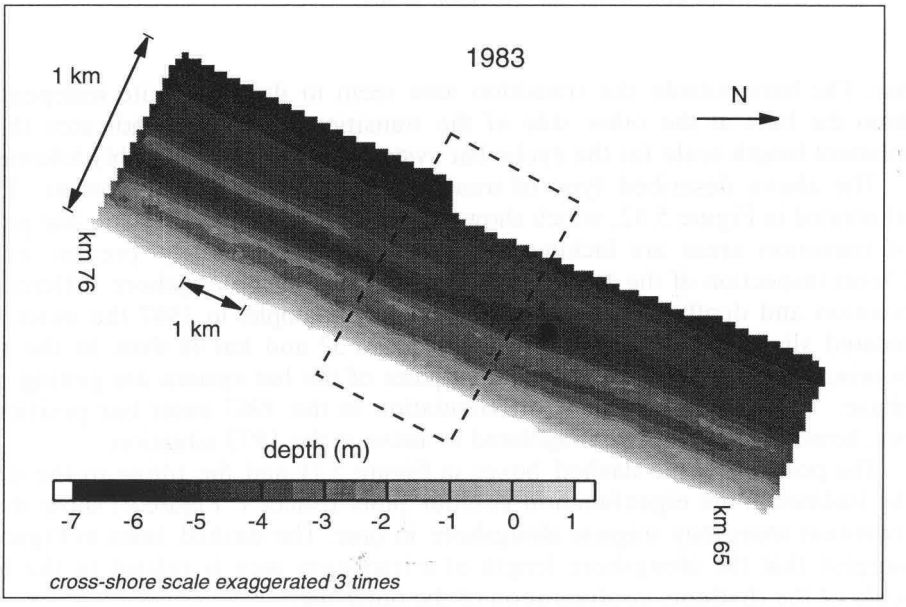

Figure 5.9: Nearshore bathymetry between km 65 and km 76 in 1983 (JARKUS data base). (Dashed box marks the transition area.)

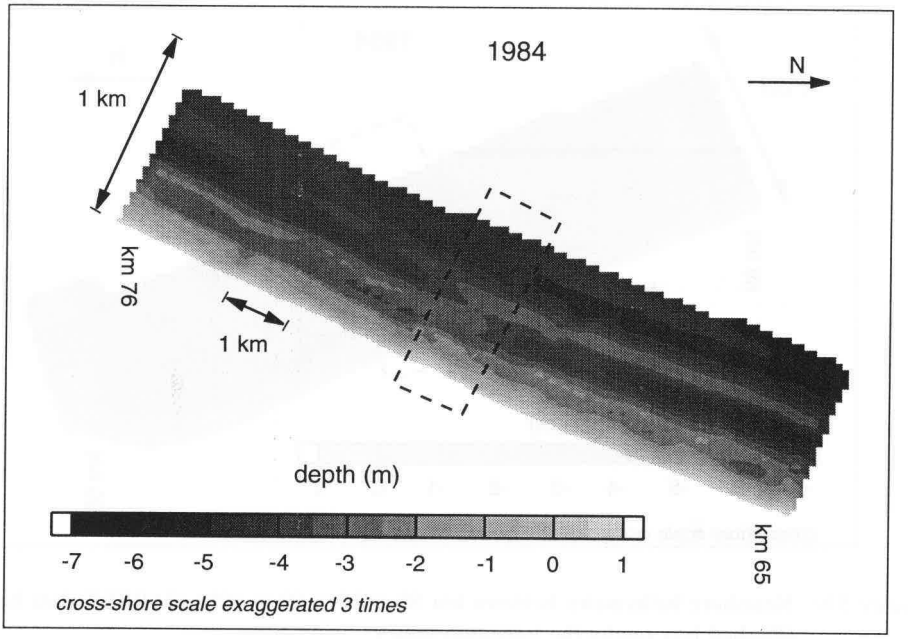

Figure 5.10: Nearshore bathymetry between km 65 and km 76 in 1984 (JARKUS data base). (Dashed box marks the transition area.)

bar. The bars outside the transition area seem to develop quite independently from the bars at the other side of the transition area. This indicates that the inherent length scale for the cyclic bar system behaviour is probably kilometres.

The above described type of transition area is not always present. This is illustrated in Figure 5.12, which shows that in 1967 the characteristic bar patterns of transition areas are lacking, whereas they are obviously present in 1973. Closer inspection of the 1967 picture reveals that small alongshore differences in position and depth of the outer bar exist. For example, in 1967 the outer bar is located slightly farther offshore between km 37 and km 41 than in the neighbouring areas. This may be a sign that parts of the bar system are getting out of phase. The small alongshore differentiation in the 1967 outer bar position can not, however, be simply extrapolated to arrive at the 1973 situation.

The position of the dashed boxes in Figure 5.11 and the tilting to the right of the isolines in the eigenfunction contour plots (Sheet 1: Figure c) show that the transition areas may migrate alongshore in time. The dashed lines in Figure 5.12 suggest that the alongshore length of a transition area is related to the length scale of the rhythmic configuration of the outer bar.

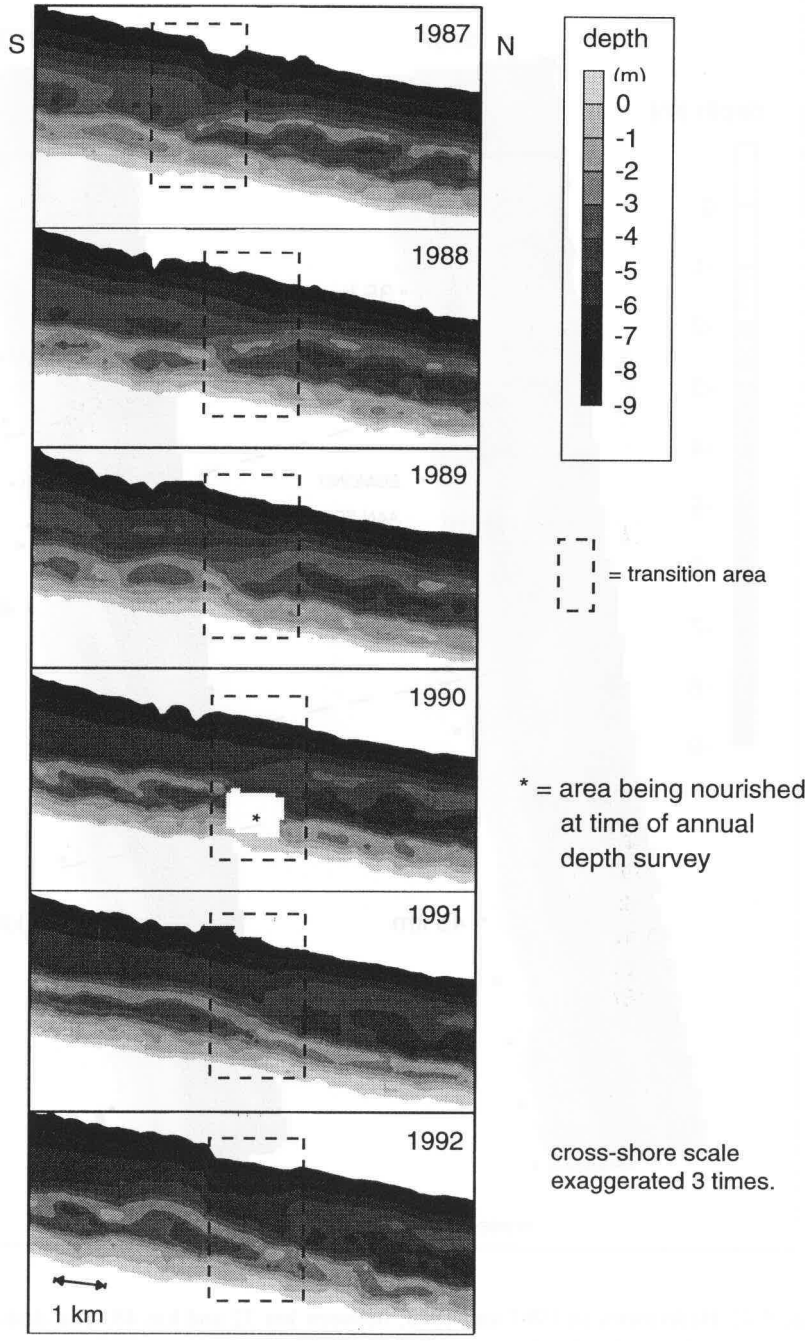

Figure 5.11: Bar behaviour between km 32.50 and km 42.75.

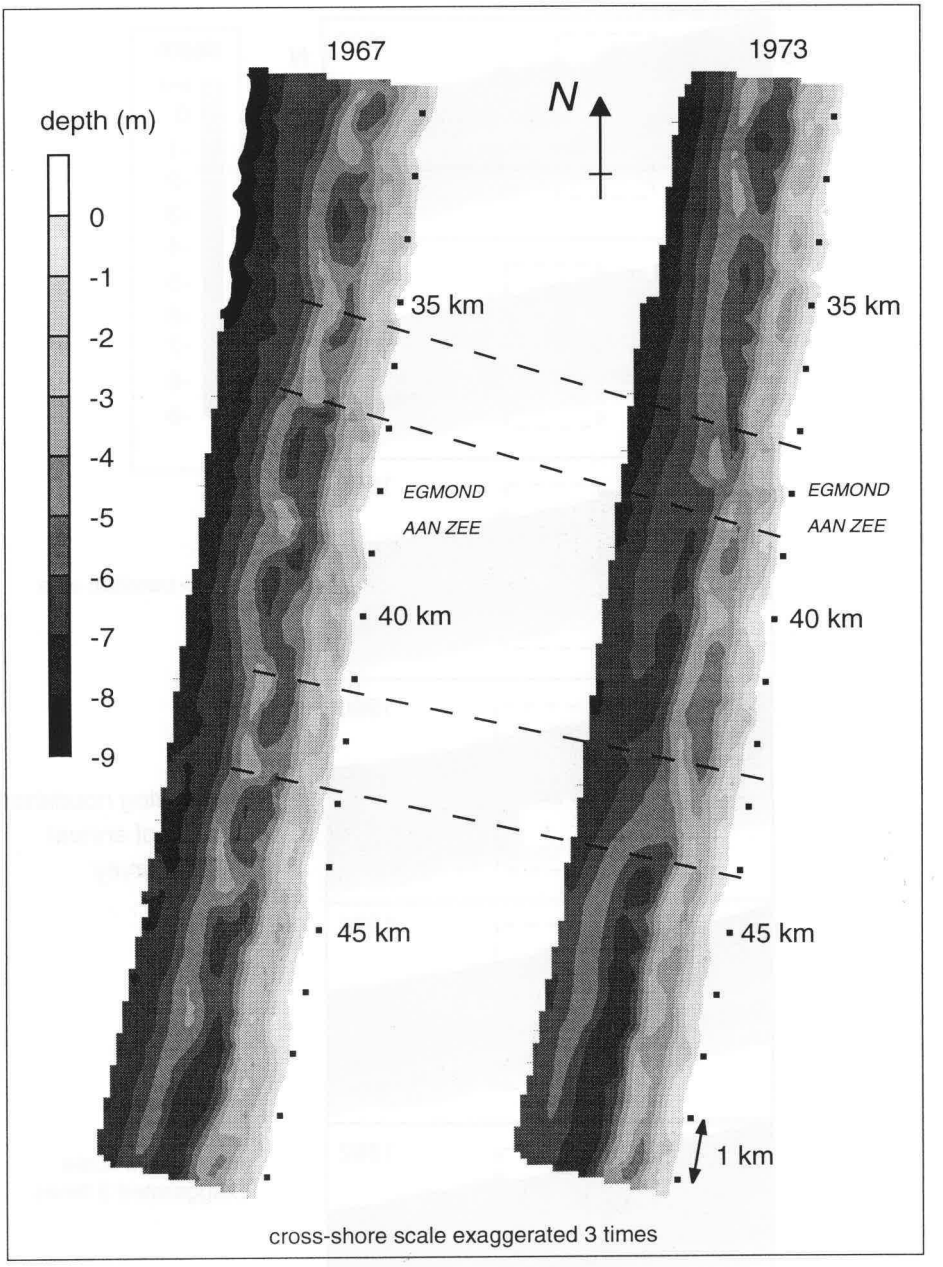

Figure 5.12: Bathymetry in 1967 and 1973, between km 32 and km 49. The dashed lines indicate the development of two transition areas.

Besides cyclic behaviour and alongshore 'out-of-phase' developments, other -more well known- developments occur: the development of rhythmic topography. The presence of rhythmic topography in the Noord-Holland bar system, especially in the outer bar, can be deduced from the 'folds' in the isolines of equal weightings (Section 4.2.3). These folds indicate that these rhythmic features may exist over a period of several years. Figure 5.13 and 5.14 illustrate the stability of these phenomena. Some changes occur, however, such as a slow alongshore migration (Figure 5.13). The spacing of the crescentic bar horns is remarkably constant though. The latter indicates either that the outer bar of the Noord-Holland bar system is seldomly active, or that the control of the existing morphology on the water motion is such that it stabilises the existing morphology.

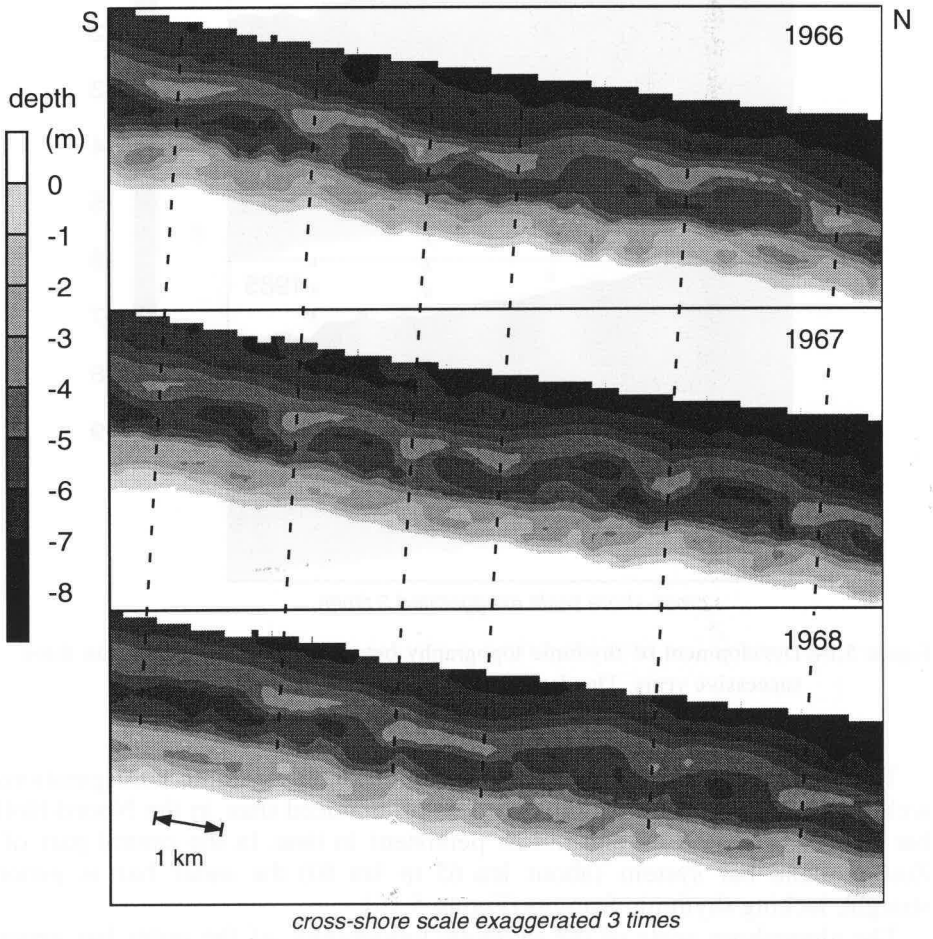

Figure 5.13: Development of rhythmic topography between km 35 and km 47 in three successive years. The dashed lines are parallel.

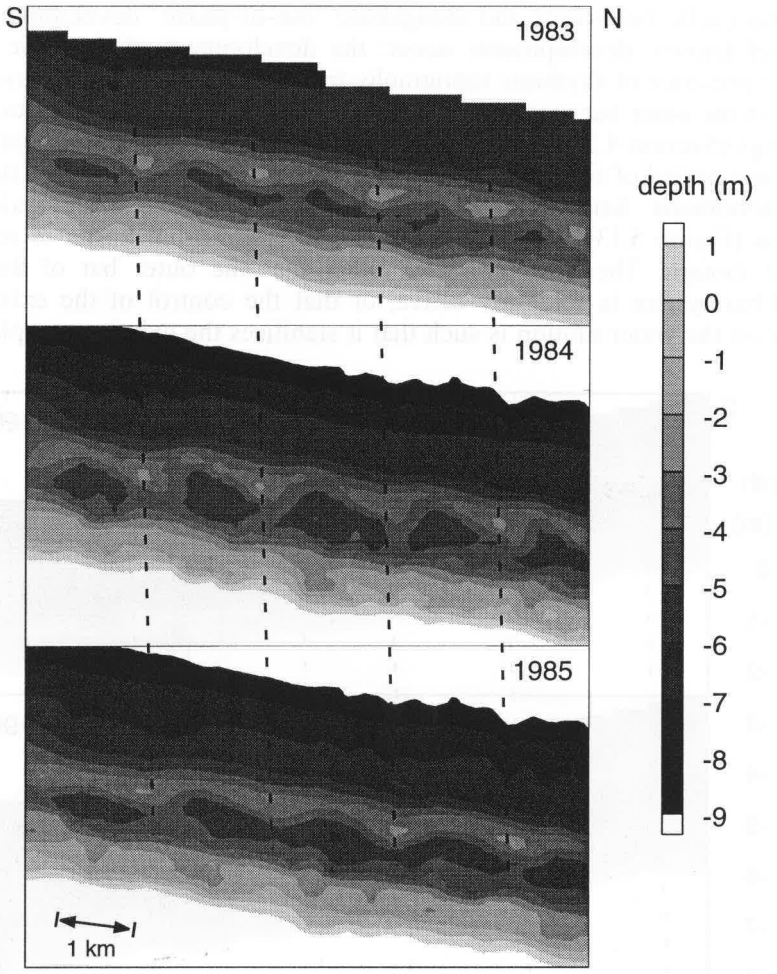

Figure 5.14: Development of rhythmic topography between km 32 and km 39 in three successive years. The dashed lines are parallel.

The bars in the Zuid-Holland bar system exhibit rhythmic configurations as well, but these rhythmic patterns are less pronounced than in the Noord-Holland bar system (Figure 5.15) and not as persistent in time. In the central part of the Zuid-Holland bar system (about km 65 to km 80) the outer bar is generally straight, lacking rhythmic features (Figure 5.16).

The alongshore scale of the rhythmic topography of the outer bar generally varies between about 1 and 3 km, with an average of about 2 km (Figure 5.17). These scales not only relate to very regular rhythmic structures, such as present in 1967 in the Noord-Holland bar system, but also to more irregular patterns,

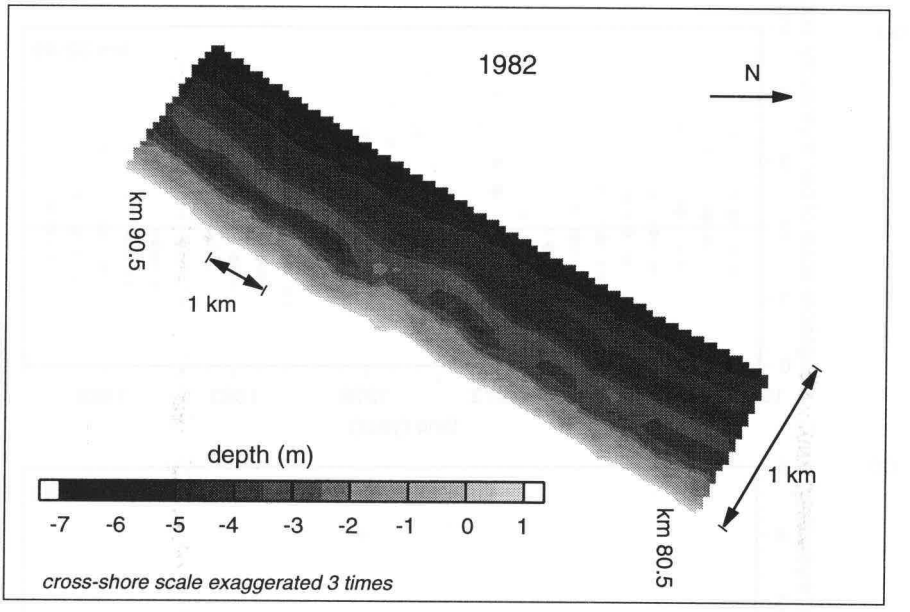

Figure 5.15: Nearshore bathymetry between km 80.5 and km 90.5 in 1982.

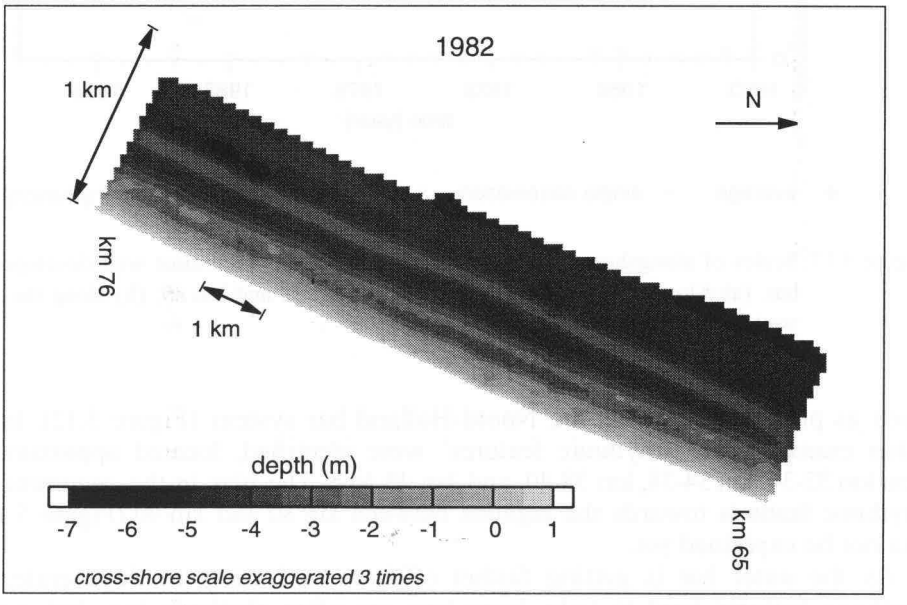

Figure 5.16: Nearshore bathymetry between km 65 and km 76 in 1982.

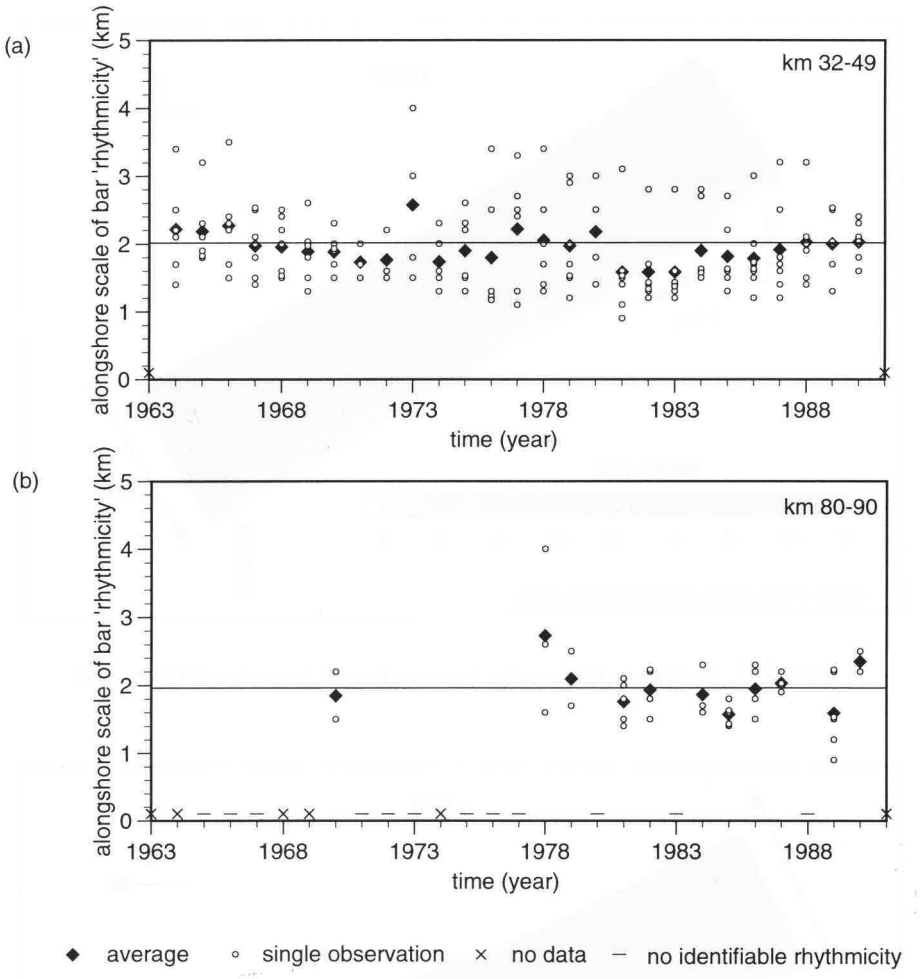

Figure 5.17: Scales of alongshore 'rhythmicity', observed in the outermost well-developed bar. (a) Along the stretch of coast between km 32 and km 49; (b) along the stretch of coast between km 80 and km 90.

such as present in 1973 in the Noord-Holland bar system (Figure 5.12). In the latter example, four 'rhythmic features' were identified, located approximately near km 32-34, km 34-38, km 38-40, and km 40-44.5. The bias in the occurrence of rhythmic features towards the eighties between km 80 and km 90 (Figure 5.17b), can not be explained yet.

As the outer bar is getting farther offshore and starts to degenerate, the rhythmic features tend to fade. Inner bars are often rhythmic too, but with a smaller length scale and not as persistent in time as the rhythmic patterns of the

outer bar. The minimum observable length scale for rhythmic configurations of the inner bar is 500 m, given the 250 m spacing of the cross-shore profiles. The cross-shore decrease in the length-scale of rhythmic topography towards the shoreline is consistent with observations along other coastlines (Greenwood and Davidson-Arnott, 1979; Goldsmith et al., 1982; Short and Aagaard, 1993).

The degeneration of the outer bar topography seems to occur mainly due to lowering of the bar top and not due to (simultaneous) filling of the landward located trough (Figure 5.18). The lowering of the bar relief seems to be an irreversible process, once the bar starts to degenerate it will not be rebuild as a pronounced bar again.

The second and third eigenfunctions in region 3 and 4 reveal that, on average, a lower elevation of the crest of the outer bar is accompanied by a more seaward position of the inner bar (Figure 5.19). This relationship is also illustrated in Figure 5.11. The deeper position of the crest of the outer bar may be caused by degeneration of the bar feature as well as by a seaward migration of the bar to deeper water.

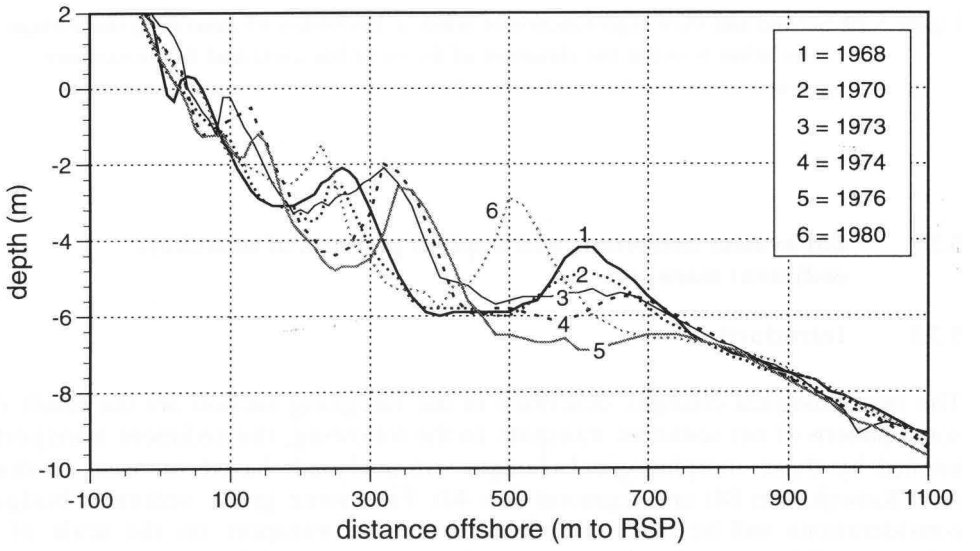

Figure 5.18: Degeneration of the outer bar. (Km 40, TAW data base.)

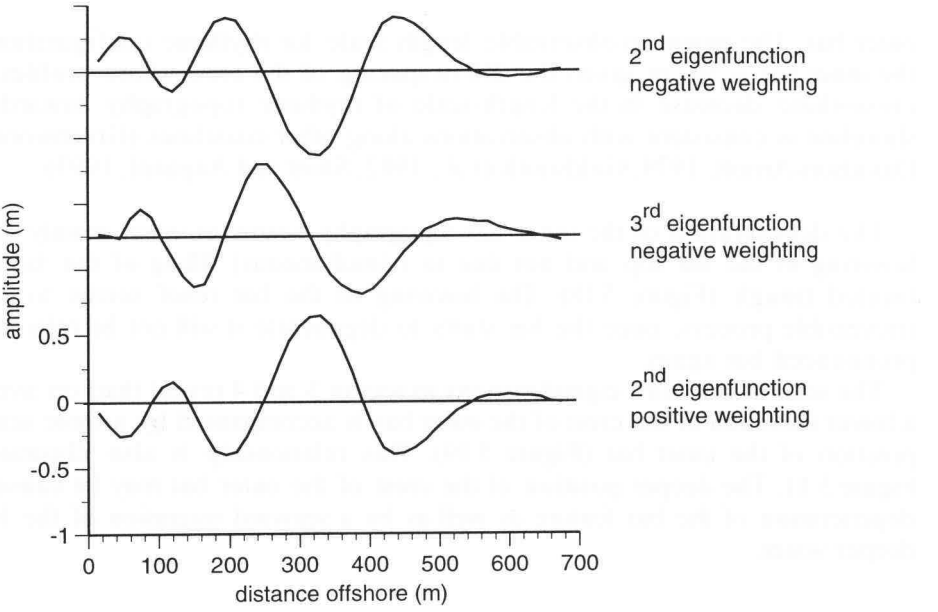

Figure 5.19: Second and third eigenfunction of window km 84-km 85 describing the average correlation between the elevation of the outer bar crest and the cross-shore position of the bar located landward of it.

5.3 Bar system behaviour and implied patterns of nearshore sediment transport

5.3.1 Introduction

The morphological changes described in the foregoing section are the result of some pattern of net sediment transport. In the following, the sediment transports implied by these morphological changes are analysed, based on case studies near Katwijk (km 84) and Egmond (km 40). First some gross sediment budget considerations will be made to infer directions of transport on the scale of a coherent offshore moving bar (typical alongshore scale 10 km). Next, transport patterns will be analysed in more detail by inferring transports from depth changes on the scale of the individual profile (typical alongshore scale is profile spacing, that is 250 m).

In the following, all transport rates are expressed in terms of a 'volume transport rate'. A 'volume transport rate' refers to a transport rate in which the transported sediment volume is expressed as a sediment volume including pores, i.e. as a volume that the sediment will occupy when being deposited. Assuming a

pore volume of about 40 % (Allen, 1985), a volume transport rate of for example 65 $m^3 m_a^{-1} yr^{-1}$ equals a 'normal' transport rate of about 40 $m^3 m_a^{-1} yr^{-1}$ (i.e. excluding pores) or about $1*10^5$ kg $m_a^{-1} yr^{-1}$ (ρ_{sed}=2650 kg/m^3).

5.3.2 Sediment transport patterns based on gross sediment budget considerations

Near Katwijk, the maximum volume of sediment enclosed in the outer bar prior to its degeneration is approximately 250 to 300 cubic meter per meter alongshore ($m^3 m_a^{-1}$) , taking the lower branch of the profile bundle envelope as the reference datum (Figure 5.20). This particular definition of bar volume was chosen because it refers to the total volume of sediment that is involved in the behaviour of this feature.

With the vanishing of the outer bar feature, the bar sediment may be transported offshore (C_s), onshore (C_{inner}), and alongshore (L_{ob}) (Figure 5.21). When the sediment is transported offshore (C_s) and/or carried away alongshore due to large-scale longshore transport gradients (L_{ob}), the cyclic bar behaviour represents a net loss of sediment from the inshore (on the alongshore scale of a coherent offshore moving bar). When the sediment is transported onshore (C_{inner}) it will only be lost from the inshore when it is transported further onshore into the beach and dune area (C_{db}), or when it is carried away alongshore by large-scale longshore transport gradients (L_{inr}). As will be argued in the following paragraphs, it appears that the sediment of the degenerating outer bar is transported (mainly) onshore towards the inner part of the nearshore zone, without being lost from the inshore area.

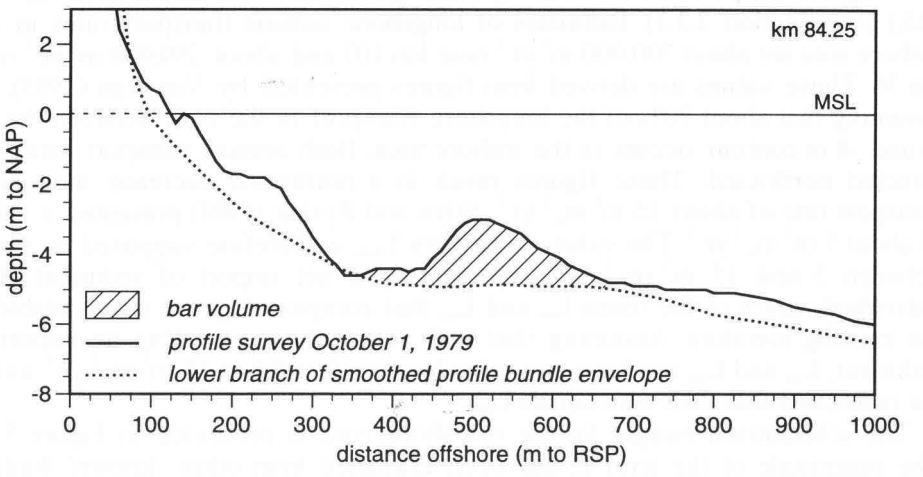

Figure 5.20: Definition sketch of bar volume.

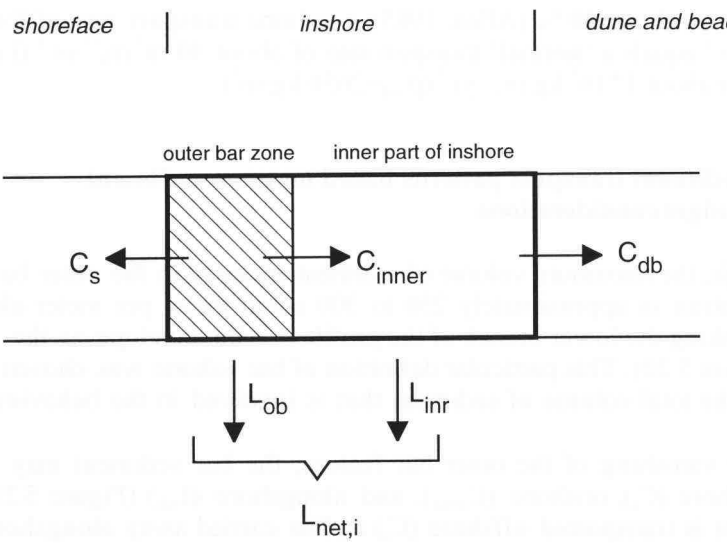

Figure 5.21: Potential transport components that may be involved in the degeneration of the outer bar and which may cause (subsequent) loss of this sediment form the inshore area. Considered length scale is that of a coherent offshore moving bar system. Codes are explained in the text.

Along the stretch of coast where the Zuid-Holland bar system is located, the dune and beach zone is accreting at a rate of about 5 to 10 $m^3 m_a^{-1} yr^{-1}$ (De Ruig and Louisse, 1991; also see Section 2.3.3). The inshore area has been described as being about stable as well as being eroding at a rate of about 2 to 3 $m^3 m_a^{-1} yr^{-1}$ (ΔS_i) (see Section 2.3.3). Estimates of longshore volume transport rates in the inshore area are about 700,000 $m^3 yr^{-1}$ near km 103 and about 290,000 $m^3 yr^{-1}$ near km 76. These values are derived from figures presented by Van Rijn (1995), by assuming that about 70% of the longshore transport in the zone between the +3 m and -8 m contour occurs in the inshore area. Both annual transport rates are directed northward. These figures result in a northward decrease in volume transport rate of about 15 $m^3 m_a^{-1} yr^{-1}$. Stive and Eysink (1989) presented a value of about 5 $m^3 m_a^{-1} yr^{-1}$. The value of the term $L_{net,i}$ is therefore supposed to range between 5 and 15 $m^3 m_a^{-1} yr^{-1}$, representing a net import of sediment. The individual values of the terms L_{ob} and L_{inr} that compose $L_{net,i}$ are not available in the existing literature. Assuming that both terms are representing an import of sediment, L_{ob} and L_{inr} can have any value between 0 and 5 to 15 $m^3 m_a^{-1} yr^{-1}$ under the restriction that their sum equals $L_{net,i}$.

The schematised budget for the nearshore zone is presented in Figure 5.22. The magnitude of the term C_s has been estimated from other 'known' budget terms. Considering the uncertainties in the 'known' budget terms in the inshore and 'dune and beach' area, 'known' budget terms for the zone seaward of the

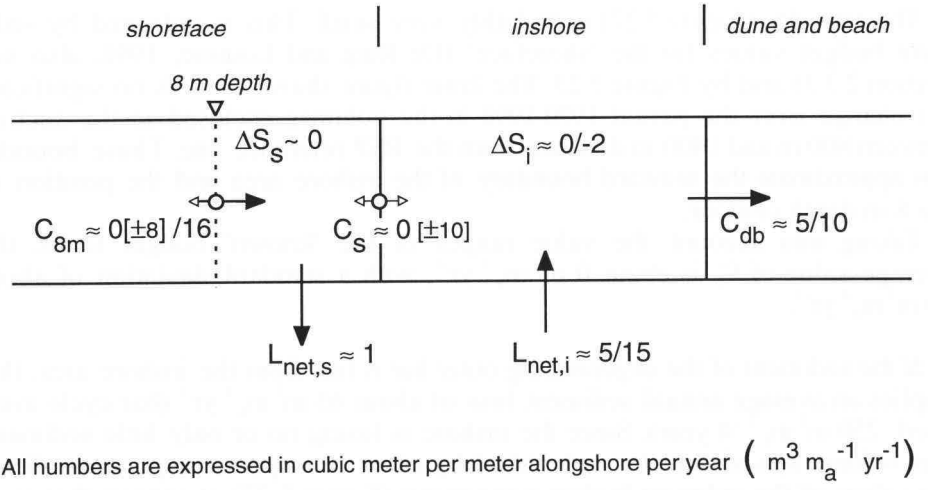

Figure 5.22: Sediment budget situation near Katwijk (sources: De Ruig, 1989; Roelvink and Stive, 1989; Stive and Eysink, 1989; De Ruig and Louisse, 1991; Van Rijn, 1995). Considered length scale is that of a coherent offshore moving bar system. The arrows indicating the longshore transport gradient only refer to import or export of sediment, and not to the geographical direction of the transport (i.e. northward or southward).

inshore area are used in the estimation of C_s as well. A best estimate of C_s is derived by using two equations (onshore transport having a positive sign):

$$C_s = \Delta S_i + C_{db} - L_{net,i} \tag{5.1}$$

$$C_s = C_{8m} + L_{net,s} - \Delta S_s \tag{5.2}$$

The term C_{8m} (Figure 5.22) may vary between 0 ± 8 $m^3\ m_a^{-1}\ yr^{-1}$ (Van Rijn, 1995) and 16 $m^3\ m_a^{-1}\ yr^{-1}$ in landward direction (Roelvink and Stive, 1989).

The term $L_{net,s}$ (Figure 5.22) will be order 1 $m^3\ m_a^{-1}\ yr^{-1}$. This quantity is derived from calculated longshore transports rates at 8 m depth at km 103 and km 76 (Van Rijn, 1995). These transports result in a gradient of the longshore volume transport at this depth of about $0.7*10^3$ $m^3\ m_a^{-1}\ yr^{-1}$ per meter cross-shore, inducing a sediment loss by longshore transport. Towards shallower water the longshore transport rates will probably increase somewhat, due to increased sediment stirring by the waves, but it is not straightforward whether the gradients will increase too. The distance between the 8 m depth contour and the seaward boundary of the breaker bar zone is about 600 m. Therefore, the term $L_{net,s}$ will be order 1 $m^3\ m_a^{-1}\ yr^{-1}$.

The term ΔS_s (Figure 5.22) is probably very small. This is indicated by sediment budget values for the 'shoreface' (De Ruig and Louisse, 1991; also see Section 2.3.3) and by Figure 5.23. The latter figure shows there is no significant net change over the period 1970-1990 in the volumes enclosed in the section between 800 m and 1400 m distance from the RSP reference line. Those boundaries approximate the seaward boundary of the inshore area and the position of the 8 m depth contour.

Taking into account the value ranges of the 'known' budget terms, the average value of C_s is about 0 $m^3\ m_a^{-1}\ yr^{-1}$, with a standard deviation of about 10 $m^3\ m_a^{-1}\ yr^{-1}$.

If the sediment of the degenerating outer bar is lost from the inshore area, this implies an average annual sediment loss of about 65 $m^3\ m_a^{-1}\ yr^{-1}$ (bar cycle averaged: 250 $m^3\ m_a^{-1}$ /4 year). Since the inshore is losing no or only little sediment, this volume loss should be replenished by other transport components. Given the values of the sediment budget components (Figure 5.22) it appears that most

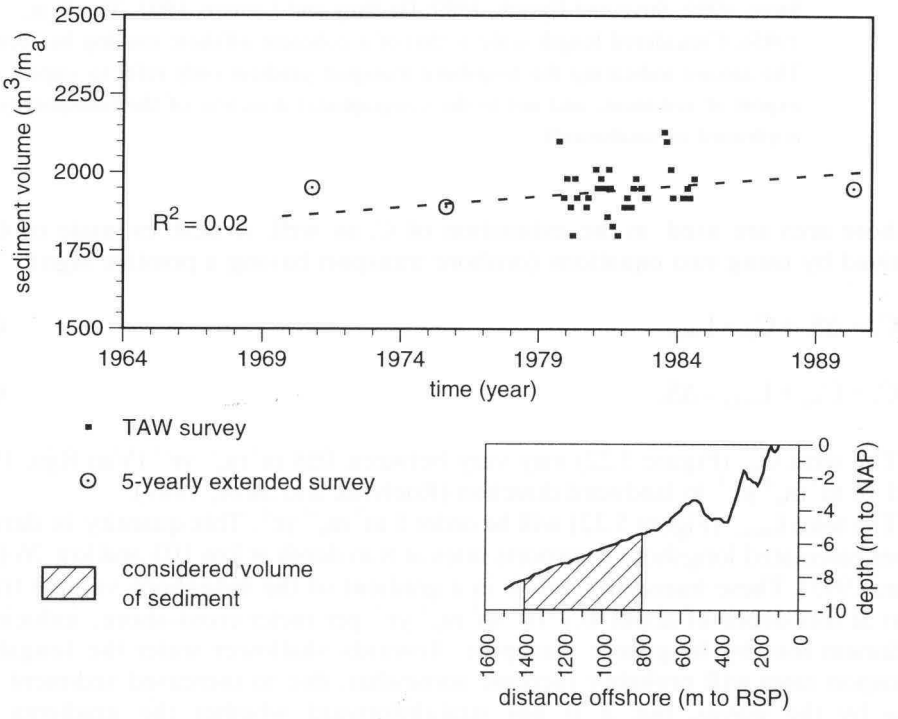

Figure 5.23: Change in sediment volume over the period 1970-1990 in the 600 m wide zone between 800 m and 1400 m seaward of the RSP reference line, near Katwijk (km 84.25). Lower limit is 10 m -NAP.

of the sediment of the degenerating outer bar has to stay within the inshore area. Therefore C_{inner} (Figure 5.21) will be the most important transport component in the degeneration process of the outer bar. Consequently, the cyclic bar behaviour appears to be essentially a cross-shore redistribution of sediment.

5.3.3 Sediment transport patterns based on profile considerations

The establishment that cyclic bar behaviour has to be a cross-shore sediment redistribution process originates from gross budget considerations on the scale of a coherent offshore moving bar. To study to what extend this concept applies on the scale level of an individual cross-shore profile, sediment transport directions will be inferred from changes in the cross-shore profile.

Morphologic changes in a cross-shore profile consist of depth changes through time at all cross-shore positions x. These changes in depth occur due to gradients in the cross-shore and longshore volume transport, respectively $\partial q_x/\partial x$ and $\partial q_y/\partial y$. The terms q_x and q_y are expressed in terms of cubic meters per meter per unit of time. This yields:

$$\partial h/\partial t = \partial q_x/\partial x + \partial q_y/\partial y \qquad (5.3)$$

To investigate whether the cyclic bar behaviour is also a dominantly cross-shore sediment redistribution process on the scale level of individual profiles, the alongshore transport gradient $\partial q_y/\partial y$ will be assumed to be zero. Equation 5.3 then reduces to:

$$\partial h/\partial t = \partial q_x/\partial x \qquad (5.4)$$

The cross-shore transport rate q_x at location x can be derived by integrating expression 5.4:

$$q_x(x) = \int_0^x (\partial h/\partial t)\, dx + q_x(0) \qquad (5.5)$$

where x = 0 is located at the seaward boundary of the inshore area.

The second right hand term in equation 5.5 equals C_s (Figure 5.22). Therefore, the value of $q_x(0)$ is assumed to be zero on the time-scale of the cyclic bar system behaviour. The first right hand term in equation 5.5 can be approximated from the profile measurements (Figure 5.24a), because these reveal $\Delta h/\Delta t$ as a function of x (Figure 5.24b). Next, $q_x(x)$ over the time interval Δt between two profile surveys can be solved (Figure 5.24c).

In the example shown in Figure 5.24, a sediment gain of about 75 $m^3 m_c^{-1}$ occurred. In case of cross-shore sediment redistribution alone, the transport at the left hand side of the figure should have been equal to zero. Over the same

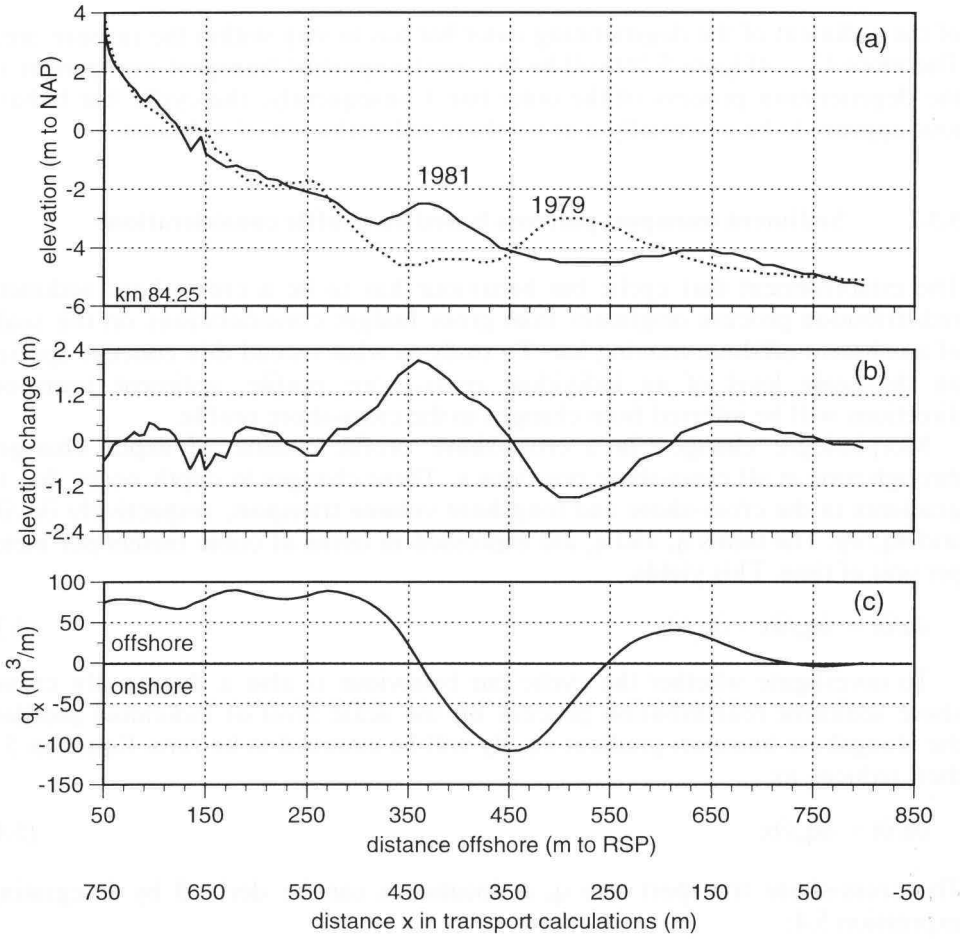

Figure 5.24: Derivation of net cross-shore transport Q_x near km 84.25, period 1979-1981. (a) Cross-shore profiles; (b) net elevation change over the period 1979-1981; (c) net cross-shore transport over the period 1979-1981, for a zero cross-shore transport at the offshore boundary, and a zero longshore transport gradient.

time interval, nearby profile lines appear to be losing sediment (Figure 5.25a). The observed sediment gain in the profile line at km 84.25 appears to be explained by the occurrence of alongshore redistribution of sediment simultaneously with the degeneration of the outer bar. The alongshore redistribution deals with the developments of rhythmic topography, mostly in the inner part of the nearshore, and with the behaviour of the outer bar attachment near km 85.5 (Figure 5.25b and Figure 5.26). The average sediment gain in the inner part of the nearshore (zone 50 m - 450 m) is about 75 m^3 m_a^{-1}, whereas the average sediment loss in the

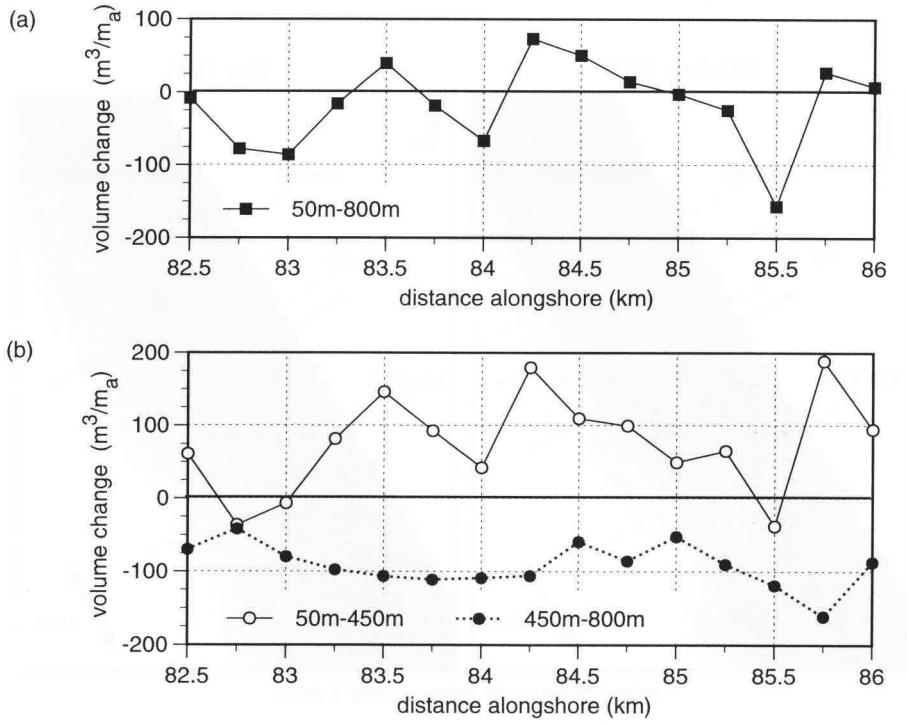

Figure 5.25: Volume change in the nearshore zone per profile cross-section of 1 m width, over the period 1979-1981. (a) Zone 50 m -800 m seaward of RSP; (b) zone 50 m - 450 m seaward of RSP, and zone 450 m - 800 m seaward of RSP.

outer part of the nearshore (zone 450 m - 800 m) is about 90 $m^3\ m_a^{-1}$. These figures add up to a net nearshore sediment loss of about 15 $m^3\ m_a^{-1}$. This loss may be real, but may as well be attributable to measurement errors (Section 3.2).

The longshore transports associated with the longshore redistribution of sediment in the inner nearshore can be approximated with help of equation 5.3. Equation 5.3 can not be solved for every cross-shore position in the profile, because no knowledge is available on the cross-shore distribution of alongshore transports to be prescribed at the longshore boundary. However, equation 5.3 can be used in a modified form:

$$\partial A/\partial t = Q_x + \partial Q_y/\partial y \qquad (5.6)$$

where: $A = \int_{50\text{ m RSP}}^{450\text{ m RSP}} h\,dx$ and $Q_x = \int_{50\text{ m RSP}}^{450\text{ m RSP}} q_x\,dx$ and $Q_y = \int_{50\text{ m RSP}}^{450\text{ m RSP}} q_y\,dx$.

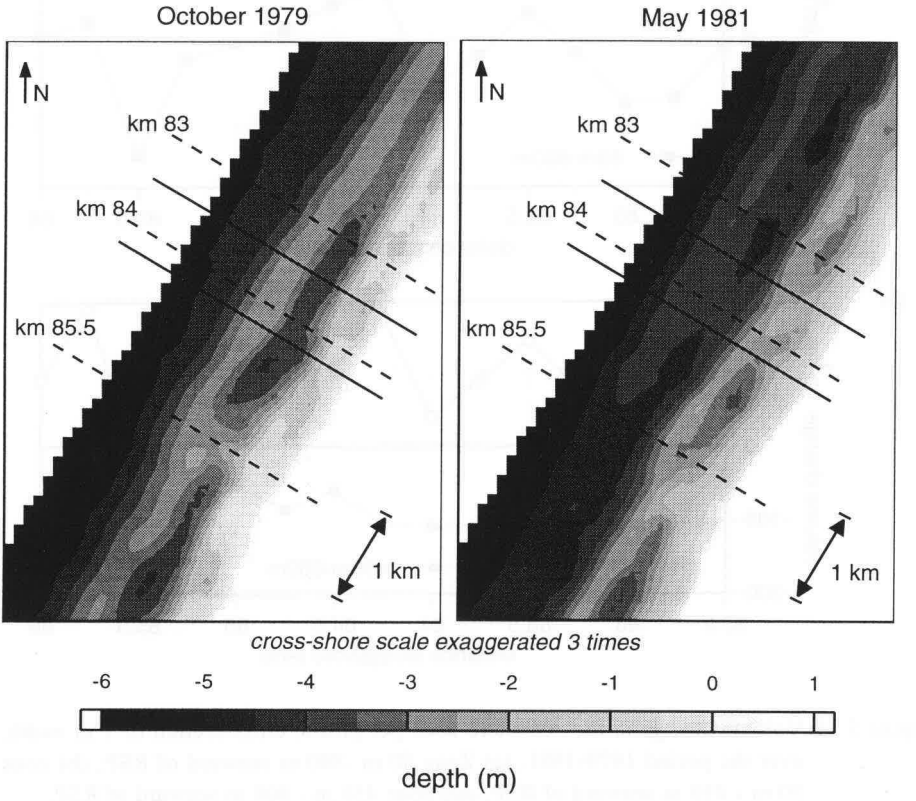

Figure 5.26: Bathymetry in the vicinity of km 84.25, in 1979 and 1981.

In this modified equation, h and q_y are integrated over a cross-shore interval. The selected interval extends from 50 m to 450 m seaward of the RSP reference line. The term $\partial h/\partial t$ is then replaced by $\partial A/\partial t$, which represents the difference between two profiles in terms of an area (A). The term Q_x describes the net cross-shore input of sediment into the inner nearshore. Q_y is the total longshore transport in the zone 50 m to 450 m seaward of the RSP reference line. Integration of equation 5.6 over the longshore stretch between km 82.5 and km 86 will yield an approximation of the longshore transport pattern that resulted in the observed longshore redistribution of onshore transported sediment. The integrated equation reads as:

$$Q_y(y) = \int_{y_1}^{y} \{\partial A/\partial t - Q_x\}\, dy + Q_y(y_1) \qquad (5.7)$$

Near Katwijk, the net yearly averaged longshore transport in the nearshore zone is directed northward (Van Rijn, 1995). Therefore, the transport calculations start at the southern boundary of the considered stretch, that is at y_1= 86 km. The value of $Q_y(y_1)$ is set at 350,000 m^3. This is considered to be the approximate value for the mean net longshore transport at km 86 over the considered 19 month period (October 1979-May 1981). The value was derived by assuming that about half of the net annual longshore transport in the nearshore zone occurs in the zone between 50 m and 450 m from the RSP (see 'gross budget considerations'). The term Q_x is assumed to be equal to the volume change in the zone between 800 m and 450 m RSP minus the longshore averaged net loss of about 15 m^3 m_a^{-1}. The calculated net loss of about 15 m^3 m_a^{-1} is removed from the data, because of the uncertainty about the value of this net change

The cross-shore integrated longshore transport rates that may have produced the observed longshore redistribution of sediment in the inner nearshore, are shown in Figure 5.27. Any net sediment loss (or gain) can be represented in Figure 5.27b by adding a longshore gradient to the longshore transport curve.

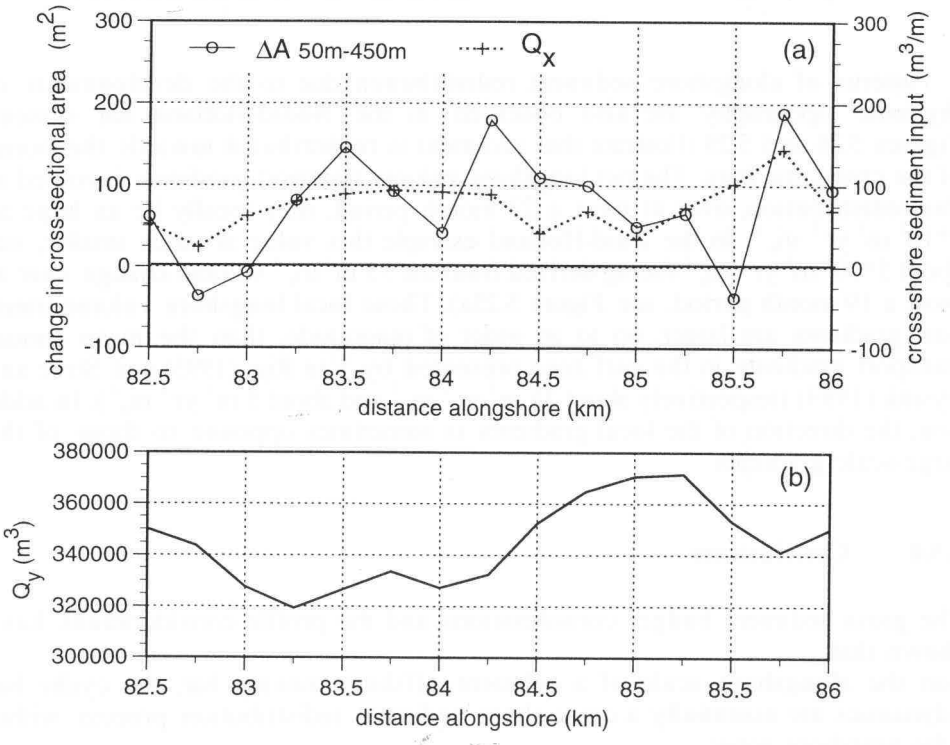

Figure 5.27: Alongshore variation near Katwijk in: (a) 1979-1981 change in cross-sectional area (ΔA) over the zone 50 m -450 m seaward of RSP, and cross-shore sediment input into this zone Q_x; (b) net longshore transport Q_y over the period 1979-1981 in the zone 50 m - 450 m seaward of RSP (northward directed).

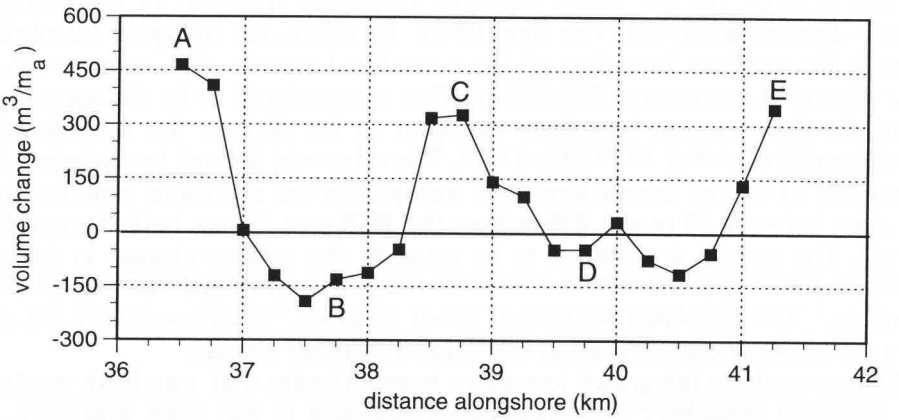

Figure 5.28: Volume change in the nearshore zone near Egmond over the period 1965-1967, per profile cross-section of 1 m width, (zone 0 m -800 m seaward of RSP).

Patterns of alongshore sediment redistribution due to the developments of rhythmic topography are also observed in the Noord-Holland bar system. Figures 5.28 and 5.29 illustrate that sediment is redistributed towards the horns of the crescentic bars. The net longshore volume transport gradients involved in this redistribution, over at most a 23 month period, may locally be as large as $2*10^2$ m^3 yr^{-1} m_a^{-1}. In the Zuid-Holland example this value is much smaller, viz. about $5*10^1$ m^3 yr^{-1} m_a^{-1} (being derived from the 75 m^3 m_a^{-1} volume change over at most a 19 month period, see Figure 5.25a). These local longshore volume transport gradients are larger, up to an order of magnitude, than the mean annual transport gradients in the surf zone presented by Van Rijn (1995) and Stive and Eysink (1989) (respectively about 15 m^3 yr^{-1} m_a^{-1} and about 5 m^3 yr^{-1} m_a^{-1}). In addition, the direction of the local gradients is sometimes opposite to those of the large-scale gradients.

5.3.4 Conclusions

The gross sediment budget considerations and the profile considerations have shown that:

- on the alongshore scale of a coherent offshore moving bar, the cyclic bar dynamics are essentially a cross-shore sediment redistribution process within the nearshore zone;
- on the scale of individual profile cross-sections, alongshore redistribution may be superimposed on the cross-shore redistribution process;
- the process of bar degeneration is associated with onshore directed sediment transport.

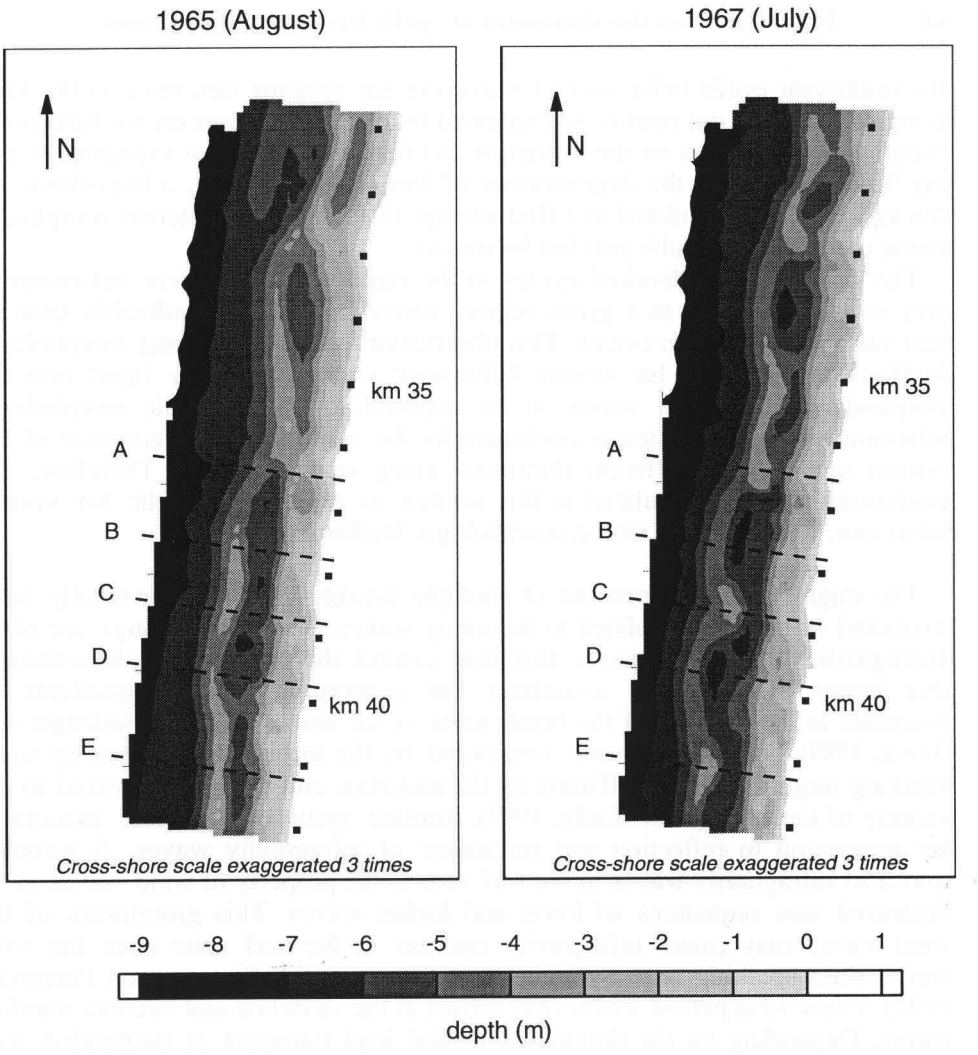

Figure 5.29: Nearshore bathymetry between km 31 and km 42 in 1965 and 1967.

These findings imply that:

- the *offshore* movement of the bar that is located landward of the degenerating outer bar, is at least partially caused by (net) *onshore* directed transport (towards its seaward slope).

Further, the observation that the landward trough is not filling in at an equal rate with the lowering of the outer bar (Section 5.2), indicates that:

- when sediment is removed from the outer bar it is 'immediately' entrained into the inner bar system and subsequently redistributed in there.

5.4 Hypothesis on the dynamics of cyclic bar system behaviour

The multi-year cyclic behaviour of nearshore bar systems described in the foregoing section, can not readily be explained by existing theories on bar behaviour. Existing theories focus on the formation and maintenance of bar topography and pay little attention to the degeneration of bars. In this section, a hypothesis on this topic will be formulated as a first attempt to formulate a coherent morphodynamic model for the multi-year bar behaviour.

The duration of individual cycles in the multi-year bar system behaviour is very constant in time in a given region, considering the considerable year-to-year variability in storm events. This observation points to a strong morphologic feedback in the cyclic bar system behaviour; no cyclic energy input into the morphodynamic system seems to be required to obtain cyclic morphologic behaviour. This impression is confirmed by the simultaneous occurrence of bar system cycles with different durations along one coastline. Therefore, the mechanism that is formulated in this section to explain the cyclic bar system behaviour, will include a strong morphologic feedback.

The migration and formation of multiple breaker bars have generally been attributed to processes related to incoming waves. Two main groups are often distinguished in the processes that may control the breaker bar phenomenon. One group of processes associates bar generation with the gradients of processes in the vicinity of the break point of the waves (e.g. see Sallenger and Howd, 1989). For example, sand suspended by the turbulence induced by wave breaking might be carried offshore by the undertow and then be deposited in the vicinity of the breakpoint (Dally, 1987). Another group of processes associates bar generation to reflection and resonance of infragravity waves. A possible source of infragravity waves in the surf zone is the property of wind waves to be organised into sequences of lower and higher waves. This groupiness of the wind waves may cause infragravity motions in the surf zone once the wind waves start breaking (e.g. Symonds and Bowen, 1984; Watson and Peregrine, 1992). These long period waves may reflect at the shoreline and become standing waves. Depending on the dominance of bed load transport or suspended load transport, bars form under the nodes or antinodes of the standing waves (e.g. Carter et al., 1973; Holman and Bowen, 1982; Huntley et al., 1993).

Theories that relate nearshore bar formation to the non-linear interaction of the wave-driven longshore current with the seabed (e.g. Hino, 1974; Damgaard Christensen et al., 1995) seem less applicable to a multiple bar system situation. The longshore current based models generate bar systems that consist of longshore series of bars that are obliquely to transversely oriented to the shoreline. Multiple bar systems, however, consist of a cross-shore series of bars of which the outer ones are often oriented quite parallel to the shoreline.

Another model concept that does not belong to one of the two main groups of theories, relates bar formation to the interaction of the first and second harmonic of shoaling waves in a regular wave field (e.g. Boczar-Karakiewicz and Davidson-

Arnott, 1987; Boczar-Karakiewicz et al., 1995). This highly idealised model concept produces nearshore bars with a realistic cross-shore scaling. It is not obvious yet, however, to what extent the proposed mechanism is valid in a random wave field and under breaking waves. The latter are conditions in which natural bar systems have been observed to change (e.g. Birkemeier, 1984; Sallenger et al., 1985; Lippmann et al., 1993).

Considering the important role of wind waves in the proposed mechanisms for bar generation, it seems reasonable to assume that the forcing of the cyclic bar behaviour is also to a large extent determined by wave-related processes.

Next, it is assumed that the outer bar governs the cyclic behaviour of the bar system, i.e. as long as the outer bar remains well developed, the inner bars will not migrate further offshore (see also Kroon, 1994). This type of correlation between the behaviour of the outer bar and the behaviour of the inner bars has been shown to exist along the Holland coast (Section 5.2), and has also been observed near Terschelling (Ruessink and Kroon, 1994). However, the proposed cause-effect relation has not been proven to exist. Nevertheless, the proposed cause-effect relation is intuitively attractive, because the outer bar obviously exerts a control on the wave field that approaches the inner bar system, especially during high wave conditions (Carter, 1988). The deeper the outer bar crest is located the higher the waves that can pass unbroken towards the inner bar(s). Further, the depth of the outer bar crest influences the location of the excitation of long period waves due to the breaking of (groupy) waves. Additionally, the location and depth of the outer bar may play a role in selecting resonant infragravity wave modes (Aagaard, 1990).

Following from the assumption on the role of the outer bar, the key to explaining the cyclic nature of the bar system behaviour lies in explaining the systematic degeneration of the outer bar at a certain, relatively constant, distance from the shoreline. The formulation of a hypothesis to explain the degeneration of the outer bar starts from the simple notion that the alternation of bar-maintaining conditions and bar-degenerating conditions determines the fate of a bar. A bar will not disappear as long as bar-maintaining conditions are stronger and/or occur more frequently than the bar-degenerating conditions. The observation that the outer bar disappears at a certain distance from the shoreline or -probably more appropriate- at a certain depth, expresses that for some reason bar-degenerating conditions start to dominate bar-maintaining conditions. The following step is to specify what these bar-maintaining and bar-degenerating processes are.

The two main groups of theories on breaker bar formation relate the formation and maintaining of the bar topography to the breaking of waves. Therefore, the conditions that favour the existence of a bar feature are expected to be related to conditions with breaking waves. Further, observations exist of a nearshore bar well within the zone of breaking waves becoming better developed (Birkemeier, 1984; Sallenger et al., 1985; Lippmann et al., 1993). Larson and Kraus (1992)

observed that the volume growth and offshore movement of an outer bar, in a double bar system, only occurred during the more energetic storms. Therefore, it is concluded that conditions with wave breaking on the outer bar are able to maintain a barred topography.

Little is known about conditions that favour the in situ degeneration of a bar feature (not to confuse with the disappearance of a bar feature due to the welding of the bar to the beach). Near Duck (North Carolina, USA) the volume of the outer bar was observed to decrease gradually under the influence of non-breaking waves. The outer bar never showed a tendency to move significantly onshore as a unit, but it appeared to experience steady onshore transport across its body under the action of non-breaking waves (Larson and Kraus, 1992). These observations on the morphologic development of the outer bar are very similar to the morphologic development of a degenerating outer bar along the Holland coast. Therefore, it is concluded that conditions of non-breaking waves on the outer bar favour degeneration of this bar.

The observation that the degeneration of the outer bar goes with onshore directed transport (Section 5.3; Larson and Kraus, 1992) leaves only a selected group of potentially responsible degeneration processes. Wave-related processes outside the surf zone that are potentially able to transport sediment onshore are: wave asymmetry, boundary layer streaming, and the combination of obliquely incident waves and a mean longshore current. Boundary layer streaming, or the Longuet-Higgins effect, is a near-bottom flow in addition to the Stokes drift. This flow is induced by a time-averaged, net downward transfer of momentum into the boundary layer which is compensated by viscous diffusion (Van Rijn, 1994).

The near-bed flow due to the Longuet-Higgins effect is generally directed onshore, but under (very) asymmetric waves the net streaming in the boundary layer has been observed to become directed offshore (Ribberink and Al-Salem, 1992; Van Rijn, 1993). This implies that degeneration of the outer bar due to this process can only occur during relatively calm conditions. Profile observations from the TAW data base have shown that during the calm summer season changes in the outer bar topography are negligible. Therefore, it seems unlikely that the boundary layer streaming is the process responsible for the degeneration of the outer bar. The inactivity of the outer bar during the summer season further indicates that the degeneration of the outer bar is not caused by the combination of a longshore current (tide or wind driven) with obliquely incident, symmetric waves. As a consequence, wave asymmetry is the most likely process to cause the degeneration of the outer bar, with or without the help of longshore currents. It is expected that especially conditions with highly asymmetric waves on the outer bar are effective in degenerating the outer bar, because these conditions will mainly occur during the 'winter storm period' in which the outer bar has been observed to degenerate.

Asymmetric waves passing the outer bar without breaking will theoretically cause a cross-shore transport gradient across the outer bar (because of the changing water depth), moving the bar onshore. The outer bar, however, has not

been observed to move onshore nor did the trough fill in with sediment. This discrepancy can be explained by the presence of a longshore current that is stronger in the trough than on the bar crest. The sediment that passes the bar crest can not be deposited at the landward side of the bar because it is kept in transport by the longshore current in the trough (cf. Greenwood and Davidson-Arnott, 1979). Since the trough will be just outside the surf zone during the considered conditions, the longshore current has to be driven mainly by the tide and the wind.

The outer bar sediment has to end up in the inner bar system (see Section 5.3). Therefore, the longshore transported sediment has to cross the trough. This crossing may occur because of some remaining wave asymmetry, or some remaining obliqueness in the wave approach.

During the conditions that waves are highly asymmetric on the outer bar, rather intense wave breaking will occur on the inner bar. This will induce currents in the inner nearshore zone, which may occur in the horizontal plane (cell circulation) and in the vertical plane (undertow). In case the horizontal type of circulation dominates, the sediment that crosses the trough will be entrained into the inner bar system along the stretches with onshore directed flow. The sediment may be redistributed alongshore or may be deposited at the seaward side of the inner bar by the seaward flowing rip currents. If the vertical circulation type of water motion dominates, the sediment that crosses the trough will be deposited seaward of the breaker zone, probably at the lower seaward slope of the inner bar.

The often observed rhythmic configurations of the nearshore bars, especially in the Noord-Holland bar system, may be considered cause or evidence of the occurrence of horizontal circulations. The observed longshore redistribution in the inner nearshore of the onshore transported sediment may also indicate that horizontal circulations occur. However, the longshore redistribution of sediment does not necessarily occur at the same time as the degeneration of the outer bar. No observations are available of the character of the nearshore circulation during the conditions that induce the degeneration of the outer bar. Therefore, it is not possible to be decisive on how the sediment of the degenerating outer bar is included in the inner bar system.

Summarising, the conditions that maintain the outer bar are those with (intensive) wave breaking on the outer bar, i.e. the 'severe' storm events. The conditions that will favour bar degeneration are the conditions with highly asymmetric waves on the outer bar. These conditions will probably occur when the highest waves of the wave field just start to break on the outer bar, i.e. the 'mild' storm events. The characterisations of the strength of the storm events are in quotes because they do not represent an absolute strength of storm events, but a relative strength. One storm event can be 'severe' for a shallow located outer bar and can be considered 'mild' for an outer bar at a deeper position. This concept of relative strength of a storm gives the key to explaining the final disappearance of the outer bar.

During a storm with well-developed wave breaking on the outer bar, the migration of this bar, if any, will be directed offshore (Birkemeier, 1984; Sallenger et al., 1985; Aagaard, 1993; Lippmann et al., 1993; Sunamura and Takeda, 1993). Because the mean sea bed is sloping seawards, the bar crest will be located at a larger depth after offshore migration. This implies that somewhat larger storms are required to create again bar-maintaining conditions. Larger storms occur less frequently and therefore the 'severe' storm conditions will also occur less frequently on the new position of the outer bar. In addition, some of the formerly 'severe' storm events will become 'mild' storm events for this outer bar.

The frequency of occurrence of the bar-degenerating conditions, or the 'mild' storms, does not necessarily increase with a deeper position of the bar crest. The change in frequency of occurrence of these conditions will depend on the wave climate distribution of the wave heights. Wave conditions that formerly produced wave breaking on the outer bar will now produce highly asymmetric waves on the new, deeper position of the outer bar. At the same time, some of the wave conditions that formerly produced asymmetric waves on the outer bar, will now produce symmetric waves on the deeper positioned bar. Therefore, with the deeper position of the outer bar, the frequency of occurrence of bar-maintaining conditions is expected to decrease, while the change in frequency of occurrence of bar-degenerating conditions will depend on the wave climate.

In the early stage of the 'life' of a bar -i.e. in between its 'birth' near the shoreline and its 'passing away' far offshore- the bar may also build up during the offshore migration. In that case, the crest of the bar does becomes located less deep than implied by the bed slope and the distance of offshore migration. This bar growth slows down or neutralises the effect of offshore migration on the frequency of occurrence of 'severe' storms. At some moment, however, a storm brings the bar crest below a certain 'critical' depth, where the bar-degenerating conditions start to dominate the bar-maintaining conditions. From that moment onwards the bar is doomed to die away, because the dominance of bar-degeneration will keep increasing by positive feedback. Once the degeneration of the outer bar starts, the frequency of occurrence of bar-maintaining conditions will become smaller and smaller, increasing the relative dominance of bar-degenerating conditions more and more. This feedback will reinforce the process of bar degeneration.

5.5 Discussion

The observation of the existence of multi-year cyclic bar system behaviour offers a new perspective on the generation of a multiple bar system. Current theories on multiple bar system formation assume that the bars are generated approximately in the position where they are currently present; being generated by higher mode edge waves or by the renewed breaking of regenerated broken waves. However, the generation of a multiple bar system may also be a sequential process.

In the sequential development of a multiple bar system, initially a breaker bar develops near the shoreline, for example due to infragravity mechanisms or breakpoint mechanisms. In certain wave climates this bar may weld to the beach in 'summer' and be formed again in 'winter' (the classic seasonal cycle). In other wave climates, however, onshore directed transport processes may be too weak or occur too infrequently relative to the transport processes that move the bar offshore. In this situation the initial bar may migrate net offshore. If this bar migrates far enough in an offshore direction a new bar can be generated near the shoreline. The notion 'far enough' may relate, for example, to a sufficient distance for wave regeneration or to a sufficient distance for the resonance of a new edge wave mode. If this new bar near the shoreline also becomes a permanent bar, a multiple bar system has been formed. As long as the outer bar keeps moving net offshore under the governing wave climate, more bars may be generated near the shoreline. With sufficient longshore current velocities in the trough landward of the outer bar, the fate of the outer bar is to degenerate offshore. 'Severe' storms will move the bar farther offshore and asymmetric waves (or 'mild' storms) will degenerate the bar instead of move it onshore (according to the proposed hypothesis on cyclic bar system behaviour).

To conclude, the cyclic bar system behaviour is a type of bar behaviour that has also been observed on other locations. Ruessink and Kroon (1994) describe similar bar behaviour along the island of Terschelling (The Netherlands). The episodic, non-stationary behaviour of a double bar system at Duck (North Carolina, USA) described by Birkemeier (1984) and Lippmann et al. (1993) probably addresses the same phenomenon as observed along the Dutch coast. This indicates that the cyclic, multi-year bar behaviour observed along the Holland coast is not a unique phenomenon resulting from some unique set of site-specific conditions. This systematic multi-year, cyclic bar system behaviour might be a more common phenomenon for multiple bar systems, which has not been noticed so often because of the lack of systematic long-term monitoring of these bar systems.

5.6 Conclusions

Along the Holland coast, the multi-year behaviour of multiple bar systems consists of systematic cyclic behaviour in which all bars migrate in a net offshore direction, with the outer bar fading away and a new bar being generated near the shoreline. This cyclic behaviour may be coherent over large alongshore distances, but the cyclic development may as well get 'out-of-phase' alongshore. The alongshore change in the phase of the bar behaviour cycle may be sharp or more gradual. A typical length scale for the transition area between parts of the bar system in a different phase, is about 2 kilometre. A transition area may migrate alongshore, but does not necessarily do so. In the transition area, the outer bar from one side of the transition area tends to attach to the inner bar at the other side of the transition area. The bars outside the transition area seem to

develop quite independently from the bars at the other side of the transition area. This indicates that the inherent length scale for the cyclic bar system behaviour is probably kilometres.

The cyclic bar behaviour appears to be essentially a cross-shore redistribution process. Therefore, the disappearance of the outer bar goes with onshore directed transport. This onshore transported sediment is not deposited in the trough landward of the outer bar, but is immediately redistributed in the inner bar system. This implies that the sediment required for the growth of the inner bar during its offshore migration originates (for the greater part) from the outer bar.

On the scale of individual profile cross-sections, the transport pattern is more complex than just cross-shore redistribution. On this scale, longshore sediment redistribution patterns superimposed on the cross-shore redistribution can be recognised, especially in the inner nearshore.

The behaviour exhibited by the multiple bar systems along the Holland coast points to a strong morphologic feedback in the mechanism that explains the cyclic bar system behaviour. No cyclic energy input into the morphodynamic system seems to be required to obtain cyclic morphologic behaviour.

To explain the observed cyclic bar system behaviour a central role is attributed to the behaviour of the outer bar. As long as the outer bar remains well developed at a certain position, the inner bar(s) can not move net offshore and will only move to and fro within a limited cross-shore range. Only as the outer bar disappears the inner bar can migrate net offshore (and it will, because it experiences the same wave climate as its predecessor). It is hypothesised that the consistently occurring degeneration of the outer bar can be explained by the balance between conditions that favour bar degeneration and conditions that favour bar existence. The conditions that cause degeneration of the outer bar are hypothesised to be those with highly asymmetric waves on the outer bar. The conditions that favour bar existence are hypothesised to be those with breaking waves on the outer bar.

6 THE SYSTEMATIC, OFFSHORE DEGENERATION OF THE OUTER BAR

6.1 Introduction

In this chapter, the hypothesis on the dynamics of the cyclic bar system behaviour, formulated in Chapter 5, will be evaluated. The hypothesis can not be verified rigorously yet, because no observations exist on the nearshore water motion during the degeneration of the outer bar. Model simulations can not be used as a provisional substitute for field observations, because 3D morphological models of barred nearshore environments are not available (Roelvink and Brøker, 1993). Therefore, the verification of the hypothesis in this chapter is only tentative. The verification will deal with quantifying elements of the proposed morphodynamic feedback process, such that they can be judged on their (qualitative) agreement with the proposed hypothesis.

An important element of the proposed morphodynamic system is the relation between the development stage of the outer bar and the wave climate integrated balance of 'mild' storms and 'severe' storms on this bar. The analysis of this topic requires insight in the frequency of occurrence of conditions with highly asymmetric waves on the outer bar, in relation to the position of that bar and the governing deep water wave climate. Similarly, the frequency of occurrence of conditions with breaking waves on the outer bar is of interest. To analyse these types of parameters, a model is required to translate information of the offshore wave climate to nearshore parameters. Those nearshore parameters will be defined in the following section. The model that is developed to derive these parameters from offshore wave climate data is described in Section 6.3 (Van Rijn and Wijnberg, 1994). Additionally, the model provides estimates of near-bottom orbital velocities and velocity asymmetries, in order to obtain more insight in the intensity of the bar-degenerating conditions.

The values of the nearshore wave climate parameters, in relation to various bar development stages, will be evaluated at two locations. One location is in the Noord-Holland bar system and one is in the Zuid-Holland bar system, viz. near Egmond (km 41.50) and near Katwijk (km 84.25). Differences in the nearshore wave climate parameters at the two locations may indicate which factors are responsible for the different duration of the bar system cycle in respectively the Noord-Holland bar system and the Zuid-Holland bar system.

6.2 Definition of wave climate parameters on the outer bar

So far, the conditions that favour degeneration of the outer bar and the conditions that favour the existence of the bar feature were defined qualitatively, viz. as 'mild storm' conditions with very asymmetric waves and as 'severe storm'

conditions with more intensive breaking of waves. Analysis of the change in balance between these conditions requires a quantitative definition of these conditions. Since the onset of breaking plays an important role in the formulated hypothesis, the boundaries between the conditions will be specified in terms of the fraction of breaking waves (Q_b) on the outer bar.

First, a boundary should be specified between 'morphologically active' conditions and 'morphologically inactive' conditions. During the latter conditions, the sediment is not necessarily completely immobile, but any sediment transport under these conditions does not result in noticeable morphological change. The outer bar is morphologically inactive during the calm summer season when waves are generally less than 1 m in height. Therefore, the boundary should be chosen such that wave classes 0-0.5 m and 0.5-1.0 m are generally excluded from the set of 'morphologically active' conditions. In a first approximation, the boundary is chosen at wave conditions for which at least 0.1% of the waves break on the outer bar, yielding:

$$\textit{morphologically inactive conditions} : \quad Q_b < 0.001 \tag{6.1}$$

$$\textit{morphologically active conditions} : \quad Q_b \geq 0.001 \tag{6.2}$$

Next, a boundary should be specified between 'bar-degenerating' conditions and 'bar-maintaining' conditions. Specifying this boundary deals with specifying at what amount of wave breaking the degenerating effect of asymmetric waves is balanced by -or is altered by- processes that are induced by wave breaking, such as undertow or infragravity waves. In a first approximation, the boundary is chosen at wave conditions for which 5% of the waves break on the outer bar, yielding:

$$\textit{bar-degenerating conditions} : \quad 0.001 \leq Q_b \leq 0.05 \tag{6.3}$$

$$\textit{bar-maintaining conditions} : \quad Q_b > 0.05 \tag{6.4}$$

As will be clear, the bar-degenerating conditions and the bar-maintaining conditions together make up the morphologically active conditions.

The occurrence of the two modes of morphologically active conditions will be expressed in terms of mean annual occurrence of these conditions, based on wave climate data. Therefore, the wave climate integrated parameters that will be evaluated for varying development stages of the outer bar read as:

%MAIN = mean annual percentage of occurrence of bar-maintaining conditions on the outer bar ('severe storm') (6.5)

%DGEN = mean annual percentage of occurrence of bar-degenerating conditions on the outer bar ('mild storm') (6.6)

%ACT = mean annual percentage of occurrence of morphologically active conditions on the outer bar (= %DGEN + %MAIN) (6.7)

The balance between bar-maintaining and bar-degenerating conditions for varying bar development stages will be characterised by the ratio R:

$$R = \%DGEN / (\%DGEN + \%MAIN) = \%DGEN / \%ACT \quad (6.8)$$

The extent to which the values of the four wave climate integrated parameters are sensitive to the specification of the boundaries between them (Q_b=0.1% and Q_b=5%), will be discussed in Section 6.4.

In this study, the parameters 6.5 to 6.8 will be derived from the offshore wave climate. For a given outer bar topography, the percentage of waves that is breaking on the outer bar (Q_b) during certain offshore wave conditions has to be determined. The value of Q_b is needed to classify those conditions according to the definitions given in 6.1 to 6.4. If $Q_b \geq 0.001$, the annual probability of occurrence of those wave conditions will be added either to %MAIN or %DGEN, depending on the value of Q_b. If, for example, during certain offshore wave conditions 10% of the waves is breaking on the outer bar, then the annual probability of occurrence of those conditions will be added to %MAIN. If only 2% of the waves is breaking on the outer bar, the annual probability of occurrence of those conditions will be added to %DGEN. Repeating this procedure for all possible offshore wave conditions, the final values of parameters 6.5 to 6.8 can be determined. The model that is used to compute the percentage of waves that is breaking on the outer bar is described in the following section.

6.3 Model for estimating wave climate parameters on the outer bar

6.3.1 Introduction

Two types of models are commonly used to describe the propagation and transformation of waves over a barred nearshore profile: parametric models and probabilistic models. Parametric models describe the onshore propagation of a wave field in terms of a (single peaked) wave spectrum, represented by a single wave height and wave period. Assumptions have to be made on the shape of the spectrum as waves start to break. A popular method is that proposed by Battjes and Janssen (1978) which is based on a Rayleigh distribution of wave heights that is truncated at the breaker wave height. To define the breaker wave height separate functions are specified. Additionally, a function has to be specified to estimate the percentage of breaking waves.

Probabilistic models describe the onshore propagation of a wave field in terms of many individual waves schematising the wave field (wave-by-wave approach). Based on a probability-density function of wave height and wave period in deep

water, many waves are propagated onshore and wave characteristics are determined by combining the properties of the individual waves at all cross-shore locations. Such a Monte-Carlo simulation technique is computationally intensive but does not rely on any assumptions about the spectrum in the surf zone. A faster alternative is to schematise the probability-density function into discrete series of wave height classes and corresponding wave periods, each having a certain probability of occurrence (Mase and Iwagaki, 1982). Each wave height class, schematised by a single wave height and wave period, is assumed to propagate onshore independently of the other classes. The 'individual' wave shoals until an empirical criterion for breaking is satisfied. After all classes have been propagated onshore, general wave statistics such as H_{rms} or $H_{1/3}$ can be calculated. More important -for this study- is that the percentage of breaking waves follows directly from adding the probabilities of the wave classes that break at a certain location. So no additional functions have to be specified to derive this parameter.

The amount of waves breaking on the outer bar is an essential topic in the proposed hypothesis. Both modelling approaches require a criterion to define the wave breaking height, but only parametric models require additional assumptions on the shape of the wave spectrum in shallow water depth, and an additional function to estimate the percentage of breaking waves. Therefore, in this study a probabilistic model type was used: the WAVIS-model (Van Rijn and Wijnberg, 1994). The WAVIS-model (WAVes In the Surf-zone) has been developed as a research model for diagnostic modelling. It uses the approach of schematising the wave field by a discrete series of wave classes. The model described by Van Rijn and Wijnberg (1994) has been extended with formulations that determine statistics of the near-bottom asymmetry of orbital velocities.

6.3.2 Wave model description

In the WAVIS-model, waves are assumed to propagate unidirectionally (i.e. without wave reflection) towards a straight beach with parallel depth contours. The transformation processes incorporated in the model are: refraction, shoaling by depth variations, shoaling by depth-averaged longshore currents (Doppler shifting), energy dissipation by bottom friction and energy dissipation by wave breaking. In addition, wave-induced set-up and set-down are included in the model. Wind- and tide-induced variations in the mean water level can be specified as an input condition.

The transformation processes of shoaling and breaking are assumed to be unaffected by wave-wave interaction and wave overtaking. Long wave effects and wave reflection are not included. Shoaling is modelled by linear small amplitude wave theory. Near-bottom orbital velocities are estimated by using second-order Stokes in combination with an empirical formulation for very shallow water (Kroon and Van Rijn, 1993).

The cross-shore transformation and propagation of waves is calculated by solving the wave action balance, which reads as:

$$\frac{d}{dx}\left(\frac{EC_{g,r}\cos\theta + v_x}{\omega_r}\right) + \frac{D_{bf} + D_{br}}{\omega_r} = 0 \tag{6.9}$$

where:

E = $\rho g H^2/8$ = wave energy per unit area (kg m^2 s^2 m^{-2});
ρ = fluid density (kg m^{-3});
g = acceleration of gravity (m s^{-2});
H = wave height (m);
C_g = nC_r = relative wave group velocity (m s^{-1});
n = $0.5[1+2kh/\sinh(2kh)]$ = coefficient (-);
k = $2\pi/L$ = wave number (m^{-1});
L = wave length (m);
h = water depth (m);
C_r = L/T_r = wave propagation velocity relative to current (m s^{-1});
T_r = $T/[1-(T|v|\cos\phi/L)]$ = wave period relative to current (s);
T = wave period (s) (constant);
v = depth-averaged velocity vector (m s^{-1});
ϕ = angle between wave propagation direction and current direction (rad);
θ = $\arcsin[(C_r/C_{r,0})\sin\theta_0]$ = angle of wave ray and x-axis normal to the coast (rad);
v_x = depth-averaged velocity component in x-direction (m s^{-1});
ω_r = $2\pi/T_r$ = relative wave angular frequency (rad s^{-1});
x = coordinate normal to shoreline (m);
D_{bf} = energy dissipation per unit area by bottom friction (kg m^2 s^2 m^{-2});
D_{br} = energy dissipation per unit area by breaking (kg m^2 s^2 m^{-2}).

The wave length (L) is defined by the dispersion relation including the current refraction effect (Doppler shifting):

$$\left(\frac{L}{T} - |v|\cos\phi\right)^2 = \frac{gL}{2\pi}\tanh\left(\frac{2\pi h}{L}\right) \tag{6.10}$$

The energy dissipation by bottom friction (D_{bf}) is described by (Putnam and Johnson, 1949):

$$D_{bf} = \frac{\rho f_w}{6\pi}\left(\frac{\omega_r H}{\sinh(2\pi h/L)}\right)^3 \tag{6.11}$$

The friction coefficient (f_w) is specified as an input parameter. The value of f_w was found to be 0.01 by calibration (Van Rijn and Wijnberg, 1994).

As long as waves are not breaking D_{br}= 0. If the local wave height (H) calculated by the model exceeds the local maximum possible wave height (H_{max}) the waves are assumed to break. H_{max} is the wave height associated with wave breaking either on depth or on steepness. H_{max} is specified by:

$$H_{\max} = \text{minimum } [\gamma h, 0.14L\tanh(kh)] \tag{6.12}$$

The value of the breaking coefficient γ varies with the character of the waves and the slope of the bottom (e.g. Southgate, 1993). In the WAVIS model γ is defined as a function of the ratio of the local average bottom slope (tanβ) and the local wave steepness (H/L) (Figure 6.1). The local average bottom slope is specified over a distance of half the local wave length seaward of the local coordinate. On the landward side of a sand bar, where a 'negative' bottom slope occurs, tanβ is set to zero (Dally, 1992). The γ-curve presented in Figure 6.1 was obtained by calibration (Van Rijn and Wijnberg, 1994).

The energy dissipation by breaking (D_{br}) is described by:

$$D_{br} = 0.25\alpha_1\rho g\left(\frac{H^2 - H_{\max}^2}{T_r}\right) \qquad \text{if } H > H_{max} \tag{6.13}$$

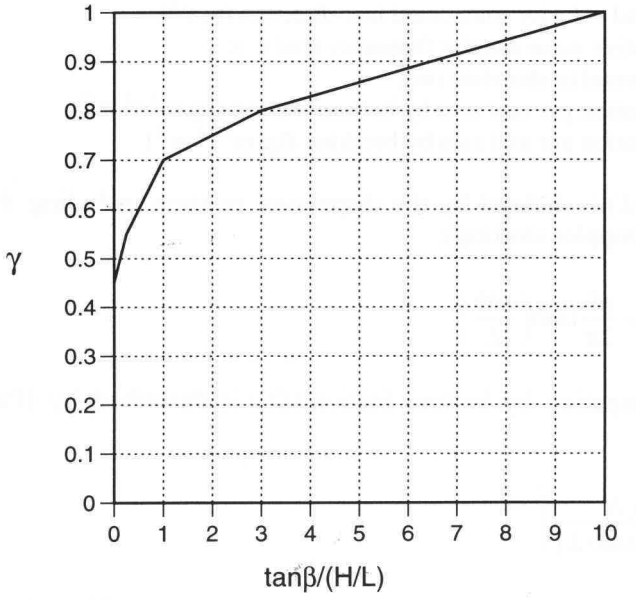

Figure 6.1: Breaking coefficient γ

where $\alpha_1 = 1.5$, yielding a gradual transition to a zero dissipation for $H=H_{max}$. The α_1 coefficient in equation 6.13 was found by calibration using laboratory and field data (Van Rijn and Wijnberg, 1994).

Expression 6.13 is a modified form of the often used expression based on the analogy between the dissipation of energy in a breaking wave and in the dissipation of energy in a bore (Battjes and Janssen, 1978; Roelvink, 1993):

$$D_{br} = 0.25\alpha_2 \rho g \frac{H^2}{T_r} \tag{6.14}$$

where α_2 is a calibration coefficient ($\alpha_2 \approx 1$).

The modification is based on the expression proposed by Dally et al. (1985) which states that the rate of energy dissipation due to breaking is proportional to the difference between the local energy flux and some stable energy flux. The concept of a stable energy flux originates from the observation that wave height stabilises at some value over a uniform depth following the initiation of breaking. This effect is not predicted by energy dissipation models based on the bore analogy (Dally et al., 1985). The expression proposed by Dally et al. reads as:

$$\frac{\partial EC_g}{\partial x} = \frac{-K}{h}\left(EC_g - EC_{g,s}\right) \tag{6.15}$$

where EC_g is a depth-integrated, time-averaged energy flux as given by shallow water linear wave theory, K is a dimensionless decay coefficient ($K \approx 0.15$), h is the still water depth, and $EC_{g,s}$ is the energy flux associated with the stable wave that the breaking wave is striving to attain.

The wave set-up and set-down are determined by solving the time-averaged momentum balance, neglecting inertial effects and bed-shear stress. The time-averaged momentum balance reads as:

$$\frac{dS_{xx}}{dx} + \rho g(h+s)\frac{ds}{dx} - \tau_{sf} = 0 \tag{6.16}$$

where:

S_{xx} = onshore radiation force per unit crest length (kg m s^2 m^{-1});
s = set-up/set-down (m);
τ_{sf} = shear stress at water surface to account for the wind effect and the breaking roller effect (kg m s^{-2} m^{-2}).

In this study τ_{sf} was set at zero. The onshore radiation force component (S_{xx}) is described by:

$$S_{xx} = (n\text{-}0.5+n\cos^2\theta)E \tag{6.17}$$

Wave statistics, such as $H_{1/3}$, computed by the WAVIS model and wave statistics derived from field measurements generally showed good agreement (Van Rijn and Wijnberg, 1994). Wave heights in very shallow water, however, may be underestimated as well as overestimated. This may be related to assumptions in the model, such as no wave-wave interaction, no reflection, and no long wave effects, because these processes all become more important close to the shoreline.

Figures 6.2 and 6.3 show two examples of verification runs, one for comparison with field data obtained along the Holland coast (Wolf, 1993) and one for comparison with laboratory data (Grassmeijer and Sies, 1994). The latter data set allowed verification of the fraction of breaking waves, a type of data that was lacking for the field conditions.

6.3.3 Near-bed orbital velocity asymmetries

The asymmetry (A) of the near-bottom, peak orbital velocities of non-breaking waves is defined as:

$$A = \hat{u}_{\delta on}/\hat{u}_{\delta off} \tag{6.18}$$

where:

$\hat{u}_{\delta on}$ = onshore directed peak orbital velocity at the top of the wave-boundary layer (m s^{-1});

$\hat{u}_{\delta off}$ = offshore directed peak orbital velocity at the top of the wave-boundary layer (m s^{-1}).

The onshore and offshore directed near-bottom peak orbital velocities are estimated from the -calculated- surface elevation amplitude and wave length by second order Stokes wave theory:

$$\hat{u}_{\delta on} = \hat{u}_{\delta 1} + \hat{u}_{\delta 2} \tag{6.19}$$

$$\hat{u}_{\delta off} = \hat{u}_{\delta 1} - \hat{u}_{\delta 2} \tag{6.20}$$

where:

$$\hat{u}_{\delta 1} = \pi H/[T \sinh(2\pi h/L)] \tag{6.21}$$

$$\hat{u}_{\delta 2} = 3\pi^2 H^2/[4\, T\, L\, (\sinh(2\pi h/L))^4] \tag{6.22}$$

In shallow water second order Stokes does not apply. Following the formulations used in the TRANSPOR model (Van Rijn, 1993) - which will be used for diagnostic transport calculations in Section 6.6- an empirical formula presented by Kroon and Van Rijn (1993) is used to estimate the near-bottom peak orbital velocities when $h < 0.01 g T^2$. These empirical formulas read as:

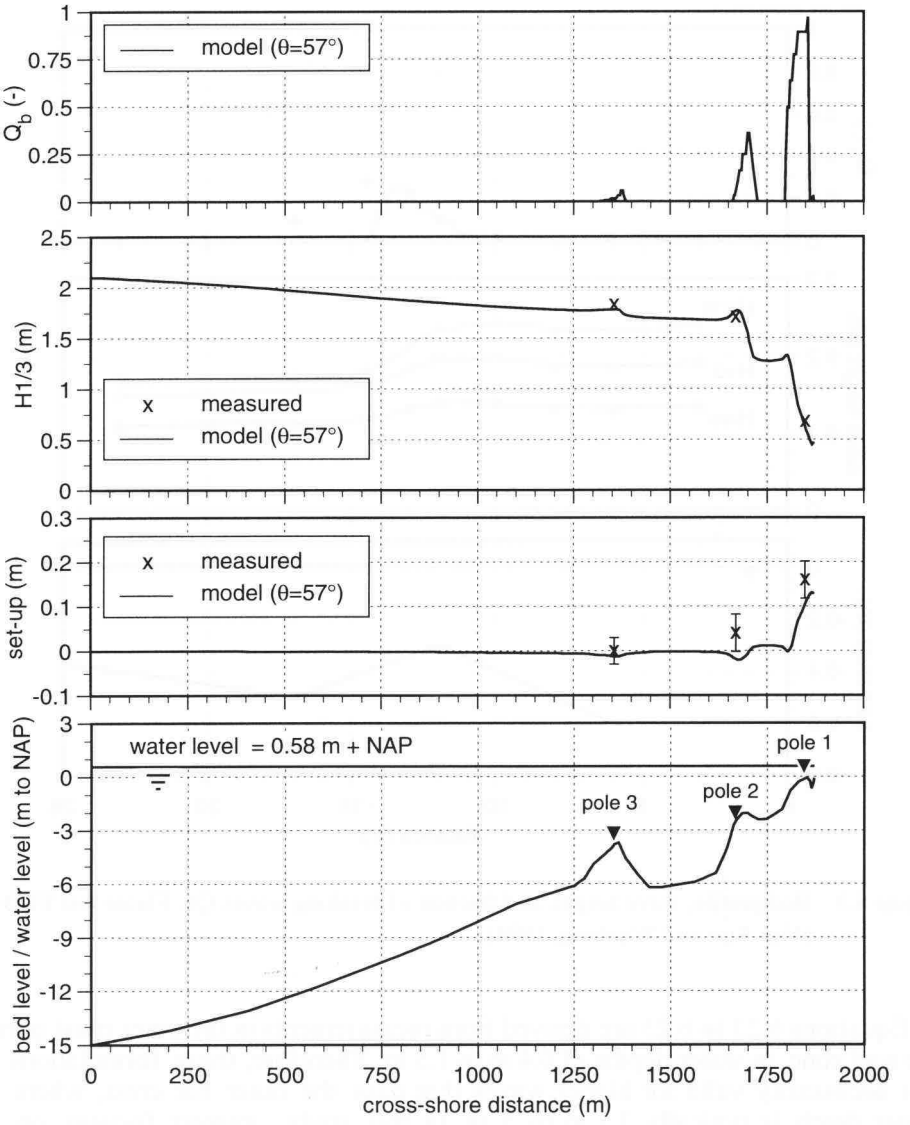

Figure 6.2: Bed profile, wave height, mean water level and fraction of breaking waves Q_b. Egmond, 9 October 1992, The Netherlands (Van Rijn and Wijnberg, 1994).

$$\hat{u}_{\delta on} = \beta \hat{u}_{\delta l} \tag{6.23}$$

$$\hat{u}_{\delta off} = (2-\beta)\hat{u}_{\delta l} \tag{6.24}$$

where: $\beta = 1 + 0.3(H/h)$ (6.25)

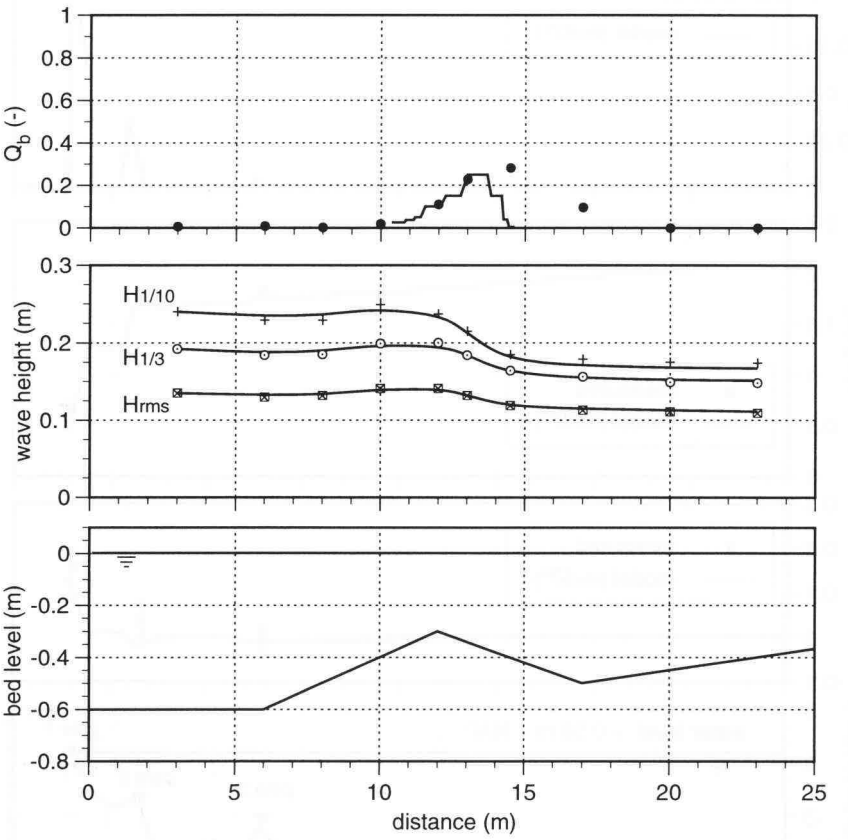

Figure 6.3: Bed profile, wave height, and fraction of breaking waves Qb. Flume test TUD-B2 (Van Rijn and Wijnberg, 1994).

Equations 6.23 to 6.25 are derived from measurements in the inner most part of the surf zone, in water depths of 0.4 m to 1.5 m. Therefore, these formulations are not necessarily valid for higher waves that pass the outer bar crest, where the water depth is typically 3.5 m to 5 m. In this study, interest focuses on the asymmetry on the outer bar for conditions with nearly no breaking waves at that bar. This implies that only the asymmetry of the highest waves in the simulated wave field -i.e. waves with a low frequency of occurrence- will be described by these empirical formulas. From field observations in the outer nearshore zone near Egmond (Houwman and Hoekstra, 1994) and Terschelling (Ruessink, pers. comm.), it appears that the formulations that are used to estimate the near-bottom orbital velocity (equations 6.19 to 6.25) produce realistic values, as will be shown hereafter.

For the Terschelling site, five hydrodynamic conditions were simulated (Table 6.1). Longshore currents were present during these conditions, but these were not included in the model simulations, because no information on the cross-shore distribution of the longshore current was available. The offshore conditions are measured by a wave buoy at about 15 m water depth. The nearshore conditions are measured by electromagnetic current meters and a pressure sensor mounted on a tripod. This tripod is positioned on a bar crest at 3.5 m -NAP (Figure 6.4). The current measurements are obtained about 0.5 m above the bed.

The calculated wave heights on the bar crest compare well to the measured values (Figure 6.5a). The near-bed peak onshore velocities are predicted reasonably well, although there is a slight tendency to overestimate the velocities (Figure 6.5b). The asymmetry in the peak near-bed orbital velocities is generally underpredicted (Figure 6.5c). The model underestimates the near-bed asymmetries especially for the larger near-bed orbital velocities (Figure 6.6).

To verify in a more general sense whether near-bed velocity asymmetries are correctly predicted relative to the value of the peak onshore velocities, the relation between computed values of those two parameters is compared to the

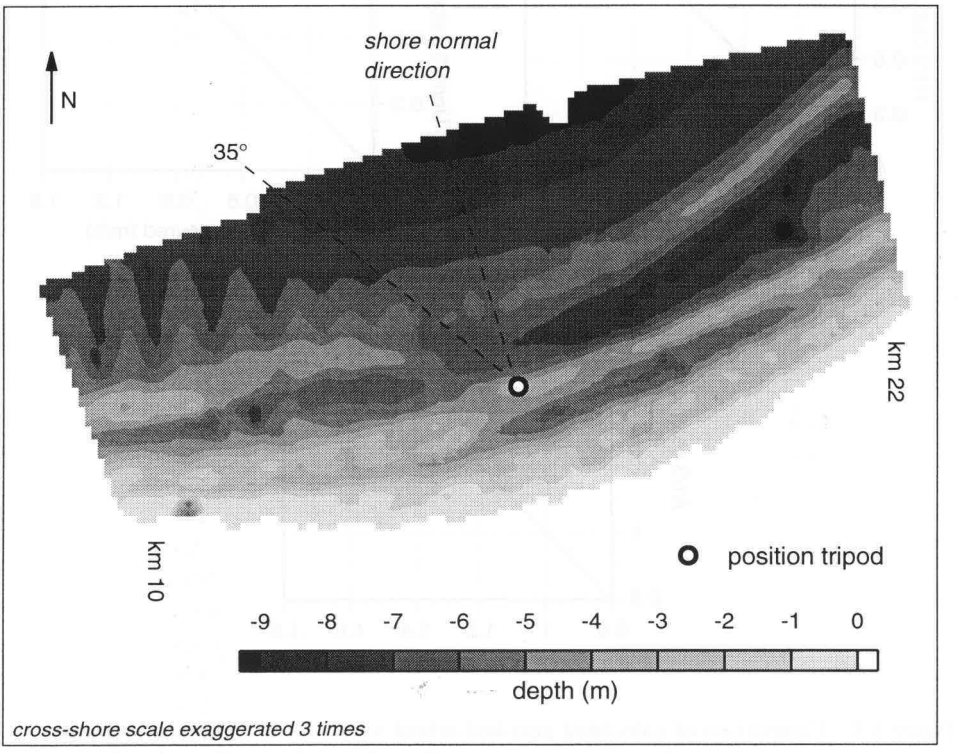

Figure 6.4: Tripod position for measuring near-bed velocity at the Terschelling field site, April 1993 (courtesy B.G. Ruessink).

Table 6.1 : Some hydrodynamic properties of the conditions that were used for model verification at the Terschelling site.

Case	ID number Terschelling data set (burst no.)	H_{m0} offshore (m)	Angle of incidence offshore (deg)		Water depth near tripod (m)	Longshore current near tripod (m/s)
			to the North	to the shore normal		
1	260	1.51	308	34	4.2	0.22
2	270	1.32	313	29	4.2	0.43
3	271	1.30	319	23	4.4	0.30
4	272	1.20	314	28	4.5	0.21
5	273	1.19	310	32	4.3	0.05

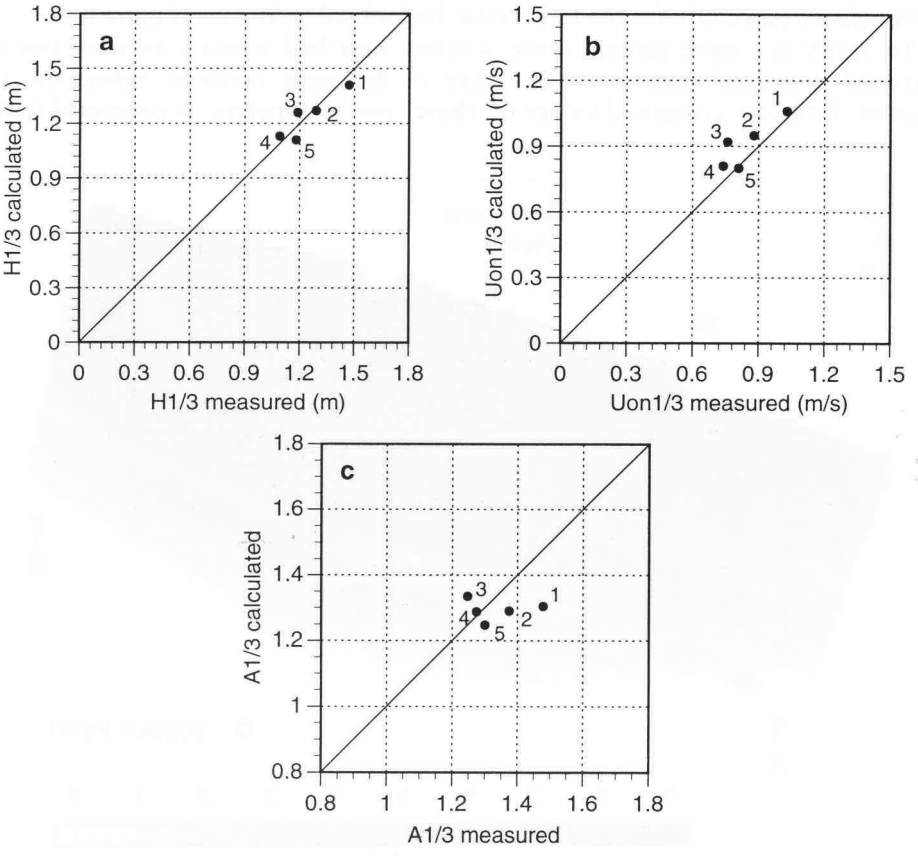

Figure 6.5: Comparison of calculated near-bed orbital velocities to field measurements collected near Terschelling (courtesy B.G. Ruessink). (a) Wave height; (b) near-bed, peak onshore orbital velocity; (c) asymmetry of near-bed, peak orbital velocities.

relation between measured values obtained near Egmond (Figure 6.7). The near-bed current measurements are obtained at most 0.5 m above the bed, at the crest of the outer bar at about 3.5 m -NAP (Figure 6.8) (Houwman and Hoekstra, 1994). The presented measured asymmetries may slightly underestimate the actual asymmetries, because the sampling rate was only 1 Hz (Houwman and Hoekstra,

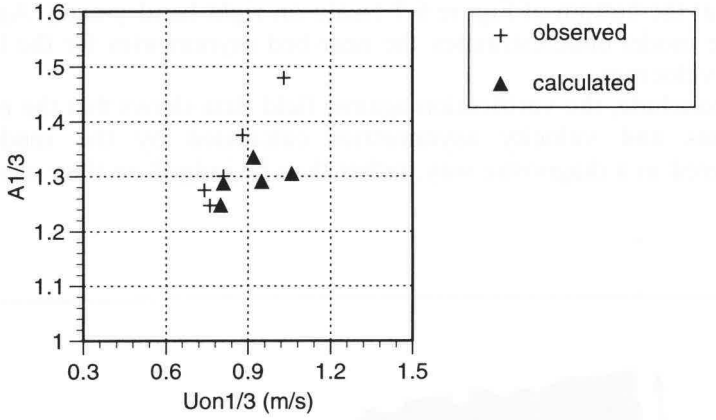

Figure 6.6: Asymmetry of near-bed, orbital velocities as a function of near-bed, peak onshore orbital velocity. Observations from Terschelling site and model computations.

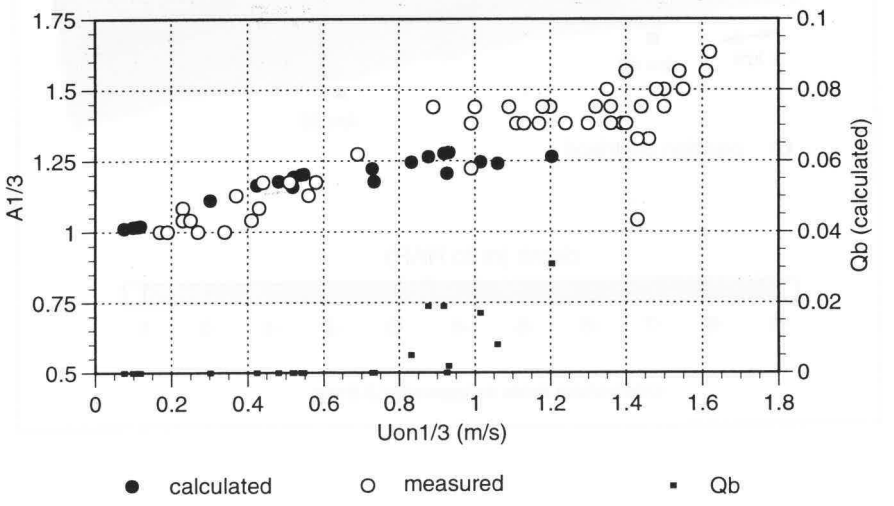

Figure 6.7: Asymmetry of near-bed, orbital velocities as a function of near-bed, peak onshore orbital velocity, at about 3.5 m water depth. Calculated values relate to non-breaking part of the wave field. Fraction of breaking waves indicated at right hand axis. (Source measured data: Houwman and Hoekstra, 1994).

1994). The calculated values relate to a set of systematically varied wave heig
and angles of incidence that produce little or no breaking waves on the outer
(Table 6.2). The latter restriction is applied because the calculated velocities a
asymmetries only relate to the non-breaking fraction of the incoming wav
Therefore, only conditions with a maximum percentage of breaking waves of
are plotted. The fraction of breaking waves going with the various conditions
shown at the bottom of Figure 6.7 (scale on right hand y-axis). Again, it appe
that the model underestimates the near-bed asymmetries for the larger near-b
orbital velocities.

To conclude, the verification against field data shows that the near-bed orb
velocities and velocity asymmetries calculated by the model should
considered in a diagnostic way, rather than be judged on their absolute values

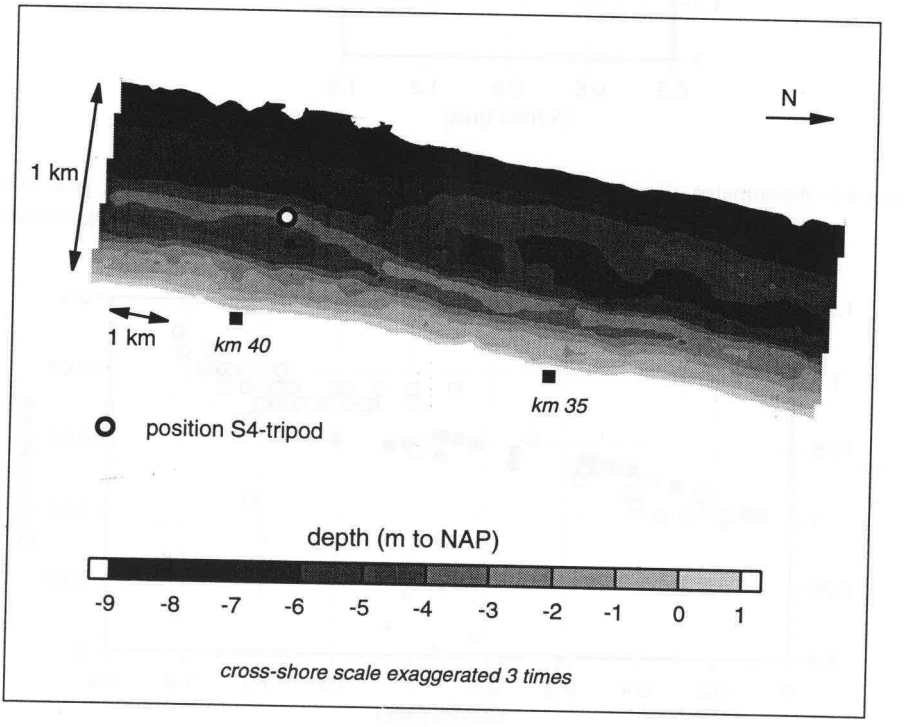

Figure 6.8: Tripod position for measuring near-bed velocity at Egmond field site, September 1991.

Table 6.2: Offshore wave input for model calculations presented in Figure 6.7, including resulting fraction of breaking waves Q_b at the bar crest.

Angle (deg)	H_{m0} (m)	Q_b	Angle (deg)	H_{m0} (m)	Q_b	Angle (deg)	H_{m0} (m)	Q_b
0	0.25	0.000	30	1.25	0.019	75	0.25	0.000
0	0.75	0.000	45	0.25	0.000	75	0.75	0.000
0	1.25	0.019	45	0.75	0.000	75	1.25	0.000
15	0.25	0.000	45	1.25	0.005	75	1.75	0.000
15	0.75	0.000	60	0.25	0.000	75	2.25	0.000
15	1.25	0.019	60	0.75	0.000	75	2.75	0.008
30	0.25	0.000	60	1.25	0.000	75	3.25	0.031
30	0.75	0.000	60	1.75	0.017			

6.4 Wave climate parameters on the outer bar

6.4.1 Wave model input

To analyse the relation between the development stage of the outer bar and the wave climate integrated balance of 'mild' storms and 'severe storms', the wave climate integrated parameters %ACT, %MAIN, %DGEN, and R have to be determined for various bar topographies. To obtain these parameters for a given outer bar topography, the following procedure was followed. The offshore wave climate data are available as a matrix of H_{m0} wave height classes and wave direction sectors in which each 'cell' has a certain frequency of occurrence $f_{H,\alpha}$. Of every wave climate 'cell' (H_{m0}, α, $f_{H,\alpha}$) that contains onshore propagating waves, the fraction of breaking waves Q_b on the outer bar is calculated by the WAVIS model. The wave height H_{m0} is the mid value of the represented H_{m0} wave height class, and the wave direction α is the mid value of the represented wave direction sector. Depending on the calculated fraction of breaking waves, each wave climate cell is classified into one of the following categories: 'morphologically inactive', 'bar-degenerating' or 'bar-maintaining'. Next, the frequencies of occurrence $f_{H,\alpha}$ of all wave climate cells falling in one category are added, in order to obtain the wave climate integrated percentage of occurrence of that category (%ACT, %DGEN, %MAIN) on the given outer bar topography.

To run the WAVIS model, the following input has to be specified:
- a probability density function of wave height, wave period and wave direction, in terms of a series of discrete classes (to be prescribed at the seaward boundary of the model);
- a water level, relative to mean sea level (tide, storm surge, wind set-up);
- a cross-shore bottom profile, relative to mean sea level.

In the following, the input for the wave model to derive %ACT, %DGEN, %MAIN, and R for various bar topographies near Katwijk and Egmond are presented.

The offshore wave field

To provide a probability density function of wave height, wave period and wave direction for each wave climate condition (H_{m0}, α, $f_{H,\alpha}$), representative wave fields have to be synthesised for each of the individual conditions. A representative wave field is synthesised by assuming a Rayleigh wave height distribution. Based on this distribution, a wave field is generated with a H_{m0} wave height that equals the mid of the considered wave height class. The Rayleigh distribution of wave heights reads as:

$$P(H>H^*)= \exp-[(H^*/H_{rms})^2] \tag{6.26}$$

H* represents the upper boundary of some arbitrarily defined wave height class. H_{rms} is derived from the specified mid-class H_{m0} value by using the relation $H_{rms}=H_{m0}/\sqrt{2}$. At the input boundary, all waves in the wave field are assumed to propagate in the same direction. This propagation direction equals the central value of the wave direction sector that is under consideration.

The wave periods associated with each of the Rayleigh distributed wave heights are specified by an empirical relation between wave height and wave period, which reads as:

$$T= 6H^{0.333} \tag{6.27}$$

This correlation has been derived from a wave climate averaged relationship between H_{m0} and $T_{1/3}$ and is shown in Figure 6.9. $T_{1/3}$ has been estimated from T_{m02} by an empirical relationship. This relationship has been derived from wave buoy measurements at 15 m water depth near Terschelling, The Netherlands. This empirical relationsip reads as:

$$T_{1/3} = 1.23\ T_{m02} + 1.03 \tag{6.28}$$

Figure 6.10 shows the measurements on which this relationship is based (Ruessink, pers. comm.). Each dot represents hourly averaged values of the wave period in terms of $T_{1/3}$ and T_{m02}. The linear relationship was fitted to a subset of the data, namely only to the conditions dominated by wind waves. The open circles in Figure 6.10 indicate conditions with considerable swell. This becomes apparent from Figure 6.11 which shows the relation between wave height and wave period. The open circles represent the conditions with wave heights of about 0.5 m and wave periods of more than 8 seconds.

The relationship 6.27 has been specified in analogy to the theoretically derived relation $T = 5H^{0.5}$ by Sverdrup-Munk-Brettschneider (see Van Rijn, 1994),

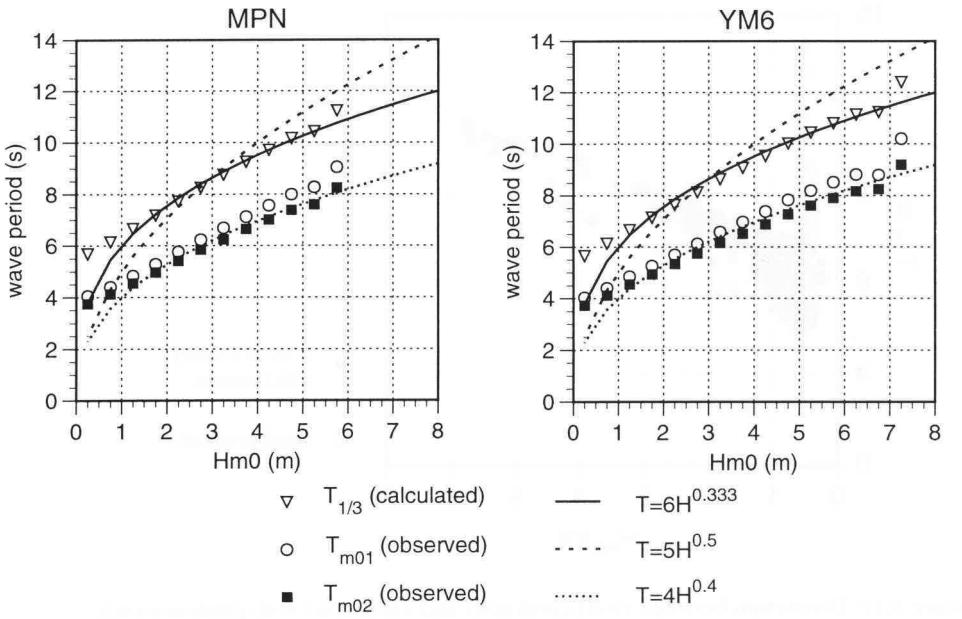

Figure 6.9: Empirical relationships between wave height and wave period at wave station MPN and wave station YM6 (unpublished data *Rijkswaterstaat*).

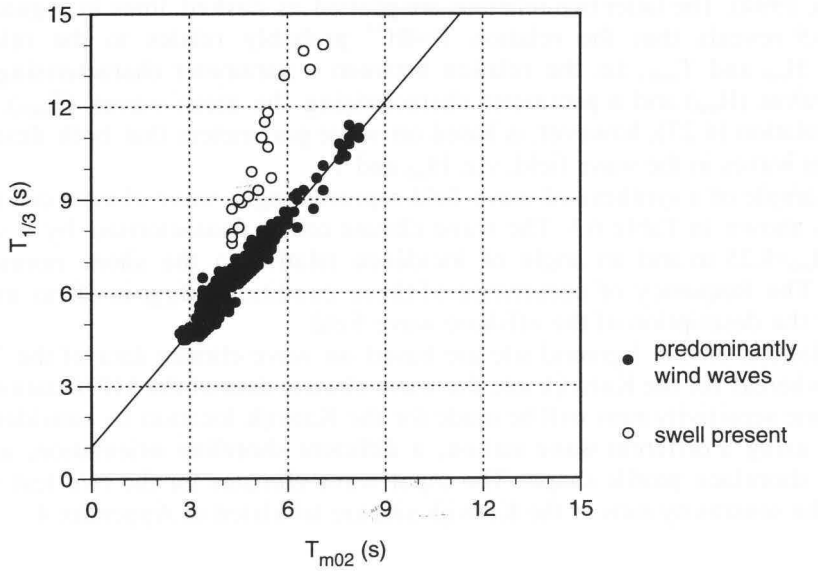

Figure 6.10: Empirical relationship between T_{m02} and $T_{1/3}$. Linear regression applied to conditions with predominantly wind waves (wave buoy Terschelling).

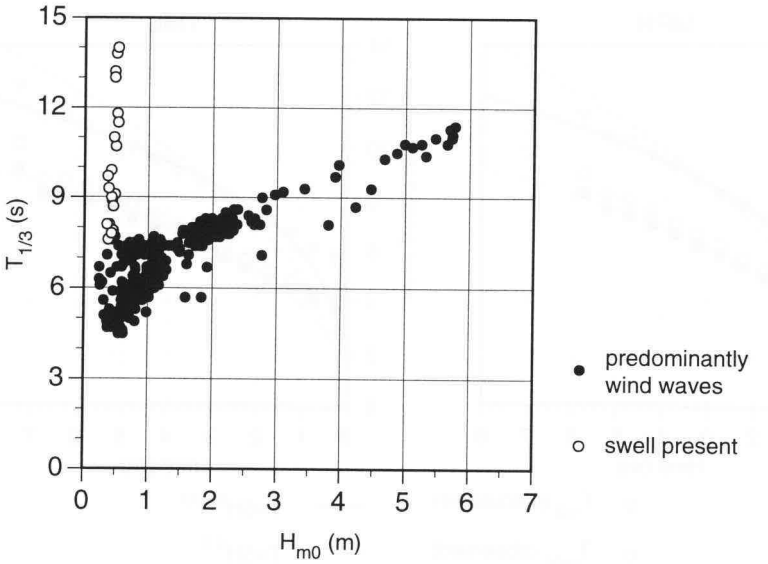

Figure 6.11: Distinction between swell conditions and conditions with predominantly wind waves (wave buoy Terschelling).

and the empirical relationship $T = 4H^{0.4}$ that was proposed for the North Sea (see Van Rijn, 1994). The latter two relations are plotted as dashed lines in Figure 6.9. Figure 6.9 reveals that the relation $T=4H^{0.4}$ probably relates to the relation between H_{m0} and T_{m01}, i.e. the relation between a parameter characterising the higher waves (H_{m0}) and a parameter characterising the mean waves (T_{m01}). The applied relation (6.27), however, is based on wave parameters that both describe the higher waves in the wave field, viz. H_{m0} and $T_{1/3}$.

An example of a synthesised wave field representing a wave climate cell (H_{m0}, α, $f_{H,\alpha}$) is shown in Table 6.3. The wave climate cell is characterised by a wave height H_{m0}=1.25 m and an angle of incidence relative to the shore normal of α=37.5°. The frequency of occurrence of these conditions, $f_{H,\alpha}$, is of no importance for the description of the offshore wave field.

Calculations on the Egmond site are based on wave climate data of the YM6 station, whereas for the Katwijk site the wave climate data of the MPN station are used. Some sensitivity runs will be made for the Katwijk location to consider the effect of using a different wave station, a different shoreline orientation, and a different shoreface profile shape. The input wave climates for the two test sites and for the sensitivity runs at the Katwijk site are tabulated in Appendix 4.

Table 6.3: Discrete representation of an offshore wave field approaching the coast at 37.5° to the shore normal. The H_{m0} wave height of the wave field is 1.25 m.

Wave height class p to be represented (m)	Characteristic wave height H (m)	Characteristic wave period T (s)	Probability of wave height class p	Angle of incidence α (deg)
0.00-0.25	0.125	3.0	0.077	37.5
0.25-0.50	0.375	4.3	0.197	37.5
0.50-0.75	0.625	5.1	0.239	37.5
0.75-1.00	0.875	5.7	0.209	37.5
1.00-1.25	1.125	6.2	0.143	37.5
1.25-1.50	1.375	6.7	0.079	37.5
1.75-2.00	1.625	7.1	0.036	37.5
2.00-2.25	1.875	7.4	0.014	37.5
2.25-2.50	2.125	7.7	0.004	37.5
2.50-2.75	2.375	8.0	0.001	37.5

The water levels

The water level input conditions are derived from empirical relations between the water level and the wave conditions (wave height and wave direction), based on data supplied by Rijkswaterstaat. The WAVIS-model assumes a straight beach and parallel depth contours and therefore does not distinguish between waves coming in at the same angle to the shore normal but at opposite sides of it. Therefore, relations between water level and wave conditions are merged for waves approaching the shore normal at the same angle but at opposite sides of it. Figure 6.12 shows the correlation between wave height and water level for varying wave direction sectors. The input water levels for the varying wave conditions are tabulated in Appendix 5, for the Egmond site and Katwijk site respectively.

The profile shapes

The calculations to transfer the offshore wave climate to nearshore parameters on the outer bar, start at the water depth of the wave station that is used in the calculations. That is at 18 m water depth for runs in which the MPN wave climate is used and at 21 m water depth for runs in which the YM6 wave station is used. The offshore part of the cross-shore profile has been derived from shape functions specified by Postma and Kroon (1986). For the inshore part of the profile, various outer bar topographies have been used, representing various stages of the outer bar development (Figure 6.13). For the Egmond site, the outer bars with the bar crests at 4.3 m -NAP respectively 5.7 m -NAP are in degenerating stages. For the Katwijk site, the outer bars with bar crest positions at 4 m and 4.6 m -NAP are in degenerating stages. The outer bar with its crest at 3.6 m -NAP

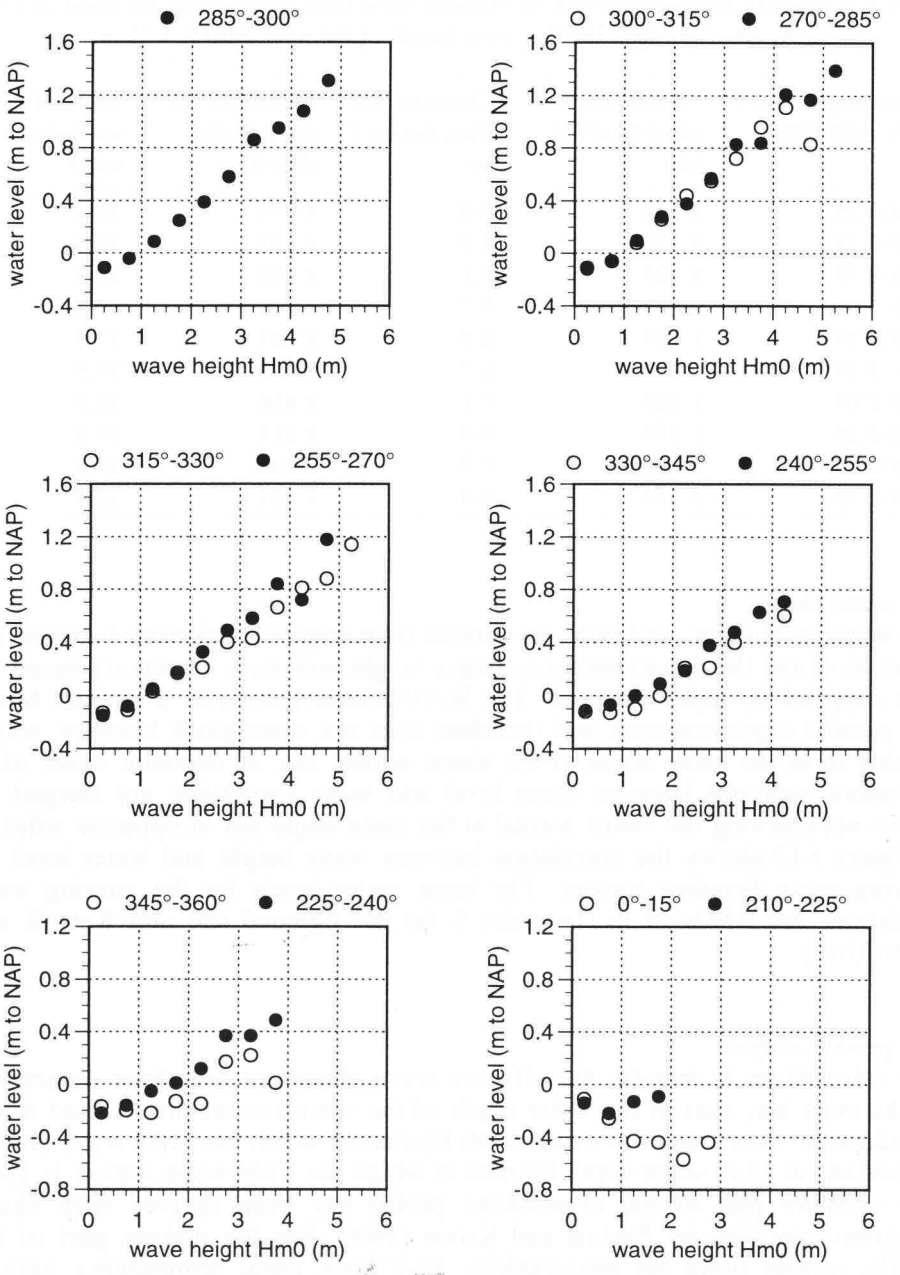

Figure 6.12: Relation between wave height and water level for varying angles of wave propagation (relative to the North). Data collected at station MPN (unpublished data *Rijkswaterstaat*).

seems to be in an early stage of degeneration or about on the threshold of degeneration. Near the Egmond site, the outer bar is still in a non-degenerating stage when its crest is at 3.6 m depth. Two examples of the composite input profiles used in the model runs are shown in Figure 6.14.

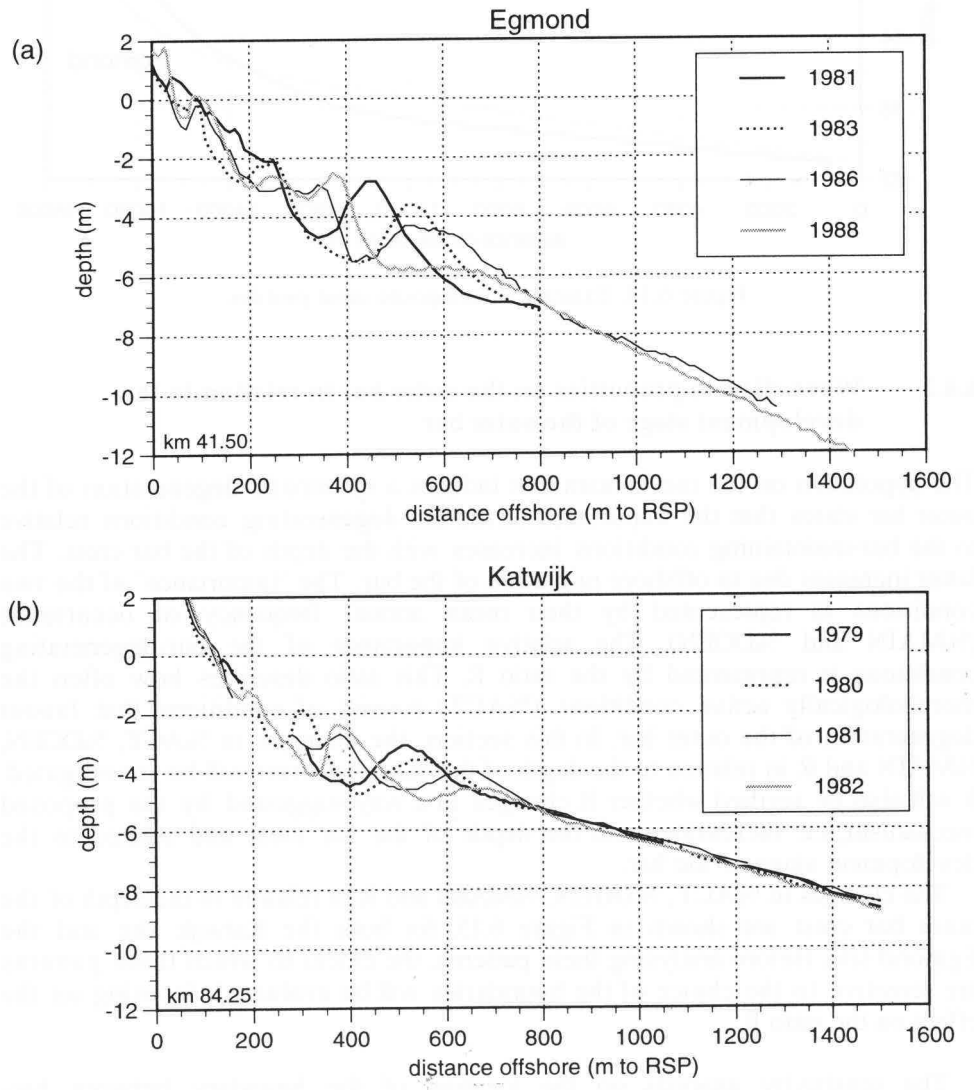

Figure 6.13: Nearshore profiles representing various development stages of the outer bar . (a) Profiles used in the Egmond computations; (b) profiles used in the Katwijk computations.

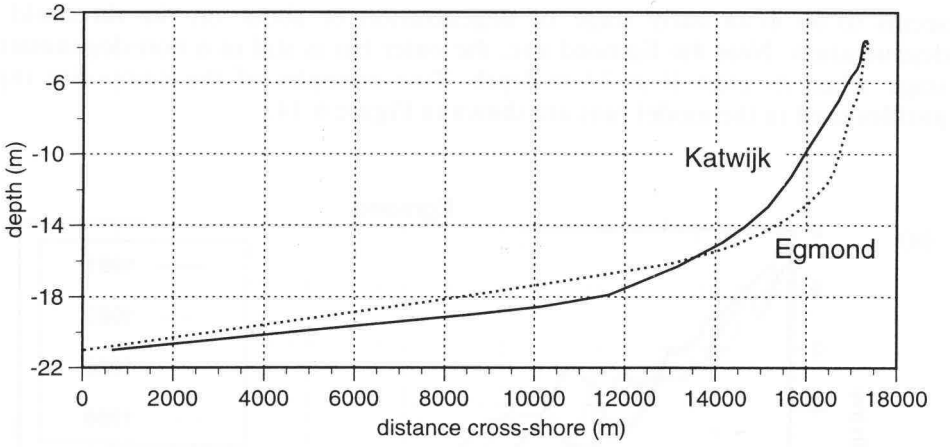

Figure 6.14: Example of composite input profiles

6.4.2 Wave climate properties on the outer bar in relation to the development stage of the outer bar

The hypothesis on the mechanism that induces a systematic degeneration of the outer bar states that the importance of the bar-degenerating conditions relative to the bar-maintaining conditions increases with the depth of the bar crest. The latter increases due to offshore migration of the bar. The 'importance' of the two conditions is represented by their mean annual frequency of occurrence (%MAIN and %DGEN). The relative importance of the bar-degenerating conditions is represented by the ratio R. This ratio describes how often the morphologically active conditions (%ACT) consist of conditions that favour degeneration of the outer bar. In this section, the changes in %ACT, %DGEN, %MAIN and R in relation to the depth of the outer bar crest will be investigated. It will also be verified whether R changes in a way suggested by the proposed mechanism, i.e. increasing with the depth of the bar crest and related to the development stage of the bar.

The changes in %ACT, %DGEN, %MAIN and R in relation to the depth of the outer bar crest are shown in Figure 6.15, for both the Katwijk site and the Egmond site. Before analysing these patterns, the extent to which these patterns are sensitive to the choice of the boundaries will be evaluated, focusing on the effect on the ratio R.

The sensitivity analysis on the location of the boundary between bar-degenerating and bar-maintaining conditions consists of varying this boundary between Q_b=0.04 and Q_b=0.06. This appears to affect the balance between these conditions mainly on the shallower bars that are still in a non-degenerating stage (Figure 6.16a,b). The cause of this sensitivity is shown in Figure 6.17. Figure 6.17

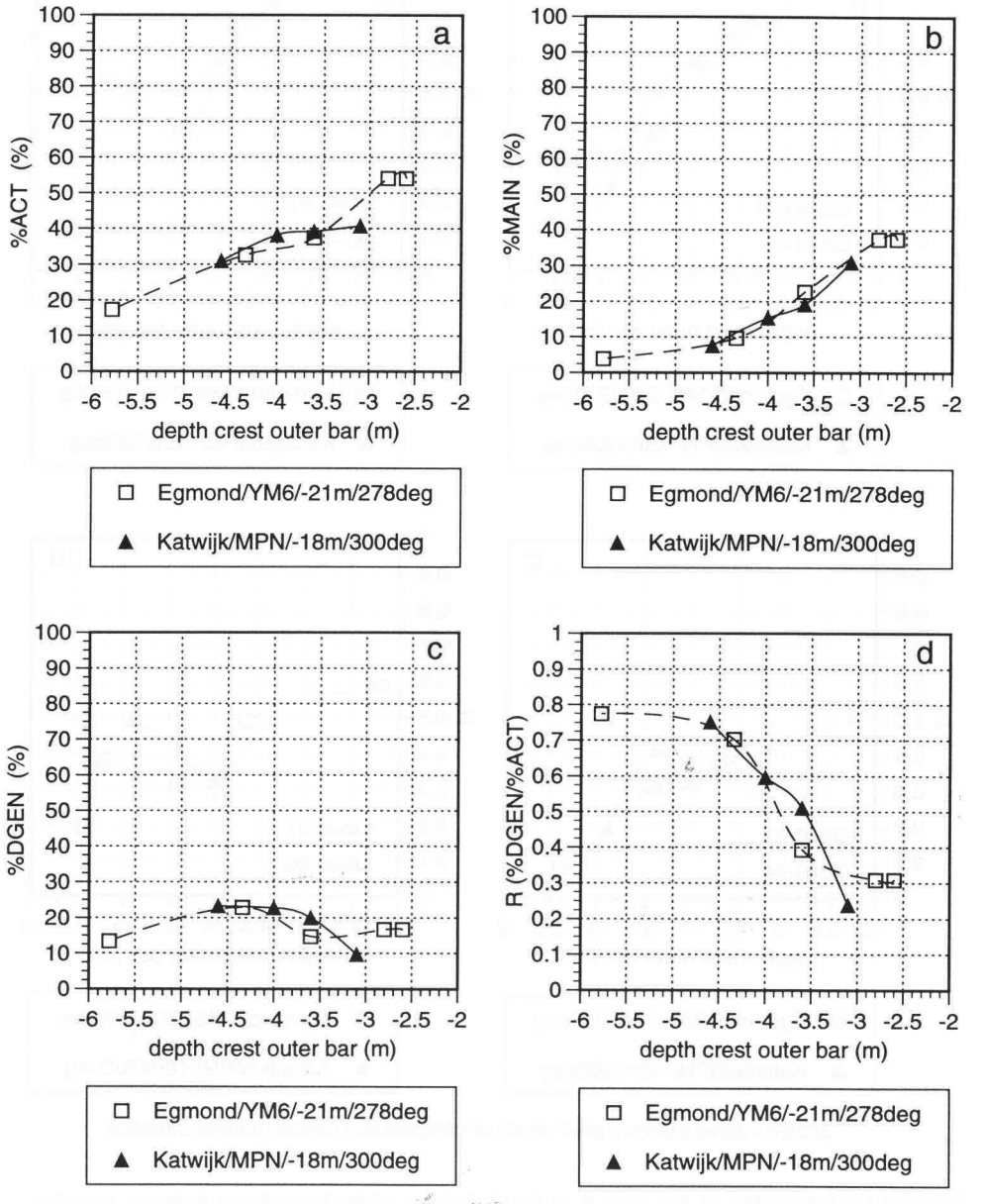

Figure 6.15: Nearshore wave climate parameters as a function of development stage of the outer bar. (a) %ACT; (b) %MAIN; (c) %DGEN; (d) ratio R.

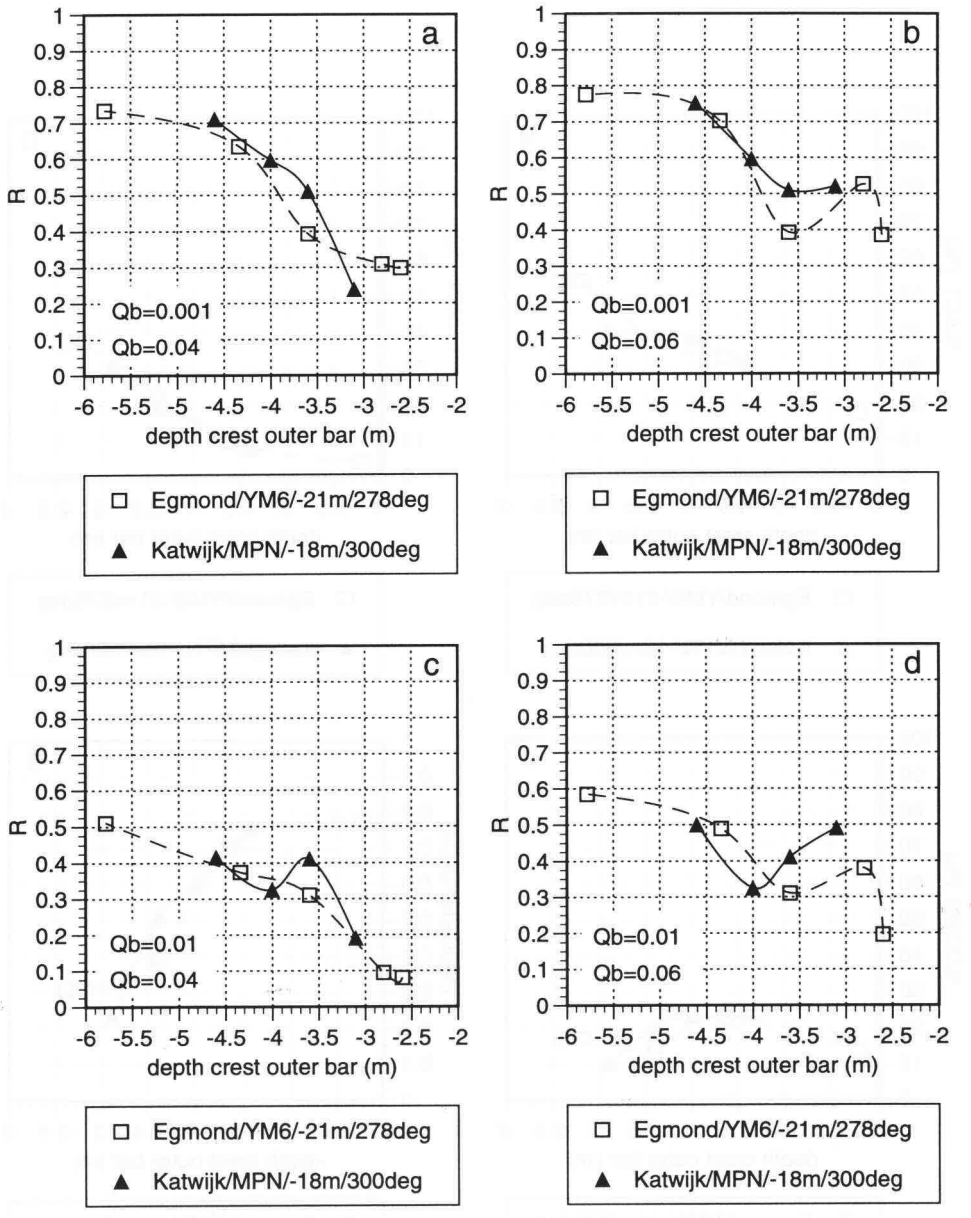

Figure 6.16: Sensitivity of the ratio R to the definition of the boundaries between morphologically inactive conditions, bar-maintaining conditions, and bar-degenerating conditions. (a) Boundaries at Q_b=0.001 and Q_b=0.04; (b) boundaries at Q_b=0.001 and Q_b=0.06; (c) boundaries at Q_b=0.01 and Q_b=0.04; (d) boundaries at Q_b=0.01 and Q_b=0.06.

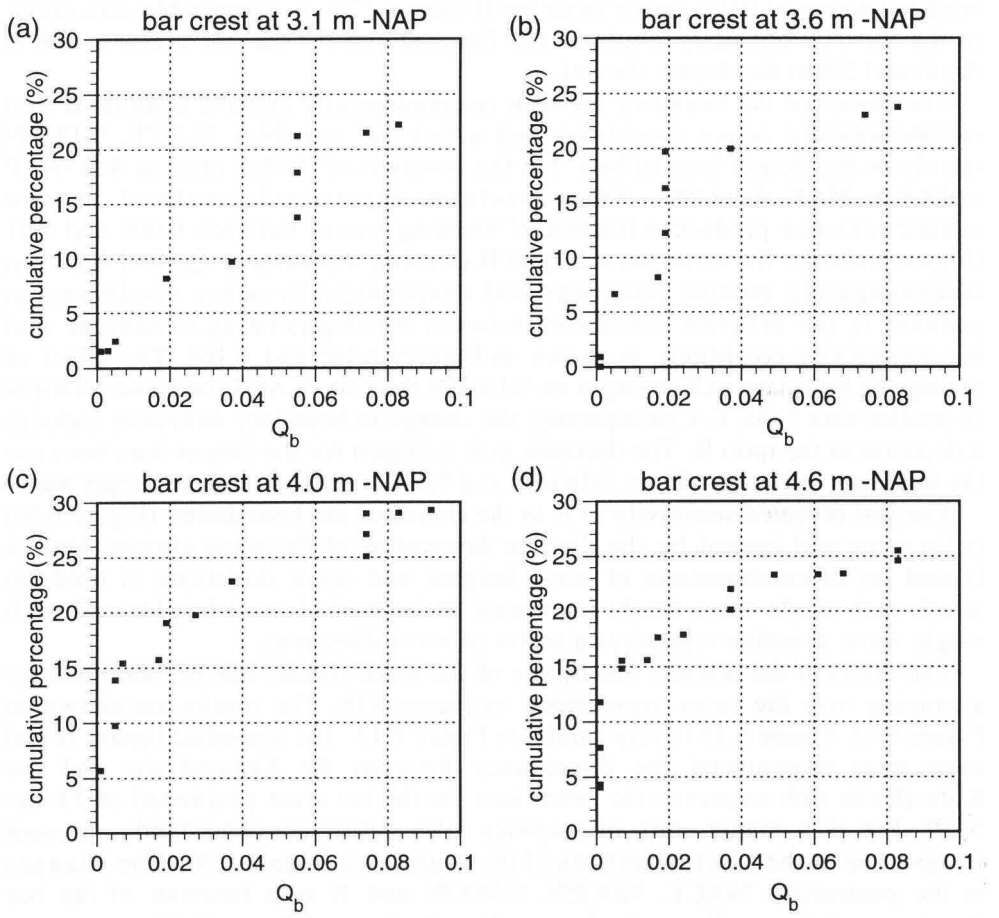

Figure 6.17: Cumulative percentage of occurrence of wave conditions with increasingly higher fractions of breaking waves on the outer bar, for $Q_b \geq 0.001$. (a) Bar crest at 3.1 m -NAP; (b) bar crest at 3.6 m -NAP; (c) bar crest at 4.0 m -NAP; (d) bar crest at 4.6 m -NAP. (Katwijk site.)

presents the cumulative percentage of occurrence of wave conditions with increasingly higher fractions of breaking waves on the outer bar. The cumulating starts at a fraction of breaking waves of 0.001. The cumulative curves are produced for the four bar development stages at the Katwijk site. It appears that for the bar crest at 3.1m -NAP, the variables %DGEN, %MAIN -and consequently R- will be quite sensitive to the location of the boundary at Q_b=0.05. For the bar crest at 3.1m -NAP, about 11 % of the wave climate is enclosed in the discretely defined wave climate cells that produce a fraction of

breaking waves of 0.055 on the outer bar (Figure 6.17a). A comparable sensitivity to the Q_b=0.05 boundary exists at the Egmond site for the bar crests at 2.6 m depth and 2.8 m depth (not shown).

The choice of the boundary between morphologically inactive conditions and morphologically active conditions will affect the variables %ACT, %DGEN mainly on the deeper located bars. For the positions of the bar crest at 4 m -NAP and 4.6 m -NAP, about 15% of the wave climate appears to be enclosed in wave climate cells that produce a fraction of breaking waves between 0.001 and 0.01 (Figure 6.17c,d). The effect on the ratio R of using a boundary Q_b=0.01 between morphologically inactive conditions and morphologically active conditions, in addition to the different boundaries between bar-degenerating conditions and bar-maintaining conditions, is shown in Figures 6.16c and 6.16d. The effect of raising the boundary will be larger on %DGEN than on %ACT, because %DGEN is smaller than %ACT. Consequently, the change in boundary definition induces a decrease in the ratio R. The decrease in R is largest for the deeper bars because the boundary variation affects %DGEN and %ACT mainly on these deeper bars.

The just revealed sensitivity of R to the choice of the boundaries (Figure 6.16) is for some part caused by the discrete description of the wave climate. Only a limited set of combinations of wave heights and wave directions is used, in which each single wave height represents an interval of wave heights and each single wave direction represents a sector of wave directions.

The effect of the discrete description of the wave climate can be smoothed by averaging over the cases represented in Figure 6.16. The results are shown in Figure 6.18. Figure 6.18 is very similar to Figure 6.15. The smoothed figures reveal even more pronounced the discrepancy between the Egmond site and the Katwijk site with respect to the conditions on the bar crest positioned at 3.6 m - NAP. For that matter, this discrepancy also remained consistently present irrespective of the exact definitions of the boundaries (Figure 6.16). The changes in the parameters %ACT, %DGEN, %MAIN and R as a function of the bar development stage will now be discussed on the basis of Figure 6.18.

The percentage of time that morphologically active conditions occur on the outer bar (%ACT) decreases steadily with the increase of depth of the bar crest (Figure 6.18a). A difference between the Egmond site and the Katwijk site seems to occur for the shallower positions of bars (bar crests shallower than 3.5 m - NAP), when bars at both sites are still in the non-degenerating stage of their development. Regarding the outer bars in the non-degenerating stage, the percentage of time the morphologically active conditions occur might be slightly larger at the Egmond site than at the Katwijk site.

The percentage of time that bar-maintaining conditions occur on the outer bar (%MAIN) decreases steadily with the increase of depth of the bar crest as well (Figure 6.18b). Regarding the outer bars of which the bar crest is positioned shallower than 4 m -NAP, the bar-maintaining conditions occur slightly more often near Egmond than near Katwijk.

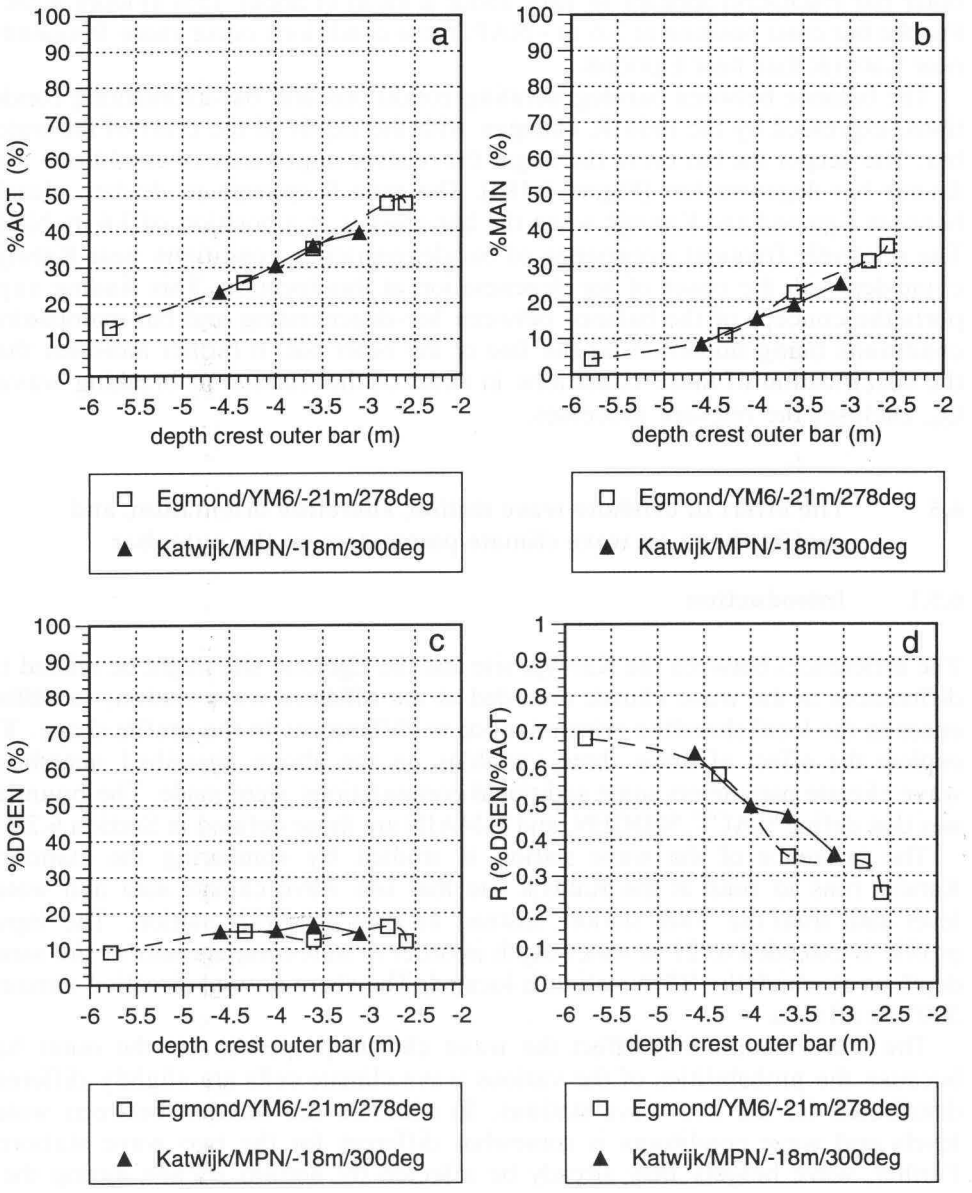

Figure 6.18: Smoothed values of the nearshore wave climate parameters as a function of development stage of the outer bar. (a) %ACT; (b) %MAIN; (c) %DGEN; (d) ratio R.

The percentage of time that conditions occur that favour degeneration of the outer bar (%DGEN) appears to vary about a mean of about 15% (Figure 6.18c). For the bar crest position at 3.6 m - NAP, these conditions occur more frequently near Katwijk than near Egmond.

The balance between bar-degenerating conditions and bar-maintaining conditions, expressed by the ratio R, changes with the depth of the crest of the outer bar. The deeper the bar crest, the larger the relative importance of conditions that favour bar degeneration (Figure 6.18d). The ratio R appears to deviate clearly between Egmond and Katwijk when the bar crest is at a position of 3.6 m -NAP. The relatively frequent occurrence of bar-degenerating conditions near Katwijk coincides with the onset of bar degeneration at this location. This finding supports the concept of the balance between bar-degenerating and bar-maintaining conditions being important for the fate of the outer bar. It further indicates that the specification of these conditions in terms of the fraction of breaking waves Q_b, encloses the relevant processes.

6.5 The effect of offshore wave station, shoreline orientation, and profile shape on wave climate parameters on the outer bar

6.5.1 Introduction

The differences between the Katwijk site and the Egmond site might be related to differences in the wave climate recorded at the offshore wave station, to differences in the local shoreline orientation, or to differences in the profile shape. To explore the effect of these three variables on the above described nearshore wave climate parameters some additional computations were made. The boundaries that define %ACT, %DGEN, and %MAIN are those defined in Section 6.2.

The influence of the wave station is studied by comparing the standard Katwijk runs to runs at the Katwijk site that use wave climate data and water level data from the YM6 station, instead of from the MPN station. The input profile is extended to 21 m water depth in order to start computations at the same depth as at which the YM6 station is located. The shore normal direction remains 300° for all runs.

The wave station may affect the wave climate properties on the outer bar because the probabilities of the various wave climate cells are slightly different distributed for the two wave stations. In addition, the relation between water levels and wave conditions is somewhat different for the two wave stations. Further, wave heights may already be affected by bottom friction during their onshore propagation across the stretch from 21 m to 18 m water depth (about 11 km length). Generally, bottom friction only affects the highest waves included in the offshore wave distribution. These highest waves, however, are the waves that are involved in the breaking on the outer bar in case of a small value of Q_b.

The influence of the shoreline orientation is studied by comparing runs that differ in the shore normal direction, viz. a shore normal direction of 300° versus a

shore normal direction of 278°. All runs use the Katwijk profiles (starting at 21 m water depth) and the YM6 wave climate and water level data.

The shoreline orientation may affect the wave climate properties on the outer bar, because it influences the angle of incidence of the various wave climate cells relative to the shoreline. For example, for a given offshore wave direction a certain wave height class may produce a fraction of breaking waves on the outer bar of just 0.001. These same waves may pass the outer bar without breaking when the shoreline orientation is closer to the wave direction. The waves will then approach the coast more obliquely, and the increased refraction will result in a reduction of the wave height. Further, the shoreline orientation determines which directional sectors of the offshore wave climate are involved in the determination of nearshore wave climate parameters.

The influence of the profile shape is studied by comparing runs that differ in the input profiles, viz. the Katwijk profiles (starting at 21 m water depth) versus the Egmond profiles. All runs use the YM6 wave climate and water level data, and the applied shore normal direction is 278°.

The profile shape may affect the wave climate properties on the outer bar, because it influences both the nearshore wave height and the breaker criterion γ. The wave height on the outer bar is influenced by the profile shape because the profile shape affects the degree of refraction of obliquely incident waves. Refraction on its turn affects the wave height and therefore is of influence on the wave height at the crest of the outer bar. The breaker criterion is influenced by the profile shape because its value depends on the bed slope (Section 6.3.2).

6.5.2 Sensitivity of wave climate parameters on the outer bar to offshore wave station, shoreline orientation and profile shape

The effect of the wave station, the shoreline orientation, and the profile shape, on the percentage of time that morphologically active conditions occur on the outer bar varies with the depth of the bar crest (Figure 6.19). When the bar crest is located at 3.6 m water depth, the value of %ACT is quite insensitive to the differences in shoreline orientation, wave station, and profile shape that exist between the Katwijk site and the Egmond site (Figure 6.19a,b,c). For deeper positions of the bar crest the use of the YM6 wave station in the computations reduces %ACT (Figure 6.19a). The difference in shoreline orientation between Katwijk and Egmond seems to affect the value of %ACT only for the bar crest position around 4 m water depth (Figure 6.19b). The difference in profile shape between Katwijk and Egmond seems to cause lower values of %ACT for the shallowest and deepest bar crest position of the Katwijk site (assuming a smooth curve between the values at the various bar crests). For the bar crest position at 4 m water depth, the shape of the Katwijk profile seems to cause a slightly larger value of %ACT (Figure 6.19c).

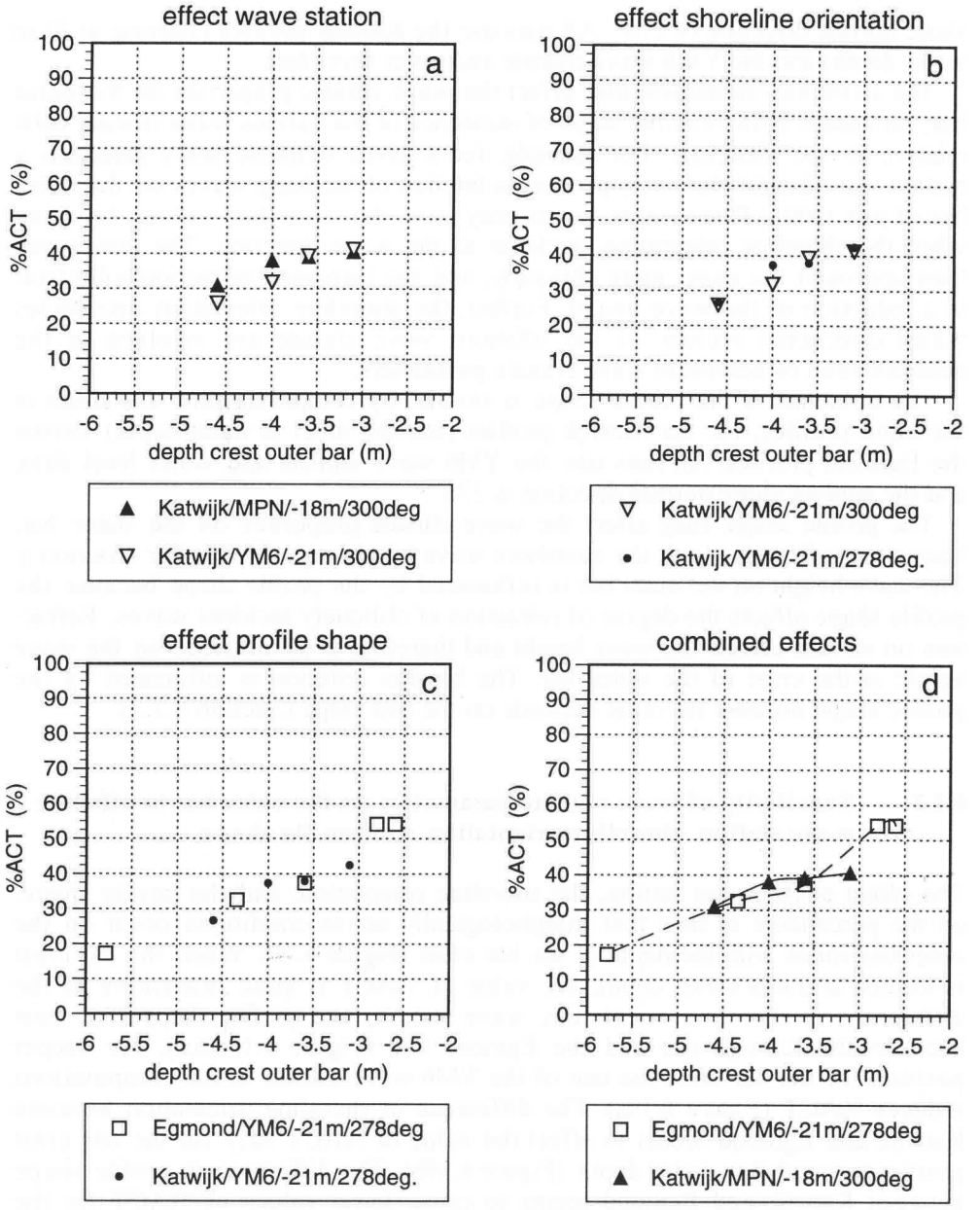

Figure 6.19: Sensitivity of the parameter %ACT to differences in (a) input wave climate (MPN vs. YM6), (b) shoreline orientation (shore normal direction to the North of 300° vs. 278°), and (c) shape of the shoreface profile (Katwijk profile vs. Egmond profile); (d) base case.

The foregoing sensitivity computations indicate that the difference in %ACT between the Katwijk and the Egmond site, for shallow positions of the bar crest (Figure 6.19d and 6.18a), is mainly caused by the difference in profile shape.

The percentage of time conditions occur that favour the degeneration of the outer bar appears to be sensitive to differences in the wave station, in the shoreline orientation, as well as in the profile shape (Figure 6.20a,b,c). The use of a different wave station in the computations influences %DGEN at all positions of the outer bar, both increasing and decreasing the percentage (Figure 6.20a). For the bar crest positioned at 3.6 m depth the effect is the smallest. The difference in the orientation of the shoreline affects %DGEN on (outer) bars of which the crest is positioned shallower than about 4 m (Figure 6.20b). The difference in profile shape between Katwijk and Egmond seems to cause lower values of %DGEN for the shallowest and deepest bar crest position of the Katwijk site (assuming a smooth curve between values at the various bar crests) (Figure 6.20c).
The foregoing sensitivity computations indicate that the deviation in %DGEN between the Katwijk and the Egmond site for the bar crest position at 3.6 m water depth (Figures 6.20d and 6.18c) is mainly caused by the difference in shoreline orientation.

The percentage of time bar-maintaining conditions occur seems to be most sensitive to the orientation of the shoreline, affecting %MAIN for the shallower positions of the outer bar crest (6.21b). The wave station and the profile shape hardly affect %MAIN (Figure 6.21a,c). Consequently, the deviation in %MAIN between the Katwijk and the Egmond site for the bar crest position at 3.1 m and 3.6 m water depth (Figures 6.21d and 6.18b) is mainly caused by the difference in shoreline orientation.

The balance between bar-maintaining and bar-degenerating conditions (R) is sensitive to the differences in wave station, in shoreline orientation as well as in profile shape (Figure 6.22a,b,c). The effect on R of differences in these variables between Egmond and Katwijk, appears to cancel out for deeper positions of the outer bar (more than 4 m depth) (Figures 6.22d and 6.18d). On the outer bar at 3.6 m -NAP, however, the effects do not cancel out. The resulting difference in R appears to be mainly caused by the difference in shoreline orientation. The difference in ratio R between Egmond and Katwijk for the shallower bar crest positions shown in Figure 6.18d is mainly due to sensitivity to the discrete representation of the wave field, cf. Figure 6.22d and Figure 6.18d (also see Section 6.4.2). The difference in the ratio R between the Egmond site and the Katwijk site for the bar crest located at 3.6 m -NAP, appears to coincide with a difference in behaviour of that bar. The outer bar near Katwijk just starts to degenerate whereas the outer bar near Egmond is still in a non-degenerating stage when its crest is at 3.6 m -NAP. Therefore, the shoreline orientation is probably an important parameter in inducing differences between Katwijk and Egmond in the moment of onset of bar degeneration.

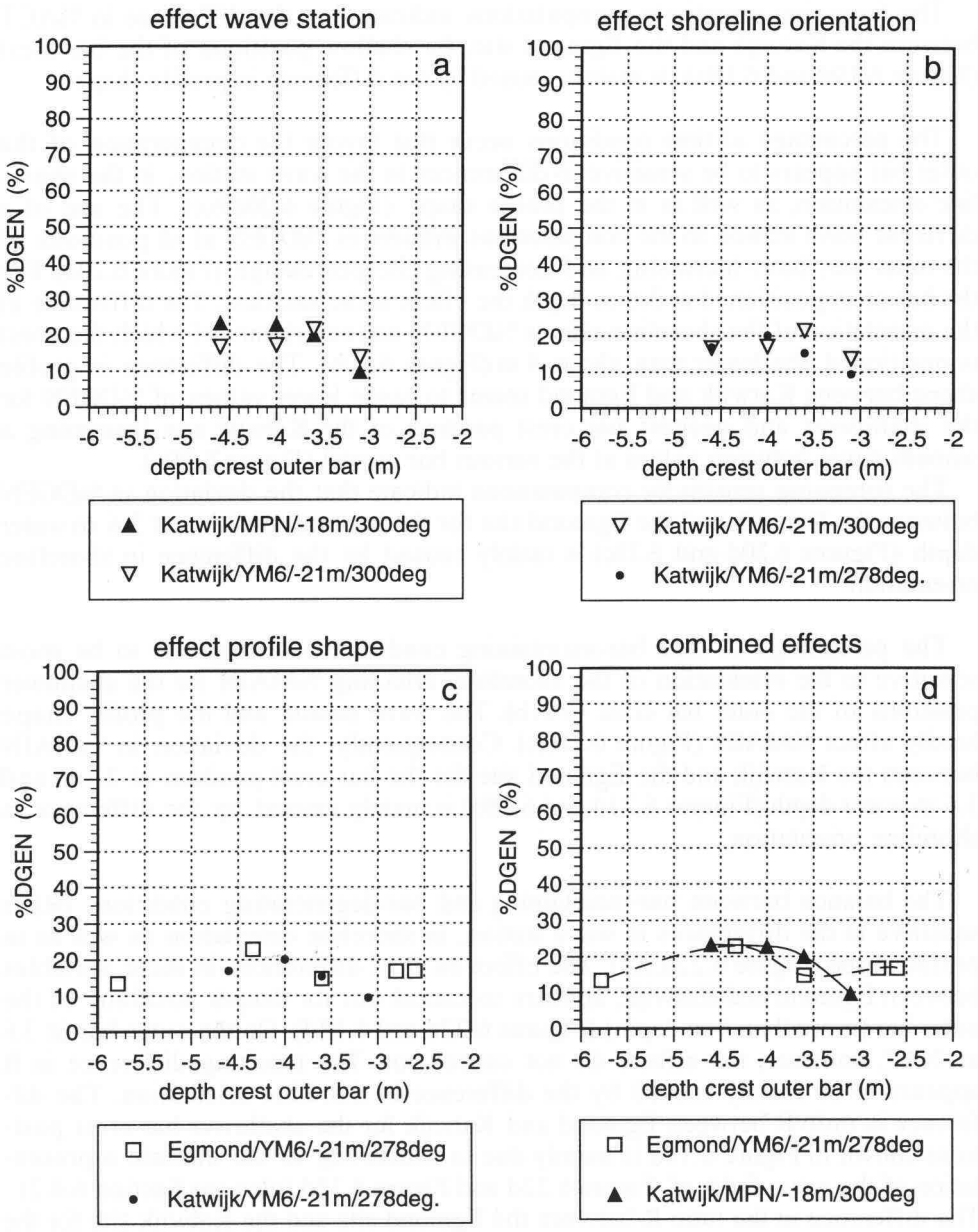

Figure 6.20: Sensitivity of the parameter %DGEN to differences in (a) input wave climate (MPN vs. YM6), (b) shoreline orientation (shore normal direction to the North of 300° vs. 278°), and (c) shape of the shoreface profile (Katwijk profile vs. Egmond profile); (d) base case.

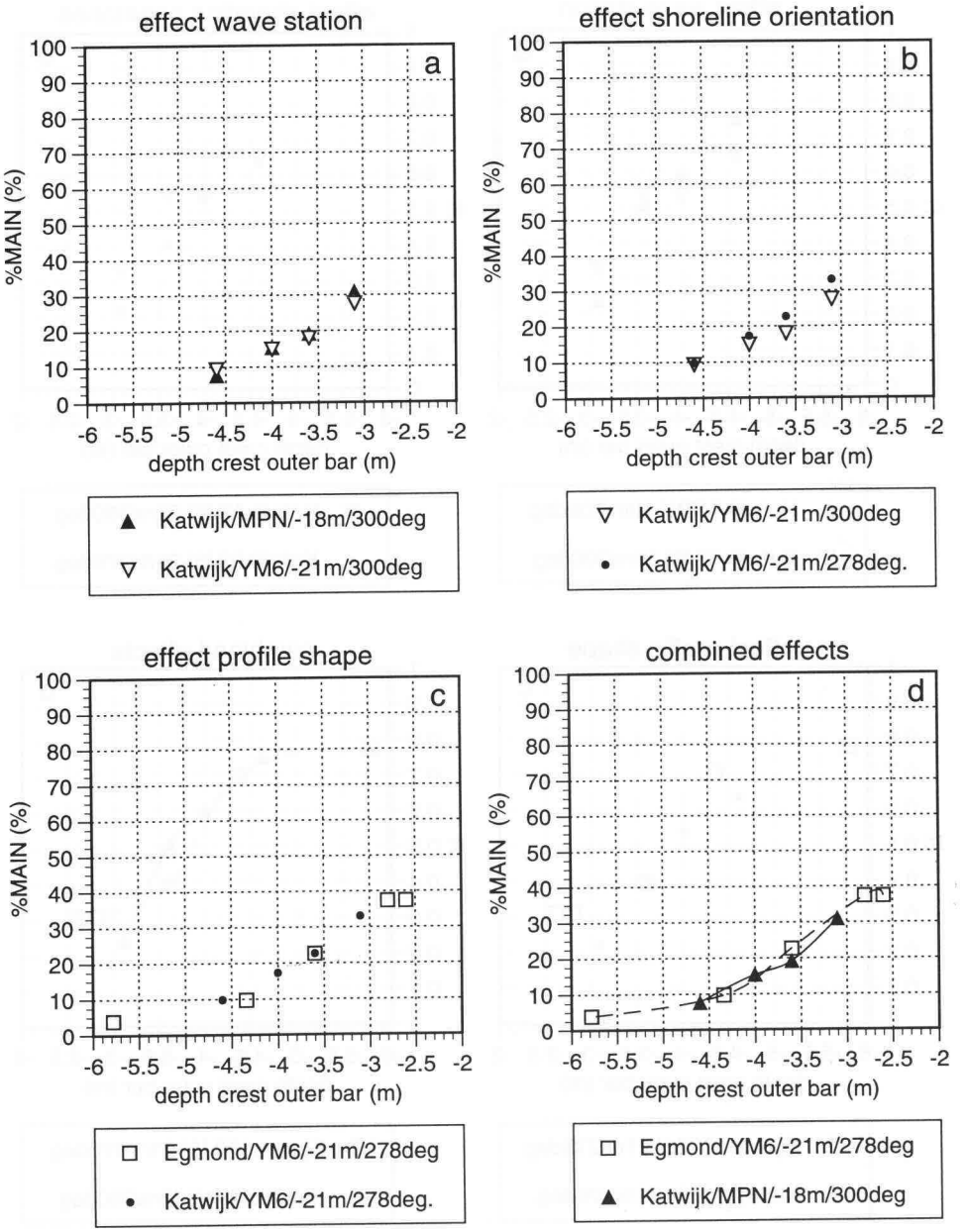

Figure 6.21: Sensitivity of the parameter %MAIN to differences in (a) input wave climate (MPN vs. YM6), (b) shoreline orientation (shore normal direction to the North of 300° vs. 278°), and (c) shape of the shoreface profile (Katwijk profile vs. Egmond profile); (d) base case.

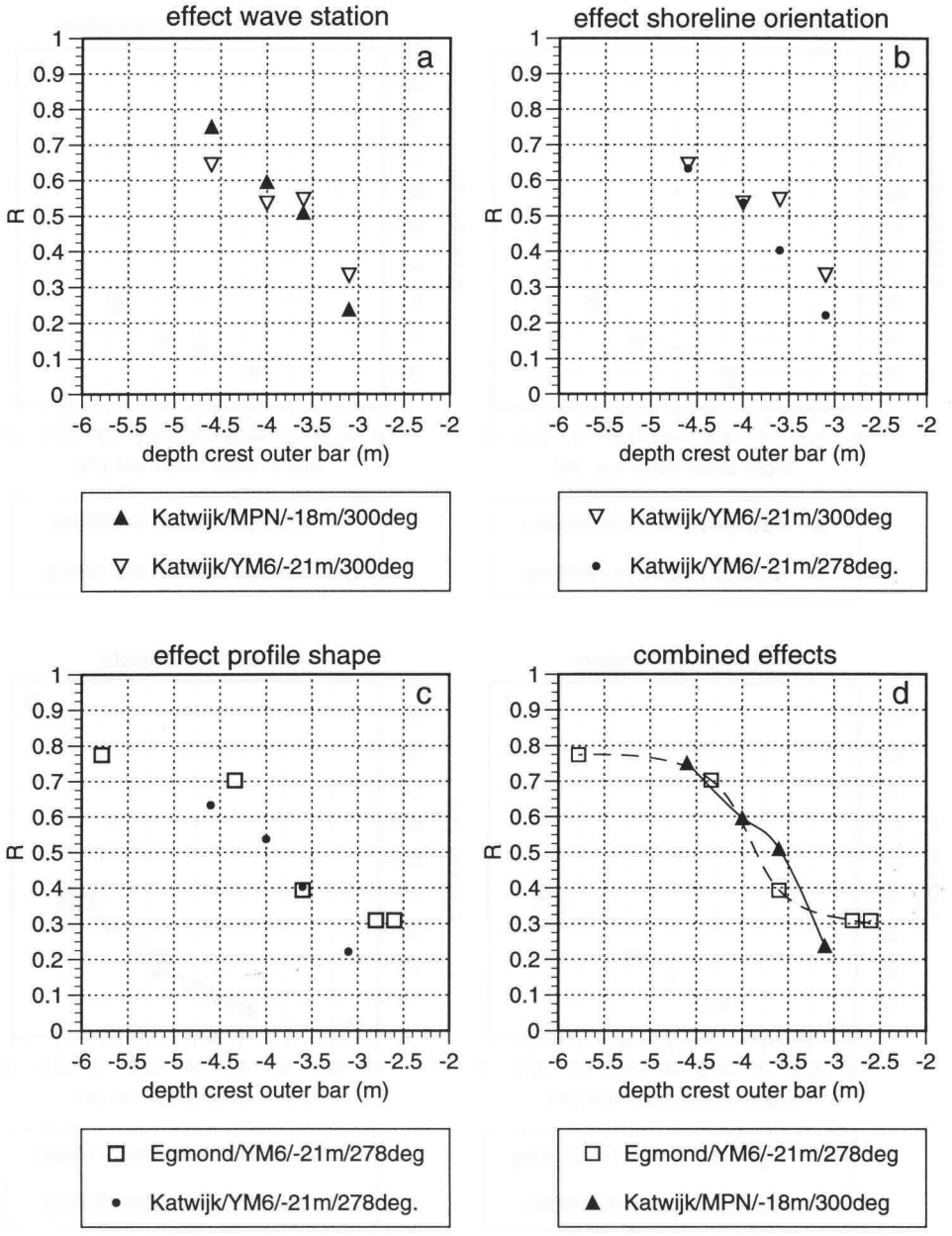

Figure 6.22: Sensitivity of the parameter R to differences in (a) input wave climate (MPN vs. YM6), (b) shoreline orientation (shore normal direction to the North of 300° vs. 278°), and (c) shape of the shoreface profile (Katwijk profile vs. Egmond profile); (d) base case.

6.5.3 The relation between shoreline orientation and the occurrence of bar-degenerating conditions

The difference in the ratio R between Egmond and Katwijk was found to be mainly caused by the difference in shoreline orientation of these two sites, in which especially the effect on %DGEN appeared to be important. To study the effect of shoreline orientation on %DGEN, the computations on the effect of shoreline orientation on %DGEN (Figure 6.20) were analysed in more detail. Figure 6.23 presents the distribution of %DGEN over the offshore wave conditions. To derive Figure 6.23, the wave classes that compose %DGEN were grouped according to the angle of incidence relative to the shore normal. For each angle of incidence relative to the shore normal, the total percentage of occurrence of bar-degenerating conditions was determined, as well as the weighted mean wave height (the weighting being based on the frequency of occurrence of the wave height class).

The change in shoreline orientation -from 300° to 278° shore normal direction- has different effects on the distribution of %DGEN over the offshore wave conditions in the quadrant south of the shore normal and in the quadrant north of the shore normal. The effects also differ for different positions of the bar crest.

For bar crest positions at 3.1 m and 3.6 m -NAP, the change in shore normal direction from 300° to 278° results in the southerly quadrant in a decrease of very oblique and relatively high waves and a small increase in less oblique waves that are on average of lower height. In the northerly quadrant, the change in shoreline orientation results in a decrease of intermediate oblique and relatively low waves and a small increase of waves that are very oblique and of larger height.

For bar crest positions at 4.0 m and 4.6 m -NAP, the change in shore normal direction from 300° to 278° results in the southerly quadrant in a small decrease of very oblique and relatively high waves going with a relatively large increase in less oblique waves that are on average of lower height. In the northerly quadrant, the change in shoreline orientation results in a decrease of intermediate oblique and relatively low waves. This decrease goes with an increase of waves that approach the coast more oblique and have larger heights for the bar positioned at 4.0 m -NAP.

The differences in distribution of %DGEN over the offshore wave conditions shown in Figure 6.23 imply that the shoreline orientation may influence the intensities of the degeneration process. Very obliquely incident waves with relatively large offshore wave heights will have a longer wave period than less obliquely incident waves with smaller wave heights. On the same bar crest, the longer period waves will exhibit larger near-bottom orbital velocities than the shorter period waves, which may influence the intensity of the bar degeneration process. These changes are rather subtle, but since sediment transport is a non-linear process they may play a role in explaining differences between Egmond and Katwijk in the degeneration rate of the outer bar.

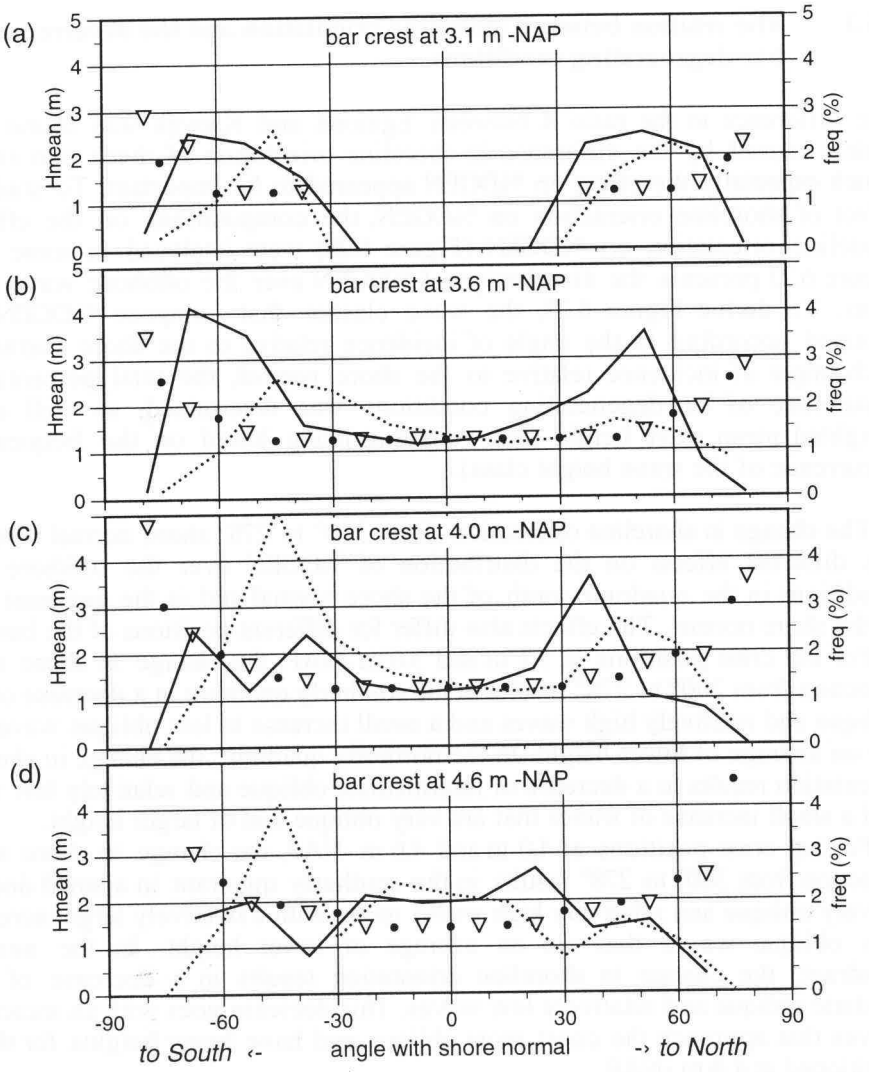

Figure 6.23: Distribution of %DGEN over the angles of incidence (defined offshore) for shore normal directions of 300° and 278°; the average offshore wave heights that produce those nearshore bar-degenerating conditions are shown as well. Outer bar crests at: (a) 3.1 m -NAP, (b) 3.6 m -NAP, (c)) 4.0 m -NAP, and (d) at 4.6 m -NAP. (Shoreface profile Katwijk, YM6 wave station.)

6.6 On the transport capacity during bar-degenerating conditions

6.6.1 Introduction

Bar-degenerating conditions occur only a limited amount of time per year. To support the formulated hypothesis, sediment should be transported onshore on the outer bar during these conditions at the right order of magnitude. The degeneration of the outer bar near Katwijk over the period 1981-1983 is used as a test case (Figure 6.24). Typical annual cross-shore transport patterns during the degeneration stage of the outer bar can be derived from the changes in profile shape (equation 5.5). Figure 6.24 reveals that a net onshore transport across the bar crest occurs of about 30 $m^3 m_a^{-1} yr^{-1}$. The net onshore transport of sediment landward of the bar crest should be attributed to a combination of waves and (increased) longshore current velocities, according to the formulated hypothesis.

In the following, transports on the outer bar during the bar-degenerating conditions are estimated. The transports will be calculated at the seaward slope and at the crest of the 1981 and 1982 outer bar configurations. For two reasons longshore currents are not included in the calculations. Firstly, synoptic current measurements on and near the outer bar, over a variety of wind conditions, are lacking. This implies that all combinations of tide and wind-driven currents to be put into the transport model have to be subjectively synthesised, including the unknown velocity differences across the bar. Secondly, the transport calculations presented in this section are meant to be no more than rough indicators of transport capacity, because too little is known about the near-bed transport in the nearshore zone under field conditions (Greenwood and Osborne, 1991).

6.6.2 Transport gradients across the outer bar

Magnitudes of the transports during bar-degenerating conditions are computed by using the TRANSPOR model, described in Van Rijn (1993). TRANSPOR computes bed load transport and suspended load transport under combined waves and currents. Near-bed peak orbital velocities are computed according to equations 6.19 to 6.25 (see Section 6.3.3). The TRANSPOR model requires the following input parameters: wave height, peak wave period, water depth, grain size (D_{50}, D_{90}, D_{SS} = grain size suspended sediment), depth-averaged mean (longshore) current, angle between waves and current, wave-related bed-roughness height, current-related bed-roughness height, water temperature and salinity. Optionally, the return current (compensating mass transport between wave crest and trough) can be switched off or set at a fixed value. Similarly, the wave-induced time-averaged near-bed velocity can be switched off or set at a fixed value (e.g. to represent near-bottom, wind- or density-driven currents). Table 6.4 contains the values of the input parameters for the TRANSPOR model as applied in this study.

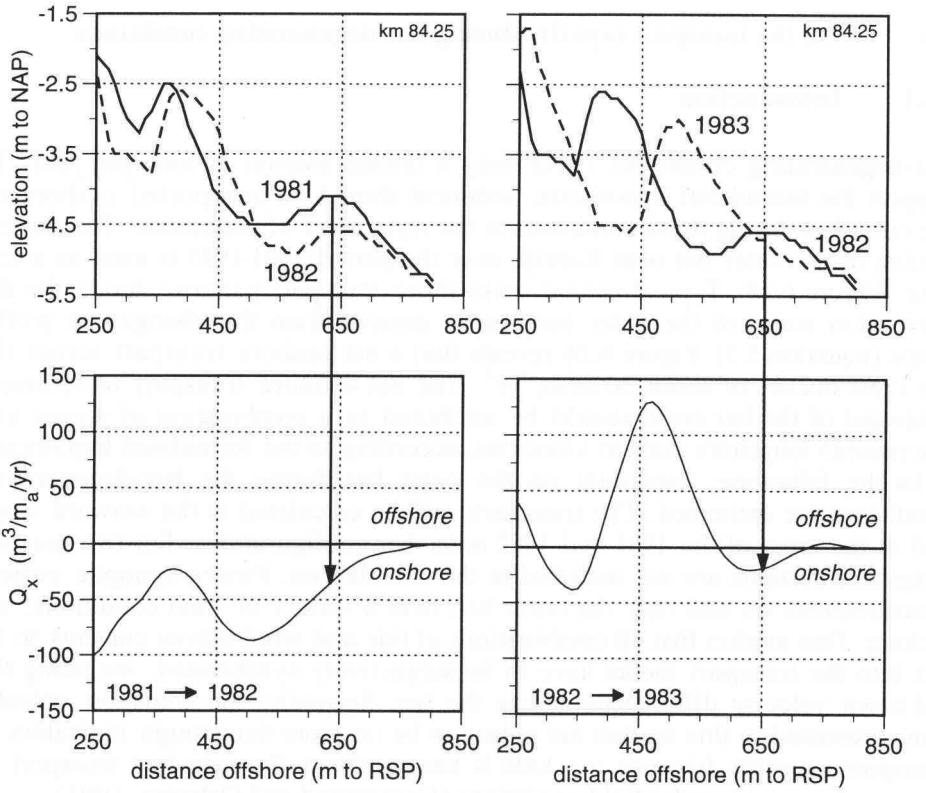

Figure 6.24: Degeneration of the outer bar and related net cross-shore transports near Katwijk: 1981-1983. (Survey dates: May 21, 1981; June 18, 1982; July 6, 1983.)

To obtain onshore directed transport in the hereafter described transport calculations, the return current had to be set to zero (Table 6.4). If the default TRANSPOR assumption of local compensation of the mass flux is applied, only offshore transport is calculated. This is due to the dominance of suspended load transport with the mean current. Measurements presented by Aagaard and Greenwood (1994) show that the assumption of a (local) zero return current is not unrealistic, even under conditions of more severe breaking than during bar-degenerating conditions. Their measurements revealed that on a bar crest under conditions of non-saturated wave breaking, the (weak) mean current was directed even onshore, instead of offshore as might have been expected.

The required assumption of non-local compensation of the mass flux implies that, according to the TRANSPOR model, net onshore transport across the outer bar only occurs if the water circulation is occurring (mainly) in the horizontal plain, instead of in the vertical plain.

Table 6.4: Values of TRANSPOR input parameters

TRANSPOR input parameters		
Significant wave height	:	$H_{1/3}$ crest outer bar (WAVIS)
Peak wave period	:	$T_{1/3}$ (WAVIS)
Water depth	:	water depth crest outer bar
Depth averaged longshore current	:	0 m/s
Return current	:	0 m/s
Wave-induced time-averaged near-bed velocity	:	as calculated by TRANSPOR
D_{50} grain size	:	0.00020 m
D_{90} grain size	:	0.00030 m
D_{SS} = grain size suspended sediment	:	0.00018 m
Wave-related bed-roughness height	:	0.01 m
Current-related bed-roughness height	:	0.01 m
Water temperature	:	12 °C
Salinity	:	29 ‰

The onshore transport on the outer bar is hypothesised to occur during conditions that the fraction of breaking waves varies between 0.001 and 0.05. The wave parameters $H_{1/3}$ and $T_{1/3}$ at the crest of the outer bar during these conditions -as determined by the WAVIS model- are used as input parameters in the TRANSPOR model. Combining the calculated transport rate with the frequency of occurrence of those conditions results in an estimate of the mean annual transport capacity during bar-degenerating conditions. A pore volume of 40% was applied to estimate the annual transport in terms of onshore transported bar volume. An example of the computation of the mean annual volume transport during bar-degenerating conditions is shown in Table 6.5.

To verify whether the proposed bar-degenerating conditions are potentially able to transport sufficient sediment onshore, transport gradients are calculated from the lower end of the seaward slope of the outer bar (5.5 m -NAP) to the crest of the outer bar (4 m and 4.6 m -NAP respectively) (Table 6.6). For the bar development stage in which the bar crest is located at 4 m water depth (1981) the mean annual volume transport gradient across the bar is about 45 $m^3 m_a^{-1} yr^{-1}$. For the bar crest location at -4.6 m (1982) this gradient is about 30 $m^3 m_a^{-1} yr^{-1}$ (Table 6.6). The calculated transports mainly consist of bed load transport.

All transport rates are calculated with the same sediment characteristics. It is known though, that sediment size varies across the nearshore zone (see Section 2.2.4). Therefore, transport rates were calculated once more for the 5.5 m depth locations using finer sediment. The grain size characteristics applied are: D_{50}=0.00017 m, D_{90}=0.00022 m and D_{SS}=0.00015 m. These changes result in mean annual volume transport gradients across the outer bar of about 60 $m^3 m_a^{-1} yr^{-1}$ and about 50 $m^3 m_a^{-1} yr^{-1}$, for bar crest positions at respectively 4 m and 4.6 m water depth (Table 6.6).

Table 6.5: Example of transport computations for bar-degenerating conditions on bar crest at 4.0 m -NAP near Katwijk.

$H_{1/3}$ (m)	$T_{1/3}$ (s)	Water depth (m)	% Wave climate	Average yearly occurrence (hr yr^{-1})	Transport rate (kg $m^{-1}s^{-1}$)	Mean annual volume transport ($m^3m_a^{-1}yr^{-1}$)
1.22	6.4	4.09	3.33433	292	0.02325	15.3
1.19	6.4	4.09	4.05540	355	0.02150	17.2
1.13	6.4	3.99	4.12933	362	0.01747	14.2
1.01	6.4	3.90	5.70973	500	0.01275	14.3
1.40	7.2	3.99	3.05118	267	0.03580	21.5
1.15	7.2	3.99	1.54810	136	0.01937	5.9
1.43	7.8	4.09	0.71452	63	0.03742	5.3
1.14	7.2	3.59	0.27356	24	0.02273	1.2
						Σ= 94.9

Table 6.6: Mean annual volume transport across the outer bar near Katwijk; calculated annual transports during bar-degenerating conditions, and 'observed' net annual transports (positive is landward directed).

	Depth (m to NAP)	Mean annual volume transport ($m^3m_a^{-1}yr^{-1}$)		
		Calculated (D_{50}=200 μm)	Calculated (D_{50}=200 μm,170 μm)	'Observed'
Bar-degenerating conditions for bar crest at 4.0 m -NAP				
Bar crest	-4.0	95	95 (200 μm)	35
Seaward slope	-5.5	50	35 (170 μm)	0
Transport gradient seaward slope - crest		45	60	35
Bar-degenerating conditions for bar crest at 4.6 m -NAP				
Bar crest	-4.6	120	120 (200 μm)	20
Seaward slope	-5.5	90	70 (170 μm)	0
Transport gradient seaward slope - crest		30	50	20

Apparently, the onshore sediment transport by asymmetric waves becomes less efficient for the finer sediments. This is probably an effect of the reduction of the critical velocity for initiation of motion. This effect will probably be less pronounced when longshore currents are taken into account, because these exert a shear stress on the grains as well. Whatever the effect of additional currents, the result of the grain size sensitivity calculations draws the attention to the possible role of selective transport in the degeneration of the outer bar. Medina et al. (1994) revealed this role in the seasonal behaviour of a single bar system. For example, they showed that the erosion of the 'winter bar' started by losing fine sand, consequently inducing a coarsening of the sediment on this bar. If selective transport plays a role in the degeneration of the outer bar, this induces another uncertainty about the calculated transport rates.

The transport figures presented in Table 6.6 show that the transport gradients during bar-degenerating conditions are of the right order of magnitude to account for the degeneration of the outer bar. The amounts of onshore transport themselves, however, are considerably larger than those derived from the profile changes. This difference may be attributed to the fact that the transports derived from the profile changes ('observed' transports) are net annual values. As a consequence, these values include the effect of transports occurring during bar-maintaining conditions. For example, sediment may be transported offshore across the 5.5 m -NAP contour during the bar-maintaining conditions, balancing the sediment input that seems to occur during the bar-degenerating conditions. Since the net annual transport is directed onshore on the considered location, the gradient in offshore directed transport should be smaller than the onshore transport gradient of the bar-degenerating conditions. Too little is known about transports under conditions with moderately and intensively breaking waves to make sensible estimates of transports and transport gradients across the outer bar during the set of bar-maintaining conditions.

6.7 The duration of the bar system cycle: the Noord-Holland bar system versus the Zuid-Holland bar system

According to the proposed mechanism for the cyclic bar system behaviour (Chapter 5), the behaviour of the outer bar will determine the duration of the bar system cycle. The difference in the duration of the bar system cycle between the Noord-Holland bar system and the Zuid-Holland bar system is related to differences in the moment of onset of bar degeneration. In addition, it may also be related to differences in the time span required to degenerate the outer bar. The required time span will depend on the volume of sediment that has to be transported onshore (depending on the volume of sand enclosed in the outer bar), as well as on the strength and frequency of occurrence of the bar-degenerating processes.

Near Egmond, the maximum volume of sediment enclosed in the outer bar is about 500 $m^3 m_a^{-1}$, taking the lower branch of the profile bundle envelope as the reference level. The difference in bar volume compared to the outer bar volume in the Zuid-Holland bar system (cf. outer bar volume Katwijk of about 250 $m^3 m_a^{-1}$), may induce at most a factor 2 longer time span for bar degeneration in the Noord-Holland bar system. The observed difference between the degeneration time spans, however, is about a factor 4.

In the Zuid-Holland bar system, the frequency of occurrence of the bar-degenerating conditions is relatively constant on the outer bar in its degenerating stage (Figures 6.15c and 6.18c). In the Noord-Holland bar system, the frequency of occurrence of these conditions might decrease somewhat with the increasing depth of the crest of the outer bar once it is in its degenerating stage.

The strength of bar-degenerating processes is represented by the strength of the near-bed orbital velocities ($\hat{u}_{\delta,on,1/3}$) and the asymmetry in near-bed orbital velocities ($A_{1/3}$). Hydrodynamic parameters are preferred to transport rates, because of the aforementioned uncertainties about the absolute values of the calculated transport rates. $A_{1/3}$ and $\hat{u}_{\delta,on,1/3}$ are determined by the WAVIS model (Section 6.3.3) analogously to the calculation of a significant wave height $H_{1/3}$. It appears that for outer bars in the degenerating stage, the peak onshore velocities on the outer bar during bar-degenerating conditions ($0.001 \leq Q_b \leq 0.05$) are somewhat larger on the degenerating outer bars near Egmond than on those near Katwijk (Figure 6.25a). The velocity asymmetries on the outer bar during these conditions may be slightly larger near Egmond than near Katwijk (Figure 6.25b).

The effect of the differences in $\hat{u}_{\delta,on,1/3}$ and $A_{1/3}$ on the magnitude of the resulting onshore transport rates will depend on the grain size characteristics. Similar to the finding that finer sediments are not necessarily transported onshore more efficiently than coarser sediments, larger orbital velocities do not necessarily transport more sediment onshore than smaller orbital velocities. So, small differences may exist between the Noord-Holland and Zuid-Holland bar system in the intensity of the bar degeneration process, but it is still not clear to what extent this will induce differences in the degeneration rate of the outer bar.

Another possible reason for the variation in the duration of the bar system cycle is related to the stage of net offshore migration of the outer bar, prior to its degeneration stage. In the Zuid-Holland bar system, the onset of degeneration of the outer bar occurs at a shallower depth than in the Noord-Holland bar system. As a consequence, the outer bar of the Noord-Holland bar system has to migrate to a larger depth than the Zuid-Holland outer bar to get into the bar-degenerating environment. This additional offshore migration may take a relatively long time when compared to the offshore migration of the outer bar prior to degeneration in the Zuid-Holland bar system, because conditions during which the bar can migrate offshore will occur less frequently at deeper positions of the bar (Figure 6.18b). This might explain why the migration of the outer bar prior to degeneration requires relatively much time in the Noord-Holland bar system when compared to the Zuid-Holland bar system.

In addition, the volume of sediment involved in the offshore migration of the outer bar is larger in the Noord-Holland bar system than in the Zuid-Holland bar system. This difference allows for a more rapid migration of the outer bar in the Zuid-Holland bar system. This implies that in the Zuid-Holland bar system a 'new' outer bar may migrate more rapidly to its degeneration position than a 'new' outer bar in the Noord-Holland bar system.

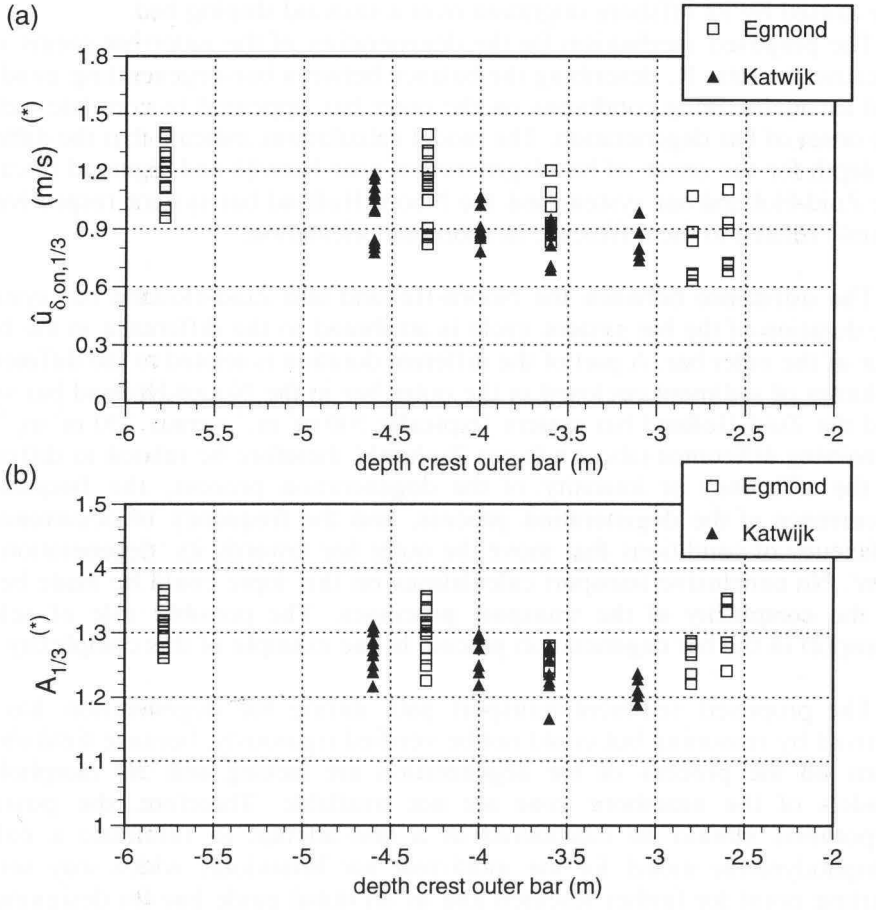

(*) *applies to non-breaking waves*

Figure 6.25: Near-bed orbital velocity properties for conditions that produce a fraction of breaking waves on the outer bar between 0.001 and 0.05. (a) Near-bed, peak onshore orbital velocity; (b) Near-bed, orbital velocity asymmetry.

6.8 Discussion and conclusions

To explain the observed cyclic bar system behaviour a central role was attributed to the behaviour of the outer bar. It was hypothesised that the consistently occurring degeneration of the outer bar could be explained by the balance between conditions that favour bar degeneration and conditions that favour bar existence. This balance was shown to change more and more in favour of the bar-degenerating conditions with an increasingly deeper position of the outer bar caused by its offshore migration over a seaward sloping bed.

The proposed mechanism for the degeneration of the outer bar seems viable, because the ratio R, describing the balance between bar-degenerating conditions and bar-maintaining conditions on the outer bar, appeared to correlate well with the onset of bar degeneration. The model calculations indicate that the difference in depth for the onset of bar degeneration near Katwijk and Egmond (located in the Zuid-Holland bar system and the Noord-Holland bar system respectively) is mainly related to the difference in shoreline orientation.

The difference between the Noord-Holland and Zuid-Holland bar system in the duration of the bar system cycle is attributed to the difference in the behaviour of the outer bar. A part of the different duration is related to the difference in volumes of sediment enclosed in the outer bar in the Noord-Holland bar system and the Zuid-Holland bar system (typically 500 $m^3 m_a^{-1}$ versus 250 $m^3 m_a^{-1}$). The remaining difference (about a factor 2) should therefore be related to differences in the efficiency or intensity of the degeneration process, the frequency of occurrence of the degeneration process, and the frequency of occurrence and efficiency of conditions that move the outer bar towards its 'degeneration position'. No conclusive transport calculations on this topic could be made because of the complexity of the transport processes. The possible role of selective transport in the bar degeneration process is one example of this complexity.

The proposed sediment transport path during bar degeneration has been derived by reasoning but could not be verified rigorously, because field observations on the process of bar degeneration are lacking and 3D morphological models of the nearshore zone are not available. Therefore, the postulated hypothesis should be considered as a first attempt to formulate a coherent morphodynamic model for the multi-year bar behaviour, which may serve as starting point for further research and as an initial guide line for designing field experiments on this topic. By no means the considerations presented in this chapter are intended to be a final proof of the postulated hypothesis. The merit of the considerations is that they support the concept in which the fate of the outer bar is determined by the balance between bar-degenerating conditions and bar-maintaining conditions. Additionally, the specification of the bar modulating conditions in terms of fraction of breaking waves on the outer bar appears to be a viable approach to define the filter for the energy input into the meso-scale morphodynamic system.

7 GENERAL DISCUSSION AND CONCLUSIONS

7.1 Decadal and sub-decadal morphologic behaviour of large coastal stretches

The case study of the behaviour of the Holland coast over the period from 1963 to 1990 increased the phenomenological knowledge on the morphological behaviour of coastal stretches over time spans of a few decades and spatial scales of tens of kilometres. In addition, some factors that play a role in this large-scale coastal behaviour were identified.

The analysis also increased the phenomenological knowledge on the behaviour of multiple bar systems on a time scale of years and a spatial scale of kilometres. Especially the phenomenological knowledge of the longshore coherence in the dynamics of the bar system increased. In addition, net transport patterns underlying the morphological changes in the bar system were revealed. A conceptual (meso-scale) morphodynamic model for the multi-year bar system behaviour was formulated and tentatively evaluated. More rigorous verification requires substantial additional information from the field.

Decadal coastal behaviour along large coastal stretches

A quantitative analysis of morphological data over large distances and long time spans is a prerequisite for the understanding of decadal behaviour of large coastal stretches. The analysis of a large amount of bathymetric data appears to require its own approach, viz. the combination of the empirical eigenfunction analysis technique with a moving window approach (Chapter 3). The analysis reveals the combined behaviour of the shoreline position and the nearshore profile shape over a period of three decades (Chapter 4).

In general, no clear trends in the development of the shape of the nearshore profile exist over the considered period. Spatially and temporally coherent fluctuations dominate the behaviour. Along certain stretches, trends in the position of the shoreline exist over the considered period. The trend in cross-shore shifting of the shoreline has no relation with the average shape of the nearshore profile. The decadal and sub-decadal shoreline fluctuations, however, are possibly related to the dynamics of the multiple bar systems. The behaviour of the multiple bar systems is remarkably systematic. The bars in the two main bar systems along the Holland coast, of respectively 30 km and 40 km length, develop in a very systematic way (in position and amplitude), such that about every 15 year respectively 4 year, the same bar topography is present. In the area with the 15 year cycle, the mean profile steepness and the shoreline position fluctuate at a similar time scale. In the other area, the relation between bar system behaviour and the shoreline and profile steepness behaviour is not evident.

Regional differences exist in decadal coastal behaviour. The differences in coastal behaviour are generally related to differences in decadal to sub-decadal

fluctuations rather than to differences in trends over the considered period of time. The alongshore changes in decadal morphologic behaviour are generally quite abrupt, often occurring over about a 2 kilometre distance. Alongshore differences in the 'energy input' into the morphodynamic system and alongshore changes in the substrate seem to be of little influence on the location of the transitions in the decadal coastal behaviour. More important are the locations of large man-made structures (harbour moles, protruding seawall) and the alongshore changes in offshore bathymetry (ebb-delta, shoreface terrace) (Chapter 2 and 4). Only one alongshore transition in behaviour could not be explained straightforwardly. This transition coincides with the transition from a groin area to a groinless area. Nevertheless, the cause-effect relation is questionable, because a similar transition along another part of the coast does not affect the behaviour. Further, nearshore sediments tend to be coarser in one area, but the transition in behaviour does not coincide with the transition in grain size.

The large engineering works seem to act as artificial headlands, creating new coastal cells that subsequently develop their own dynamics. The different coastal behaviour occurring north and south of the IJmuiden harbour moles (Chapter 4) is considered an example of this phenomenon. Consequently, large man-made structures can influence the amplitude of the natural variability of the coastal system along stretches of coast of tens of kilometres length. The difference in the variability of the shoreline position north and south of the IJmuiden harbour moles is an example of this difference in amplitude of the natural variability of the coastal system. Apparently, large engineering works can have effects that far exceed the spatial extent of the 'local' effects of these hard structures, such as the shoreline progradation close to the harbour moles.

Other human interventions along the Holland coast can generally be considered as 'noise' for the decadal behaviour of the Holland coast. Beach nourishments are generally not detected in the decadal behaviour, unless they are very large, such as near Hoek van Holland. The effect of groins on the decadal behaviour is not unambiguous from this study. According to Short (1991,1992) groins along the Holland coast serve as an irritant rather than a determinant of the morphodynamics of the beach and inner bar. Since the beach and inner bar act on much smaller time scales than decades, the effects of groins can probably be considered to be noise on the decadal time scale.

The operation of the large-scale morphodynamic system, dealing with the interaction between morphology and hydrodynamics on the scale of the entire Holland coast, could not be determined from observations because the existing data bases turned out to cover too short time spans. The appropriate length of time series for obtaining information on the operation of the large-scale morphodynamic system is expected to be a century or more. Filtering meso-scale 'noise' from the morphologic data set, such as cyclic bar system behaviour, requires at least several repetitions of the fluctuations. Five repetitions of the meso-scale bar system cycle of the Noord-Holland bar system already requires a 75 year data set.

Scales in morphodynamic systems

The lack of coherent developments concerning the morphologic state of the complete Holland coast, indicates that the JARKUS data base offers only a first glance of the behaviour of the entire Holland coast (the 'large-scale' coastal behaviour). Therefore, the time-independent morphologic characteristics (over the three decade period) should be considered describing one state in the large-scale coastal behaviour. The present-day spatial differences in mean characteristics of the shoreline position and the profile shape, indicate that large-scale coastal developments will deal with the orientation of the shoreline and the overall scaling of the nearshore bar systems. From this point of view, the observed decadal and sub-decadal morphologic behaviour is considered an expression of the 'meso-scale' morphodynamic system. The behaviour of the entire Holland coast is anticipated to occur on a 'sub-century' to century time scale.

This study further indicates that the presence of a bar system should be considered an inherent property of the large-scale morphology. This implies that for modelling developments of a barred coast over a period of decades, a barless mean profile may be a less realistic representation of the mean profile. Regarding the influence of bar topography on the distribution of wave-driven longshore currents, the effect of bar topography on longshore transports in the surf zone may not be neglected (Rønberg et al., 1991).

To conclude, the presented concept of scale levels in the coastal system (Chapter 1) is helpful in making the complexity in coastal behaviour more manageable. However, the concept is not always straightforward in its application to real-world coastal systems, because there are no universal definitions of scale levels. Consequently, the scale definitions are still site-specific, but should be analysed for more universal applicability.

Multi-year bar system morphodynamics

The morphologic behaviour of the multiple bar systems along the Holland coast consists of systematic offshore movement of all bars, with the outer bar fading away and with a new bar being generated near the shoreline. This behaviour was noticed earlier, for example by Edelman (1974) and De Vroeg (1987). This study added new knowledge on the alongshore coherence in this behaviour (Chapter 5). The cyclic behaviour may be uniform over large alongshore distances (up to 20 km), but the cyclic development may as well get 'out-of-phase' alongshore. The alongshore change in the phase of the bar behaviour cycle may be sharp or more gradual. The length scale of the transition area between two parts of the bar system in a different phase is typically 2 kilometre. A transition area may migrate alongshore but does not necessarily do so. In the transition area, the outer bar from one side of the transition area tends to attach to the inner bar at the other side of the transition area. The bars outside the transition area seem to develop quite independently from the bars at the other side of the transition area. This indicates

that the inherent length scale for the cyclic bar system behaviour is probably kilometres.

The cyclic bar system behaviour appeared to be essentially a cross-shore redistribution of sediment in the nearshore zone. This implies that the degeneration of the outer bar is associated with net onshore directed transport. On the scale level of individual cross-sections, a longshore sediment redistribution pattern is superimposed, especially in the inner nearshore (Chapter 5). The sediment of the degenerating outer bar does not accumulate in the trough located landward of it, but is immediately enclosed into the inner bar system. Therefore, the net seaward migration of the inner bar feature, going with the degeneration of the outer bar, is partly induced by net onshore directed transport.

In the explanation of the cyclic behaviour, an important role was attributed to the outer bar. The systematic degeneration of the outer bar is considered to be the key element of the cyclic nature of the bar system behaviour. The hypothesised mechanism for the systematic degeneration of the outer bar at a relatively constant distance offshore, i.e. at a relatively constant 'mean' depth, seemed viable (Chapter 6). The essence of the proposed mechanism is that the importance of bar-degenerating conditions (asymmetric waves) compared to bar-maintaining conditions (breaking waves) increases with depth (Chapter 5 and Chapter 6). The mechanism was only evaluated tentatively and needs a more rigorous verification as well as a critical re-evaluation on the basis of additional field observations. In addition, the topic of bar formation near the shoreline and the subsequent net seaward migration needs further attention. For a proper analysis of that topic, morphologic data with a higher resolution (especially in time) than currently available should be obtained.

The morphologic control in the multi-year behaviour of a multiple bar system is strong. As a consequence, the exact annual sequence in storm events seems less important for the overall duration of a cycle than the fact *that* a number of varying storm events occurs each year. In other words, the individual realisations of storm and calm weather sequences are not important as long as they originate from a constant probability function of wave height, wave period, and wave direction (i.e. a constant wave climate). In addition, the strong morphologic control may influence the sensitivity of the bar system to changes in the wave climate. Probably, the forcing wave climate has to change over a time span that is larger than the autonomous time scale of the bar behaviour to become apparent in the behaviour of the bar system. For example, a change in the wave climate with respect to number, strength, and direction of storm events should persist over at least a 4 year period to become apparent in the bar behaviour of the Zuid-Holland bar system. In the Noord-Holland bar system it should persist over at least a 15 year period. If such a relation applies, the Zuid-Holland bar system should be sensitive to shorter fluctuations in the wave climate than the Noord-Holland bar system.

Bar behaviour observed from other multi-year data sets of nearshore bathymetry (Birkemeier, 1984; Lippmann et al., 1993; Ruessink and Kroon, 1994) indicates that the cyclic multi-year bar behaviour observed along the Holland coast is not a unique phenomenon resulting from some unique set of site-specific

conditions. Possibly, cyclic bar system behaviour is a common type of multi-year behaviour of multiple bar systems, which has not been noticed very often so far because of the lack of systematic long-term monitoring of these bar systems.

7.2 Recommendations for further research

The length of time series required for the analysis of large-scale morphodynamic systems from data (probably more than a century), may be discouraging for progress on the subject in the near future. However, continuation of the monitoring programs (JARKUS and 5-yearly extended surveys) is essential. The obtained data offer the only opportunity to verify models that address the coastal behaviour at spatial and temporal scales that are relevant to coastal management. Moreover, and maybe even more important, the systematic monitoring can reveal never anticipated phenomena (cf. the cyclic bar system behaviour on the meso-scale level). The phenomenological knowledge will be very helpful in the formulation of models that address coastal behaviour at time scales of years to decades and spatial scales of kilometres to tens of kilometres.

A sensible topic for further research is the understanding of the morphodynamics that generate the fluctuations in the 'coastal cells' created by large man-made structures. Those fluctuations occur on temporal and spatial scales of many years and many kilometres. Available data bases match these scales. Along the Holland coast, the fluctuations seem to be to related the multi-year behaviour of the multiple bar systems. Recommendations for further research therefore deal with the morphodynamics of the complete bar system.

Recommendations for further research are:

- Verification and re-evaluation of the proposed mechanism of bar degeneration by gathering field data during the conditions of bar degeneration. These observations should reveal whether bar degeneration is caused by highly asymmetric, non-breaking waves, and whether flow circulation occurs in the horizontal or vertical plane during periods that the outer bar degenerates. In addition, the importance of selective transport in the morphodynamics of the bar system should be determined.
- Explanation of the generation of a new bar near the shoreline and the subsequent net offshore migration. This will require more frequent observations of the nearshore morphology than provided by JARKUS. Video-monitoring systems such as introduced by Lippmann and Holman (1989) provide a valuable tool to obtain more information on this topic.
- Identification of the mechanisms that cause the different bar morphologies north and south of IJmuiden. This knowledge is essential for understanding when and why the overall characteristics of a bar system will change. This type of bar system dynamics seems to occur on a large time scale (decades). Therefore, model experiments can be a valuable tool to investigate this morphodynamic topic (cf. Hulscher et al., 1993)

SUMMARY

The general aim of this study is to increase the phenomenological knowledge of decadal behaviour of large coastal stretches and to get a qualitative insight in the governing process-response relations. To increase the phenomenological knowledge of decadal behaviour of large coastal stretches, the morphologic behaviour of the Holland coast (120 km long, sandy, wave-dominated, micro-tidal) is analysed from annual bathymetric surveys over the period 1963-1990. Alongshore changes in morphologic behaviour are correlated with alongshore changes in potentially relevant boundary conditions concerning sediment, morphology and hydrodynamic conditions. The effect of human interference along the Holland coast is also considered. Finally, some of the observed decadal behaviour is explained in terms of possibly involved physical mechanisms.

The existing phenomenological knowledge of decadal morphologic behaviour along the Holland coast is limited. Most of the previous studies deal with shoreline behaviour or sediment budgets. The spatial and temporal coherence in nearshore bathymetric changes has not yet been described satisfactorily. This may be attributed to the presence of complex behaving nearshore bar systems.

The analysis of the nearshore morphologic behaviour is based on the JARKUS data base. This data base consists of cross-shore profile lines starting at the fore dune and extending about 1 km seaward. The profiles generally have a longshore spacing of 250 m. The bathymetric data base is analysed by considering 'morphologic behaviour' as profile behaviour that exhibits alongshore coherence. The cross-shore shift of the nearshore profile is represented by the behaviour of the 1m +NAP contour, also called 'the shoreline' (NAP = Dutch ordnance datum ≈ mean sea level). The change in shape of the profile shape is described by 3 empirical eigenfunctions. These eigenfunctions describe the mean profile shape and the most pronounced deviations from the mean profile. These deviations are generally related to bar topography.

Trends in the behaviour of the shoreline over a period of three decades and trends in the behaviour of the shoreline over a period of more than a century exhibit similarities as well differences. In general, the behaviour of the profile shape exhibits no clear trends over the three decade period. The fluctuations within that period of time are often temporally and spatially coherent on scales of years and kilometres. The most noticeable behaviour is the cyclic behaviour of the multiple bar systems, consisting of net offshore movement of all bars, with the outer bar fading away and with a new bar being generated near the shoreline. No correlation is found between the mean profile shape and trends in shoreline behaviour over the three decade period. On the other hand, a relation seems to exist between the behaviour of the bars and the fluctuations in the shoreline position.

The morphologic analysis revealed that regional differences in decadal morphologic behaviour exist. Five regions can be distinguished. The transitions in behaviour occur over relatively short distances (about 2 km), and correlate with

the locations of man-made structures and alongshore changes in shoreface morphology. The alongshore changes in decadal coastal behaviour do not correlate with the alongshore changes in sediment properties and energy input (waves, wind, tides).

Obviously, the morphodynamics of the multiple bar systems play an important role in the morphologic behaviour of the Holland coast over a 3 decade period. The two main multiple bar systems along the Holland coast both exhibit cyclic behaviour. The duration of the cycle differs between the bar systems: viz. 4 year and about 15 years. The cyclic behaviour is sometimes uniform over distances up to 20 km, but can also get 'out-of-phase' in alongshore direction. The latter causes rather complex bar patterns. The behaviour of the nearshore bars indicates that the mechanism that explains the cyclic behaviour contains a strong morphologic feedback. This indicates that no cyclic external forcing is required to obtain cyclic bar system behaviour.

On the alongshore scale of a coherent offshore moving bar, the cyclic development of the bar system is essentially a cross-shore redistribution of sediment within the nearshore zone. On the scale of individual profile cross-sections, an alongshore redistribution of sediment may be superimposed on the cross-shore redistribution process. The process of bar degeneration is associated with net onshore directed sediment transport. Further, the sediment removed from the outer bar is 'immediately' entrained into the inner bar system and subsequently redistributed in there.

It is hypothesised that the cyclic behaviour is governed by the outer bar. Inner bars do not move farther offshore as long as the outer bar remains unchanged. The degeneration of the outer bar causes inner bars to move farther offshore, probably because they will experience different wave conditions. The systematic degeneration of the outer bar is hypothesised to occur due to a changing balance in the occurrence of very asymmetric waves (that degenerate the bar), and the occurrence of conditions with breaking waves (that maintain the bar topography). The balance changes due to the offshore migration of the bar.

The formulated hypothesis on the degeneration of the outer bar is tentatively evaluated. The frequencies of occurrence of conditions with breaking waves and of conditions with very asymmetric waves on the outer bar are analysed for varying development stages of the outer bar. Sites in both main bar systems are considered. To obtain these parameters from the offshore wave climate data, a probabilistic wave model is developed (Van Rijn and Wijnberg, 1994). The results of the calculations support the proposed mechanism for the degeneration of the outer bar. Additionally, transport calculations indicate that transport gradients are of the right order of magnitude to transport the outer bar sediment onshore during the proposed bar degenerating conditions.

Although the proposed morphodynamic model for the multiple bar system behaviour seems viable, it is still considered a first attempt to formulate a morphodynamic model for bar system behaviour. More rigorous verification requires substantial additional field observations.

MORFOLOGISCH GEDRAG VAN EEN KUST MET BRANDINGSBANKEN GEDURENDE EEN PERIODE VAN ENKELE DECENNIA: SAMENVATTING

Het algemene doel van het onderzoek beschreven in dit proefschrift, is het vergroten van de fenomenologische kennis van het gedrag van grote stukken kust over een tijdspanne van enkele decennia. Daarnaast is het de bedoeling (kwalitatief) inzicht te krijgen in de fysische mechanismen die het waargenomen gedrag veroorzaken. Om dit soort kennis te vergaren is een analyse gemaakt van het morfologische gedrag van de Hollandse kust (120 km lang, zandig, golf-gedomineerd en 'micro-tidal'). Deze analyse is gebaseerd op jaarlijkse metingen van de bodemligging in de kustzone in de periode 1963-1990. Kustlangse veranderingen in het morfologische gedrag zijn vergeleken met kustlangse veranderingen in mogelijke relevante randvoorwaarden betreffende sediment, morfologie en hydrodynamische condities. Ook het mogelijke effect van menselijke ingrepen is meegenomen in deze vergelijking. Voor een deel van het waargenomen gedrag is tenslotte getracht een verklaring te vinden in de vorm van mogelijk betrokken fysische mechanismen.

De bestaande fenomenologische kennis van het morfologische gedrag van de Hollandse kust over een periode van enkele decennia is beperkt. De meeste van de voorgaande studies op dit gebied hebben betrekking op het kustlijngedrag en de zandbalans. De ruimtelijke en temporele samenhang in de verandering van de bodemligging in de kustnabije zone is nog niet bevredigend beschreven. Dit laatste hangt samen met de aanwezigheid van complex bewegende brandingsbanken in deze zone.

De analyse van het morfologische gedrag in de kustnabije zone is gebaseerd op het JARKUS bestand. Het JARKUS bestand bestaat uit kustdwarse meetraaien (profielen) die beginnen op de zeereep en zich ongeveer 1 km in zeewaarste richting uitstrekken. De afstand tussen deze profielen is doorgaans 250 m. Bij de analyse van dit bestand is 'morfologisch gedrag' beschouwd als zijnde profielgedrag dat kustlangse samenhang vertoont. De kustdwarse verplaatsingen van het kustprofiel zijn beschreven door het gedrag van de 1m +NAP lijn (NAP komt ongeveer overeen met gemiddeld zeenivo). Deze lijn zal hierna ook 'de kustlijn' worden genoemd. De veranderingen in de vorm van het kustprofiel zijn beschreven met behulp van 3 empirische eigenfuncties. Deze eigenfuncties beschrijven de gemiddelde profielvorm en de grootste afwijkingen van deze gemiddelde profielvorm. Deze afwijkingen zijn in het algemeen gerelateerd aan brandingsbanken topografie.

Tussen de trends in kustlijngedrag over een periode van drie decennia en de trends in kustlijngedrag over een periode van meer dan een eeuw bestaan zowel overeenkomsten als verschillen. Het gedrag van de profielvorm vertoont in het algemeen geen trends over de beschouwde periode van 3 decennia. De veranderingen in de vorm van het profiel gedurende deze periode hangen vaak ruimtelijk en temporeel samen op schalen van respectievelijk kilometers en jaren.

Het meest opmerkelijke gedrag van de profielvorm hangt samen met het cyclische gedrag van de meervoudige brandingsbank systemen. Dit cyclische gedrag bestaat uit een netto zeewaartse verplaatsing van alle brandingsbanken, waarbij de meest zeewaartse bank geleidelijk verdwijnt en tegelijkertijd nabij de kustlijn een nieuwe bank wordt gevormd. Er is geen correlatie gevonden tussen de gemiddelde vorm van het kustprofiel en de eventuele trendmatige ontwikkelingen in de kustlijnpositie over een periode van 3 decennia. Er lijkt daarentegen wel een relatie te bestaan tussen het gedrag van de brandingsbanken en de fluctuaties in de kustlijnpositie gedurende deze periode.

Uit de morfologische analyse is verder gebleken dat er regionale verschillen bestaan in het morfologische gedrag dat de Hollandse kust gedurende een periode van 3 decennia vertoont. In totaal kunnen vijf regio's worden onderscheiden. De veranderingen in het kustnabije profielgedrag vinden plaats over relatief korte afstanden (ongeveer 2 km), en vallen samen met de locaties van civieltechnische werken (bijvoorbeeld havendammen) en met veranderingen in de morfologie van de diepere onderwateroever. De kustlangse veranderingen in kustgedrag vertonen geen correlatie met de kustlangse veranderingen in sedimenteigenschappen en 'energie toevoer' (golven, wind, getij).

De morfodynamiek van meervoudige brandingsbank systemen speelt duidelijk een belangrijke rol in het morfologische gedrag van de Hollandse kust gedurende een periode van 3 decennia. De twee voornaamste meervoudige brandingsbank systemen langs de Hollandse kust vertonen beiden cyclisch gedrag. De tijdsduur van de cyclus is echter verschillend voor deze twee banksystemen: namelijk 4 jaar en ongeveer 15 jaar. Het cyclische bankengedrag treedt soms uniform op over afstanden van wel 20 km, maar soms raakt deze cyclische bankenontwikkeling 'uit fase' in kustlangse richting. In het laatste geval kunnen complexe bankpatronen ontstaan. Het gedrag van de brandingsbanken wijst op een sterke morfologische terugkoppeling in het mechanisme dat het cyclische gedrag van het bankensysteem verklaart; er lijkt geen cyclische externe forcering nodig te zijn om het bankensysteem cyclisch gedrag te laten vertonen.

Op de schaal van een zich in het geheel zeewaarts verplaatsende bank is de cyclische ontwikkkeling van het bankensysteem in essentie een kustdwarse herverdeling van sediment in de kustnabije zone. Op de schaal van een individueel kustprofiel kan, gesuperponeerd op deze kustdwarse herverdeling, ook nog een kustlangse herverdeling van sediment plaatsvinden. De degeneratie van de buitenste bank (= meest zeewaartse bank) gaat gepaard met kustwaarts gericht sedimenttransport. Daarnaast blijkt dat het sediment dat van de buitenste bank wordt weggevoerd 'meteen' in het landwaarts gelegen deel van het bankensysteem wordt opgenomen en daar vervolgens wordt herverdeeld.

Er is een hypothese opgesteld waarin de buitenste bank het cyclische gedrag van het bankensysteem bestuurt: zolang de buitenste bank niet verandert kunnen de binnenste banken niet netto zeewaarts migreren. Wanneer de buitenste bank begint te degenereren migreren de landwaarts gelegen banken netto zeewaarts, waarschijnlijk omdat zij onder invloed van andere golfcondities komen te staan. In de hypothese wordt de systematische degeneratie van de

buitenste bank toegeschreven aan de veranderende balans in het optreden van condities met zeer asymmetrische golven (die de bank afbreken) en het optreden van condities met brekende golven (die de bank in stand houden). Deze balans verandert ten gevolge van de zeewaartse migratie van de bank.

De opgestelde hypothese over de systematische degeneratie van de buitenste bank is op een verkennende wijze geëvalueerd. Voor verschillende ontwikkelingsstadia van de buitenste bank is geanalyseerd wat de frequentie van optreden is van condities met brekende golven op de buitenste bank en van condities met zeer asymmetrische golven op de buitenste bank. Deze analyse is uitgevoerd voor twee locaties, één in elk van de twee voornaamste banksystemen. Om de frequenties van optreden van verschillende condities op de buitenste bank af te leiden uit het golfklimaat op diep water, is een probabilistisch golfmodel ontwikkeld (Van Rijn en Wijnberg, 1994). De resultaten van de berekeningen ondersteunen het voorgestelde mechanisme voor de degeneratie van de buitenste bank. Sediment transport berekeningen geven verder aan dat transport gradiënten die optreden tijdens bankafbrekende condities van de juiste orde van grootte zijn om sediment van de buitenste bank netto landwaarts te transporteren.

Het voorgestelde morfodynamische model voor de verklaring van het gedrag van meervoudige banksystemen lijkt levensvatbaar. Het moet echter nog steeds beschouwd worden als een eerste poging om een samenhangend morfodynamisch model te formuleren voor het gedrag van deze banken. Een nauwgezettere verificatie van het voorgestelde mechanisme vereist een aanzienlijke hoeveelheid aanvullende veldwaarnemingen.

REFERENCES

Aagaard, T., 1990. Infragravity waves and nearshore bars in protected, storm-dominated coastal environments. Marine Geology 94, pp. 181-203.

Aagaard, T., and B. Greenwood, 1994. Suspended sediment transport and the role of infragravity waves in a barred surf zone. Marine Geology 118, pp. 23-48.

Allen, J.R.L., 1985. Principles of physical sedimentology. George Allen and Unwin, London, 272 pp.

Arens, S.M., 1994. Aeolian processes in the Dutch Foredunes. PhD-thesis, Faculteit der Ruimtelijke Wetenschappen, University of Amsterdam, The Netherlands, 150 pp.

Aubrey, D.G., 1979. Seasonal patterns of onshore/offshore sediment movement. Journal of Geophysical Research 84 (C10), pp. 6347-6354.

Aubrey, D.G., D.L. Inman, and C.D. Winant, 1980. The statistical prediction of beach changes in southern California. Journal of Geophysical Research 85 (C6), pp. 3264-3276.

Aubrey, D.G., and R.M. Ross, 1985. The quantitative description of beach cycles. Marine Geology 69, pp. 155-170.

Augustijn, B., H. Daan, B. van Mourik, D. Messeschmidt, and B. Zwart, 1990. Stormenkalender, Chronologisch overzicht van alle stormen (windkracht 8 en hoger) langs de Nederlandse kust voor het tijdvak 1964-1990. KNMI-publikatie nr. 176, Koninklijk Nederlands Meteorologisch Instituut, De Bilt, The Netherlands, 138 pp.

Bakker, W.T., 1968. The dynamics of a coast with a groyne system. Proceedings of the 11th Conference on Coastal Engineering, pp. 492-517.

Bakker, W.T., and H.J. de Vroeg, 1988. Is de kust veilig? Analyse van het gedrag van de Hollandse kust in de laatste 20 jaar. Nota GWAO 88.017, Rijkswaterstaat, Den Haag, The Netherlands, 42 pp.

Barry, R.G., and R.J. Chorley, 1982. Atmosphere, weather and climate. Fourth edition. Methuen, London, 407 pp.

Battjes, J.A., and J.P.F.M Janssen, 1978. Energy loss and set-up due to breaking of random waves. Proceedings of the 16th International Conference on Coastal Engineering, ASCE, pp. 569-587.

Beets, D.J., 1994. Geologisch onderzoek naar de erodeerbaarheid van de vooroever. Rapport Kustgenese CL-935248, Rijks Geologische Dienst, Haarlem, 13 pp.+ figures.

Beets, D.J., L. van der Valk, and M.J.F. Stive, 1992. Holocene evolution of the coast of Holland. Marine Geology 103, pp. 423-443.

Beets, D.J., A.J.F. van der Spek, and L. van der Valk, 1994. Holocene ontwikkeling van de Nederlandse kust. RGD rapport 40.016-Projekt Kustgenese, Rijks Geologische Dienst, Haarlem, 53 pp. + figures, tables and appendices.

Birkemeier, W.A., 1984. Time scales of nearshore profile changes. Proceedings of the 19th Coastal Engineering Conference, ASCE , pp. 1507-1521.

Boczar-Karakiewicz, B., and R.G.D. Davidson-Arnott, 1987. Nearshore bar formation by non-linear wave processes - a comparison of model results and field data. Marine Geology 77, pp. 287-304.

Boczar-Karakiewicz, B., D.L. Forbes, and G. Drapeau, 1995. Nearshore bar development in southern Gulf of St. Lawrence.Journal of Waterway, Port, Coastal, and Ocean Engineering 121, pp. 49-60.

Bodge, K.R., 1992. Representing equilibrium beach profiles with an exponential expression. Journal of Coastal Research 8, pp. 47-55.

Bouwmeester, E.C., R.B. Kalf, and L. Walburg, In prep. Statistische analyse en voorspelling van de Nederlandse kustontwikkeling. RIKZ/OSF-concept mei 1994, Rijkswaterstaat, Den Haag, 49 pp.+ figures.

Bruun, P., 1988. The Bruun Rule of erosion by sea-level rise, pp. a discussion on large-scale two- and three-dimensional usages. Journal of Coastal Research 4, pp. 627-648.

Carter R.W.G., 1988. Coastal environments. An introduction to the physical, ecological and cultural systems of coastlines. Academic Press, London, 617 pp.

Carter, T.G., P.L.F., Liu, and C.C. Mei, 1973. Mass transports by waves and offshore sand bedforms. Journal of the Waterways, Harbours and Coastal Engineering Division, WW2, pp. 165-183.

Chesher, T.J., 1993. Tidal schematisation in morphodynamic area models. In: J.H. List (Ed.), Large Scale Coastal Behaviour '93, U.S. Geological Survey Open-File Report 93-381, pp. 29-32.

Christiansen, C., and D. Bowman,1990. Long-term beach and shoreface changes, NW Jutland, Denmark: effects of change in wind direction. In: J.J. Beukema, W.J.Wolff, and J.J.W.M. Brouns (Eds.), Expected effects of climatic change on marine coastal ecosystems. Kluwer, Dordrecht, pp. 113-122.

Cowell, P.J., P.S. Roy, and R.A. Jones, 1993. Simulation modelling of LSCB: parametric scaling, markovian evolution and site idiosyncrasies. In: J.H. List (Ed.), Large Scale Coastal Behaviour '93, U.S. Geological Survey Open-File Report 93-381, pp. 41-44.

Cowell, P.J., and B.G. Thom, 1994. Morphodynamics of coastal evolution. In: R.W.G. Carter and C.D. Woodroffe (Eds.), Coastal evolution: Late Quaternary shoreline morphodynamics. Cambridge University Press, Cambridge, pp. 33-86.

Dally, W.R., 1987. Longshore bar formation - surf beat or undertow? Proceedings of Coastal Sediments '87, ASCE, New York, pp. 71-86.

Dally, W.R., 1992. Random breaking waves: field verification of a wave-by-wave algorithm for engineering application. Coastal Engineering 16, pp. 369-397.

Dally, W.R., R.G. Dean, and R.A. Dalrymple, 1985. Wave height variation across beaches of arbitrary profile. Journal of Geophysical Research, 90 (C6), pp. 11917-11927.

Damgaard Christensen, E., R. Deigaard, and J. Fredsøe. Sea bed stability on a long straight coast. Proceedings of the 24th International Conference on Coastal Engineering, ASCE, pp. 1865-1879.

Davis, J.C., 1986. Statistics and data analysis in geology. Second edition. John Wiley & Sons, New York, 646 pp.

Dean, R.G., 1977. Equilibrium beach profiles: U.S. Atlantic and Gulf Coasts. Ocean Engineering Technical Report No.12, University of Delaware, Newark, USA, 45 pp.

Dean, R.G., 1991. Equilibrium beach profiles: characteristics and applications. Journal of Coastal Research 7, pp. 53-84.

De Gans, W., 1991. Kwartairgeologie van West-Nederland. Grondboor en Hamer, Vol. november 1991, pp. 103-124.

De Mulder, E.F.J., 1983. Geologische geschiedenis van de Hondsbossche Zeewering. Derde uitgave Kring van 'Vrienden van de Hondsbossche', Alkmaar, 15 pp.

De Ruig, J.H.M.,1989. De sedimentbalans van de gesloten Hollandse kust over de periode 1963 tot 1986. Nota GWAO-89.016/ZL-NXL89.42, Rijkswaterstaat, Den Haag, 43 pp. + figures.

De Ruig, J.H.M., and C.J. Louisse, 1991. Sand budget trends and changes along the Holland coast. Journal of Coastal Research 7, pp. 1013-1026.

De Swart, H.E., 1995. Limitations to predictability in morphodynamic modelling. Proceedings of ECOPS, the oceans and the poles. ZNT Bremen, pp. 63-71.

De Valk, C.F., and T.J. Zitman, 1987. Hoofcomponenten-analyse voor kustontwikkeling. Report H 317, Waterloopkundig Laboratorium, 16 pp. + figures.
De Vriend, H.J., 1991. Mathematical modelling and large-scale coastal behaviour, Part 1: Physical processes. Journal of Hydraulic Research 29, pp. 727-740.
De Vriend, H.J., M. Capobianco, T. Chesner, H.E. de Swart, B. Latteux, and M.J.F. Stive, 1993. Approaches to long-term modelling of coastal morphology: a review. Coastal Engineering 21, pp. 225-269.
De Vriend, H.J. and J.A. Roelvink, 1989. Innovatie van kustverdediging, inspelen op het kustsysteem. Kustverdediging na 1990, Technisch Rapport 19, Rijkswaterstaat, Den Haag, 37 pp. + Appendices.
De Vroeg, J.H.,1987. Schematisering brandingsruggen met behulp van jaarlijkse kustmetingen. Dept. of Civil Engineering, Techical University Delft, 37 pp. + figures + appendices.
Dijkman, M.J., W.T. Bakker, and J.H. De Vroeg, 1990. Prediction of coastline evolution for the Holland coast. Proceedings of the 22nd International Conference on Coastal Engineering, ASCE, pp. 1935-1947.
Dolan, R., B.P. Hayden, and W. Felder, 1977. Systematic variations in inshore bathymetry. Journal of Geology 85, pp. 129-141.
Edelman, T., 1961. Erosie en aanwas van het kustvak Den Helder-Hoek van Holland. Nota WWK 61-1, Rijkswaterstaat, Den Haag,The Netherlands, 7 pp.+ figures.
Edelman, T., 1974. Bijdrage tot de historische geografie van de Nederlandse kuststrook. Rijkswaterstaat/directie waterhuishouding en waterbeweging. Den Haag, The Netherlands, 84 pp.
Eversdijk, P.J., 1989. Harde kustverdediging. Kustverdediging na 1990, Technisch Rapport 16, Rijkswaterstaat, Den Haag, 129 pp.
Fanos, A.M., O.E. Frihy, A.A. Khafagy, and P.D. Komar, 1991. Processes of shoreline change along the Nile Delta coast of Egypt. Proceedings of Coastal Sediments '91, ASCE, pp. 1547-1557.
Fenster, M.S., and R. Dolan, 1993. Historical shoreline trends along the Outer Banks, North Carolina: processes and responses. Journal of Coastal Research 9, pp. 172-188.
Fisher, N., R. Dolan, and B. Hayden, 1984. Variations in large-scale beach amplitude along the coast. Journal of Sedimentary Petrology 54, pp. 73-85.
Getijtafels, 1991. Getijtafels voor Nederland 1992. SDU Uitgeverij, Den Haag, 155 pp.
Glim, G.W., and G.C. Visser, 1981. Nauwkeurigheid van kustlodingen. Rapport WWKZ-81.H002, Rijkswaterstaat, 21 pp.
Goldsmith, V., D. Bowman, and K. Kiley, 1982. Sequential stage development of crescentic bars: Hahoterim beach, southeastern Mediterranean. Journal of Sedimentary Petrology 52, pp. 0233-0249.
Grassmeijer, B.T., and E.M. Sies, 1994. Sand concentrations and transport in breaking wave conditions. MSc Thesis, Dept. of Coastal Engineering., Delft University of Technology, Delft, The Netherlands.
Greenwood, B., and R.G.D. Davidson-Arnott, 1979. Sedimentation and equilibrium in wave-formed bars: a review and case study. Canadian Journal of Earth Sciences 16, pp. 312-332.
Greenwood, B., and P.D. Osborne, 1991. Equilibrium slopes and cross-shore velocity asymmetries in a storm dominated, barred nearshore system. Marine Geology 96, pp. 211-235.
Groenendijk., F.C., in prep.. Voorspelling Nederlandse kust. Overzichtsrapport. Werkdocument RIKZ/94-0__, Rijkswaterstaat, Den Haag, 22 pp.
Helsloot, I.C.M., 1989. Profielbeschrijving voor de Hollandse kust gebruikmakend van spectraal analyse. Dept. of Physical Geography, Utrecht University, The Netherlands, 121 pp.

Hino, M., 1974. Theory on formation of rip-current and cuspidal coast. Coastal Engineering in Japan 17, pp. 23-37.

Holman, R.A., and A.J. Bowen, 1982. Bar, bumps and holes: models for the generation of complex beach topography. Journal of Geophysical Research 87 (C1), pp. 457-468.

Hoozemans, F.M.J., 1989. Het windklimaat ter hoogte van de Nederlands kust over de periode 1907-1980. Analyse van lichtschipwaarnemingen. Nota GWAO-89.010, Rijkswaterstaat/ Dienst Getijdewateren, Den Haag, 82 pp.

Hoozemans, F.M.J., 1990. Long term changes in wind and wave climate on the North Sea. Proceedings of the 22nd International Conference on Coastal Engineering, ASCE, pp. 1888-1894.

Houwing, E.J., 1991. Analyse van de TAW-profielen, Egmond aan Zee en Katwijk aan Zee. GEOPRO-report 1991.019, Dept. of Physical Geography, Utrecht University, The Netherlands, 20 pp. + tables and figures.

Houwman, K., and P. Hoekstra, 1994. Shoreface hydrodynamics. Report Part 1: field measurements Egmond aan Zee. IMAU-report 94-2, Dept. of Physical Geography, Utrecht University, The Netherlands, 29 pp. + figures.

Hulscher, S.J.M.H., H.E. de Swart, and H.J. de Vriend, 1993. The generation of offshore tidal sand banks and sand waves. Continental Shelf Research 13, pp. 1183-1204.

Huntley, D.A., M. Davidson, P. Russell, Y. Foote, and J. Hardisty, 1993. Long waves and sediment movement on beaches: recent observations and implications for modelling. Journal of Coastal Research 15 Special Issue, pp. 215-229.

Inman, D.L., M. Hany, S. Elwany, A.A. Khafagy, and A. Golik, 1992. Nile Delta profiles and migrating sand blankets. Proceedings of the 23rd International Conference on Coastal Engineering, ASCE, pp. 3273-3284.

Kalf, R., L. Walburg, and T. Nijland, 1993. Validatie Jarkus-gegevens in het kader van het project Kustgenese. Report GWAO-93.133x, Rijkswaterstaat Dienst Getijdewateren, Den Haag, 6 pp. + Appendices.

Khafagy, A.A., M.G. Naffaa, A.M. Fanos, and R.G. Dean, 1992. Nearshore coastal changes along the Nile Delta shores. Proceedings of the 23rd International Conference on Coastal Engineering, ASCE, pp. 3260-3272.

Knoester, D., 1990. De morfologie van de Hollandse kustzone (analyse van het JARKUS-bestand 1964-1986). Nota GWAO-90.010, Rijkswaterstaat/Dienst Getijdewateren, Den Haag, 85 pp.

Kohsiek, L.H.M., 1988. Kustafslag en -aangroei in Nederland. Verleden tot heden (1860-1985) en toekomst (2000). Nota GWAO-88.007, Rijkswaterstaat/Dienst Getijdewateren, Den Haag, 29 pp.

Komar, P.D., 1976. Beach processes and sedimentation. Prentice-Hall, Englewood Cliffs, New Yersey, 429 pp.

Kroon, A., and L.C. Van Rijn, 1993. Suspended sediment fluxes in the nearshore zone at Egmond aan Zee, The Netherlands. Dept. of Physical Geography, Utrecht University, Utrecht, The Netherlands.

Kroon, A., 1994. Sediment transport and morphodynamics of the beach and nearshore zone near Egmond, The Netherlands. PhD thesis, Utrecht University, The Netherlands, 275 pp.

Larson, M., and N.C. Kraus, 1992. Analysis of cross-shore movement of natural longshore bars and material placed to create longshore bars. Technical Report DRP-92-5. CERC, 89 pp. + Appendices.

Larson, M., and N.C. Kraus, 1993. Prediction of cross-shore sediment transport at different spatial and temporal scales. In: J.H. List (Ed.), Large Scale Coastal Behaviour '93, U.S. Geological Survey Open-File Report 93-381, pp. 96-99.

Larson, M., and N.C. Kraus, 1994. Temporal and spatial scales of beach profile change, Duck, North Carolina. Marine Geology 117, pp. 75-94.

Latteux, B., 1993. Techniques for long-term morpohological simulation under tidal current action. In: J.H. List (Ed.), Large Scale Coastal Behaviour '93, U.S. Geological Survey Open-File Report 93-381, pp. 100-103.

Liang, G., and R.J. Seymour, 1991. Complex principal component analysis of wave-like sand motions. Proceedings of Coastal Sediments '91, ASCE, pp. 2175-2186.

Lins, H.F., 1985. Storm-generated variations in nearshore beach topography. Marine Geology 62, pp. 13-29.

Lippmann, T.C., and R.A. Holman, 1989. Quantification of sand bar morphology: a video technique based on wave dissipation. Journal of Geophysical Research 94 (C1), pp. 995-1011.

Lippmann, T.C., R.A. Holman, and K.K. Hathaway, 1993. Episodic, nonstationary behaviour of a double bar system at Duck, North Carolina, U.S.A., 1986-1991. Journal of Coastal Research 15 Special Issue, pp. 49-75.

List, J.H., 1993. (Ed.), Large Scale Coastal Behaviour '93, U.S. Geological Survey Open-File Report 93-381, 238 pp.

Louisse, C.J., M.J.F. Stive, and J. Wiersma (Eds.), 1990. The Dutch coast; report of a session on the 22nd International Conference on Coastal Engineering 1990. Preprints of the papers to be published by the American Society of Civil Engineers. Rijkswaterstaat, 165 pp.

Mase, H. , and Y. Iwagaki, 1982. Wave height distributions and wave grouping in the surf zone. Proceedings of the 18th International Conference on Coastal Engineering, ASCE, pp. 58-76.

Medina, R., M.A. Losada, I.J. Losada, and C. Vidal, 1994. Temporal and spatial relationship between sediment grain size and beach profile. Marine Geology 118, pp. 195-206.

North, G.R., T.L. Bell, R.F. Calahan, and F.J Moeng, 1982. Sampling errors in the estimation of empirical orthogonal functions. Monthly Weather Review 110, pp. 699-706.

Oosterwijk, H.J.M., and M.H.J. Ettema, 1987. Aansluiting hoogte- en dieptemetingen JARKUS m.b.t. de waterpassing. Report GWIO-87,022, Rijkswaterstaat, DGW, 10 pp.

Ostrowski, R., Z. Pruszak, and R.B. Zeidler, 1990. Multi-scale nearshore and beach changes. Proceedings of the 22nd International Conference on Coastal Engineering, ASCE, pp. 2101-2116.

Pool, M.A, 1992. Modelmatige, grootschalige profielanalyse van centraal Hollandse kustsecties. Internal report Kustgenese (Werkgroep 1). Utrecht University, Faculty of Earth Sciences: 32 pp. + Appendices.

Postma, R., and A. Kroon, 1986. Mathematische profielanalyse van de onderzeese oever en de aansluitende zeebodem voor de Nederlandse kust. Kustgenese, Universiteit Utrecht-RWS/DGW, notitie GWAO-86.375, 37 pp. + figures.

Putnam, J.A., and J.W. Johnson, 1949. The dissipation of wave energy by bottom friction. EOS, Trans. AGU 30, pp. 67-74.

Resio, D.T, R. Dolan, B.P. Hayden, and L. Vincent, 1977. Systematic variations in offshore bathymetry. Journal of Geology 85, pp. 105-113.

Rijkswaterstaat, 1994. Wave climate data period 1979/1982-1991, unpublished.

Ribberink, J.S., and A.A. Al-Salem, 1992. Time-dependent sediment transport phenomena in oscillatory boundary-layer flow under sheet flow conditions. Report H 840.20, Part VI, Delft Hydraulics, The Netherlands, 25 pp. + Figures, Tables, and Appendix.

Roelvink, J.A., 1993. Dissipation in random wave groups incident on a beach. Coastal Engineering 19, pp. 127-150.

Roelvink, J.A., and I. Brøker, 1993. Cross-shore profile models. Coastal Engineering 21, pp. 163-191.

Roelvink, J.A, and M.J.F. Stive, 1989. Voorspelling ontwikkeling kustlijn 1990-2090, fase 3. Deelrapport 3.4: Initieel sedimenttransport model voor de Hollandse kust. Waterloopkundig Laboratorium, Report H825.

Roelvink, J.A., and M.J.F. Stive, 1990. Sand transport on the shoreface of the Holland coast. Proceedings of the 22nd International Conference on Coastal Engineering, ASCE, pp. 1909-1921.

Rønberg, J.K, I.B. Hedegaard, and R. Deigaard, 1991. Sensitivity of longshore and cross-shore transport, Part I: The influence of profile evolution on littoral drift. MAST G6 Coastal Morphodynamics Mid-term Workshop, 4 pp.

Roskam, A.P., 1988. Golfklimaten voor de Nederlandse kust. Rijkswaterstaat, Nota GWAO-88.046, 21 pp. + figures.

Roskam, A.P., 1992. Eerste resultaten van golfrichtingsmetingen in de Noordzee met de Wavec-boei; periode 1985-1989. Werkdocument GWAO-92.126x/ Notitie GWAO-91.10083, Rijkswaterstaat, Den Haag, 62 pp. + appendices.

Roskam, B., 1994. Werkdocument RIKZ/OS-94.152x (concept). De opbouw van datafiles voor golfklimatologie in HYDRA. Overzichts rapportage. Rijkswaterstaat/RIKZ, 48 pp. + Appendices.

Ruessink, B.G., and A. Kroon, 1994. The behaviour of a multiple bar system in the nearshore zone of Terschelling, The Netherlands: 1965-1993. Marine Geology 121, pp. 187-197.

Sallenger, A.H., R.A. Holman, and W.A. Birkemeier, 1985, Storm-induced response of a nearshore-bar system. Marine Geology 64, pp. 237-257.

Sallenger, A.H., and P.A. Howd, 1989. Nearshore bars and the break-point hypothesis. Coastal Engineering 12, pp. 301-313.

Scientific Committee on Ocean Research Working Group 89, 1991. The response of Beaches to sea-level changes: a review of predictive models. Journal of Coastal Research 7, pp. 895-921.

Sha, L.P., 1990. Sedimentological studies of the ebb-tidal deltas along the West Frisian Islands, the Netherlands. PhD-thesis, Dept. of Earth Sciences, Utrecht University, 160 pp.

Shore Protection Manual, 1984. Volume 1. Department of the Army, Waterways Experiment Station, Corps of Engineers, Coastal Engineering Research Center. U.S. Gouvernment Printing Office, Washington.

Short, A.D., 1991. Beach morphodynamic systems of the central Netherlands coast, Den Helder to Hoek van Holland. GEOPRO-report 1991.01, Dept. of Physical Geography, Utrecht University, The Netherlands, 106 pp.

Short, A.D., 1992. Beach systems of the central Netherlands coast: processes, morphology and structural impacts in a storm driven multi-bar system. Marine Geology 107, pp. 103-137.

Short, A.D., and T. Aagaard, 1993. Single and multi-bar beach change models. Journal of Coastal Research 15 Special Issue, pp. 141-157.

Southgate, H.N., 1993. Review of wave breaking in shallow water. Society of Underwater Technology Conference on Wave Kinematics and Environmental Forces, London. HR Walingford published paper no. 71, 14 pp.

Staatscommissie Kraus, 1911. Staatscommissie in zake den toegang tot Nederland door het Noordzeekanaal. Verslag aan Hare majesteit de Koningin. Tweede deel. Gebroeders J.&H. van Langenhuysen, 's-Gravenhage, 23 pp. + bijlagen.

StatSoft, 1991. CSS-Statistica, version 3C.

Stive, M.J.F., 1989. Voorspelling ontwikkeling kustlijn 1990-2090. Kustverdediging na 1990, Technisch Rapport 5, Rijkswaterstaat, Den Haag, 66 pp. + Appendices.

Stive, M.J.F., and W.D. Eysink, 1989. Voorspelling ontwikkeling kustlijn 1990-2090, fase 3. Deelrapport 3.1: Dynamisch model van het Nederlandse kustsysteem. Waterloopkundig Laboratorium, Report H 825, 66 pp. + tables and figures.

Stolk, A., 1989. Zandsysteem kust - een morfologische karakterisering. Kustverdediging na 1990, Technisch Rapport 1, Dept. of Physical Geography, Utrecht University, Report GEOPRO 1989-02, 97 pp.

Sunamura, T., and I. Takeda, 1993. Bar movement and shoreline change: predictive relations. Journal of Coastal Research 15 Special Issue, pp. 125-140.

Symonds, G. and A.J. Bowen, 1984. Interactions of nearshore bars with incoming wave groups. Journal of Geophysical Research 89 (C2), pp. 1953-1959.

Terwindt, J.H.J., 1969. Bewerking van de oeverlodingen en strandwaterpassingen van drie gebieden langs de kust van Delfland. Report K426, Rijkswaterstaat/ Deltadienst, 11pp.

Terwindt, J.H.J., and J.A. Battjes, 1990. Research on large-scale coastal behaviour. Proceedings of the 22nd International Conference on Coastal Engineering, ASCE, pp. 1975-1983.

Terwindt, J.H.J., and A. Kroon, 1993. Theorethical concepts of a parameterization of coastal behaviour. In: J.H. List (Ed.), Large Scale Coastal Behaviour '93, U.S. Geological Survey Open-File Report 93-381, pp. 193-196.

Terwindt, J.H.J., and K.M. Wijnberg, 1991. Thoughts on large-scale coastal behaviour. Proceedings of Coastal Sediments '91, ASCE, pp. 1476-1487.

Van Alphen, J., 1987. De morfologie en lithologie van de brandingszone tussen Terheijde en Egmond aan Zee. Rijkswaterstaat, Report NZ-N-87.28, 22 pp.

Van Alphen, J.S.L.J., and M.A. Damoiseaux, 1988. Geomorfologische kaart van de Nederlandse kustwateren, schaal 1:250,000. K.N.A.G. Geografisch Tijdschrift 22, pp. 161-167.

Van Alphen, J.S.L.J., W.P.M. de Ruijter and J.C. Borst, 1988. Outflow and three-dimensional spreading of Rhine River water in the Netherlands coastal zone. In: J. Dronkers and W. van Leussen (Eds.), Physical processes in estuaries. Springer-Verlag, Berlin, pp. 70-92.

Van Bemmelen, C.E., 1988. De korrelgrootte-samenstelling van het strandzand langs de Nederlandse Noordzee-kust. Universiteit Utrecht, Vakgroep Fysische Geografie, GEOPRO-rapport 1988-01., 38 pp. + bijlagen.

Van de Meene, J.W.H, 1994. The shoreface-connected ridges along the Central Dutch coast. PhD-thesis, Utrecht University, 222 pp.

Van den Berg, J.H., 1987. Toelichting bij de isallobatenkaart Voordelta. Nota ZL-87.0020, Rijkswaterstaat/Direktie Zeeland, 49 pp. + appendiecs.

Van der Valk, L., 1992. Mid- and late-Holocene coastal evolution in the beach-barrier area of the western Netherlands. Thesis Vrije Universiteit Amsterdam, Febodruk, Enschede, 235 pp.

Van Ommering, G., 1988. De Rijnmond bij Katwijk. Duin 1, pp. 3-6.

Van Rijn, L.C., 1993. Principles of sediment transport in rivers, estuaries and coastal seas. Aqua Publications, Amsterdam, The Netherlands.

Van Rijn, L.C., 1994. Principles of fluid flow and surface waves in rivers, estuaries, seas and oceans. Second edition, Aqua Publications, Amsterdam, The Netherlands

Van Rijn, L.C., 1995. Sand budget and coastline change of the Central Dutch Coast between Den Helder and Hoek van Holland. Report H2129, Delft Hydraulics, The Netherlands.

Van Rijn, L.C., and K.M. Wijnberg, 1994. One-dimensional modelling of individual waves and wave-induced longshore currents in the surf zone; the WAVIS model. IMAU-report R 94-09. Institute for Marine and Atmospheric research Utrecht, Utrecht University, The Netherlands, 55 pp. + 1 Appendix.

Van Vessem, P., and A. Stolk,1990. Sand budget of the Dutch coast. Proceedings of the 22nd International Conference on Coastal Engineering, ASCE, pp. 1895-1908.

Van Straaten, L.M.J.U., 1961. Directional effects of winds, waves and currents along the Dutch North Sea coast, Part 2. Geologie en Mijnbouw 40, pp. 363-391.
Verhagen, H.J., 1989a. Grote civiele werken. Kustverdediging na 1990, Technisch Rapport 13, Rijkswaterstaat, Den Haag, 33 pp.
Verhagen, H.J., 1989b. Sand waves along the Dutch coast. Coastal Engineering 13, pp. 129-147.
Verhagen, H.J., and Van Rossum, H., 1989. Strandhoofden en paalrijen. Kustverdediging na 1990, Technisch Rapport 12, Rijkswaterstaat, Den Haag, 40 pp.
Veugen, L.L.M., 1984. De nauwkeurigheid van strandprofielen, fotogrammetrische acquisitie. Rapport MDLK-R-8403, Rijkswaterstaat/Meetkundige Dienst, 20 pp.
Vincent, L., R. Dolan, B. Hayden, and D. Resio, 1976. Systematic variations in barrier-island topography. Journal of Geology 84, pp. 583-594.
Visser, M., W.P.M. de Ruijter, and L. Postma, 1991. The distribution of suspended matter in the Dutch Coastal zone. Netherlands Journal of Coastal Research 27, pp. 127-143.
Visser, M., 1993. On the transport of fine marine sediment in the Netherlands coastal zone. PhD thesis, Utrecht University, The Netherlands, 169 pp.
Watson, G. and D.H. Peregrine, 1992. Low frequency waves in the surfzone. Proceedings of the 23rd International Conference on Coastal Engineering, ASCE, pp. 818-831.
Warrick, R.A., and H. Oerlemans, 1990. Sea level rise. In: J.T. Houghton, G.J. Jenkins, and J.J. Ephraums (Eds.), Climate Change, the IPCC scientific assessment. Cambridge University Press, Cambridge, pp. 257-281.
Weishar, L.L., and W.L. Wood, 1983. An evaluation of offshore and beach changes on a tideless coast. Journal of Sedimentary Petrology 53, pp. 0847-0858.
Wentholt, L.R., 1912. Stranden en strandverdediging. Thesis, Technical University Delft, Technische boekhandel en drukkerij J. Waltman Jr., Delft, 237 pp.
Westerhof, W.E., E.F.J. de Mulder, and W. de Gans, 1987. Toelichtingen bij de Geologische kaart van Nederland, 1:50.000. Blad Alkmaar West (19W). Rijks Geologische Dienst, Haarlem, 227 pp.
Winant, C.D., D.L.Inman, and C.E. Nordstrom, 1975. Description of seasonal beach changes using empirical eigenfunctions. Journal of Geophysical Research 80, pp. 1979-1986.
Wiersma, J., 1991. De ontwikkeling van de Hollandse kust; een kwestie van schaal. Grondboor en Hamer, Vol. november 1991, pp. 129-134.
Wijnberg, K.M., and F.C.J. Wolf, 1994. Three-dimensional behaviour of a multiple bar system. Proceedings of Coastal Dynamics '94, ASCE, pp. 59-73.
Wijnberg, K.M., and J.H.J. Terwindt, 1995. Extracting decadal morphological behaviour from high-resolution, long-term bathymetric surveys along the Holland coast using eigenfunction analysis. Marine Geology 126.
Wolf, F.C.J., 1993. Data summary field measurements Egmond aan Zee. September-November 1992. Dept. of Physical Geography, Utrecht University. The Netherlands.
Zagwijn, W.H., 1986. Nederland in het Holoceen. Staatsuitgeverij, 's-Gravenhage, 46 pp.
Zarillo, G.A., and J.T. Liu, 1988. Resolving bathymetric components of the upper shoreface on a wave-dominated coast. Marine Geology 82, pp. 69-186.
Zitman, T.J., M.J.F . Stive, and J. Wiersma, 1990. Reconstruction of the Holocene Evolution of the Dutch coast. Proceedings of the 22nd International Conference on Coastal Engineering, ASCE, pp. 1876-1887.

APPENDICES

Appendix 1 Model estimates of wave refraction effects near wave station MPN

To verify whether the observed reduction in wave height near station MPN of the onshore propagating waves can be explained by refraction, some model calculations were conducted (Table A.1). The seaward boundary for the calculations was chosen at 21 m water depth, equalling the water depth near station YM6. The wave model used for estimating the change in wave height, is described in Section 6.3. The bottom topography between the input boundary and station MPN was schematised as a smoothly sloping bottom profile (see Section 6.4.1). The water levels mentioned in the third column refer to the mean water level changes that have been observed to correlate with varying wave conditions (Section 6.4.1).

The model runs in which $\alpha=0°$ give an indication of the decrease in wave height due to bottom friction. This decrease in wave height may be less realistic for some conditions because input of energy by the wind is not included in the model. The two locations are about 11 km apart, so the effect of strong winds will not be negligible over such a distance. Therefore, the effect of refraction on wave height is estimated indirectly, viz. by considering the difference at station MPN in $H_{1/3}$ for the two angles of wave approach ('$\Delta H_{1/3}$ due to refraction'). The calculated effect of refraction on wave height compares well to the observed reduction in wave height near station MPN compared to station YM6.

Table A.1: Estimated effect of refraction on wave height near MPN

Sea bed at 21 m -NAP (comparable to YM6)				*Sea bed at 18 m -NAP (MPN)*	
$H_{1/3}$ (m)	α* (deg)	Water level (m to NAP)	$T_{1/3}$ (s)	$H_{1/3}$ (m)	$\Delta H_{1/3}$ due to refraction (m)
0.75	0	0.0	5.4	0.74	
0.75	45	-0.1	5.4	0.74	0.00
1.25	0	0.1	6.4	1.21	
1.25	60 (SSW)	-0.1	6.4	1.16	0.05
2.25	0	0.4	7.8	2.13	
2.25	60 (SSW)	0.1	7.8	1.94	0.18
3.25	0	0.7	8.8	2.97	
3.25	60 (SSW)	0.3	8.8	2.61	0.36
4.25	0	1.0	9.7	3.76	
4.25	30	0.8	9.7	3.66	0.10
5.25	0	1.3	10.4	4.50	
5.25	30	1.2	10.4	4.37	0.13

*) α = angle of wave approach relative to the shore normal

Appendix 2 Stratigraphy along the Holland coast

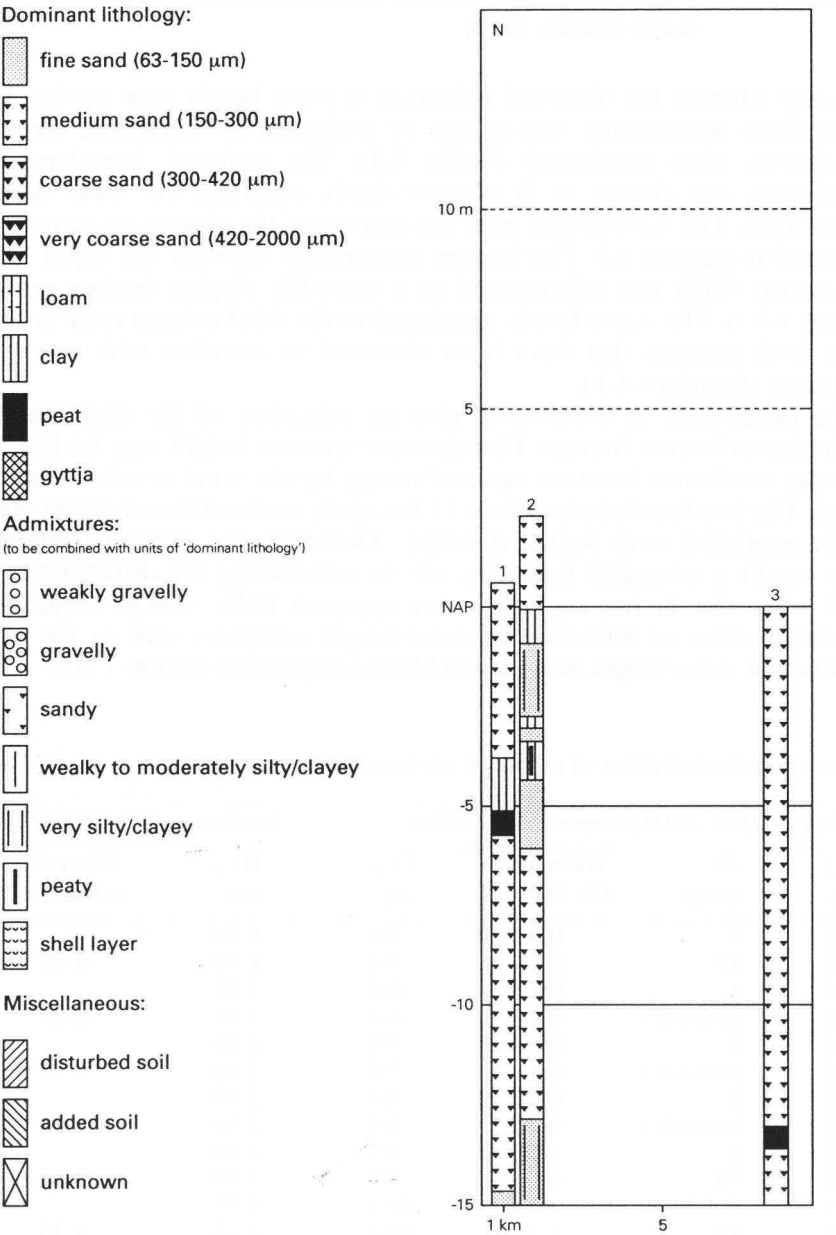

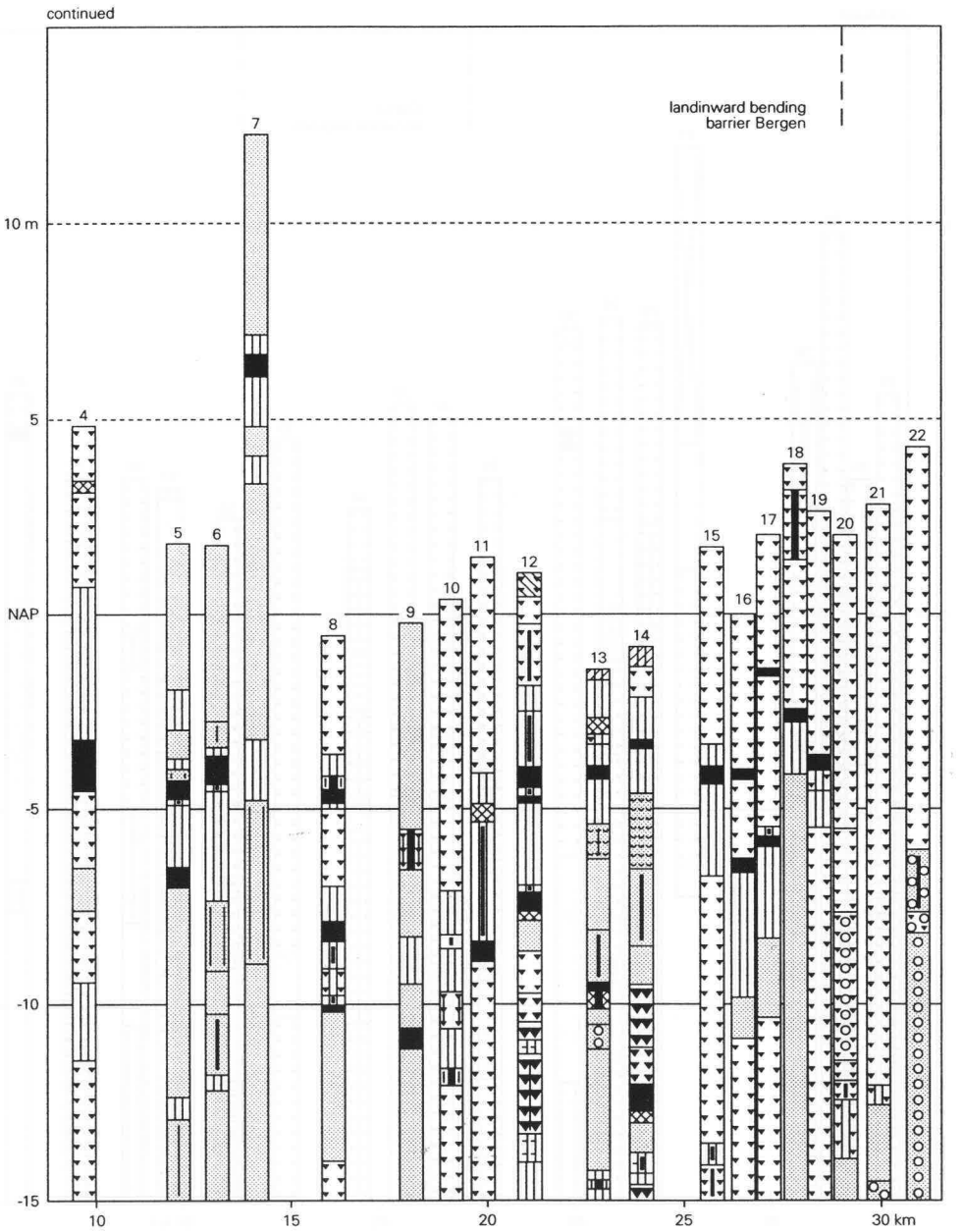
continued
landinward bending
barrier Bergen
10 m
5
NAP
-5
-10
-15
4
5
6
7
8
9
10
11
12
13
14
15
16
17
18
19
20
21
22
10
15
20
25
30 km

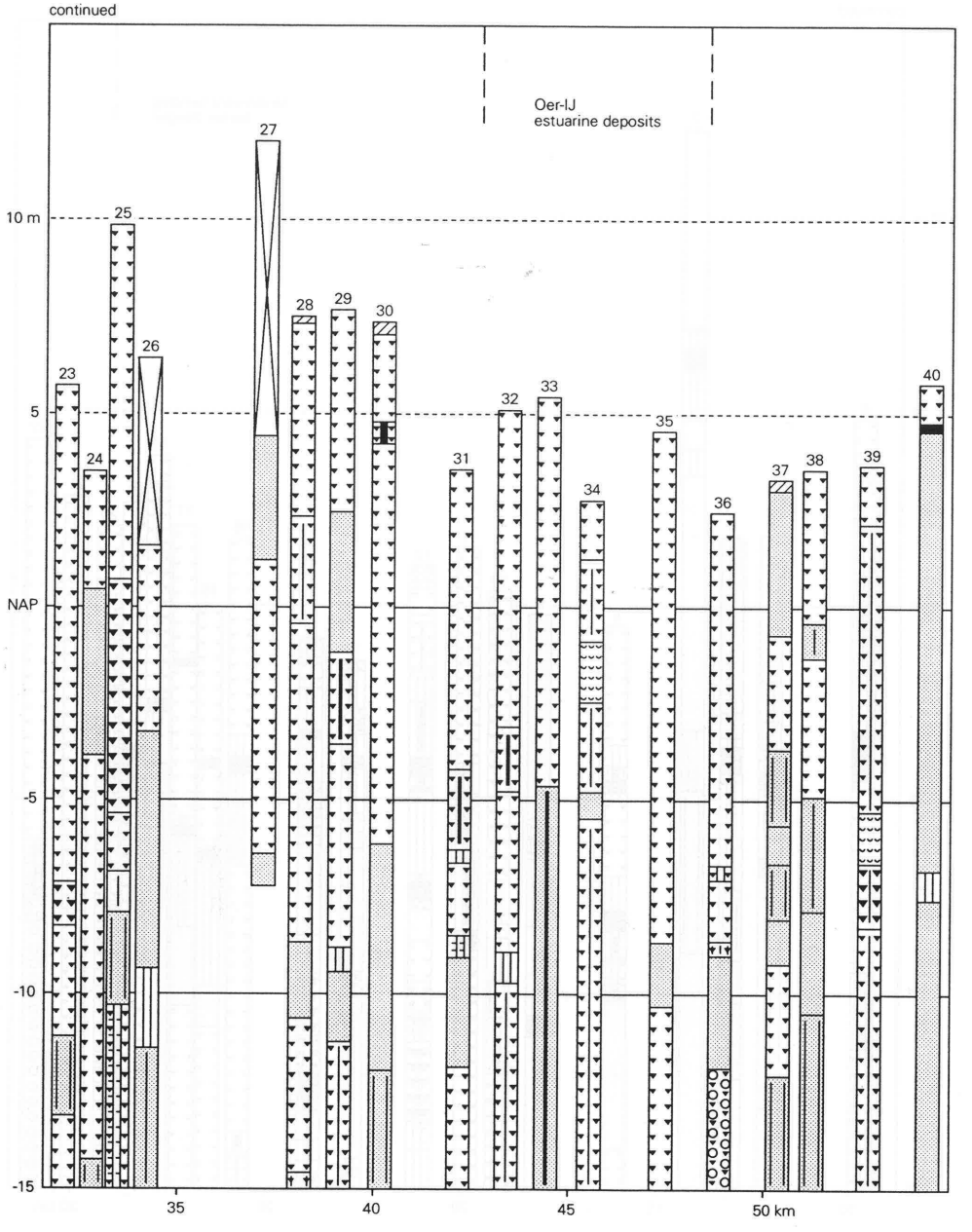
continued
Oer-IJ
estuarine deposits
10 m
5
NAP
-5
-10
-15
23
24
25
26
27
28
29
30
31
32
33
34
35
36
37
38
39
40
35
40
45
50 km

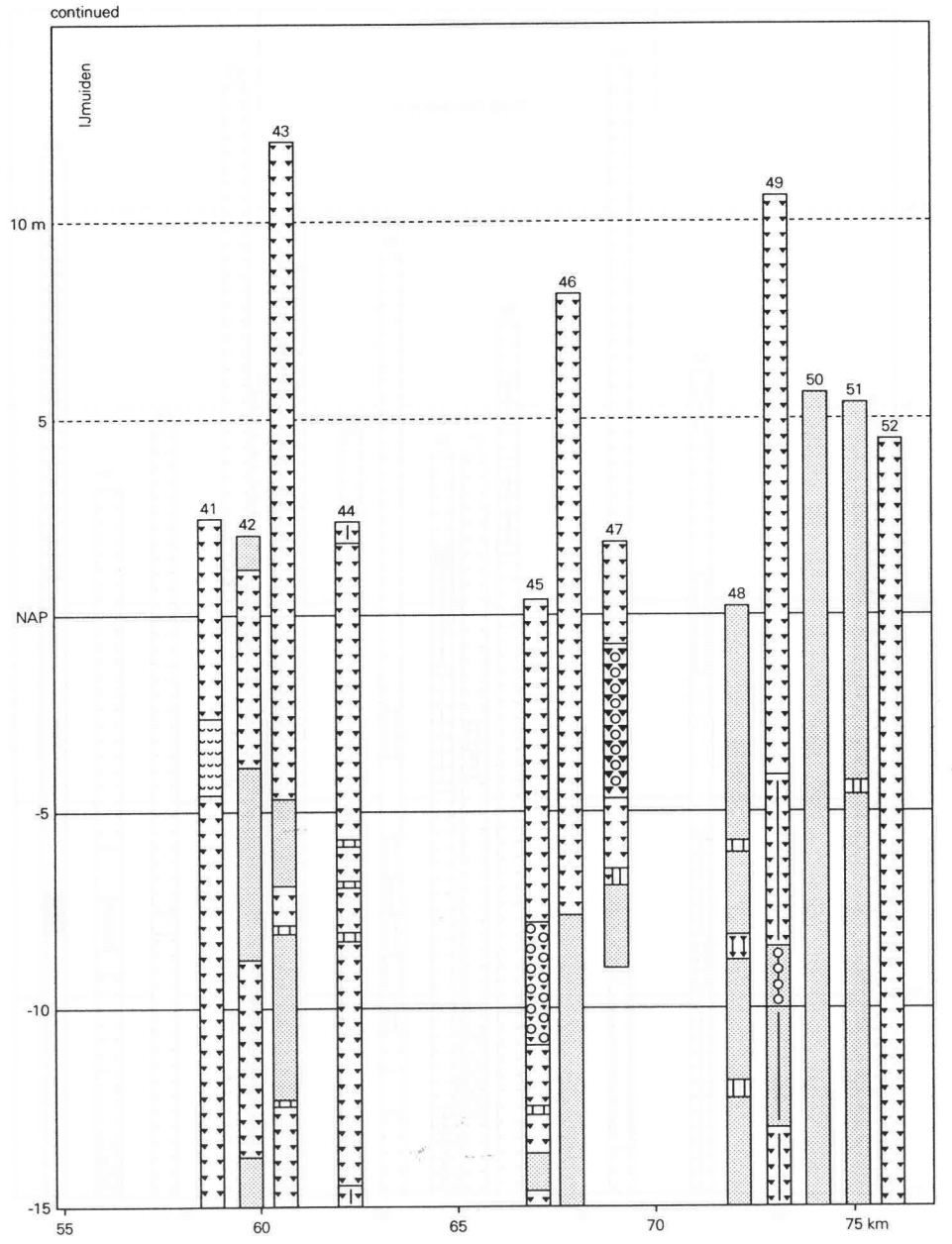
continued
IJmuiden
10 m
5
NAP
-5
-10
-15
41
42
43
44
45
46
47
48
49
50
51
52
55
60
65
70
75 km

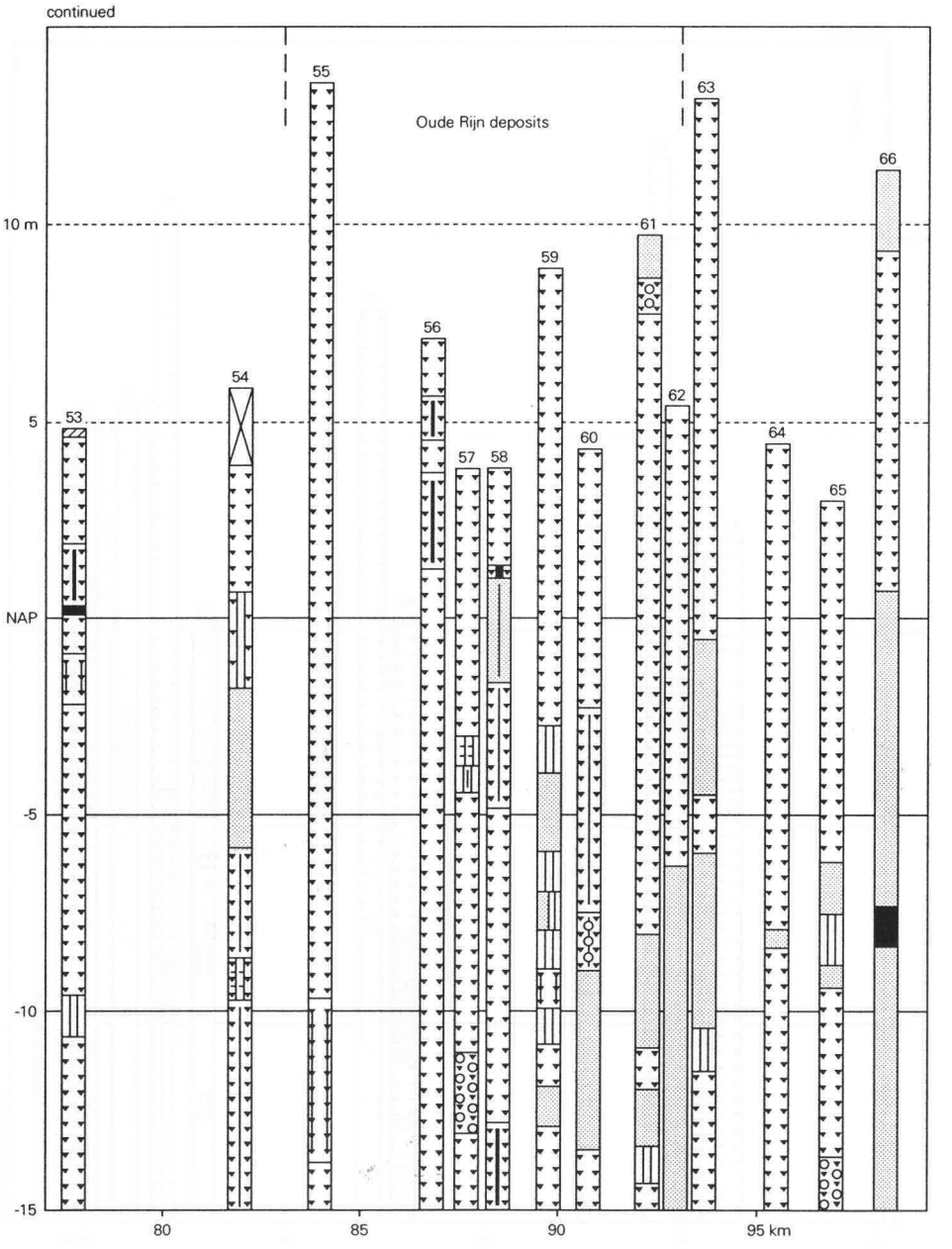
continued
Oude Rijn deposits
10 m
5
NAP
-5
-10
-15
53
54
55
56
57
58
59
60
61
62
63
64
65
66
80
85
90
95 km

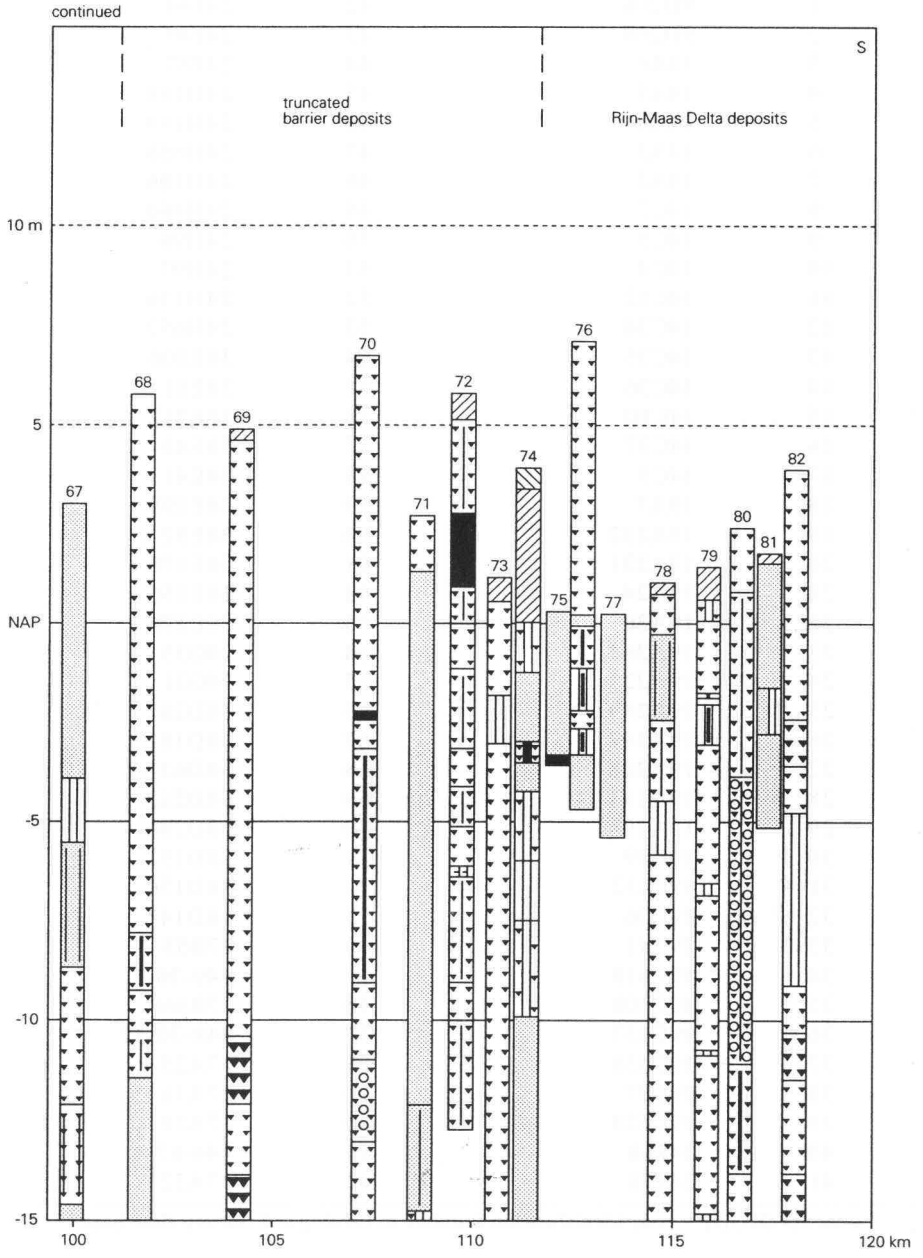
continued
S
truncated
barrier deposits
Rijn-Maas Delta deposits
10 m
5
NAP
-5
-10
-15
67
68
69
70
71
72
73
74
75
76
77
78
79
80
81
82
100
105
110
115
120 km

Table A.2: Core identification numbers in Geological Survey data base.

Core no.	Core ID (RGD) *	Core no.	Core ID (RGD) *
1	9D206	42	24F44
2	9D208	43	24F45
3	14A6	44	24F87
4	14A5	45	24H188
5	14A4	46	24H189
6	14A3	47	24H656
7	14A2	48	24H106
8	14C7	49	24H460
9	14C5	50	24H96
10	14C4	51	24H97
11	14C12	52	24H136
12	14C34	53	24H652
13	14C35	54	30E106
14	14C36	55	30E111
15	14C10	56	30E212
16	14C37	57	30E43
17	14C9	58	30E41
18	19A7	59	30E199
19	19A232	60	30E92
20	19A231	61	30E178
21	19A24	62	30E156
22	19A30	63	30E179
23	19A264	64	30G35
24	19A227	65	30G31
25	19A249	66	30D207
26	19A347	67	30D181
27	19A208	68	30D63
28	19A193	69	30D212
29	19A194	70	30D206
30	19C89	71	30D15
31	19C152	72	30D176
32	19C36	73	30D147
33	19C41	74	37B53
34	19C618	75	449-70-1
35	19C100	76	37B168
36	19C157	77	448-70-11
37	19C558	78	37A25
38	19C77	79	37A36
39	19C621	80	37A28
40	24F60	81	444-67-1
41	24F76	82	37A223

* core ID (RGD) = core identification number in Geological Survey data base.

Appendix 3 Accuracy of the 1896 position and the present-day position of the 7 m and 10 m depth contour

Knoester (1990) determined the 1896 position and the present-day position of the 7 m and 10 m depth contour. The present-day position of the contours, relative to the RSP reference line, was derived by averaging over the 1965, 1970, 1975, and 1980 extended profile surveys. The 1896 positions of the two contours were derived by Knoester from profile surveys carried out during the period 1895-1898. These surveys were conducted relative to the position of the waterline during low tide. Knoester used surveys of the low tide mark in 1890 and 1900 to estimate the 1896 position of the low tide waterline relative to the RSP reference line.

The accuracy of the position of the 7 m and 10 m depth contour is influenced by various factors, such as:

- the accuracy of the depth measurement device;
- the accuracy of determining the elevation of the sea level relative to NAP at the time of the depth measurement;
- the accuracy of positioning the depth measurement relative to the RSP reference line;
- the small bed slopes at 7 m and 10 m water depth (order 1:250).

An estimate of the accuracy of the positions of the 7 m depth contour and 10 m depth contour in 1896 is obtained by assuming that: (a) the bed slope at 7 m -NAP and 10 m -NAP are equal to the mean bed slope between these two contours, and (b) the inaccuracy of the depth values (relative to NAP) in 1896 is about twice as large as it is today, viz. 0.5 m in 1896 versus 0.25 m today (see Section 3.2). The accuracy of the depth measurement and the bed slope combine into an estimate of the accuracy of the 1896-position of the 7 m and 10 m depth contours (Figure 2.29).

Between km 50 and km 110 the accuracy of the two depth contour positions is about 120 m. North of km 50 the accuracy improves to about 30 m near km 20 (Figure A.1). On average, the accuracy of the 1896-positions of the two depth contours is about 100 m. The present-day position of the contours, as used by Knoester (1990), is the result of averaging over 4 surveys. Therefore, the accuracy of the contour positions will be relatively good, viz. about 30 m between km 50 and km 110, and north of km 50 the accuracy improves to about 15 m near km 20.

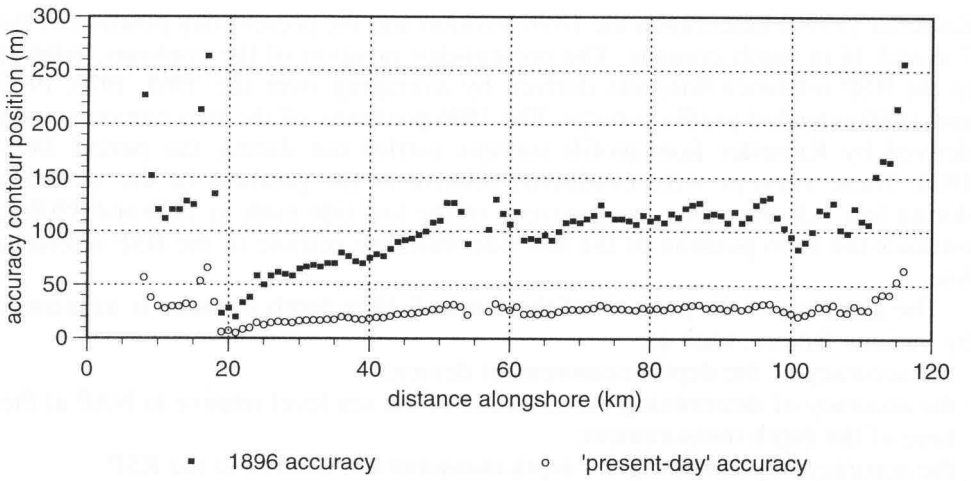

Figure A1: Estimates of the accuracy of the position of the 7 m and 10 m depth contour

Appendix 4 Input wave climates

Table A.3: Input wave climate (in % occurrence) applied in 'Katwijk' case study. (Wave station MPN, shore normal direction 300° to the North.)

Wave height	Angle of incidence (deg)						
(m)	7.5	22.5	37.5	52.5	67.5 (SW)	67.5 (N)	79
0.25	4.55430	6.45640	4.80204	2.69397	0.39590	1.21983	0.39749
0.75	5.85448	7.91442	8.36502	7.37362	1.19410	2.30125	0.60187
1.25	3.33422	4.05540	4.12933	5.70973	1.52558	0.88831	0.20276
1.75	1.87956	2.25296	2.02117	3.05118	1.54810	0.27356	0.03540
2.25	1.11365	1.16185	0.93007	1.29712	0.71452	0.05472	
2.75	0.61155	0.61153	0.55035	0.59547	0.25105	0.02898	
3.25	0.35080	0.32178	0.17379	0.15450	0.06756		
3.75	0.23815	0.18020	0.04498	0.06118	0.01612		
4.25	0.09008	0.10622	0.04825	0.03534	0.00000		
4.75	0.06431	0.04176	0.01609	0.00000	0.00320		
5.25	0.01611	0.03858	0.00645	0.00000			
5.75		0.00961		0.00324			

Table A.4: Input wave climate (in % occurrence) applied in 'Egmond' case study and in profile shape sensitivity analysis. (Wave station YM6, shore normal direction 278° to the North.)

Wave height	Angle of incidence (deg)					
(m)	0	15	30	45	60	75
0.25	0.93242	1.88755	2.63806	2.33104	2.88057	2.02779
0.75	2.04678	4.40055	5.15102	4.05560	4.06323	3.69931
1.25	1.34555	2.72145	3.559	4.21103	3.31272	2.77068
1.75	0.78082	1.62226	1.97859	3.56669	2.40300	1.24703
2.25	0.51929	0.94381	1.25455	2.16046	1.74729	0.57991
2.75	0.35629	0.57609	0.62547	1.25082	0.95899	0.28045
3.25	0.15160	0.29566	0.39414	0.73148	0.40176	0.15163
3.75	0.12885	0.26530	0.20851	0.29567	0.16294	0.08338
4.25	0.10234	0.16299	0.10239	0.13265	0.07965	0.02655
4.75	0.06067	0.08717	0.06443	0.06057	0.06826	0.01895
5.25	0.01893	0.06068	0.02269	0.02655	0.02271	0.00000
5.75	0.02651	0.01135	0.00760	0.01139	0.00753	0.00375
6.25	0.01134	0.01135		0.00377	0.00753	0.00375
6.75		0.00379		0.00377	0.00000	
7.25					0.00377	

Table A.5: Input wave climate (in % occurrence) applied in shoreline orientation sensitivity analysis and wave station sensitivity analysis.
(wave station YM6, shore normal direction 300° to the North.)

Wave height (m)	Angle of incidence (deg)							
		22.5	37.5	52.5	67.5 (SW)	67.5 (N)	79 (SSW)	79 (NNE)
0.25	3.20282	2.87688	3.28993	2.55464	0.38658	1.16743	0.14592	0.45295
0.75	4.81368	4.48772	5.54147	5.93180	1.61466	2.27422	0.36576	1.14657
1.25	2.39544	2.99055	3.81306	4.80611	2.56604	1.55405	0.53443	0.65763
1.75	1.56919	1.82312	2.20974	2.28181	2.52438	0.55717	0.50789	0.26153
2.25	0.87553	1.08404	1.27730	1.28869	1.59571	0.23119	0.49274	0.06634
2.75	0.57993	0.69361	0.64061	0.58749	0.91350	0.10235	0.29564	0.05685
3.25	0.31082	0.32592	0.34868	0.33352	0.55716	0.04927	0.10992	0.00947
3.75	0.25774	0.21982	0.19705	0.17060	0.20470	0.01137	0.04358	0.00380
4.25	0.14409	0.16299	0.11751	0.07963	0.07200	0.00381	0.01517	0.00380
4.75	0.09853	0.09853	0.08344	0.03788	0.02271		0.00948	
5.25	0.03788	0.04548	0.05306	0.01514	0.00000			
5.75	0.01138	0.03790	0.01132	0.00754	0.00000			
6.25	0.00378	0.01134	0.01511	0.00375	0.00377			
6.75			0.00379		0.00377			
7.25			0.00377					

Appendix 5 Input water levels

Table A.6: Input water levels for varying wave conditions applied in 'Katwijk' case study. (Wave station MPN, shore normal direction 300° to the North.)

Wave height (m) representing mid of 0.5 m wide wave height class	Wave direction (deg) representing mid of 15° wide wave direction sector wave direction rela			
	7.5 and 22.5	37.5	52.5 and 67.5 (SW)	67.5 (N) and 79
0.25	-0.2	-0.2	-0.2	-0.2
0.75	0.0	-0.1	-0.1	-0.2
	0.1	0.0	-0.1	-0.3
1.75	0.2	0.1	0.0	-0.4
2.25	0.4	0.2	0.1	-0.4
2.75	0.5	0.3	0.2	-0.5
3.25	0.7	0.5	0.3	
3.75	0.8	0.7	0.5	
4.25	1.0	0.8	0.6	
4.75	1.1	1.0	0.8	
5.25	1.3	1.2	0.9	
5.75			1.1	

Table A.7: Input water levels for varying wave conditions, applied in shoreline orientation sensitivity analysis and wave station sensitivity analysis. (Wave station YM6, shore normal direction 300° to the North.)

Wave height (m) representing mid of 0.5 m wide wave height class	Wave direction (deg) representing mid of 15° wide wave direction sector wave direction relative to shore normal (= 300° to N)					
	7.5 and 22.5	37.5	52.5 and 67.5 ('S')	67.5 ('N')	79 ('S')	79 ('N')
0.25	-0.1	-0.1	-0.1	-0.2	0.0	-0.2
0.75	0.0	0.0	-0.1	-0.2	0.0	-0.3
1.25	0.1	0.1	0.0	-0.2	0.0	-0.3
1.75	0.2	0.1	0.1	-0.2	0.0	-0.4
2.25	0.3	0.2	0.1	-0.2	0.0	-0.4
2.75	0.4	0.3	0.2	-0.2	0.0	-0.5
3.25	0.6	0.4	0.3	-0.2	0.0	-0.5
3.75	0.7	0.5	0.4	-0.2	0.0	-0.6
4.25	0.9	0.6	0.5	-0.2	0.0	-0.6
4.75	1.1	0.7	0.6			
5.25	1.2	0.9	0.7			
5.75	1.4	1.0	0.8			

Table A.8: Input water levels for varying wave conditions applied in 'Egmond' case study and profile shape sensitivity analysis.
(Wave station YM6, shore normal direction 278° to the North.)

Wave height (m) representing mid of 0.5 m wide wave height class	Wave direction (deg) representing mid of 15° wide wave direction sector wave direction relative to shore normal (= 278° to N)			
	0° and 15°	30° and 45°	60°	75°
0.25	-0.1	-0.1	-0.1	0.0
0.75	0.0	0.0	-0.1	0.0
1.25	0.1	0.1	0.0	0.0
1.75	0.2	0.2	0.0	0.0
2.25	0.3	0.3	0.0	0.0
2.75	0.5	0.4	0.1	0.0
3.25	0.6	0.5	0.2	0.0
3.75	0.8	0.6	0.3	0.0
4.25	0.9	0.7	0.4	0.0
4.75	1.1	0.75	0.5	0.0
5.25	1.3	0.8	0.7	0.0
5.75	1.5	0.9	0.8	0.0
6.25	1.7	1.0	1.0	0.0
6.75	1.9	1.1	1.1	

CURRICULUM VITAE

Kathelijne Wijnberg werd geboren op 10 september 1966 in Eindhoven. In 1984 behaalde zij het diploma VWO aan het Strabrecht College in Geldrop. Aansluitend ging zij fysische geografie studeren aan de Universiteit Utrecht. In februari 1990 behaalde zij daar haar doctoraal diploma, met als specialisatie 'fysisch geografische proceskunde'. Hierin richtte zij haar aandacht vooral op de morfodynamiek van kust- en riviersystemen. Na haar afstuderen werd zij tot 1 januari 1991 aangesteld als toegevoegd onderzoeker aan dezelfde universiteit. Als toegevoegd onderzoeker voerde zij een verkennende studie uit naar de geschiktheid van bestaande gegevens bestanden voor het analyseren van grootschalig kustgedrag. Deze studie mondde uit in een onderzoeksvoorstel dat gehonoreerd werd door de Universiteit Utrecht met een aanstelling als Assistent in Opleiding. Het tijdens deze aanstelling uitgevoerde onderzoek heeft geleid tot dit proefschrift. Vanaf januari 1996 zal zij als post doc gaan deelnemen aan het Marine Science and Technology (MAST) programma van de Europese Gemeenschap in het project 'Prediction of Aggregated-scale Coastal Evolution' (PACE). Een deel van haar onderzoek zal zij gaan uitvoeren in de Verenigde Staten aan de Oregon State University in Corvallis.

NEDERLANDSE GEOGRAFISCHE STUDIES / NETHERLANDS GEOGRAPHICAL STUDIES

1 G MIK & J H STIKKELBROEK Verkiezingen in Rotterdam -- Amsterdam/Rotterdam 1985: Knag/Economisch-Geografisch Instituut Erasmus Universiteit Rotterdam. 130 pp, 51 figs, 8 tabs. ISBN 90-6809-009-7 Dfl 17,50

2 S MUSTERD Verschillende structuren en ontwikkelingen van woongebieden in Tilburg -- Amsterdam 1985: Knag/Geografisch en Planologisch Instituut VU. 292 pp, 104 figs, 44 tabs. ISBN 90-6809-010-0 Dfl 27,75

3 M J TITUS Urbanisatie, integratie en demografische respons in Jakarta -- Amsterdam/Utrecht 1985: Knag/Geografisch Instituut Rijksuniversiteit Utrecht. 380 pp, 14 figs, 202 tabs. ISBN 90-6809-012-7 Dfl 39,50

4 H SCHENK Views on Alleppey -- Amsterdam 1986: Knag/Instituut voor Sociale Geografie Universiteit van Amsterdam. 246 pp, 41 figs, 36 tabs. ISBN 90-6809-011-9 Dfl 29,50

5 P J BOELHOUWER & F M DIELEMAN (red) Wonen in de stad -- Amsterdam/Utrecht 1986: Knag/Geografisch Instituut Rijksuniversiteit Utrecht. 138 pp, 41 figs, 32 tabs. ISBN 90-6809-013-5 Dfl 19,50

6 P LUKKES & J H M VAN ROODEN De makelaardij in onroerende goederen in Nederland -- Amsterdam/Groningen 1986: Knag/Geografisch Instituut Universiteit Groningen. 102 pp, 9 fig, 28 tab ISBN 90-6809-015-1 Out of print

7 P P P HUIGEN Binnen of buiten bereik? Een sociaal-geografisch onderzoek in ZW-Friesland -- Amsterdam/ Utrecht 1986: Knag/Geografisch Instituut Universiteit Utrecht. 276 pp, 58 figs, 72 tabs. ISBN 90-6809-014-3 Dfl 34,00

8 V M VAN DALEN & L VAN DER LAAN (red) Werken aan de kust; verslag van het Knag-symposium over de plannen tot uitbreiding van de Ned. kust -- Amsterdam 1986: Knag. 78 pp, 8 figs, 2 tabs. ISBN 90-6809-016-X Dfl 14,00

9 H KNIPPENBERG Deelname aan het lager onderwijs in Nederland gedurende de 19e eeuw -- Amsterdam 1986: Knag/Instituut Sociale Geografie Universiteit Amsterdam. 268 pp, 29 fig, 81 tab. ISBN 90-6809-017-8 Dfl 29,00

10 H J A BERENDSEN (red) Het landschap van de Bommelerwaard -- Amsterdam/Utrecht 1986: Knag/Geografisch Instituut Rijksuniversiteit Utrecht. 186 pp, 71 figs, 2 maps. ISBN 90-6809-019-4 Dfl 34,50

11 M DE SMIDT (red) Regionale statistiek: organisatie en onderzoek -- Amsterdam/Utrecht 1986: Knag/Geografisch Instituut Rijksuniversiteit Utrecht. 86 pp, 17 figs, 9 tabs. ISBN 90-6809-020-8 Dfl 14,95

12 J M VAN MOURIK Pollen profiles of slope deposits in the Galician area (NW Spain) -- Amsterdam 1986: Knag/ Fysisch-Geografisch en Bodemkundig Laboratorium Universiteit van Amsterdam. 174 pp, 55 figs, 4 tabs. ISBN 90-6809-018-6 Out of print

13 J J HARTS & L HINGSTMAN Verhuizingen op een rij -- Amsterdam/Utrecht 1986: Knag/Geografisch Instituut Rijksuniversiteit Utrecht. 312 pp, 54 figs, 108 tabs. ISBN 90-6809-022-4 Dfl 38,50

14 A VAN SCHAIK Colonial control and peasant resources in Java -- Amsterdam 1986: Knag/Instituut voor Sociale Geografie Universiteit van Amsterdam. 214 pp, 14 figs, 31 tabs. ISBN 90-6809-021-6 Dfl 27,00

15 L L J M DIRRIX, T K GRIMMIUS & P VAN DER VEEN The functioning of periodic markets in the Bombay Metropolitan Region -- Amsterdam/Groningen 1986: Knag/Geografisch Instituut Rijksuniversiteit Groningen. 200 pp, 38 figs, 47 tabs. ISBN 90-6809-030-5 Out of print

16 J G BORCHERT, L S BOURNE & R SINCLAIR (eds) Urban Systems in Transition -- Amsterdam/Utrecht 1986: Knag/ Geografisch Instituut Rijksuniverseit Utrecht. 248 pp, 41 figs, 48 tabs. ISBN 90-6809-028-3 Dfl 24,90

17 P W BLAUW Suburbanisatie en sociale contacten -- Amsterdam/Rotterdam 1986: Knag/Faculteit der Economische Wetenschappen Erasmus Universiteit Rotterdam. 168 pp, 68 tabs. ISBN 90-6809-024-0 Dfl 25,00

18 H J SCHOLTEN, R J VAN DE VELDE & P PADDING Doorstroming op de Nederlandse woningmarkt; geanalyseerd en gemodelleerd -- Amsterdam/Utrecht 1986: Knag/Geografisch Instituut Rijksuniversiteit Utrecht. 116 pp, 38 figs, 22 tabs. ISBN 90-6809-025-9 Dfl 13,00

19 F M DIELEMAN, A W P JANSEN & M DE SMIDT (red) Metamorfose van de stad; recente tendenzen van wonen en werken in Nederlandse steden -- Amsterdam/Utrecht 1986: Knag/Geografisch Instituut Rijksuniversiteit Utrecht. 134 pp, 31 figs, 22 tabs. ISBN 90-6809-026-7 Out of print

20 E VOS, M NIEUWENHUIS, M HOOGENDOORN & A SENDERS Vele handen; vrouw en werk in Latijns Amerika -- Amsterdam 1986: Knag/Geografisch en Planologisch Instituut VU. 210 pp, 9 figs, 7 tabs ISBN 90-6809-027-5 Dfl 30,00

21 J H J VAN DINTEREN & H W TER HART (red) Geografie en kantoren 1985 -- Amsterdam/Nijmegen 1986: Knag/Geografisch en Planologisch Instituut Katholieke Universiteit. 144 pp, 15 fig, 15 tabs ISBN 90-6809-029-1 Dfl 17,00

22 J VIJGEN, R VAN ENGELSDORP GASTELAARS Stedelijke bevolkingskategorieën in opkomst; stijlen en strategieën in het alledaagse bestaan -- Amsterdam 1986: Knag/Instituut voor Sociale Geografie Universiteit van Amsterdam. 122 pp, 3 figs, 40 tabs. ISBN 90-6809-031-3 Dfl 15,00

23 H J MÜCHER Aspects of loess and loess-derived slope deposits -- Amsterdam 1986: Knag/Fysisch-Geografisch en Bodemkundig Laboratorium Universiteit v Amsterdam. 268 pp, 42 figs, 9 tabs. ISBN 90-6809-032-1 Out of print

24 P HENDRIKS De relationele definitie van begrippen -- Amsterdam/Nijmegen 1986: Knag/Geografisch en Planologisch Instituut Katholieke Universiteit Nijmegen. 282 pp, 28 figs, 7 tabs. ISBN 90-6809-033-X Dfl 30,00

25 J M G KLEINPENNING (ed) Competition for rural and urban space in Latin America; its consequences for low income groups -- Amsterdam/Nijmegen 1986: Knag/Geografisch en Planologisch Instituut Katholieke Universiteit Nijmegen. 178 pp, 36 figs, 11 tabs. ISBN 90-6809-034-8 Dfl 22,50

26 J BUURSINK & E WEVER (red) Regio en ontwikkeling -- Amsterdam/Nijmegen 1986: Knag/Geografisch-Planologisch Instituut Katholieke Universiteit Nijmegen. 160 pp, 41 figs, 50 tabs. ISBN 90-6809-035-6 Dfl 20,00

27 G CLARK, P DOSTAL & F THISSEN (eds) Rural research and planning: the Netherlands and Great Britain -- Amsterdam 1987: Knag/Instituut voor Sociale Geografie Universiteit van Amsterdam. 88 pp, 6 figs, 4 tabs. ISBN 90-6809-037-2 Dfl 10,00

28 W M KARREMAN & M DE SMIDT (red) Redevoeringen en kleine geschriften van Prof A C de Vooys -- Amsterdam/ Utrecht 1987: Knag/Geografisch Instituut Rijksuniversiteit Utrecht. 156 pp, 8 figs, 5 tabs. ISBN 90- 6809-036-4 Dfl 21,70

29 G PEPERKAMP (red) Mens en milieu in de derde wereld -- Amsterdam/Nijmegen 1987: Knag/Geografisch en Planologisch Instituut Katholieke Universiteit Nijmegen. 146 pp, 17 figs, 11 tabs. ISBN 90-6809-038-0 Dfl 20,00

30 A R WOLTERS & A PIERSMA Beschermde reservaten? -- Amsterdam/Groningen 1987: Knag/Geografisch Instituut Rijksuniversiteit Groningen. 184 pp, 47 figs, 4 tabs. ISBN 90-6809-039-9 Out of print

31 W J VAN DEN BREMEN & P H PELLENBARG (red) Het geografisch plechtanker: eenheid in verscheidenheid. Liber amicorum Rob Tamsma – Amsterdam/Groningen 1987: Knag/Geografisch Instituut Rijksuniversiteit Groningen. 336 pp, 58 figs, 22 tabs. ISBN 90-6809-040-2 Dfl 35,00

32 G MIK Segregatie in het grootstedelijk milieu – Amsterdam/Rotterdam 1987: Knag/Economisch-Geografisch Instituut Erasmus Universiteit Rotterdam. 252 pp, 48 figs, 45 tabs. ISBN 90-6809-041-0 Dfl 25,00

33 H J M GOVERDE Macht over de Markerruimte – Amsterdam/Nijmegen 1987: Knag/Geografisch en Planologisch Instituut Katholieke Universiteit Nijmegen. 480 pp, 26 figs, 22 tabs. ISBN 90-6809-042-9 Dfl 57,50

34 P P GROENEWEGEN, J P MACKENBACH & M H STIJNENBOSCH (red) Geografie van gezondheid en gezondheidszorg – Amsterdam/Utrecht 1987: Knag/Geografisch Instituut Rijksuniversiteit Utrecht. 132 pp, 25 fig, 19 tabs ISBN 90-6809-043-7 Dfl 19,70

35 R TER BRUGGE & E WEVER (red) Energiebeleid; het Nederlandse energiebeleid in ruimtelijk perspectief – Amsterdam/Groningen/Nijmegen 1987: Knag/Geografisch Instituut Rijksuniversiteit Groningen/Geografisch en Planologisch Instituut Katholieke Universiteit. 132 pp, 21 figs, 18 tabs. ISBN 90-6809-044-5 Dfl 18,00

36 J A VAN DER SCHEE Kijk op kaarten – Amsterdam 1987: Knag/Geografisch en Planologisch Instituut van de Vrije Universiteit Amsterdam. 312 pp, 42 figs, 58 tabs. ISBN 90-6809-045-3 Dfl 39,50

37 O VERKOREN & J VAN WEESEP (eds) Spatial mobility and urban change – Amsterdam/Utrecht 1987: Knag/Geografisch Instituut Rijksuniversiteit Utrecht. 180 pp, 17 figs, 45 tabs. ISBN 90-6809-051-8 Dfl 24,75

38 M W DE JONG New economic activities and regional dynamics – Amsterdam 1987: Knag/Economisch-Geografisch Instituut Universiteit van Amsterdam. 200 pp, 26 figs, 27 tabs. ISBN 90-6809-046-1 Dfl 29,00

39 A C M JANSEN Bier in Nederland en België; een geografie van de smaak – Amsterdam 1987: Knag/Economisch-Geografisch Instituut Universiteit van Amsterdam. 282 pp, 14 figs, 7 tabs. ISBN 90-6809-047-X Dfl 37,50

40 Y C J BROUWERS, M C DEURLOO & L DE KLERK Selectieve verhuisbewegingen en segregatie; de invloed van de etnische samenstelling van de woonomgeving op verhuisgedrag – Amsterdam 1987: Knag/Instituut voor Sociale Geografie Universiteit van Amsterdam. 112 pp, 9 figs, 22 tabs. ISBN 90-6809-048-8 Dfl 16,00

41 R J SCHOUW & F M DIELEMAN Echtscheiding en woningmarkt – Amsterdam/Utrecht 1987: Knag/Geografisch Instituut Rijksuniversiteit Utrecht. 98 pp, 8 figs, 21 tabs. ISBN 90-6809-049-6 Dfl 14,95

42 J G GROENENDIJK De positie van dorpen in het beleid van Nederlandse plattelandsgemeenten – Amsterdam 1987: Knag/Instituut Sociale Geografie Universiteit Amsterdam. 314 pp, 22 fig, 55 tab ISBN 90-6809-050-X Dfl 31,50

43 J G BORCHERT & J BUURSINK (red) Citymarketing en geografie – Amsterdam/Nijmegen 1987: Knag/Geografisch en Planologisch Instituut Katholieke Universiteit. 172 pp, 32 figs, 14 tabs. ISBN 90-6809-052-6 Out of print

44 J J M ANGENENT & A BONGENAAR (eds) Planning without a passport: the future of European spatial planning – Amsterdam 1987: Knag/Siswo. 184 pp, 26 figs, 7 tabs. ISBN 90-6809-053-4 Dlf 24,90

45 R C VAN DER MARK, A H PERRELS & J J REYNDERS Kansen voor het Noorden; een beleidsstrategisch onderzoek naar nieuwe technologie – Amsterdam/Utrecht 1987: Knag/Geografisch Instituut Rijksuniversiteit Utrecht/Economische Faculteit Vrije Universiteit Amsterdam. 168 pp, 54 figs, 41 tabs. ISBN 90-6809-054-2 Dfl 22,50

46 J J STERKENBURG Rural development and rural development policies: cases from Africa and Asia – Amsterdam/Utrecht 1987: Knag/Geografisch Instituut Rijksuniversiteit Utrecht. 196 pp, 13 figs, 14 tabs. ISBN 90- 6809-055-0 Dfl 26,50

47 C CORTIE Alkmaar, van streekcentrum naar groeikern – Amsterdam 1987: Knag/Instituut voor Sociale Geografie Universiteit van Amsterdam. 204 pp, 28 figs, 39 tabs. ISBN 90-6809-056-9 Dfl 25,00

48 J A A M KOK & P H PELLENBARG (red) Buitenlandse bedrijven in Nederland – Amsterdam/Groningen 1987: Knag/Geografisch Instituut Rijksuniversiteit Groningen. 112 pp,. 17 figs, 30 tabs. ISBN 90-6809-059-3 Out of print

49 T DIETZ Pastoralists in Dire Straits; survival strategies and external interventions in a semi-arid region – Amsterdam 1987: Knag/Instituut voor Sociale Geografie Universiteit van Amsterdam. 332 pp, 34 figs, 66 tabs. ISBN 90-6809-057-7 Dfl 43,00

50 F J J H VAN HOORN Onder anderen; effekten van de vestiging van Mediterranen in naoorlogse wijken – Amsterdam/Utrecht 1987: Knag/Geografisch Instituut Rijksuniversiteit Utrecht. 226 pp, 36 figs, 55 tabs. ISBN 90-6809-060-7 Dfl 29,70

51 M J DIJST & C CORTIE Universiteit en revitalisering – Amsterdam 1987: Knag/Instituut voor Sociale Geografie Universiteit van Amsterdam. 140 pp, 6 figs, 13 tabs. ISBN 90-6809-058-5 Dfl 17,00

52 Planologie als kleurbepaling; de rol van toonaangevende instellingen en bedrijven op de ontwikkeling van de Amsterdamse Museum- en Concertgebouwbuurt – Amsterdam 1987: Knag/Centrum Beleidsadviserend Onderzoek. 164 pp, 2 figs, 23 tabs. ISBN 90-6809-061-5 Dfl 25,00

53 J VERHORST & M H STIJNENBOSCH Bedrijvigheid en stadsvernieuwing; analyse van de bedrijvigheidsontwikkeling in enkele stadsvernieuwingsgebieden in Utrecht en Den Haag – Amsterdam/Utrecht 1987: Knag/ Geografisch Instituut Rijksuniversiteit Utrecht. 112 pp, 47 figs, 25 tabs. ISBN 90-6809-063-1 Dfl 15,70

54 B G J DRIESSEN, R VERHOEF & J G P TER WELLE-HEETHUIS Overheid en bevolkingsontwikkelingen; een onderzoek naar autonome en niet-autonome bevolkingsontwikkelingen in Arnhem en Utrecht – Amsterdam/Utrecht 1987: Knag/Geografisch Instituut Rijksuniversiteit Utrecht. 166 pp, 53 figs, 42 tabs.. ISBN 90-6809-064-X Dfl 23,30

55 O A L C ATZEMA, P P P HUIGEN, A G A DE VOCHT & C R VOLKERS De bereikbaarheid van voorzieningen in Noord-Nederland – Amsterdam/Utrecht 1987: Knag/Geografisch Instituut Rijksuniversiteit Utrecht. 220 pp, 49 figs, 122 tabs. ISBN 90-6809-065-8 Dfl 24,00

56 P C BEUKENKAMP, G A HOEKVELD & A MUDDE (red) Geografie en onderwijstelevisie – Amsterdam/Utrecht 1987: Knag/Geografisch Instituut Rijksuniversiteit Utrecht. 222 pp, 29 figs, 6 tabs. ISBN 90-6809-066-6 Dfl 26,50

57 G CARDOL Ruimte voor agribusiness-complexen; structuur, positie en dynamiek van het Noordlimburgse tuinbouwcomplex – Amsterdam/Nijmegen 1988: Knag/Geografisch en Planologisch Instituut Katholieke Universiteit Nijmegen. 312 pp, 34 figs, 57 tabs.. ISBN 90-6809-067-4 Dfl 30,00

58 M JANSEN-VERBEKE Leisure, recreation and tourism in inner cities – Amsterdam/Nijmegen 1988: Knag/Geografisch en Planologisch Instituut Katholieke Universiteit. 316 pp, 61 fig, 51 tabs. ISBN 90-6809-068-2 Out of print

59 A H H M KEMPERS-WARMERDAM Vergrijzen in het groen; het bereik van ouderen en de bereikbaarheid van voorzieningen in landelijke gebieden – Amsterdam/Utrecht 1988: Knag/Geografisch Instituut Rijksuniversiteit Utrecht. 236 pp, 47 figs, 70 tabs. ISBN 90-6809-069-0 Dfl 29,50

60 P J BOELHOUWER De verkoop van woningwetwoningen -- Amsterdam/Utrecht 1988: Knag/Geografisch Instituut Rijksuniversiteit Utrecht. 208 pp, 49 figs, 122 tabs. ISBN 90-6809-070-4 Dfl 29,30

61 A G J DIETVORST & M C JANSEN-VERBEKE De binnenstad: kader van een sociaal perpetuum mobile; een literatuurstudie naar tijdsbesteding en binnenstadsgebruik -- Amsterdam/Nijmegen 1988: Knag/Geografisch en Planologisch Instituut Katholieke Universiteit Nijmegen. 240 pp, 10 tabs. ISBN 90-6809-071-2 Dfl 30,00

62 H SCHRETTENBRUNNER & J VAN WESTRHENEN Empirische Forschung und Computer im Geographie-unterricht -- Amsterdam 1988: Knag/Centrum v Educatieve Geografie VU. 120 pp, 27 figs. ISBN 90-6809-072-0 Out of print

63 H J A BERENDSEN & H VAN STEIJN (red) Nieuwe karteringsmethoden in de fysische geografie -- Amsterdam/ Utrecht 1988: Knag/Geografisch Instituut Utrecht. 176 pp, 56 figs, 24 tabs. ISBN 90-6809-073- 9 Dfl 22,50

64 A G J DIETVORST & J P M KWAAD (eds) Geographical research in the Netherlands 1978-1987 -- Amsterdam. 1988: Knag/IGU Netherlands. 262 pp, 7 figs, 2 tabs. ISBN 90-6809-074-7 Dfl 33,00

65 J VAN WEESEP Appartementsrechten; het gebruik van het splitsingregime -- Amsterdam/Utrecht 1988: Knag/ Geografisch Instituut Rijksuniversiteit Utrecht. 94 pp, 4 figs, 16 tabs. ISBN 90-6809-075-5 Dfl 14,50

66 T W A EPPINK Choice of mathematical models in geographic research considering alternatives -- Amsterdam/ Nijmegen 1988: Knag/Geografisch en Planologisch Instituut Katholieke Universiteit Nijmegen. 244 pp, 74 figs, 49 tabs. ISBN 90-6809-076-3 Dfl 30,00

67 J HINDERINK & E SZULC-DABROWIECKA (eds) Successful rural development in Third World Countries - Amsterdam/Utrecht 1988: Knag/Geografisch Instituut Rijksuniversiteit Utrecht. 256 pp, 14 figs, 20 tabs. ISBN 90-6809-077-1 Dfl 31,50

68 S BARENDS, J D H HARTEN, J RENES, J VERHORST & K E VAN DER WIELEN (red) Planning in het verleden -- Amsterdam /Utrecht 1988: Knag/Geografisch Instituut Universiteit Utrecht. 192 pp, 71 figs. ISBN 90-6809-078-X Dfl 26,00

69 J MANSVELT BECK The rise of a subsidized periphery in Spain -- Amsterdam 1988: Knag/Instituut voor Sociale Geografie Universiteit van Amsterdam. 286 pp, 15 figs, 28 tabs. ISBN 90-6809-079-8 Dfl 37,50

70 S SMITH Kleinschalige industrie in Latijns Amerika; een studie van de ontwikkelingsmogelijkheden in Aguascalientes, Mexico -- Amsterdam/Nijmegen 1988: Knag/Geografisch en Planologisch Instituut Katholieke Universiteit Nijmegen. 422 pp, 4 figs, 16 tabs. ISBN 90-6809-080-1 Dfl 42,50

71 W DWARKASING, D HANEMAAYER, M DE SMIDT & P P TORDOIR Ruimte voor hoogwaardige kantoren; onderzoek naar toplocaties voor de commerciële kantorensector -- Amsterdam/Utrecht/Leiden/Delft 1988: Knag/Geografisch Instituut Utrecht/Research voor Beleid/Inro-tno. 112 pp, 7 figs, 44 tabs. ISBN 90-6809-081-X Out of print

72 P J KORTEWEG Dynamiek en immobiliteit in naoorlogse woonwijken in Alkmaar, Haarlem en Purmerend -- Amsterdam/Utrecht 1988: Knag/Geografisch Instituut Rijksuniversiteit Utrecht. 144 pp, 21 figs, 34 tabs. ISBN 90-6809-082-8 Dfl 20,90

73 P J WIJERS Land prices in Tokyo -- Amsterdam 1988: Knag/Economisch-Geografisch Instituut Universiteit van Amsterdam. 84 pp, 12 figs, 8 tabs. ISBN 90-6809-084-4 Dfl 47,50

74 J VAN MOURIK (red) Landschap in beweging; ontwikkeling en bewoning van een stuifzandgebied in de Kempen -- Amsterdam 1988: Knag/Faculteit Ruimtelijke Wetenschappen Universiteit van Amsterdam. 197 pp, 95 figs, 1 tab. ISBN 90-6809-083-6 Dfl 30,00

75 W J M OSTENDORF Het sociaal profiel van de gemeente; woonmilieudifferentiatie en de vorming van het stadsgewest Amsterdam -- Amsterdam 1988: Knag/Instituut voor Sociale Geografie Universiteit van Amsterdam. 192 pp, 12 figs, 26 tabs. ISBN 90-6809-085-2 Dfl 23,00

76 J DE BRUIN & J A KOETSIER (red) De kracht van de regio; sociaal-economische ontwikkelingsmogelijkheden van de regio -- Amsterdam 1988: Knag/Instituut voor Sociale Geografie Universiteit van Amsterdam. 104 pp, 12 figs, 6 tabs. ISBN 90-6809-086-0 Dfl 15,00

77 A G M VAN DER SMAGT & P H J HENDRIKS (red) Methoden op een keerpunt; opstellen aangeboden aan prof drs P J W Kouwe -- Amsterdam/Nijmegen 1988: Knag/Geografisch en Planologisch Instituut Katholieke Universiteit Nijmegen. 170 pp, 29 figs, 10 tabs. ISBN 90-6809-087-9 Dfl 25,00

78 C VAN DER POST, Migrants and migrant-labour absorption in large and small centres in Swaziland -- Amsterdam/ Utrecht 1988: Knag/Geografisch Instituut Utrecht. 310 pp, 32 figs, 84 tabs. ISBN 90- 6809-088-7 Dfl 35,00

79 L J DE HAAN Overheid en regionale integratie van de savanne in Togo 1885-1985 -- Amsterdam 1988: Knag/Instituut v Sociale Geografie Universiteit van Amsterdam. 304 pp, 31 figs, 65 tabs. ISBN 90-6809-089-5 Dfl 33,00

80 L H VAN WIJNGAARDEN-BAKKER & J J M VAN DER MEER (eds) Spatial sciences, research in progress: Proceedings of the symposium "Spatial sciences, research in progress" -- Amsterdam 1988: Knag/ Faculteit Ruimtelijke Wetenschappen Universiteit van Amsterdam. 112 pp, 16 figs, 2 tabs. ISBN 90-6809-091-7 Dfl 24,00

81 F M H M DRIESSEN & J H VAN HOUWELINGEN Vrije tijd en korte verblijfsrecreatie -- Amsterdam/Utrecht 1988: Knag/Bureau Driessen. 256 pp, 25 figs, 146 tabs. ISBN 90-6809-095-X Dfl 15,00

82 G HOEKVELD-MEIJER & G J SCHUTTE Aardrijkskunde gebiedenderwijs; tekst en uitleg bij het schrijven, lezen, denken en leren over gebieden en verschijnselen in gebieden -- Amsterdam 1988: Knag/Centrum voor Educatieve Geografie Vrije Universiteit Amsterdam. 252 pp, 76 figs, 12 tabs. Out of print

83 P K DOORN Social structure and spatial mobility: composition and dynamics of the Dutch labour force -- Amsterdam/Utrecht 1989: Knag/Geografisch Instituut Rijksuniversiteit Utrecht. 262 pp, 72 figs, 41 tabs. ISBN 90-6809-092-5 Dfl 31,50

84 A LOEVE Buitenlandse ondernemingen in regionaal perspectief; vestigingsstrategieën en regionale effecten van buitenlandse bedrijven in Nederland -- Amsterdam/Utrecht 1989: Knag/Geografisch Instituut Rijksuniversiteit Utrecht. 272 pp, 49 figs, 78 tabs. ISBN 90-6809-093-3 Dfl 32,00

85 D H DE BAKKER Ruraal nederzettingenpatroon en beleid; ontwikkelingen in ZW-Friesland -- Amsterdam/Utrecht 1989: Knag/Geografisch Instituut Universiteit Utrecht. 230 pp, 32 figs, 68 tabs. ISBN 90-6809-094-1 Dfl 29,00

86 L J PAUL (ed) Post-war development of regional geography; with special attention to the United Kingdom, Belgium, and the Netherlands -- Amsterdam/Utrecht 1989: Knag/Geografisch Instituut Rijksuniversiteit Utrecht. 88 pp, 15 figs, 5 tabs. ISBN 90-6809-096-8 Dfl 14,00

87 P HOEKSTRA River outflow, depositional processes and coastal morphodynamics in a monsoon-dominated deltaic environment, East Java, Indonesia -- Amsterdam/Utrecht 1989: Knag/Geografisch Instituut Rijksuniversiteit Utrecht. 220 pp, 77 figs, 24 tabs. ISBN 90-6809-097-6 Dfl 28,50

88 E LENSINK Intermediaire diensten in landelijke gebieden -- Amsterdam/Nijmegen 1989: Knag/Faculteit Beleidswetenschappen Katholieke Universiteit Nijmegen. 246 pp, 21 figs, 65 tabs. ISBN 90-6809-098-4 Dfl 30,00

89 P P P HUIGEN & M C H M VAN DE VELDEN (red) De achterkant van verstedelijkt Nederland; de positie en funktie van landelijke gebieden in de Nederlandse samenleving -- Amsterdam/Utrecht 1989: Knag/Geografisch Instituut Rijksuniversiteit Utrecht. 181 pp, 25 figs, 46 tabs. ISBN 90-6809-100-X Out of print

90 J H J VAN DINTEREN Zakelijke diensten en middelgrote steden, een onderzoek naar dienstverleningsbedrijven in Noord-Brabant, Gelderland en Overijssel -- Amsterdam/Nijmegen 1989: Knag/Faculteit der Beleidswetenschappen Katholieke Universiteit Nijmegen. 312 pp, 28 figs, 84 tabs. ISBN 90-6809-099-2 Dfl 40,00

91 L VAN DER LAAN, H SCHOLTEN & G A VAN DER KNAAP Het regionaal arbeidsaanbod in Nederland -- Amsterdam/Rotterdam 1989: Knag/Economisch-Geografisch Instituut Erasmus Universiteit Rotterdam. 128 pp, 27 figs, 28 tabs. ISBN 90-6809-101-8 Dfl 17,50

92 C CLARK, P HUIGEN & F THISSEN (eds) Planning and the future of the countryside: Great Britain and the Netherlands -- Amsterdam 1989: Knag/Instituut voor Sociale Geografie Universiteit van Amsterdam. 240 pp, 25 figs, 43 tabs. ISBN 90-6809-102-6 Dfl 35,00

93 J A VAN DEN BERG Variability of parameters for modelling soil moisture conditions; studies on loamy to silty soils on marly bedrock in the Ardêche drainage basin, France -- Amsterdam/Utrecht 1989: Knag/Geografisch Instituut Rijksuniversiteit Utrecht. 214 pp, 76 figs, 16 tabs. ISBN 90-6809-103-4 Dfl 28,50

94 O VERKOREN Huizen op de hoogvlakte; een residentieel-geografische verkenning van La Paz, Bolivia -- Amsterdam/Utrecht 1989: Knag/Geografisch Instituut Rijksuniversiteit Utrecht. 210 pp, 29 figs, 16 tabs. ISBN 90-6809-104-2 Dfl 32,00

95 G MIK (red) Herstructurering in Rotterdam; modernisering en internationalisering en de Kop van Zuid -- Amsterdam/Rotterdam 1989: Knag/Economisch Geografisch Instituut Erasmus Universiteit Rotterdam. 324 pp. 86 figs, 54 tabs. ISBN 90-6809-105-0 Dfl 30,00

96 P BEEKMAN, P VAN LINDERT, J POST & W PRINS Huisvestingsbeleid en informele bouw in de derde wereld -- Amsterdam 1989: Knag/Instituut voor Sociale Geografie Universiteit van Amsterdam. 174 pp, 9 figs, 25 tabs. ISBN 90-6809-106-9 Dfl 30,00

97 J G L PALTE Upland farming on Java, Indonesia -- Amsterdam/Utrecht 1989: Knag/Geografisch Instituut Rijksuniversiteit Utrecht. 256 pp, 15 figs, 38 tabs. ISBN 90-6809-107-7 Dfl 34,50

98 P VAN GENUCHTEN Movement mechanisms and slide velocity variations of landslides in varved clays in the French Alps -- Amsterdam/Utrecht 1989: Knag/Geografisch Instituut Rijksuniversiteit Utrecht. 160 pp, 70 figs, 17 tabs. ISBN 90-6809-108-5 Dfl 25,00

99 M DE SMIDT & E WEVER (eds) Regional and local economic policies and technology -- Amsterdam/Utrecht/Nijmegen 1989: Knag/Geografisch Instituut Rijksuniversiteit Utrecht/Geografisch en Planologisch Instituut Katholieke Universiteit Nijmegen. 156 pp, 53 figs, 36 tabs. ISBN 90-6809-109-3 Dfl 24,00

100 P J H RIEMENS On the foreign operations of third world firms -- Amsterdam 1989: Knag/Instituut voor Sociale Geografie Universiteit van Amsterdam. 148 pp, 20 tabs. ISBN 90-6809-110-7 Dfl 30,00

101 G B M PEDROLI The nature of landscape; a contribution to landscape ecology and ecohydrology with examples from the Strijper Aa landscape -- Amsterdam 1989: Knag/Fysisch-Geografisch en Bodemkundig Laboratorium Universiteit van Amsterdam. 164 pp, 43 figs, 18 tabs. ISBN 90-6809-111-5 Dfl 25,00

102 H LEENAERS The dispersal of metal mining wastes in the catchment of the river Geul, Belgium-the Netherlands -- Amsterdam/Utrecht 1989: Knag/Geografisch Instituut Rijksuniversiteit Utrecht. 230 pp, 95 figs, 52 tabs. ISBN 90-6809-112-3 Dfl 30,00

103 G A HOEKVELD, G SCHOENMAKER & J VAN WESTRHENEN Wijkende grenzen -- Amsterdam 1989: Knag/Centrum voor Educatieve Geografie VU. 216 pp, 38 figs, 24 tabs. ISBN 90-6809-113-1 Out of print

104 P C J DRUIJVEN Mandenvlechters en Mexcalstokers in Mexico -- Amsterdam 1990: Knag/Instituut voor Sociale Geografie Universiteit van Amsterdam. 294 pp, 21 figs, 55 tabs. ISBN 90-6809-114-X Dfl 38,50

105 W BLEUTEN De verwatering van meststoffen; analyse en modellering van de relaties tussen landgebruik en waterkwaliteit in het stroomgebied van de Langbroeker Wetering -- Amsterdam/Utrecht 1990: Knag/Geografisch Instituut Rijksuniversiteit Utrecht. 262 pp, 80 figs, 31 tabs. ISBN 90-6809-115-8 Dfl 37,00

106 J VAN WEESEP & P KORCELLI (eds) Residential mobility and social change; studies from Poland and the Netherlands -- Amsterdam/Utrecht 1990: Knag/Geografisch Instituut Rijksuniversiteit Utrecht. 182 pp. 46 figs, 34 tabs. ISBN 90-6809-116-6 Dfl 29,50

107 M VAN HERWIJNEN, R JANSSEN & P RIETVELD Herbestemming van landbouwgrond -- Amsterdam 1990: Knag/Instituut Milieuvraagstukken Vrije Universiteit. 110 pp, 33 figs, 12 tabs. ISBN 90-6809-117-4 Dfl 25,00

108 D H DRENTH De informatica-sector in Nederland tussen rijp en groen -- Amsterdam/Nijmegen 1990: Knag/Faculteit Beleidswetenschappen Katholieke Universiteit. 268 pp, 24 figs, 87 tabs. ISBN 90-6809-118-2 Dfl 37,50

109 H KNOL & W MANSHANDEN Functionele samenhang in de noordvleugel van de Randstad -- Amsterdam/Utrecht 1990: Knag/Economisch-Geografisch Instituut Universiteit van Amsterdam/Geografisch Instituut Rijksuniversiteit Utrecht. 112 pp, 26 figs, 27 tabs. ISBN 90-6809-119-0 Dfl 19,50

110 C D EYSBERG The Californian wine economy -- Amsterdam/Utrecht 1990: Knag/Geografisch Instituut Rijksuniversiteit Utrecht. 272 pp, 64 figs, 26 tabs. ISBN 90-6809-121-2 Dfl 29,75

111 J W A DIJKMANS Aspects of geomorphology and thermoluminescence dating of cold climate eolian sands -- Amsterdam/Utrecht 1990: Knag/Geografisch Instituut Rijksuniversiteit Utrecht. 256 pp, 119 figs, 19 tabs. ISBN 90-6809-120-4 Dfl 36,50

112 H TER HEIDE (ed) Technological change and spatial policy -- Amsterdam/Utrecht 1990: Knag/Geografisch Instituut Rijksuniversiteit Utrecht. 218 pp, 9 figs, 31 tabs. ISBN 90-6809-122-0 Dfl 29,00

113 I L M VAN HEES De ontwikkeling van een woningmarktmodel en zijn toepassing op Italië -- Amsterdam/Nijmegen 1990: Knag/Faculteit der Beleidswetenschappen Katholieke Universiteit Nijmegen. 196 pp, 12 figs, 26 tabs. ISBN 90-6809-123-9 Dfl 35,00

114 M R HENDRIKS Regionalisation of hydrological data: effects of lithology and land use on storm runoff in east Luxembourg -- Amsterdam/Utrecht 1990: Knag/Geografisch Instituut Rijksuniversiteit Utrecht. 174 pp, 23 figs, 50 tabs. ISBN 90-6809-124-7 Dfl 26,00

115 P H RENOOY The informal economy -- Amsterdam 1990: Knag/Regioplan. 204 pp, 12 figs, 21 tabs. ISBN 90-6809-125-5 Dfl 35,00

116 J H T KRAMER Luchthavens en hun uitstraling -- Amsterdam/Nijmegen 1990: Knag/Faculteit der Beleidswetenschappen Katholieke Universiteit Nijmegen. 312 pp, 47 figs, 60 tabs. ISBN 90-6809-126-3 Dfl 55,00

117 M DE KWAASTENIET Denomination and primary education in the Netherlands 1870-1984 -- Amsterdam/ Florence 1990: Knag/Instituut voor Sociale Geografie Universiteit van Amsterdam/European University Institute Florence. 268 pp, 28 figs, 39 tabs. ISBN 90-6809-127-1 Dfl 36,00

118 W P M F IVENS Atmospheric deposition onto forests: an analysis of the deposition variability by means of throughfall measurements -- Amsterdam/Utrecht 1990: Knag/Geografisch Instituut Rijksuniversiteit Utrecht. 156 pp, 53 figs, 36 tabs. ISBN 90-6809-128-X Dfl 25,00

119 R HASSINK Herstructurering en innovatiebevordering in het Ruhrgebied -- Amsterdam/Utrecht 1990: Knag/Geografisch Instituut Rijksuniversiteit Utrecht. 122 pp, 20 figs, 18 tabs. ISBN 90-6809-120-8 Dfl 24,00

120 P P SCHOT Solute transport by groundwater flow to wetland ecosystems; the environmental impact of human activities -- Amsterdam/Utrecht 1991: Knag/Geografisch Instituut Rijksuniversiteit Utrecht. 136 pp, 27 figs, 9 tabs. ISBN 90-6809-130-1 Dfl 25,00

121 S DEN HENGST & B DE PATER (red) Externe relaties en regionale ontwikkeling: voorbeelden uit Spanje en Portugal -- Amsterdam/Utrecht 1991: Knag/Geografisch Instituut Rijksuniversiteit Utrecht. 198 pp, 31 figs, 27 tabs. ISBN 90-6809-131-X Dfl 29,50

122 J KROES Onvolledige opstrek op de Nederlandse zandgronden -- Amsterdam/Utrecht 1991: Knag/Geografisch Instituut Rijksuniversiteit Utrecht. 256 pp, 65 figs. ISBN 90-6809-132-8 Dfl 35,00

123 H S VERDUIN-MULLER Serving the knowledge-based society: research on knowledge products -- Amsterdam/ Utrecht 1991: Knag/Geografisch Inst. Universiteit Utrecht. 116 pp, 3 figs. ISBN 90-6809-133-6 Dfl 24,00

124 F MULDER Assessment of landslide hazard -- Amsterdam/Utrecht 1991: Knag/Geografisch Instituut Rijksuniversiteit Utrecht. 156 pp, 59 figs, 25 tabs. ISBN 90-6809-134-4 Dfl 29,50

125 M VIS Processes and patterns of erosion in natural and disturbed Andean forest ecosystems -- Amsterdam 1991: Knag/Fysisch Geografisch en Bodemkundig Laboratorium Universiteit van Amsterdam. 190 pp, 70 figs, 40 tabs. ISBN 90-6809-136-0 Dfl 12,00

126 V EIFF Beleid voor bedrijfsterreinen -- Amsterdam 1991: Knag/Instituut voor Sociale Geografie Universiteit van Amsterdam. 214 pp, 13 figs, 18 tabs. ISBN 90-6809-135-2 Dfl 37,50

127 O ATZEMA Stad uit, stad in; residentiele suburbanisatie in Nederland -- Amsterdam/Utrecht 1991: Knag/ Geografisch Instituut Rijksuniversiteit Utrecht. 274 pp, 57 figs, 80 tabs. ISBN 90-6809-137-9 Dfl 37,50

128 M HULSHOF Zatopec moves; networks and remittances of US-bound migrants from Oaxaca, Mexico -- Amsterdam 1991: Knag/Instituut voor Sociale Geografie Universiteit van Amsterdam. 106 pp, 6 figs, 14 tabs. ISBN 90-6809-138-7 Dfl 18,50

129 J M J DOOMERNIK Turkse moskeeën en maatschappelijke participatie; de institutionalisering van de Turkse Islam in Nederland en de Duitse Bondsrepubliek -- Amsterdam 1991: Knag/Instituut voor Sociale Geografie Universiteit van Amsterdam. 200 pp, 30 figs, 1 tab. ISBN 90-6809-139-5 Dfl 32,50

130 M DE SMIDT, A GRANBERG & E WEVER (eds) Regional development strategies and territorial production complexes; a Dutch-USSR perspective -- Amsterdam 1991: Knag. 216 pp, 25 figs., 40 tabs. ISBN 90-6809-140-9 Dfl 29,50

131 P MISDORP Centrale begrippen in de sociale geografie; een conceptuele analyse van engelstalige leerboeken -- Amsterdam 1991: Knag/Iparto 316 pp, 39 figs, 51 tabs. ISBN 90-6809-141-7 Dfl 39,50

132 M DE SMIDT & E WEVER (eds) Complexes, formations and networks -- Utrecht/Nijmegen 1991: Knag/ Geografisch Instituut Rijksuniversiteit Utrecht/ Faculteit Beleidswetenschappen Katholieke Universiteit Nijmegen. 150 pp, 32 figs, 17 tabs. ISBN 90-6809-142-5 Out of print

133 I I Y CASTEL Late Holocene eolian drift sands in Drenthe -- Amsterdam/Utrecht 1991: Knag/Geografisch Instituut Rijksuniversiteit Utrecht. 162 pp, 49 figs, 15 tabs. ISBN 90-6809-143-3 Dfl 29,50

134 J G BORCHERT & M DE KRUYF Bevolkingsgroei ter wille van het voorzieningenniveau? -- Utrecht 1991: Knag/ Faculteit Ruimtelijke Wetenschappen Rijksuniversiteit Utrecht. 78 pp, 4 figs, 15 tabs ISBN 90-6809-144-1 Dfl 18,00

135 R VAN DER VAART Educatief ontwerpen met geografie; een studie betreffende de structurering van geografische kennis voor educatieve doeleinden -- Utrecht 1991: Knag/Faculteit Ruimtelijke Wetenschappen Rijksuniversiteit Utrecht. 256 pp, 84 figs. ISBN 90-6809-145-X Dfl 36,00

136 P VAN LINDERT Huisvestigingsstrategieën van lage-inkomensgroepen in La Paz -- Utrecht 1991: Knag/Faculteit Ruimtelijke Wetenschappen Rijksuniversiteit Utrecht. 320 pp, 34 figs, 26 tabs. ISBN 90-6809-146-8 Dfl 34,50

137 J M M VAN AMERSFOORT & H KNIPPENBERG (eds) States and nations: the rebirth of the 'nationalities question' in Europe -- Utrecht/Amsterdam 1991: Knag/Instituut voor Sociale Geografie Universiteit van Amsterdam. 198 pp, 20 figs, 12 tabs. ISBN 90-6809-147-6 Dfl 29,50

138 P VAN TEEFFELEN Dienstencentra en rurale ontwikkeling; een onderzoek naar het aanbod en gebruik van overheidsdiensten in Mali, Afrika -- Utrecht 1992: Knag/Faculteit Ruimtelijke Wetenschappen Rijksuniversiteit Utrecht. 256 pp, 70 figs, 40 tabs. ISBN 90-6809-148-4 Dfl 34,50

139 T H M VAN DER LOOP Industrial dynamics and fragmented labour markets. Construction firms and labourers in India -- Utrecht/Amsterdam 1992: Knag/Instituut voor Sociale Geografie Universiteit van Amsterdam. 350 pp, 30 figs, 71 tabs. ISBN 90-6809-149-2 Dfl 49,50

140 H VAN DER WUSTEN (ed) The urban political arena; geographies of public administration -- Utrecht/Amsterdam 1992: Knag/Instituut voor Sociale Geografie Universiteit van Amsterdam. 192 pp, 28 figs, 12 tabs. ISBN 90-6809-150-6 Dfl 35,00

141 B D HOEKSTRA Informatienetwerken rondom bedrijven; de bibliotheek als informatieleverancier voor het bedrijfsleven -- Utrecht/Groningen 1992: Knag/Faculteit Ruimtelijke Wetenschappen Rijksuniversiteit Groningen. 112 pp, 16 figs, 8 tabs. ISBN 90-6809-151-4 Dfl 25,00

142 H SCHRETTENBRUNNER & J VAN WESTRHENEN (eds) Empirical research and geography teaching -- Utrecht/Amsterdam 1992: Knag/Centrum voor Educatieve Geografie Vrije Universiteit Amsterdam. 190 pp, 48 figs, 38 tabs. ISBN 90-6809-152-2 Dfl 30,00

143 J VAN BECKUM & C VAN DER BURG Naar een online videotex geografisch informatiesysteem voor educatieve toepassingen; het Giset Project 1987-1992 -- Utrecht 1992: Knag/Faculteit Ruimtelijke Wetenschappen Rijksuniversiteit Utrecht. 224 pp, 19 figs, 30 tabs. ISBN 90-6809-153-0 Dfl 29,50

144 C P TERLOUW The regional geography of the world-system: external arena, periphery, semiperiphery, core -- Utrecht 1992: Knag/Faculteit Ruimtelijke Wetenschappen Rijksuniversiteit Utrecht. 240 pp, 74 figs, 39 tabs. ISBN 90-6809-156-5 Out of print

145 R HASSINK Regional innovation policy: case-studies from the Ruhr Area, Baden-Wurttemberg and the North East of England -- Utrecht 1992: Knag/Faculteit Ruimtelijke Wetenschappen Rijksuniversiteit Utrecht. 196 pp, 27 figs, 28 tabs. ISBN 90-6809-155-7 Dfl 29,00

146 H REITSMA, T DIETZ & L DE HAAN (eds) Coping with semiaridity; how the rural poor survive in dry season environments -- Utrecht/Amsterdam 1992: Knag/Instituut voor Sociale Geografie Universiteit van Amsterdam. 202 pp, 18 figs, 19 tabs. ISBN 90-6809-154-9 Dfl 32,00

147 M HESSELS Locational dynamics of business services; an intrametropolitan study on the Randstad Holland -- Utrecht 1992: Knag/Faculteit Ruimtelijke Wetenschappen Rijksuniversiteit Utrecht. 232 pp, 25 figs, 79 tabs. ISBN 90-6809-157-3 Dfl 34,50

148 J KANT Geografen en planologen op de arbeidsmarkt; het succes op de arbeidsmarkt van geografen en planologen, afgestudeerd in de periode september 1987 - augustus 1990 -- Utrecht 1992: Knag/Stichting Geografenwerk. 176 pp, 39 figs, 41 tabs. ISBN 90-6809-158-1 Dfl 26,00

149 R VAN DER VAART (red) Aardrijkskunde in de basisvorming -- Utrecht 1992: Knag/ Faculteit Ruimtelijke Wetenschappen Rijksuniversiteit Utrecht. 176 pp, 44 figs, 2 tabs. ISBN 90-6809-159-X Dfl 32,50

150 M R SCHEFFER Trading places; fashion, retailers and the changing geography of clothing production -- Utrecht 1992: Knag/Faculteit Ruimtelijke Wetenschappen Rijksuniversiteit Utrecht. 270 pp, 37 figs, 34 tabs. ISBN 90-6809-160-3 Out of print

151 P P GROENEWEGEN & P P P HUIGEN (eds) Micro-macro vraagstukken in de sociologie en de sociale geografie -- Utrecht 1992: Knag/Faculteit Ruimtelijke Wetenschappen Rijksuniversiteit Utrecht. 140 pp, 15 figs, 9 tabs. ISBN 90-6809-161-1 Dfl 25,00

152 P VAN TEEFFELEN, L VAN GRUNSVEN & O VERKOREN (eds) Possibilities and constraints of GIS applications in developing countries -- Utrecht 1992: Knag/Faculteit Ruimtelijke Wetenschappen Rijksuniversiteit Utrecht. 126 pp, 16 figs, 11 tabs. ISBN 90-6809-162-X Dfl 24,50

153 L J PAUL, P P P HUIGEN & C R VOLKERS (eds) The changing function and position of rural areas in Europe -- Utrecht 1992: Knag/Faculteit Ruimtelijke Wetenschappen Rijksuniversiteit Utrecht. 192 pp, 34 figs, 16 tabs. ISBN 90-6809-163-8 Dfl 30,00

154 P LUCAS & G M R A VAN OORT Dynamiek in een stadsrandzone; werken en wonen in de stadsrandzone van de agglomeratie Utrecht -- Utrecht 1993: Knag/Faculteit Ruimtelijke Wetenschappen Universiteit Utrecht. 396 pp, 105 figs, 41 tabs, 20 photographs. ISBN 90-6809-164-6 Dfl 48,00

155 E DIRVEN, J GROENEWEGEN & S VAN HOOF (eds) Stuck in the region? Changing scales for regional identity -- Utrecht 1993: Knag/Vereniging van Utrechtse Geografie Studenten Vugs. 126 pp, 17 figs, 2 tabs. ISBN 90-6809-165-4 Dfl 27,50

156 G DRAAIJERS The variability of atmospheric deposition to forests; the effects of canopy structure and forest edges -- Utrecht 1993: Knag/Faculteit Ruimtelijke Wetenschappen Universiteit Utrecht. 208 pp, 54 figs, 26 tabs. ISBN 90-6809-166-2 Dfl 34,00

157 A P J DE ROO Modelling surface runoff and soil erosion in catchments using Geographical Information Systems -- Utrecht 1993: Knag/Faculteit Ruimtelijke Wetenschappen Universiteit Utrecht. 295 pp, 84 figs, 85 tabs. ISBN 90-6809-167-0 Dfl 36,00

158 R VERHOEFF De weg naar de podia; ruimtelijke aspecten van het bezoek aan podiumkunsten in Nederland -- Utrecht 1993: Knag/Faculteit Ruimtelijke Wetenschappen Universiteit Utrecht. 208 pp, 20 figs, 48 tabs. ISBN 90-6809-168-9 Dfl 35,00

159 H ZONDAG Regio en bedrijfseconomische vitaliteit -- Utrecht 1993: Knag/Faculteit Ruimtelijke Wetenschappen Universiteit Utrecht. 208 pp, 17 figs, 24 tabs. ISBN 90-6809-169-7 Dfl 34,50

160 T SPIT Strangled in structures; an institutional analysis of innovative policy by Dutch municipalities -- Utrecht 1993: Knag/Faculteit Ruimtelijke Wetenschappen Universiteit Utrecht. 192 pp, 36 figs, 11 tabs. ISBN 90-6809-170-0 Dfl 32,50

161 J HAUER & G HOEKVELD (eds) Moving regions -- Utrecht 1993: Knag/Faculteit Ruimtelijke Wetenschappen Universiteit Utrecht. 280 pp, 74 figs, 11 tabs. ISBN 90-6809-173-5 Dfl 34,50

162 A BARENDREGT Hydro-ecology of the Dutch polder landscape -- Utrecht 1993: Knag/Faculteit Ruimtelijke Wetenschappen Universiteit Utrecht. 208 pp, 34 figs, 31 tabs. ISBN 90-6809-175-1 Dfl 34,50

163 G B M HEUVELINK Error propagation in quantitative spatial modelling applications in GIS -- Utrecht 1993: Knag/ Faculteit Ruimtelijke Wetenschappen Universiteit Utrecht. 160 pp, 37 fig, 8 tab ISBN 90-6809-176-X Dfl 32,00

164 J R RITSEMA VAN ECK Analyse van transportnetwerken in GIS voor sociaal-geografisch onderzoek -- Utrecht 1993: Knag/Faculteit Ruimtelijke Wetenschappen Universiteit Utrecht. 206 pp, 56 figs, 17 tabs. ISBN 90-6809-177-8 Dfl 35,00

165 P VAESSEN Small business growth in contrasting environments -- Utrecht/Nijmegen 1993: Knag/Faculteit Beleidswetenschappen Katholieke Universiteit Nijmegen. 228 pp, 9 figs, 3 tabs. ISBN 90-6809-178-6 Dfl 35,00

166 T E TÖRNQVIST Fluvial sedimentary geology and chronology of the Holocene Rhine-Meuse delta, The Netherlands -- Utrecht 1993: Knag/Faculteit Ruimtelijke Wetenschappen Universiteit Utrecht. 176 pp, 66 figs, 13 tabs. ISBN 90-6809-179-4 Dfl 32,00

167 P J M VAN STEEN (red) Geografie in beweging; liber amicorum Pieter Lukkes -- Utrecht/Groningen 1993: Knag/ Faculteit Ruimtelijke Wetenschappen Rijksuniversiteit Groningen. 216 pp, 36 figs, 17 tabs. ISBN 90-6809-180-8 Dfl 35,00

168 E J A HARTS-BROEKHUIS & A A DE JONG Subsistence and survival in the Sahel; responses of households and enterprises to deterioriating conditions and development policy in the Mopti Region of Mali -- Utrecht 1993: Knag/ Faculteit Ruimt. Wetenschappen Universiteit Utrecht. 464 pp, 42 figs, 69 tabs. ISBN 90-6809-181-6 Dfl 49,50

169 F FILIUS Huishoudensopheffing en woningverlating in een vergrijzende samenleving -- Utrecht 1993: Knag/Faculteit Ruimtelijke Wetenschappen Universiteit Utrecht. 224 pp, 28 figs, 37 tabs. ISBN 90-6809-182-4 Dfl 32,50

170 V SCHUTJENS Dynamiek in het draagvlak; huishoudensontwikkelingen en winkelbestedingen in oudere naoorlogse wijken -- Utrecht 1993: Knag/Faculteit Ruimtelijke Wetenschappen Universiteit Utrecht. 240 pp, 19 figs, 31 tabs. ISBN 90-6809-183-2 Dfl 34,50

171 J KWADIJK The impact of climate change on the discharge of the River Rhine -- Utrecht 1993: Knag/Faculteit Ruimtelijke Wetenschappen Universiteit Utrecht. 208 pp, 80 figs, 20 tabs. ISBN 90-6809-184-0 Dfl 30,00

172 E C A BOLSIUS, G CLARK & J G GROENENDIJK (eds) The retreat: rural land-use and European agriculture -- Utrecht/Amsterdam 1993: Knag/Department of Human Geography Faculty of Environmental Sciences University of Amsterdam. 168 pp, 12 figs, 26 tabs. ISBN 90-6809-185-9 Dfl 33,50

173 P HOOIMEIJER, G A VAN DER KNAAP, J VAN WEESEP & R I WOODS (eds) Population dynamics in Europe; current issues in population geography -- Utrecht 1994: Knag/Faculteit Ruimtelijke Wetenschappen Universiteit Utrecht. 192 pp, 29 figs, 36 tabs. ISBN 90-6809-187-5 Dfl 35,00

174 J W H VAN DE MEENE The shoreface-connected ridges along the Dutch coast -- Utrecht 1994: Knag/Faculteit Ruimtelijke Wetenschappen Universiteit Utrecht. 246 pp, 83 figs, 28 tabs. ISBN 90-6809-188-3 Dfl 44,00

175 F R BRUINSMA De invloed van transportinfrastructuur op ruimtelijke patronen van economische activiteiten -- Utrecht/Amsterdam 1994: Knag/Vakgroep Ruimtelijke Economie Vrije Universiteit. 272 pp, 33 figs, 64 tabs. ISBN 90-6809-189-1 Dfl 42,50.

176 H CLOUT (ed) Europe's cities in the late twentieth century -- Utrecht/Amsterdam 1994: Knag/Department of Human Geography University of Amsterdam. 218 pp, 50 figs, 39 tabs. ISBN 90-6809-190-5 Dfl 35,00.

177 S M DE JONG Applications of reflective remote sensing for land degradation studies in a Mediterranean environment -- Utrecht 1994: Knag/Faculteit Ruimtelijke Wetenschappen Universiteit Utrecht. 256 pp, 64 figs, 31 tabs. ISBN 90-6809-191-3 Dfl 39,00.

178 A KROON Sediment transport and morphodynamics of the beach and nearshore zone near Egmond, the Netherlands -- Utrecht 1994: Knag/Faculteit Ruimtelijke Wetenschappen Universiteit Utrecht. 284 pp, 138 figs, 9 tabs. ISBN 90-6809-192-1 Dfl 39,00.

179 C P TERLOUW (eds) Methodological exercises in regional geography: France as an example -- Utrecht/Amsterdam 1994: Knag/Faculteit Ruimtelijke Wetenschappen Universiteit Utrecht/Centrum voor Educatieve Geografie Vrije Universiteit Amsterdam. 226 pp, 96 figs, 15 tabs. ISBN 90-6809-193-X Dfl 36,00.

180 H HUISMAN Planning for rural development: experiences and alternatives; Cases from Indonesia and Lesotho -- Utrecht 1994: Knag/Faculteit Ruimtelijke Wetenschappen Universiteit Utrecht. 240 pp, 9 figs, 36 tabs. ISBN 90-6809-194-8 Dfl 37,00.

181 P DICKEN & M QUÉVIT (eds) Transnational corporations and European regional restructuring -- Utrecht 1994: Knag/Faculteit Ruimtelijke Wetenschappen Universiteit Utrecht. 168 pp, 5 figs, 54 tabs. ISBN 90-6809-195-6 Dfl 30,00.

182 H TER HEIDE & D WIJNBELT Tussen kennen en kunnen: over de verbinding van onderzoek en ruimtelijk ontwerp; verslag van een verkenning en van een symposium -- Utrecht/Den Haag 1994: Knag/Faculteit Ruimtelijke Wetenschappen Universiteit Utrecht/Rijksplanologische Dienst. 160 pp, 11 figs, 1 tab. ISBN 90-6809-196-4 Dfl 29,00

183 M GROTHE, H J SCHOLTEN & M VAN DER BEEK GIS, noodzaak of luxe? Een verkenning naar het gebruik van geografische informatiesystemen bij private ondernemingen in Nederland -- Utrecht/Amsterdam 1994: Knag/Vakgroep Ruimtelijke Economie Vrije Universiteit Amsterdam. 128 pp, 21 figs, 27 tabs. ISBN 90-6809-199-9 Dfl 49,95

184 M F P BIERKENS Complex confining layers; a stochastic analysis of hydraulic properties at various scales -- Utrecht 1994: Knag/Faculteit Ruimtelijke Wetenschappen Universiteit Utrecht. 272 pp, 102 figs, 29 tabs. ISBN 90-6809-200-6 Dfl 39,00

185 F BARNHOORN, R JANSEN, H TH RIEZEBOS & J J STERKENBURG Sustainable development in Botswana; an analysis of resource mangement in three communal development areas -- Utrecht 1994: Knag/Faculteit Ruimtelijke Wetenschappen Universiteit Utrecht. 160 pp, 21 figs, 46 tabs. ISBN 90-6809-201-4 Dfl 35,00

186 A HARTS-BROEKHUIS & O VERKOREN (eds) No easy way out; essays on Third World development in honour of Jan Hinderink -- Utrecht 1994: Knag/Faculteit Ruimtelijke Wetenschappen Universiteit Utrecht. 392 pp, 21 figs, 16 tabs. ISBN 90-6809-202-2 Dfl 59,00

187 A C M VAN WESTEN Unsettled: low-income housing and mobility in Bamako, Mali -- Utrecht 1995: Knag/Faculteit Ruimtelijke Wetenschappen Universiteit Utrecht. 336 pp, 31 figs, 48 tabs. ISBN 90-6809-203-0 Dfl 43,00

188 F VAN DAM Meer voor minder; schaalverandering en bereikbaarheid van voorzieningen in landelijke gebieden in Nederland -- Utrecht 1995: Knag/Faculteit Ruimtelijke Wetenschappen Universiteit Utrecht. 346 pp, 119 figs, 56 tabs. ISBN 90-6809-204-9 Dfl 45,00

189 F VAN REISEN & M TACKEN (eds) A future of telework; towards a new urban planning concept? -- Utrecht/Delft 1995: Knag/Faculteit Bouwkunde TU Delft. ca 200 pp. ISBN 90-6809-205-7 Dfl 37,50

190 W P A VAN DEURSEN Geographical Information Systems and Dynamic Models; development and application of a prototype spatial modelling language -- Utrecht 1995: Knag/Faculteit Ruimtelijke Wetenschappen Universiteit Utrecht. 206 pp, 44 figs, 8 tabs. ISBN 90-6809-206-5 Dfl 38,00

191 F THISSEN Bewoners en nederzettingen in Zeeland: op weg naar een nieuwe verscheidenheid -- Utrecht/Amsterdam 1995: Knag/Instituut voor Sociale Geografie Universiteit van Amsterdam. ca 200 pp. ISBN 90-6809-207-3 Dfl 37,50

192 A ROMEIN Labour markets and migrant absorption in small towns: the case of northern Costa Rica -- Utrecht 1995: Knag/Faculteit Ruimtelijke Wetenschappen Universiteit Utrecht. 190 pp, 24 figs, 47 tabs. ISBN 90-6809-208-1 Dfl 36,00

193 G J ASHWORTH & J WAALKENS (red) Geografie en milieu: trend of traditie? -- Utrecht/Groningen 1995: Knag/Faculteit der Ruimtelijke Wetenschappen Rijksuniversiteit Groningen. 152 pp, 14 figs, 9 tabs. ISBN 90-6809-209-X Dfl 32,50

194 A FEDDES Woningmarkt, regulering en inflatie: het na-oorlogse volkshuisvestingsbeleid van tien Noordwest-Europese landen vergeleken -- Knag/ Faculteit Ruimtelijke Wetenschappen Universiteit Utrecht. 464 pp, 69 figs, 75 tabs. ISBN 90-6809-210-3 Dfl 60,00

195 K M WIJNBERG Morphologic behaviour of a barred coast over a period of decades -- Knag/ Faculteit Ruimtelijke Wetenschappen Universiteit Utrecht. ca 250 pp. ISBN 90-6809-211-1 Dfl 45,00

Publications of this series can be ordered from KNAG / NETHERLANDS GEOGRAPHICAL STUDIES, P.O. Box 80123, 3508 TC Utrecht, The Netherlands (Fax +31 30 535523). Prices include packing and postage by surface mail. Orders should be prepaid, with cheques made payable to "Netherlands Geographical Studies". Please ensure that all banking charges are prepaid. Alternatively, American Express, Eurocard, Access, MasterCard, BankAmericard and Visa credit cards are accepted (quote card number and expiry date with your signed order).

Sheet 1

Alongshore coherence in the temporal behaviour of the shoreline and the profile shape

***(a)* Anomaly position +1m contour**

landward ▮▮▮▮ seaward

-10 10 m

Cross-shore shifting of the sub-aqueous profile represented by the cross-shore shifting of the 1m +NAP contour relative to its time-averaged position.

***(b)* Anomaly mean depth at 750 m offshore**

deeper ▮▮▮▮ shallower

-0.2 0.2 m

Profile steepness variations, represented by the deviations from the local mean depth at 750 m from the shoreline (derived from local first empirical eigenfunctions).

***(c)* Normalised weightings on eigenfunction 2**

▮▮▮▮

-0.5 0.5

Behaviour of secondary morphologic features represented by the weightings on the re-arranged second empirical eigenfunctions (Figure 4.2).

***(d)* Normalised weightings on eigenfunction 3**

▮▮▮▮

-0.5 0.5

Behaviour of secondary morphologic features represented by the weightings on the re-arranged third empirical eigenfunctions (Figure 4.2).

White rectangular areas represent missing data
Dashed lines indicate boundaries of LSCB-regions